

FACULTY OF MEDICINE.
DEPARTMENT OF ORAL HEALTH SCIENCES
ORAL IMAGING CENTRE
Kapucijnenvoer 7 block a box 7001
B-3000 LEUVEN, BELGIUM
tel. + 32 16 32 00800
<http://gbiomed.kuleuven.be>



Livia Corpas

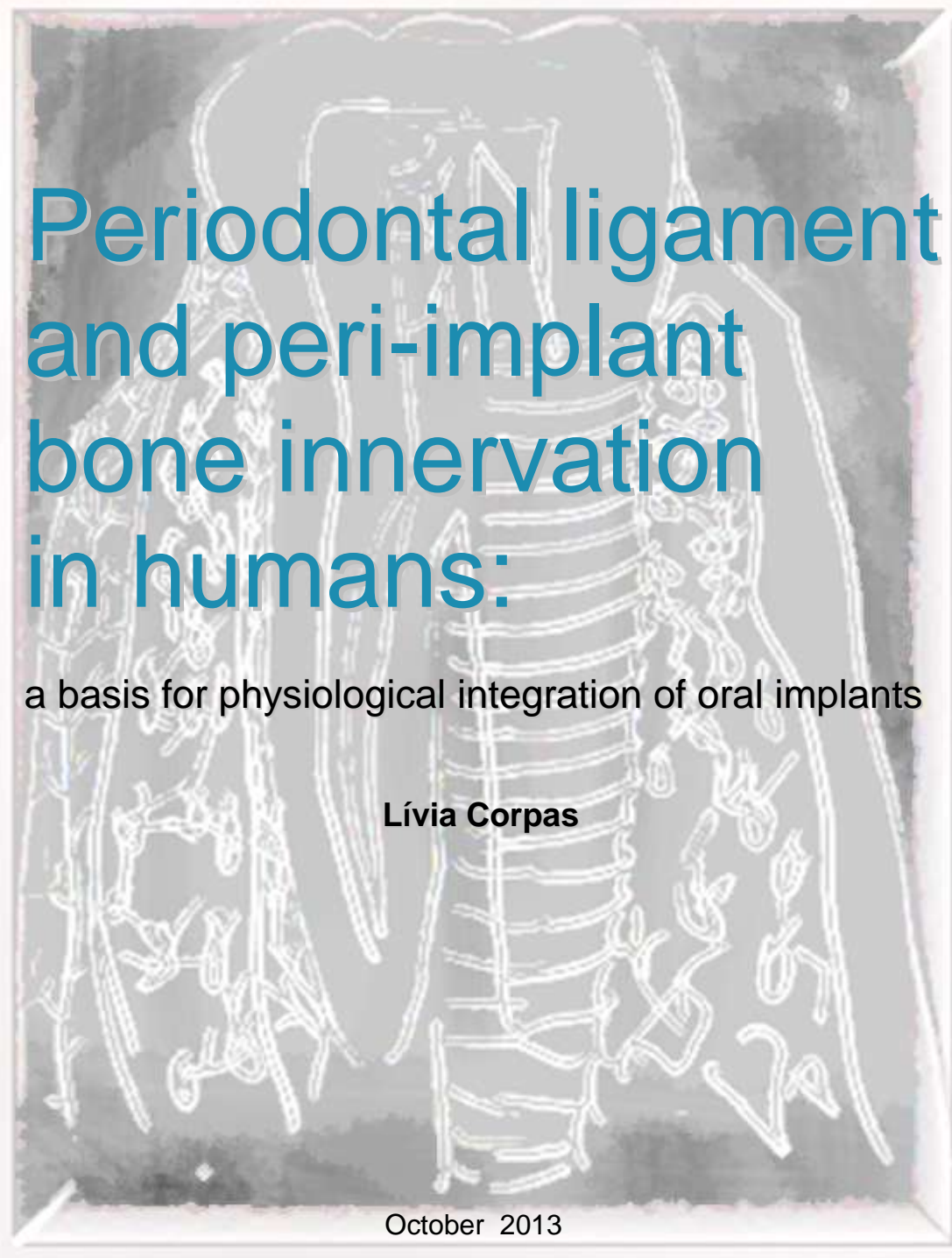
PERIODONTAL LIGAMENT AND PERI-IMPLANT BONE INNERVATION IN HUMANS: A
BASIS FOR PHYSIOLOGICAL INTEGRATION OF ORAL IMPLANTS

October 2013

KU LEUVEN

universiteit
hasselt

DOCTORAL SCHOOL
BIOMEDICAL SCIENCES



**KU Leuven
Biomedical Sciences Group
Faculty of Medicine
Department of Oral Health Sciences
Oral Imaging Centre**



Periodontal ligament and peri-implant bone innervation in humans: a basis for physiological integration of oral implants

Lívia CORPAS

Promoter:
Prof. Dr. Reinhilde Jacobs
Co-promoter:
Prof. Dr. Ivo Lambrichts

Dissertation presented in
partial fulfilment of the
requirements for the
degree of Doctor in
Biomedical Sciences

October 2013

KU Leuven
Group Biomedical Sciences
Faculty of Medicine
Department of Oral Health Sciences
Oral Imaging Centre



Periodontal ligament and peri-implant bone innervation in humans: a basis for physiological integration of oral implants

Lívia CORPAS

Jury:

Promoter: Prof. Dr. Reinhilde Jacobs, KU Leuven, Belgium
Co-promoter: Prof. Dr. Ivo Lambrichts, Hasselt University, Belgium
Chair: Prof. Dr. Dominique Declerck, KU Leuven, Belgium
Secretary: Prof. Dr. Joke Duyck, KU Leuven, Belgium
Jury members: Prof. Dr. Antoon De Laat, KU Leuven, Belgium
Prof. Dr. Izabel Regina Fischer Rubira-Bullen USP/FOB, Brazil
Prof. Dr. Constatinus Politis, KU Leuven–Hasselt University, Belgium
Prof. Dr. Serge Schepers, Hospital St. Jan Genk, Belgium
Prof. Dr. Marjan Vandersteen, Hasselt University, Belgium
Dr. Patrick Semal, Royal Belgian Institute of Natural Sciences, Brussels, Belgium

Leuven, October 2013
Doctoral thesis in Oral Health Sciences

Acknowledgments

This thesis would not be possible without the help and work of many people to whom I would like to express my gratitude here.

First of all, I would like to thank Prof. Rik Torfs, Rector at KULeuven, Prof. Jan Goffin, Dean of the Faculty of Medicine and Prof. Dominique Declerck, head of the Department of Oral Health Sciences. My special thanks is extended to the staff of Doctoral School of Biomedical Sciences, Prof. Bart Nuttin, research director and Prof. John Creemers, director. The assistance provided by their administrative team, Els Wellens and Katleen Vercammen was greatly appreciated. I would also like to acknowledge Prof. Luc de Schepper, Rector at Hasselt University and Prof. Sven Hendrix, director of the Doctoral School for Medicine & Life Sciences at Hasselt University.

It was a great honour to be as PhD student at both institutions: KULeuven and Hasselt University. I am very grateful to those who have made it possible for me to study abroad. In this way, I would like to thank Prof. Wellington Bonachela, for his support and for showing me the opportunity to try the scholarship at KULeuven, and specially to the staff of International Office at KULeuven, for their support and help from the beginning till the end. I am particularly grateful for the assistance given by Hilde Nijs and Edmund Guzman.

I would like to offer my thanks to my promoter Prof. Reinhilde Jacobs for having accepted me as her PhD student, for kindly receiving me at KULeuven and for following and supporting this work over all those years, together with my co-promoter Prof. Ivo Lambrichts. I would also like to thank Prof. Ivo Lambrichts for opening to me the doors of Hasselt University and for the training and teaching on histology. I thank both of them for their work and time spent on this thesis.

I wish to acknowledge the help provided by Dr. Bart Vandenberghe, Dr. Bruno Collaert, Prof. Christiano Oliveira, Prof. Ignace Naert, Prof. Joke Duyck, Dr. Yan Huang, Dr. Tom Struys, Dr. Wendy Martens, Prof. Marc Quirynen, Mr. Marc Jans, Dr. Olivia Nackaerts, Prof. Xin Liang, Dr. Patrick Semal, Dr. Emmanuel Gilissen and Prof. Rubens Raimundo. Thanks for their work and collaboration which helped to improve several chapters of this thesis.

My gratitude goes also towards all members of the Examining Committee for taking their time to review this manuscript: Prof. Ghislain Opdenakker, chair of the Examining Committee, Prof. Joke Duyck, Prof. Antoon De Laat, Prof. Izabel Regina Fischer Rubira-Bullen, Prof. Constatinus Politis, Prof. Serge Schepers, Prof. Marjan Vandersteen and Dr. Patrick Semal. I would like to express my very great appreciation to their useful comments and suggestions to this work.

A great thanks to all staff members of the Oral and Maxillofacial Surgery Department at East Limburg Hospital in Genk. I am particularly grateful to all assistance and care of all lovely nurses who work there. My special word of thanks goes also to Prof. Constantinus Politis, Prof. Serge Schepers and Dr. Luc Vrielinck for allowing me to conduct part of my thesis there. I thank them for their help, trust and support to my researches.

Another special thanks goes to all my colleagues and friends at the Oral Imaging Center and Oral Health Sciences Department with whom I was always very glad to share my working (and after working) hours at the University or just enjoying Leuven: Ali, Aline, Andres, Eduardo, Jeroen, Joe, Marcio, Maryam, Mostafa, Pisha, Ruben, Yan and all Brazilians who have passed by and helped to turn me back to my Brazilian way of being: Izabel, Fernando, Paulo, Soraya, Francisco, Ivete, Marcia, Rejane, Christiano, João, Ana Carolina, Emanuela, Monikelly, Laura, Karla, Evelise, Germana, Fernanda and Thais.

I am especially grateful to Olivia Nackaerts, Xin Liang and Bart Vandenberghe for helping me in the very beginning to get used to my new life in Belgium and for their amazing friendship throughout the years. I would like to particularly thank Bart Vandenberghe, for his friendship, help and professional support. I also thank him for always believing in me, even at those moments that I did not, and for helping me to understand that it is not a problem to be myself. Thanks for being there for me not only as a trustful colleague, but also (much better and funnier) as a very supportive friend.

Last, but not least, I would like to thank my Brazilian and Belgian families and friends outside-professional borders. Without them, I am nothing...Special thanks to my husband, William Gisgand, for giving me so much love, for his patience, for the courage he gave me to get through those tough years of PhD, for his beautiful artwork in the cover of this thesis, specially made for me in the middle of the Brazilian Amazon, and mainly, for being always there for me, anytime of the day or night; to my parents, Nanci and Osvaldo for their unconditional support and love along all my life and for the great moments we could spend here in Belgium. Special thanks to my father, Osvaldo Corpas, my eternal professional source of inspiration and advices. It was because of him I became a dentist and 20 years later, it is him who gives me the drive to continue....

Thank you all!

Table of Contents

Preface	7
List of abbreviations	8
Chapter 1 – General introduction and aims	9
PART 1: HISTOLOGICAL ASSESSMENT	17
Chapter 2 – Periodontal ligament innervation and mechanosensory function in teeth: a review and novel 3D-approach	18
Introduction	20
I- Assessment of PDL nerve fibres	24
I.I Origin of the PDL innervation	24
I.II Characteristics and distribution of nerve fibres in the PDL	26
II –Assessment of PDL nerve endings	33
II.I Morphology of PDL mechanoreceptors	33
II.II Neurophysiological aspects of PDL mechanoreceptors	36
II.III Connections to Central Nervous System	44
II.IV Functional significance of nerve fibres and ending in the PDL	47
II.V Periodontal neuropeptides and neural growth factors	59
III – Influence of oral treatments and future approaches in PDL	63
III.I Influence of oral treatments	63
III.II Future research approaches in the PDL structures	67
IV – Three dimensional reconstruction of human periodontal ligament structures using light microscopy imaging	70
Conclusions	80
Chapter 3 – Distribution of nerve fibers in the periodontal ligament	89

Chapter 4 – Other PDL special structures: Epithelial Rest of Malassez and Cementicles	108
Chapter 5 – The peri-implant innervation: Literature review and histological findings in humans	129
PART 2: RADIO-ANATOMICAL ASSESSMENT	151
Chapter 6 – Peri-implant bone characterization: bone structure and density	152
Chapter 7 – Mandibular neurovascular canals: Influence of inter-specific, secular and geographical variability	179
Chapter 8 – Mandibular neurovascular canals: Influence of oral status and implant treatment	209
Chapter 9 – General discussion and conclusions	237
Summary - Samenvatting	253
References	258
Curriculum Vitae	265

Preface

This thesis is based on the following papers:

- **Chapter 2**

Corpas LS, Struys T, Politis C, Lambrichts I, Jacobs R. From old concepts to current knowledge on periodontal ligament innervation: a literature review. (in prep)

- **Chapter 3**

Huang Y, **Corpas LS**, Martens W, Jacobs R, Lambrichts I. Histomorphological study of myelinated nerve fibres in the periodontal ligament of human canine. *Acta Odontol Scand.* 2011; 69:279-86.

- **Chapter 4**

Struys T, Schuermans J, **Corpas L**, Politis C, Vrielinck L, Schepers S, Jacobs R, Lambrichts I. Proliferation of epithelial rests of Malassez following auto-transplantation of third molars: a case report. *J Med Case Reports.* 2010; 4:328-333.

- **Chapter 5**

Corpas LS, Lambrichts I, Quiryneen M, Collaert B, Politis C, Vrielinck L, Martens W, Struys T, Jacobs R. Bone innervation around osseointegrated implants: literature review and report of histological findings in humans. (submitted)

- **Chapter 6**

Corpas LS, Jacobs R, Quiryneen M, Huang Y, Naert I, Duyck J. Peri-implant bone tissue assessment by comparing the outcome of intra-oral radiograph and cone beam computed tomography analyses to the histological standard. *Clin Oral Implants Res.* 2011; 22:492-9.

- **Chapter 7**

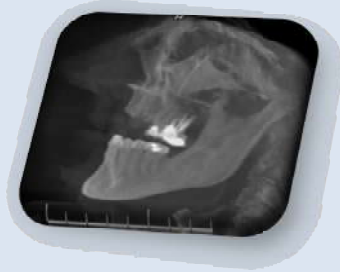
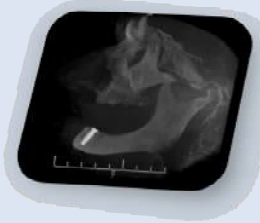
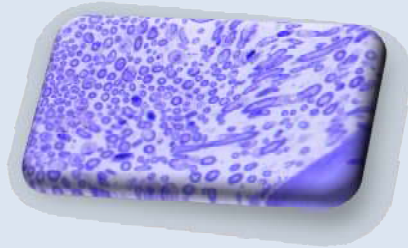
Corpas LS, Liang X, Oliveira C, Lambrichts I, Semal P, Gilissen E, Raymundo Junior R, Jacobs R. Comparative anatomy of neurovascular canals and tooth roots in mandibles of modern humans and great apes. (in prep)

- **Chapter 8**

Corpas LS, Vandenberghe B, Politis C, Schepers S, Lambrichts I, Naert I, Jacobs R. Anatomical changes in the mandibular bone after tooth extraction and implant rehabilitation in edentulous patients. (in prep)

List of abbreviations

AED	aluminium equivalent density
AFC	afibrillar cementum
BSP	bone sialoprotein
CBCT	cone beam computed tomography
CGRP	calcitonin gene-related peptide
CLS	cementicle-like structures
CNS	central nervous system
CPG	central pattern generator
EMG	electromyography
ERM	epithelial rests of Malassez
ERSH	epithelial root sheath of Hertwig
fMRI	functional magnetic resonance image
GDNF	glial cell line-derived neurotrophic factor
Hrp	horseradish peroxidase
IAN	Inferior alveolar nerve
ICMS	intra-cortical microstimulation
IO	intra-oral
IR	immunoreactive neural elements
MI	face primary motor cortex
mm	millimetre
mmAleq	millimetre aluminium equivalent
MS	mesencephalic nucleus
MSTN	main sensory trigeminal nucleus
N	number of fibers
NCP	non-collagenous matrix protein
NFP	neurofilament protein
OPN	osteopontin
PDL	periodontal ligament
PGP-9.5	protein gene product 9.5
PTHrP	parathyroid hormone-related protein
S-100	glia-specific S-100 protein
SI	face primary somatosensory cortex
SP	substance P
STTN	spinal tract of the trigeminal nucleus
TEM	transmission electron microscopy
TG	trigeminal ganglion
TrkA	tyrosine receptor kinase A
VIP	vasoactive intestinal peptide
µm	micrometer
%	percentage



Chapter 1

General introduction and aims

1.1 General Introduction:

Why assessing periodontal ligament (PDL) innervation to discuss physiological integration of implants?

The study of PDL innervation and its mechanoreceptive role in tooth function can help to improve the understanding of peri-implant innervation and its functional role in the sensory feedback mechanism. The overall aim in this thesis was to identify the most relevant elements in the understanding of oral mechanosensory function in relation to oral osseointegrated implants. For this, we have first driven on the roads of mechanoreception in teeth, searching for differences or similarities between this function in teeth and implants.

The periodontal ligament is a unique connective tissue that surrounds the roots of teeth and connects them with the alveolar bone (*Beertsen et al 1997; Berkovitz 1990*). This ligament has an abundant number of periodontal mechanoreceptors contributing to sensory feedback mechanisms (*Trulsson 2005; Trulsson 2006; Jacobs and van Steenberghe 2006; Maeda et al 1999; Jacobs and van Steenberghe 1994*). Although these structures have been extensively studied in the literature (*Lambrichts et al 1992; Linden 1990; Jacobs and van Steenberghe 1994; Long et al 1995; van Steenberghe 1979*), the real tridimensional nature of periodontal receptors intermingled with the collagen fibres has not been appropriately explored in man. In animals, it was described by Kannari in 1990. The spatial arrangement between collagen and nervous fibres influences the biomechanical environment in the complex tooth-PDL-bone, and the way loads will be sensed and transmitted to the Central Nervous System (CNS).

According to nerve fibre distribution and dimensions, some conclusions could be drawn about their physiological significance. In cats, thick isolated nerve fibres that were found in the cemental part of PDL were considered putative mechanoreceptors (*Long, Loescher and Robinson 1995*). Indeed, the diameter reported ($\approx 5\mu\text{m}$) was in the range of nerve fibres of touch and pressure (*Manzano et al 2008*). Besides mechanoreceptors, other structures identified in the PDL, like epithelial rests of Malassez and cementicles, may also have a relation to innervation. Yet, their functional role is not yet fully understood (*Haku et al 2011; Bosshardt and Nanci, 2003; Lambrichts et al 1993; Holton et al 1986*).

It is known that tooth extraction can be compared to limb amputation leading to some retrograde nervous degeneration (*Hansen 1980*). Indeed, an earlier study of Heasman (1984) has shown that the inferior alveolar nerve (IAN) in edentulous patients have on average 20% less myelinated nerve fibres than in dentate patients. Although some fibre regeneration in healed extraction sockets has been reported previously (*Gunjigake et al 2006*), those fibres do not seem to innervate new tissues in which these could be functionally active and mechanically stimulated (*Bonte et al 1993; Linden and Scott 1989*). Interestingly, implants were found to preserve bone by restoring a suitable biomechanical environment to the minimum load levels found in the normal physiological condition (*Lin et al 2010; Lin et al 2009*). It could thus be wondered whether implants would also influence nerve fibre regeneration by providing them a new functional impulse.

In oral rehabilitation, clinical observations indicated that bone-anchored prostheses in edentulous patients could transmit sensory information (*Brånemark 1999*) contributing to the physiological integration of artificial teeth. The term “osseoperception” was coined by Brånemark to indicate the perception of different external stimuli transmitted via the prosthetic limb or the anchoring implant (*Jacobs 1998*). Clinical observations by Haraldson and coworkers showed for the first time a restored oral function associated with higher bite forces and better masticatory efficiency (*Haraldson and Carlsson 1977; Haraldson and Ingervall 1979a and b; Haraldson and Carlsson 1979 and Haraldson, Carlsson and Ingervall 1979*).

Later on, several studies confirmed improved tactile function in patients rehabilitated with osseointegrated implants by comparing the tactile thresholds in edentulous patients using conventional or bone-anchored prosthesis (*Enkling et al 2012; Habre-Hallage et al 2010; Enkling et al 2010; Batista et al 2008; Enkling et al 2007; El-Sheikh et al 2003; Jacobs et al 2001; Jang and Kim 2001; Jacobs et al 1997; Jacobs et al 1993; Jacobs and van Steenberghe 1991; Lundqvist and Haraldson 1990*). Similarly, limb amputated patients rehabilitated with a bone-anchored prosthesis supported by an osseointegrated implant seem to have a subjectively improved ability to feel through their prosthesis and the anchoring implant in the bone (*Jacobs et al 2000; Jacobs et al 1998; Stenfelt et al 1998*). This was generally described as the osseoperception phenomenon by Lundborg et al (1996), Brånemark et al (1997), Rydevik (1997) and Jacobs et al (1996 and 1997) (*Rydevik 1998*).

Although differing in components and structures, both PDL and peri-implant tissues provide sensory information to the CNS (*Habre-Hallage et al 2012; Jacobs and van Steenberghe 2006; Van Loven et al 2000; Jacobs and van Steenberghe 1991*). The peri-implant bone tissues might indeed possess some tactile feedback mechanisms by load transfer (*Jacobs and van Steenberghe 1993*) and mechanoreceptor stimulation in the vicinity of the peri-implant tissues such as periosteum and more distant receptors (*Jacobs and van Steenberghe 2006; Trulsson 2005; Klineberg 2005*). According to the consensus statement on osseoperception (*Klineberg et al 2005*), those more distant receptors may include those located in muscle, joint, mucosal and cutaneous tissue. The entire consensus is reproduced in table 1.1. In the framework it is stated that “there are no data to support feedback contributions to the restoration of function from bone, bone marrow, include vasculature within, or periosteum”. This is a consensus statement dating back from 2005, even if other data were published later on (*Habre-Hallage et al 2012; Habre-Hallage et al 2010*), the role of bone innervation is not fully understood. In this way, the study of peri-implant bone innervation may help in unravelling the osseoperception phenomenon by assessing the influence of local factors in the mechanosensibility arising from osseointegrated implants in the jaw bones.

Table 1.1: Consensus statement on Osseoperception in Klineberg et al (2005)

Consensus statement
Osseoperception may be considered to be the mechanosensibility associated with osseointegrated implant rehabilitation. This phenomenon may be defined as: (i) the sensation arising from mechanical stimulation of a bone-anchored prosthesis, transduced by mechanoreceptors that may include those located in muscle, joint, mucosal, cutaneous and periosteal tissues; together with (ii) a change in central neural processing in maintaining sensorimotor function.
Framework:
The consensus statement was developed within the framework of recognition that:
1. Orofacial phenomena require tactile and kinaesthetic inputs and mechanosensibility is an appropriate description for the sensation derived from a bone-anchored prosthesis, which, together with tactile and kinaesthetic inputs, combine to allow appropriate restoration of function.
2. There are no data to support feedback contributions to the restoration of function from bone, bone marrow, included vasculature within, or periosteum.
3. There are significant data from mechanoreceptors groups in adjacent tissues, including skin, muscle and joints, the relative contributions of which need to be determined.
4. Sensorimotor cortical representation varies in ipsilateral and bilateral contributions and the varied topographical representation from orofacial afferents is considered to be an indication of the plasticity of the system in accommodation of change.

Extraction of a tooth leads to loss of the periodontal ligament space and its related innervation. When a subsequent implant is then placed and osseointegrated, the original spatial arrangement of the periodontal ligament innervation is lost, while sensory feedback is further challenged as a novel biomechanical environment is created, with potentially higher load levels. While the tactile feedback from the original periodontal ligament innervation helps to modulate force levels during chewing and biting, PDL does no longer exist around osseointegrated implants. It could therefore be questioned whether there is any remaining innervation neighbouring the implant? And if this innervation would be present, does it express some mechanoreceptive characteristics? And if so, is it sufficient to restore the sensory feedback pathway?

Although histological and neurophysiological studies would be needed to address those questions appropriately, it is a challenge to carry this out in man. Current imaging techniques could be applied to gain more information on jaw bone neurovascular canals and peri-implant bone. It may help to render tridimensional visualization and characterization of peri-implant bone in order to elucidate some features which might be of functional significance, such as bone density and structure. Those two bone parameters are of promising diagnostic use to describe bone tissue by means of digital intra-oral radiographs and cone beam computed tomography, respectively. It is known that bone density cannot be accurately predicted in CBCT images (*Casseta et al 2012; Hua et al 2009*); however bone structure seems to deserve further exploitation (*Huang et al 2013; Naitoh et al 2010; Liu et al 2007*). In the same way, digital intra-oral imaging has shown promising results in the determination of bone density (*Sun et al 2009; Nackaerts et al 2008, 2007 and 2006*).

As for jaw bone neurovascularisation, the current clinical imaging techniques allow to study neurovascular canals, while functional magnetic resonance imaging may further contribute to unravel the cortical response to receptor activation. The present thesis will further focus on the radiographical visualisation of the mandibular canal, as it can be clearly depicted on radiographic images and might help to identify changes in the innervation after tooth extraction and implant treatment. Since after tooth extraction some retrograde nerve degeneration may occur, it can then be discussed what happens to the mandibular neurovascular canals (*Jacobs et al 2002; Polland et al 2001*) and their appearance on radiographic images (*Jacobs et al 2004*).

So far no study was found comparing mandibular canals dimensions in dentate and edentulous mandible, whereas the degeneration of some fibres of inferior alveolar nerve (IAN) has been clearly demonstrated in edentulous mandibles (*Wadu et al 1997; Heasman 1984; Hansen 1980*).

Assuming that this nerve degeneration would lead to changes in the mandibular canals, one could discuss that those changes could be depicted on 3D images. However, it is important to note that great interindividual variability exist in the mandibular canal anatomy, as well as in the composition of the inferior alveolar nerve. The study of the mandibular canal variations is crucial when attempting to address the neurovascular changes potentially occurring after tooth extraction and implant placement.

All those questions should not only be studied radiologically, yet also by histological and functional approaches in order to attempt the physiological integration of oral osseointegrated implants. This thesis has focused on the radiological and histological assessments.

Aims

The main objectives of this thesis were to assess the periodontal ligament and peri-implant bone in humans by means of histological and radiological techniques and to study the intrabony canals by means of radio-anatomical assessments in dentate and edentulous subjects.

Part I-Histological assessment: To identify and characterize the presence of nerve fibres in the periodontal and peri-implant bone tissues by means of light and electron microscopy.

- Describe the historical evolution of main concepts about PDL mechanosensory function; identify needs for novel approaches in the study of periodontal ligament innervation - literature review (chapter 2).
- Analyze myelinated nerve fibre distribution in human periodontal ligament by means of light microscopy – histomorphometric study (chapter 3).

Hypothesis: Nerve fibre dimensions and distribution in human PDL are similar to that found in previous animal reports.

- Describe other specialized structures present in human periodontal ligament, Epithelial Rests of Malassez (ERM) and cementicles, discussing their relation with bone innervation – review and case report (chapter 4).
- Identify and describe myelinated nerve fibres present around implant by means of light microscopy (LM), electron microscopy (EM) (chapter 5).

Hypotheses: 1. Myelinated nerve fibres are present in the peri-implant region in humans similarly to those found in animal reports.

2. Mechanoreceptor-like structures can be found in the human peri-implant region.

- Correlate histological and radiological assessment of peri-implant bone healing (chapter 6).

Hypothesis: Tissue parameters assessed on intra-oral radiographs and cone beam computer tomograms are correlated to those found in histomorphometric analyses of the same sites.

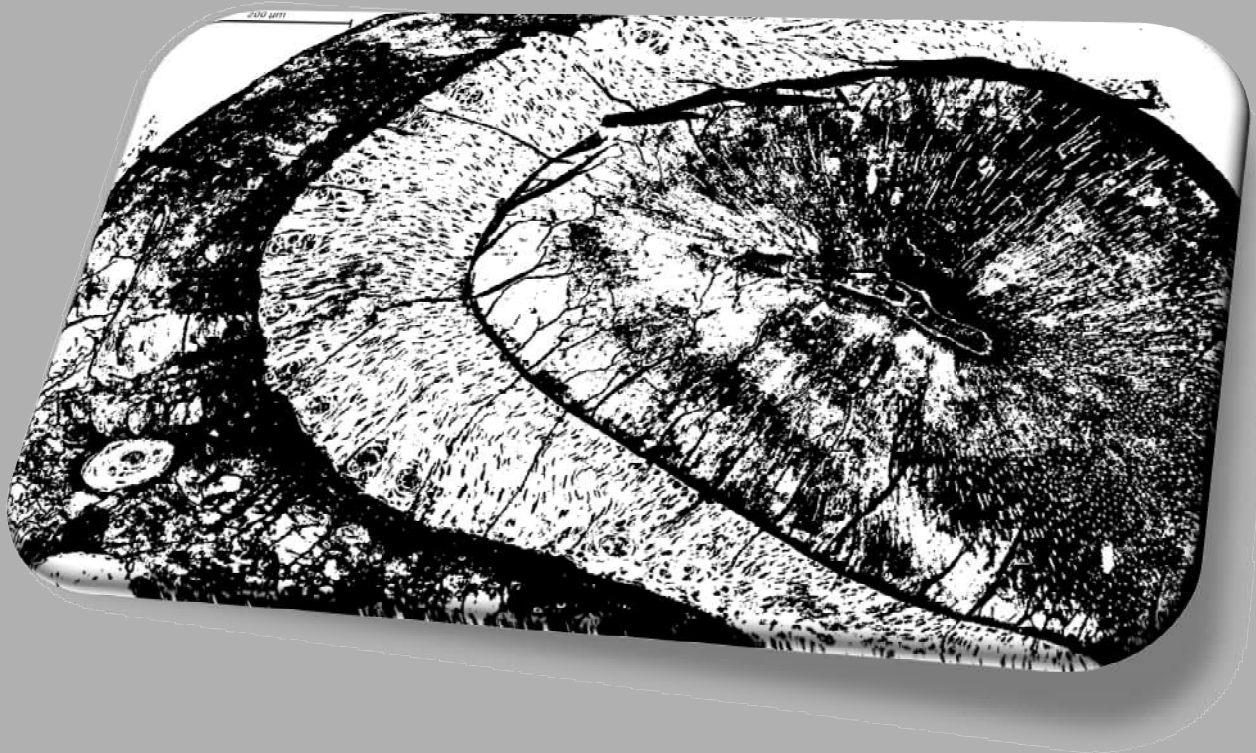
Part II-Radio-Anatomical assessment: To assess variability of mandibular neurovascular canals in humans. To verify influence of implant treatment on mandibular bone resorption and neurovascular canal dimensions.

- Describe and compare neurovascular canals of human mandibles from prehistoric, medieval and contemporary human mandibles from 7 different geographical origins to chimpanzee and gorilla mandibles by means of cone beam computed tomography (CBCT) (chapter 7).

Hypothesis: Anatomical variability of mandibular canals can be explained by secular, geographical and species differentiation.

- Assess bone resorption, mandibular neurovascular canals dimensions and their changes maximum 2 years after implant rehabilitation in edentulous patients compared to dentate patients by means of CBCT imaging (chapter 8).

Hypothesis: Dental status and implant treatment influence bone resorption and dimensional changes in the mandibular canal.



PART I

Histological assessment

Chapter 2

Periodontal ligament innervation and mechanosensory function in teeth: a review and novel 3D-approach

Publication related to this chapter:

Corpas LS, Struys T, Politis C, Lambrichts I, Jacobs R. From old concepts to current knowledge in periodontal ligament innervation: a literature review. (in prep)

From the old concepts to the current knowledge in periodontal ligament innervation: a literature review

Abstract:

Objective: This study aimed to review the literature on periodontal ligament innervation searching for evidence-based information about mechanosensory function in teeth. **Material and Methods:** Five literature reviews were used as “start-point” of the search strategy and were used to further search on PUBMED and WEB OF SCIENCE to find related articles, articles from the same authors and the citations received by those reviews. Mesh terms were chosen from the terms classifying those reviews and used in PUBMED to find relevant articles published in the last 6 years. **Results:** After using this search strategy, two collections were created. One in PUBMED and another on WEB OF SCIENCE, consisting of 258 and 105 articles, respectively. Articles from WEB OF SCIENCE were further selected on the basis of publication date (last 6 years) and the number of citations (fifteen-most cited articles). Next steps included the verification for duplicates between collections and articles classification by topics. **Conclusions:** Mechanosensory function in teeth has not been fully unravelled by the extensive number of researches on this field. Substantial advances have been made, although the challenge still exists due to the complexity to characterize the periodontal ligament. Several methods and study approaches have been designed using microneuroradiography, electrophysiological records, classic and ultrastructural histological techniques, immunohistochemical analyses and psychophysical clinical tests. The knowledge generated by these several sources is useful for a more complete understanding of the periodontal ligament innervation and its functions. However future researches need to further study the interrelationship of oral mechanosensory function with histomorphological features and spatial arrangement of the periodontal ligament within different species.

Introduction

Apart from its supportive role, the periodontal ligament (PDL) is also considered as sense organ (*Hildebrand et al 1995*). How this ligament can function in this way is explained by its specialized innervation machinery. Already in the 19th century, Linderer had described the innervation of the periodontal ligament (*Lewinsky and Stewart 1937*). Since then, a large number of histological and physiological studies have been performed in a variety of species like humans, monkeys, dogs, cats, rats, mice, guinea-pigs, ferrets, rabbits, moles, hedgehogs and caimans. Later, in the 20th and 21th centuries the studies on the PDL innervation have been reviewed regarding several aspects (*Trulsson 2007; Trulsson 2006; Trulsson and Johansson 2002; Lobezoo et al 2002; Linden 1990; Maeda et al 1999; Jacobs and van Steenberghe 1994, Kannari 1990, Maeda et al 1990, van Steenberghe 1979*). The main aspects discussed were related to the morphology, neurophysiology, trigeminal central connections and functional significance of nerve fibres and endings in the PDL.

The main concern about PDL innervation is the feedback input provided to the Central Nervous System (CNS) allowing it to regulate oral functions such as biting and chewing (*Svensson et al 2012; Svensson and Trulsson 2011; Svensson and Trulsson 2007; Lund and Kolta 2006; Lobbezoo et al 2002*). However, to build up the knowledge about PDL innervation physiology, information related to those mentioned aspects need to be gathered. In 1990, Linden reported that “by analogy with the control movement elsewhere in the body and in the view of the very large forces which can be transmitted via the tooth to the periodontium, one would expect to find a receptor mechanism that is capable of providing the basis of feedback control to the muscles of mastication” (*Linden 1990b*). Yet, up till now, this receptor mechanism has not been fully unravelled, notwithstanding the abundant literature available on this topic (*Trulsson 2007; Trulsson 2006; Trulsson and Johansson 2002; Lobbezoo et al 2002; Linden 1990b; Maeda et al 1999; Jacobs and van Steenberghe 1994, Kannari 1990, Maeda et al 1990, van Steenberghe 1979*).

Substantial advances have been made, although the challenge still exists due to the complexity to characterize the periodontal ligament. For that, several methods and study approaches have been designed using microneuroradiography, electrophysiological records, classic and ultrastructural histological techniques,

immunohistochemical analyses and psychophysical clinical tests (*Trulsson 2007; Linden 1990a; Maeda et al 1999; Lambrichts et al 1992; Kannari 1990; van Steenberghe 1979*). The knowledge generated by these several sources might be useful for a more complete understanding of the periodontal ligament innervation and its functions.

Mechanisms of mechanoreception around teeth

Functional loading causes displacement of the tooth triggering mechanoreceptors around the tooth. Those mechanoreceptors are specialized nerve endings programmed to sense and codify mechanical stimuli to the CNS (*Trulsson 2006; Lund and Kolta 2006*). In order to understand how forces are sensed by those receptors, studies have been conducted on different species, focused on a variety of teeth using various scientific methods (*Hildebrand et al 1995; Linden 1990b, Byers and Dong 1989; van Steenberghe 1979*). In this way, it has been difficult to draw clear conclusions about the function of the PDL innervation, particularly in humans, since neurophysiological as well as histological studies are complex.

The characteristics of mechanoreceptors have been studied in an effort to describe those structures as accurate as possible and to understand their functional significance (*Jacobs and van Steenberghe 1994; Linden 1990a; van Steenberghe 1979*). At first, it is important to realize that, when describing the nerve endings, one is addressing only the terminal portion of a nerve fibre. Studies describing nerve fibres should therefore be distinguished from those addressing fibre endings, or nerve endings. When studying periodontal ligament innervation, both descriptions are found in the literature and they need to be understood to be correctly interpreted. Morphological characteristics, distribution of nerve structures, and neurophysiological aspects described for nerve endings can differ to a great extent from those found for nerve fibres (*Linden 1990b*).

The nerve fibres carrying information related to touch and pressure have been described in the PDL (*Jacobs and van Steenberghe 1994*). Those and other periodontal nerve fibres are discussed in the first part of this review, to give a general view about PDL innervation. In the second part, this review focused on the PDL mechanoreceptors, their morphology, neurophysiological and functional characteristics, as well as their central connections. In the third part, the importance

of PDL innervation in particular treatments is discussed, while new approaches and future challenges of PDL innervation are highlighted. Finally, in the last part of this chapter, a 3D reconstruction of PDL is shown to propose a new approach to study PDL innervation characteristics.

Literature search:

In this search, previous reviews were used as “start-point” of our search strategy. Five reviews were selected (table 2.1) to further search on the database of the search engines PUBMED and WEB OF SCIENCE.

Table2.1: Description of literature reviews used as a basis to build the search strategy

<i>Authors</i>	<i>Years</i>	<i>Title</i>
van Steenberghe D	1979	The structure and function of periodontal innervation. A review of the literature
Linden RW	1990	An update on the innervation of the periodontal ligament.
Jacobs R, van Steenberghe D	1994	Role of periodontal ligament receptors in the tactile function of teeth: a review
Trulsson M	2006	Sensory-motor function of human periodontal mechanoreceptors
Trulsson M	2007	Force encoding by human periodontal mechanoreceptors during mastication

In the PUBMED, it was searched throughout the articles indicated as related to the 5 selected reviews in this search engine. New articles published by the same authors were also considered for this selection. In addition, medical subject headings (mesh terms) were chosen from the terms classifying those reviews. On the WEB OF SCIENCE, the search proceeded amongst the articles which had cited these reviews as their references. The results from this search are summarized in table 2.2.

The next search was based on the mesh terms selected, as follows: ("axons"[MeSH Terms] OR "axons"[All Fields]) AND ("periodontal ligament"[MeSH Terms] OR "periodontal ligament"[All Fields]) – **54 articles retrieved**; (("jaw"[MeSH Terms] OR "jaw"[All Fields]) AND ("mechanoreceptors"[MeSH Terms] OR "mechanoreceptors"[All Fields])) AND ("periodontal ligament"[MeSH Terms] OR ("periodontal"[All Fields] AND "ligament"[All Fields]) OR "periodontal ligament"[All Fields]) - **233 articles retrieved**; (((("jaw/physiology"[All Fields] OR "jaw/innervation"[All Fields]) OR "mechanoreceptors/anatomy and histology"[All Fields]) OR "mechanoreceptors/innervation"[All Fields]) OR

"mechanoreceptors/physiology"[All Fields]) AND "periodontal ligament/anatomy and histology"[All Fields]) OR "periodontal ligament/innervation"[All Fields] - **60 articles retrieved.**

The selection of articles generated by the search using mesh terms was based on the publication date (last 6 years) and the main topic discussed. The articles selected concerned the PDL innervation in normal health condition as well as PDL innervation regeneration after nerve injury, tooth movement, transplantation and reimplantation. Articles comparing PDL innervation with peri-implant innervation were selected to be used in chapter 5. The articles excluded were those not written in English language, or classified as not directly related to PDL innervation after reading the abstracts.

Table 2.2: Number of articles retrieved and selected from PUBMED and WEB OF SCIENCE related to the basic reviews

<i>Authors</i>	<i>Times cited on PUBMED</i>	<i>Related reviews on PUBMED</i>	<i>Related citation on PUBMED</i>	<i>First author in PUBMED</i>	<i>Times cited on WEB OF SCIENCE</i>
van Steenberghe D	1 article (1selected)	16 articles (4selected)	105 articles (20selected)	30 articles (19selected)	36 articles (24selected)
Linden RW	1 article (1selected)	8 articles (3selected)	100 articles (83selected)	45 articles (10selected)	11articles (6selected)
Jacobs R, van Steenberghe D	no article	17 articles (6selected)	155articles (3 selected)	22 articles (14selected)	50 articles (33selected)
Trulsson M 2006	no article	39 articles (15selected)	362 articles (33selected)	54 articles (7selected)	34 articles (22selected)
Trulsson M 2007	no article	33 articles (20selected)	323 articles (10selected)	same previous	11 articles (4selected)

After using this search strategy, two collections were created. One in PUBMED and another on WEB OF SCIENCE, consisting of 258 and 105 articles, respectively. Articles from WEB OF SCIENCE were further selected on the basis of publication date (last 6 years) and the number of citations (fifteen-most cited articles). Next steps included the verification for duplicates between collections and articles classification by topics (table 2.3). Those articles already referred in the reviews were only consulted in case of any further clarification was needed.

This review aimed to revisit the main knowledge supported by the former reviews and to add the current knowledge and trends found in the literature in the last 6 years.

Table 2.3: Topics used to classify the articles selected

Topics
Morphology (M)
Neurophysiological aspects (N)
Trigeminal/central connections (TC)
Functional significance –(FS)
General (G)
Tactile sensibility (TS)
Receptors (R)
Biochemistry/molecular (B)
Spatial arrangement (SA)
Implants (I)
Teeth (T)

I - ASSESSMENT OF PDL NERVE FIBRES

I.1 Origin of the PDL innervation:

Periodontal ligament is supplied by sensory and autonomic nerves (*Schroeder Springer 1986*). The nerve fibres in the periodontal ligament are from branches of the superior or inferior alveolar nerves (*Linden 1990b*) which are composed of both fine and thick fibre bundles. Most of the nerve fibres supplying the periodontal ligament enter it in the apical region, and some course through lateral foramina in the alveolar bone (*Schroeder 1986; Hildebrand et al 1995*). In this way, the periodontal ligament can be approached from two aspects in humans as well as in other mammalian species: first, the peripheral branches arise from the dental nerve prior to its entering in the apical foramen. Second, the branches of the nerves traveling through the interdental and interradicular septa penetrate through the openings (Volkman’s canals) of the alveolar bone proper and reach the periodontal ligament at various levels laterally (*Schroeder 1986*).

The branches entering apically run through the periodontal ligament towards the gingiva, while the branches entering laterally take either a coronal or apical course. Both fibre groups join each other to form a nerve plexus on the periodontal ligament space which comprises of coarse fibre bundles running mostly parallel to the long axis of the root, and thin nerve bundles giving off terminal branches and individual fibres. Figure 2.1 shows the appearance of those fibre bundles in histological slices of human PDL in the axial plane. At the alveolar crest, fibres running along the root join both the fibres which pass through the alveolar process and those following the periosteum. This assemblage of ligament, bone, and periosteum fibres give rise to the innervation of the gingiva (*Schroeder 1986; Lewinsky and Stuart 1937*).

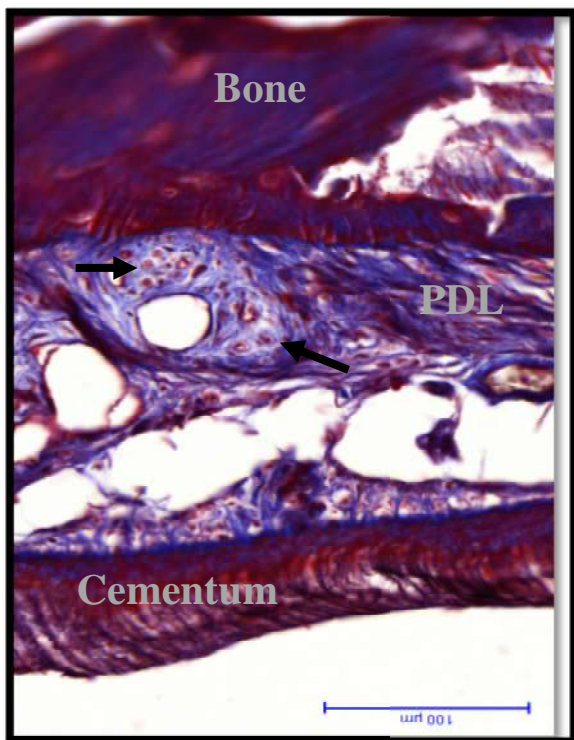


Figure 2.1: Histological slice of human PDL (thricome Masson) in the axial plane. Black arrows indicate bundles of myelinated nerve fibres parallel to the long axis of the root.

Anatomical studies show that the cell bodies of the PDL nerves have a dual origin, emanating from the trigeminal ganglion and from the trigeminal mesencephalic nucleus (*Hildebrand et al 1995; Linden 1990b; van Steenberghe 1979*). However, trigeminal and mesencephalic nerve endings are not equally distributed along the tooth root (*Linden 1990b*). Microelectrode recordings in cats, monkeys and rabbits showed that a significant proportion of all periodontal receptors have their cell bodies

in the trigeminal ganglion (*Linden 1990a*). Using anterograde transport technique, Byers and Dong (1989) reported that cat periodontal receptors with cell bodies in the trigeminal ganglion are distributed throughout the length of the root, the majority being found in the middle portion. On the other hand, cell bodies found in the mesencephalic nucleus had their nerve endings mostly confined in the lower half of the root – 50% being located below the apex. Using electrophysiological techniques, Linden and Scott (1989a) showed cell bodies in the trigeminal ganglion located in the whole area from below the fulcrum till the apex of the tooth. Contrary to the findings of Byers and Dong (1989), those from the mesencephalic nucleus were situated in a discrete area of the ligament intermediate between the fulcrum and the apex of the tooth.

This distribution pattern of cell bodies has supported the idea that PDL fibres with cell bodies in the mesencephalic nucleus participate in the mechanoreception mechanism used as a peripheral feedback to regulate oral function. Their specific location near the tooth apex and the common location with cell body from muscle spindles in the mesencephalic nucleus would corroborate for their role in muscular reflexes. In addition, the difference in the distribution of fibres with distinct cell bodies origins brought the idea that those fibres might be distributed according to the mechanical loads acting in the several regions of the PDL. The contribution of PDL nerve fibres in the muscular reflexes and the distribution of PDL mechanoreceptors will be discussed further in this review.

I.II Characteristics and distribution of nerve fibres in the PDL

Mammalian somatosensory mechanoreceptors can be classified according to their modality, conduction velocity, myelination, soma diameter and other subclasses (*see: Lumpkin and Bautista 2005*). The periodontal ligament contains both myelinated and unmyelinated nerve fibres. Most nerve fibres travel in bundles associated with blood vessels and are believed to have a vasomotor function (*Hildebrand et al 1995; van Steenberghe 1979*). The afferent sensory fibres of the periodontal ligament are between 0.5 and 1 μm in diameter when unmyelinated, and between 1 and 16 μm when myelinated (*van Steenberghe 1979*). In cats, a large

proportion of the myelinated periodontal fibres are thin myelinated fibres related to pain and temperature (A_{δ} -fibres) (Heasman and Beynon 1986). Nevertheless, these may be activated by nociception and some behave like A_{β} -fibres (touch and pressure) when recorded electrophysiologically (Hildebrand et al 1995). The A_{β} -fibres are large myelinated fibres related to mechanoreceptors of low threshold (Lumpkin and Bautista 2005). Furthermore, it is plausible that some of the unmyelinated fibres belong to the autonomic nervous system and participate in the vasomotor control (van Steenberghe 1979). It is worth to note that some variability between species occurs as has been described by Schroeder (1986).

Besides, the PDL myelinated fibres have been also described as grouped or isolated according to the proximity with other nerves and blood vessels (Long, Loescher and Robinson 1995; Loescher and Holland 1991). Fibres are classified as isolated when no more than 3 myelinated fibres were found in the surroundings, neither any blood vessels in the radius of 20 μ m. The percentage of all myelinated fibres designated as isolated in the histological studies by Loescher and Holland (1991) was 15% to 16%. According to Long, Loescher and Robinson (1995), isolated fibres found alone in the cemental half of the ligament should be considered as putative mechanoreceptors.

In the study of Loescher and Holland (1991), the location and frequency of isolated myelinated and large unmyelinated fibres were similar, and they suggested that these large unmyelinated fibres are in fact the mechanoreceptive preterminals of isolated myelinated fibres. The majority of grouped PDL nerve fibres have been observed in the alveolar portion of the ligament (Long, Loescher and Robinson 1995). Just a few myelinated fibres branching off the main bundles were observed terminating at the avascular cemental portion of the ligament (Long, Loescher and Robinson 1995).

The nerve fibres composing the periodontal ligament plexus may not be evenly distributed throughout the whole ligament space. Histological studies investigating the PDL innervation have shown that this ligament is most densely innervated at the apex of the tooth, with only a few axons extending toward the cervical margin (Maeda et al 1987; Loescher and Holland 1991 and Kubota and Osanai 1977; Byers and Holland 1977). Nevertheless, some difference according to species

exists. In man, the nerve supply seems to be more dense in the intermediate part of the ligament (*van Steenberghe 1979*). On the other hand, in moles, the apical ligament innervation was described to be much denser than that at the midroot region (*Kubota and Osanai 1977*). Since the myelinated fibres were suggested to be thicker in the apical than in the cervical tooth levels, Hildebrand et al (1995) concluded that those fibres branch and taper as they course in the PDL. Whereas thin periodontal fibres would terminate as free nerve endings, large fibres would form specialized endings of different sizes, predominantly near the apical level (*Hildebrand et al 1995*).

Like the distribution of nerve fibres along the root axis, the distribution of those fibres around the tooth root circumference was found not to be uniform. Long, Loescher and Robinson (1995) found that approximately 30% of all the grouped myelinated fibres were located in the mesial portion of the ligament, while between 30% to 50% of all isolated fibres were located in the distal portion. This figures corresponds closely to the 60% of isolated fibres recorded as being locate disto-buccally by Loescher and Holland (1991).

Regarding the distribution between alveolar and cemental portions of the PDL, most of the neural elements were found in the lateral, alveolar compartment of the ligament space in the mouse incisor (*Everts et al 1977*), while the tooth-related or cemental portion, was mostly avascular compartment, free of neural elements. This is in contrast to the report by Byers (1985) who observed neural elements of the trigeminal ganglion origin mostly in the avascular, tooth-related region in the apical third of the ligament in the rat. It is important to note that incisors in rodents are in continuously eruption, unlike in humans. Indeed, recent studies have confirmed the presence of innervation in the avascular cemental area of constinously erupting teeth (*Jayawardena et al 2002*).

Although it is believed that the discharge characteristics of an individual periodontal mechanoreceptors (terminal part of some myelinated fibres) may be governed by their location within the ligament (*Cash and Linden 1982*), much controversy is found in the distribution of nerve fibres and their endings. This may be explained by the difference among species, methods and types of teeth used in the researches.

According to Heasman and Beynon (1986), the analysis of the physiological function of peripheral nerve is assisted by ultrastructural analysis of axon size. In the human periodontal ligament, fibres of the nerve plexus were found to be, on the average, $4.5\mu\text{m}$ in diameter, with 20% of these fibres being thicker than $5.5\mu\text{m}$ (Griffin and Spain 1972). Loescher and Holand (1991) searched for the distribution of nerve fibres in the PDL in cats and its correlated functional significance. Once more, the highest density of periodontal nerve fibres was reported at the tooth apex and most were found in nerve bundles adjacent to blood vessels (figure 2.2). The diameter of both grouped ($4.72\pm 0.22\mu\text{m}$) and isolated ($4.56\pm 0.08\mu\text{m}$) myelinated fibres were similar. Similar to the studies of Griffin and Spain (1972) in humans, just 20% of the myelinated fibres in the PDL of cats had diameter greater than $6\mu\text{m}$, therefore classified as A_{β} fibres, whereas 36% of myelinated fibres in the inferior alveolar nerve have been shown to be A_{β} fibre (Loescher and Holand 1991).

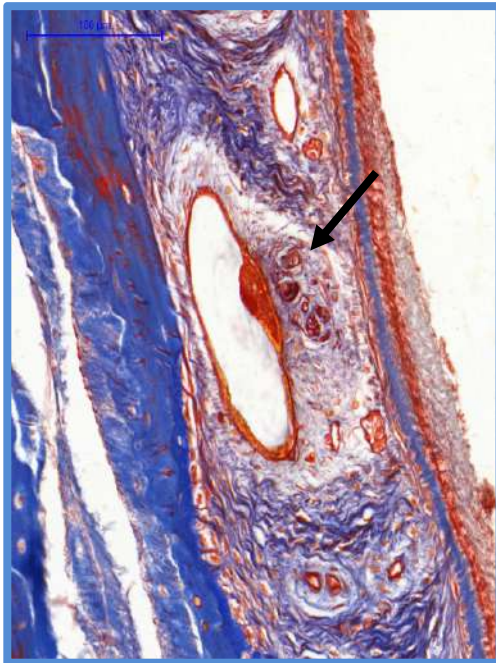


Figure 2.2: Histological slice of human PDL (thricome Masson) in the axial plane. Black arrows indicate bundles of myelinated nerve fibres near the cemental part of the PDL.

In turn, either the periodontal ligament is not innervated by the largest diameter fibres or alternatively fibres branch and narrow toward the periphery (Loescher and Holand 1991). This latter suggestion is supported by the results of electrophysiological experiments showing a reduced conduction velocity in the peripheral section of the periodontal afferent (Loescher and Robinson 1989a; Linden and Scott 1989). However, further studies should confirm if those larger diameter IAN fibres can have another functional significance apart from periodontal ligament

innervation. Moreover, myelinated fibre diameters of the inferior alveolar nerves may vary among different animals, as shown by Heasman and Beynon (1986) and by Heasman (1984) (table 2.4).

As seen in table 2.4, the fibre diameter distribution curves of human inferior alveolar nerves have peaks of density in two diameter ranges (bimodal distribution), corresponding to the A δ (pain and temperature) and A β (touch and pressure) ranges. This bimodality characteristic in humans appeared to be independent of the age and the number of teeth present (*Heasman and Beynon 1986*). Rood (1978) has reported a similar bimodal curve, peaks and diameter range, although they suggested that mandibular tooth loss would cause atrophy of some small diameter fibres. However, this hypothesis was refuted later by Heasman (1984) since two of their edentulous subjects had a unimodal curve with peak in the 3-4 μ m range, suggesting that, if any fibres had undergone atrophy following tooth loss, they would have been from the large diameter types (*Heasman 1984*). Furthermore, a trimodal curve has been reported in an edentulous subject (*Heasman and Beynon 1986*).

Table 2.4: Findings reported in Heasman and Beynon (1986)

Species	Diameter distribution	Peaks (μ m)	Diameter range (μ m)
Man	Bimodal	2-4 8-9	2-15
Cat	Bimodal	2-4 8-14	1-22
Dog	Unimodal	9-10	-
Sheep	Unimodal	-	-
rabbits	Unimodal	-	-

Besides the myelinated nerve fibres, Heasman and Beynon (1986) stated that the unmyelinated C-fibres are important in propagating both autonomic and pain impulses from periodontal membranes. Measurements of these unmyelinated fibres, which account for over 50 per cent of the total fibres in the inferior alveolar nerve of the cat, would be necessary to complete a functional analysis of this nerve in human (*Heasman and Beynon 1986*). The small unmyelinated axons in the periodontal ligament can be either sympathetic efferents or nociceptor afferent axons (*Loescher and Holland 1991; Linden 1990 a*). It has been reported that the sympathetic efferents have a direct effect on periodontal blood vessels (*Loescher and Holland 1991*). Indeed,

97% of the single, small unmyelinated axons have been observed close to neurovascular bundles, consistent with a vasomotor role (*Loescher and Holland 1991*).

Jyvasjarvi et al (1988) have identified a number of functional single C-fibres originating from the periodontal ligament. Their conduction velocities ranged between 0.3-2.5m/s (mean 1.2 ± 0.6 m/s). Some authors (Mengel et al 1992; Jyvasjarvi et al 1988) suggested that the periodontal receptors supplied by C-fibres show a polymodal response behaviour. Indeed, C-fibres responded not only to thermal and chemical stimuli applied to the periodontal space, but also to forces of high intensity manually applied to the tooth crown from different directions (Mengel et al 1992). None of the C-fibres could be excited by forces known to stimulate periodontal mechanoreceptors associated with large diameter myelinated fibres. Mei et al (1977), as cited by Linden (1990b) has reported on A δ fibres showing similar properties to those described by Jyvasjarvi et al (1988) for C-fibres. Interestingly, Sessle (2006) reports that C-fibres appear to play an important role in shaping the adult mechanoreceptive field properties of the low-threshold mechanoreceptors neurones receiving large diameter mechanosensitive afferent inputs.

Although their structure show species variations, PDL nerve fibres have their terminal portion usually like free neural endings or organized receptors described as resembling Ruffini endings. Intermediate forms also occur between Ruffini-like endings and free endings (*Lambrichts et al 1992*). According to Hildebrand et al (1995), the combined morphological and electrophysiological data indicated that large Ruffini-type terminals, as well as free endings, function as intermediate, rapidly-adapting mechanoreceptors (*Hildebrand et al 1995*). However, later studies have demonstrated that most of Ruffini-like endings in the periodontal ligament are actually slowly adapting and low threshold receptors (*Trulsson 2007 and 2006*). These adaptation properties will be discussed later in this chapter.

As for the distribution of the free and organized endings, the latter are more frequently found in the apical region (*van Steenberghe 1979*), whereas the former can be evenly distributed throughout the PDL. However, contradictory observations have also been obtained by histological and electrophysiological studies. Periodontal mechanoreceptors with their cell bodies in the mesencephalic nucleus have been observed, histologically, to be located primarily on the distal side (*Byers et al 1986*),

although electrophysiological recordings have revealed the majority of the receptors to be located on the labial to mesial surface (*Linden and Scott 1988,1989*). This pattern appears to differ according to species and raises the question of its functional significance. This does not mean that some of these fibres cannot be related to other functions, such as temperature sensibility and nociception, as already reported in this chapter. However, the respective roles of different receptors from various parts of the periodontium cannot be deduced from histological studies alone (*van Steenberghe 1979*).

In view of the complex orientation of the collagen fibres in the ligament and the presence of receptors which are bidirectionally sensitive, it is unlikely that the relationship is that simple. If the distribution of mechanoreceptors in a tooth is functionally relevant, the distribution pattern of the receptors might also be expected to vary between teeth within the same animal and species. In man, Maeda et al (1990) observed free nerve endings throughout the ligament, while specialized nerve endings appeared located in specific regions within the ligament: Ruffini-endings being present near the root apex and other specialized endings in the mid-region.

Considering the morphological analogies between structures which have been described, it can be postulated that these neural endings or part of them, are mechanoreceptors, i.e. are sensitive to mechanical stimuli applied to the teeth (*van Steenberghe 1979*). Long, Loescher and Robinson (1995) observed that the distal portion of the periodontal ligament of mandibular canine tooth in cats, is normally under compression. Unlike the study of Cash and Linden (1982) suggesting that the PDL mechanoreceptors in cats respond to tension forces. Nevertheless, some receptors were found to be bidirectionally sensitive, and therefore must also respond to compression (*Hildebrand et al 1995*).

Loescher and Holland (1991) concluded the controversy over the probable morphology of the periodontal mechanoreceptors. According to the authors, some confusion concerning the receptor morphology may have arisen from the difficulty in predicting a three-dimensional structure from a single section. Moreover, there was also a wide variation in what is recognized as a Ruffini ending. Halata et al (1985: as cited by Loescher and Holland 1991) described three variants in the human knee joint capsule and Polacek (1966: as cited by Biemesderfer et al 1978) has suggested that

Ruffini ending is not a uniform group but a range that constitutes the link between simple free endings and encapsulate endings.

II - ASSESSMENT OF PDL NERVE ENDINGS

II.I Morphology of PDL mechanoreceptors:

There has been a long debate about the morphology of the PDL mechanoreceptors (*Linden 1990b*). The current view states that all PDL mechanoreceptors in man are unencapsulated Ruffini-like endings. On the other hand, a large variety of morphologies have been described in other animals (*Trulsson 2006; Maeda et al 1999*). In 1985 and 1986, Byers and collaborators (*Byers 1985; Byers et al 1986*) have described encapsulated Ruffini-like endings in the rat molar and unencapsulated in the cat periodontal ligament.

Considering the relation with physiological properties, those mechanoreceptors have shown both rapidly and slowly adapting properties and some association with their position along the root has been mentioned. Considering the species divergences, those mechanoreceptors in man are considered all slowly adapting low-threshold stretching receptors (*Trulsson 2006; Maeda et al 1999*). Studies in rat and cat reported on slowly and rapidly adapting, as well as low and high threshold mechanoreceptors (*Linden 1990a*). However, those studies affirmed that only one morphology was found for the organized mechanoreceptors, the Ruffini-like receptors. The different physiological properties were related to the position of the mechanoreceptors along the root. In other words, mechanoreceptors located in root apex are exposed to higher loads than in the mid-root during application of same force in the tooth crown. Therefore, the mechanoreceptors located at root apex would present low-threshold and slowly adapting properties unlike the ones found in the mid-root. At this position, the mechanoreceptors presented rapidly adapting properties and a high-threshold to perceive loads applied to the tooth crown.

"There is only one type of mechanoreceptor situated within the periodontal ligament."

Millar, Halata and Linden 1989

According to Trulsson and Johansson (1996), the apparent difference in adaptation properties observed in experiments on man and animals may be explained by methodological factors. Periodontal afferents are very sensitive to the direction of the tooth loading (*Loescher and Robinson 1989; Trulsson et al 1992*). As such, a three-dimensional stimulation procedure is crucial to elucidate the slowly adapting response properties of periodontal afferents. During non-optimal stimulation conditions, a “slowly adapting” periodontal afferent can easily be mistaken as “rapidly adapting” (*Trulsson and Johansson 1996*). The fact that discharge from periodontal mechanoreceptors can be modulated by sympathetic activity complicates the picture (*Hildebrand et al 1995; Cash and Linden 1982b*).

In mature rodent incisors, periodontal Ruffini-like endings, like other mechanoreceptors, e.g. Meissner and Pacini corpuscles, are invested by Schwann cell processes with multilayered basal laminae and high levels of non-specific cholinesterase (*Hildebrand et al 1995*). Since those teeth in rodents are continuously erupting, the PDL is continuously remodeling. How the local axons and terminals behave during the continual periodontal remodeling is unknown (*Jayawardena and Takano 2006*). It is known that resection of inferior alveolar nerve in rats resulted in a greater eruption rate of the incisor.

In this way, the adult rat incisor eruption is subjected to neural influences. However, selective sympathetic denervation caused no effect, suggesting that the increased eruption rate is due to loss of sensory fibres (*Boggio et al 2004*).

“Morphologically, Ruffini endings are characterized by extensive ramifications of expanded axonal terminals and an association with specialized Schwann cells, called lamellar or terminal Schwann cells, which are categorized, based on their histochemical properties, as non-myelin-forming Schwann cells.”

Wakisaka et al 2000

Maeda et al (1999) made a comprehensive report on the morphology, cytochemical features, regeneration and development of Ruffini endings in the PDL. They reported those mechanoreceptors as the primary mechanoreceptor in the PDL, an overview about the main results reported by Maeda and collaborators in other studies is presented in table 2.5. Maeda et al (1999) described the PDL Ruffini endings as displaying dendritic ramifications with expanded terminal buttons and,

furthermore, they are ultrastructurally characterized by expanded axon terminals filled with many mitochondria and by an association with terminal or lamellar Schwann cells. The axon terminals of the periodontal Ruffini endings have finger-like projections called axonal spines or microspikes, which extend into the surrounding tissue to detect the deformation of collagen fibres. The functional basis of the periodontal Ruffini endings is further described by histochemical analysis. Their main conclusions can be summarized in four points (*Maeda et al 1999*):

1. Ruffini endings have a high potential to neuroplasticity showed by the up regulation of some neuroproteins related to regeneration and the development process even in adult animals.
2. Degeneration of Ruffini endings takes place immediately after nerve injury, with the distribution and normal morphology returning to almost normal after some days.
3. Regenerating Ruffini endings express neuropeptide Y, which is rarely observed in animals.
4. Ruffini-endings show stage-specific configurations. Mechanical stimuli due to tooth eruption and occlusion are prerequisite for the differentiation and maturation of the PDL Ruffini endings.

The morphology of the large unmyelinated “receptors” and their Schwann cells described in the study on Loescher and Holland (1991) was similar to that reported for receptors in the periodontal ligament of rat (*Byers 1985*) and cats (*Millar et al 1989*) and to lanceolate receptors found in the sinus hair of monkeys (*Halata and Munger 1980*). The finger like-projections that were seen extending into the collagen matrix may be responsible for detecting the displacement of collagen fibres and hence the tooth (*Takahashi-Iwanaga 2001; Kannari 1990*).

The Schwann cells surrounding the “receptors” were characterized by numerous pinocytotic vesicles which have been shown to contain cholinesterase activity (*Maeda et al 1999*). Similar vesicles (or caveolae) have been described on the lamellae of Meissners and Pacinian corpuscles and in the Schwann cells lanceolate hair receptors (*Halata and Munger 1980*). Loescher and Holland (1991) found no true lamellated endings although a few axons were invested by multiple cell layers. Other studies have described lamellated endings in the periodontal ligament of the cat,

carmen crocodylia, rat, and ferret (*studies are cited in Loescher and Holland 1991*). This may reflect either a difference in the interpretation of the morphological appearance or variability between species.

A few of the large unmyelinated axons were found encapsulated. The isolated myelinated preterminal axons usually had a well-defined perineural sheath surrounding them that appeared to end with the myelin (*Maeda et al 1999*). The capsule seen around the large unmyelinated axons may be an extension of this perineural sheath and is unlikely to have covered the entire receptor. Within the different species, Ruffini endings have been described with and without capsule (*Maeda et al 1999*). The entire range could be present in the periodontal ligament, but only a more extensive and three-dimensional examination would clarify this point.

“Proper mechanical stimulation to the ligament contributes to the morphological maturation of the periodontal Ruffini endings.”

Shi et al 2005

Finally, a previous study has confirmed that periodontal Ruffini endings show stage-specific morphological features intimately related to the timing of tooth eruption and occlusion (*Nakakura-Ohshima et al 1995*). Similarly, studies confirmed that neurons develop with the eruption of teeth (*Umemura et al 2010*) and that the response properties of rat's PDL mechanoreceptors matured when functional molar occlusion and transition of dietary contents from liquid to hard-diet were achieved (*Nasution et al 2002*). Moreover, Muramoto et al (2000) reported that the loss of occlusal stimuli, after extracting opposing teeth, influenced the distribution and structure of the periodontal mechanoreceptors of the rat mandibular molar.

II.II Neurophysiological aspects of PDL mechanoreceptors:

Mechanoreception function of PDL nerve fibres can be investigated by collecting data on their adaptation properties, directional sensitivity and discriminatory ability (*van Steenberghe 1979*).

Three types of adaptation properties of PDL mechanoreceptors have been historically described, e.g. slow-adapting, rapid-adapting and spontaneous firing ones (*van Steenberghe 1979*).

Table 2.5: Overview main findings reported by Maeda and collaborators, Sato and collaborators and Kannari using immunohistochemistry. NFP = Neurofilament protein; S-100= glia-specific S-100 protein; IR=immunoreactive neural elements; N=number of fibres; tSC=terminal Schwann cells.

Authors/year	Sample	Methodology	Results	Observations	Receptors Features
Maeda et al 1987	Rat molars	NFP sections in three different planes	IR clearly visualized in the 3D analysis	Densely distributed in lower half of the alveolar socket	<ul style="list-style-type: none"> ✓ Free nerve ending with a tree like ramifications tapered around periodontal fibres some reaching the cementoblastic layer; ✓ Expanded nerve terminals showing button or glove-like shape - frequently in groups within the lower third of the alveolar socket
Maeda 1987	Monkey(Macaca fuscata) incisive /molar	NFP S-100	IR NFP and IR S100: distribution molars ≈ incisors. apical region in molars: IR NFP (N) < IR S-100 (N)	Thick immunoreactive bundles entered the periodontal ligament from through slits at the bottom of the alveolar socket; thinner bundles penetrated the ligament from the lateral walls. Densely found around root apex . In upper incisors also densely found in the coronal half of labial side	<ul style="list-style-type: none"> ✓ Incisors-ramified in dendritic fashion-free endings ✓ Molar-free endings and coiled nerve endings
Sato et al 1988	Rat incisors	NFP S-100	densely innervated IR NFP	≠ Molars. Restricted to the alveolar half every region. IR S-100 (N) ≈ (N) IR NFP	<ul style="list-style-type: none"> ✓ Thick nerve bundles entered the lingual periodontal ligament in the mid-region of the alveolar socket, and immediately formed numerous Ruffini-like corpuscles. ✓ In the labial periodontal ligament, terminated in free endings.
Maeda et al 1989	Rat incisors	S-100 and electron microscopy.	electron microscopy: Ruffini endings displayed expanded axoplasmic spines filled with a large number of mitochondria and neurofilaments	Numerous Ruffini endings distributed in the alveolus-related part of the lingual periodontal ligament	<ul style="list-style-type: none"> ✓ Some of the spines directly contacted the surrounding collagen fibres via finger like projections. The axoplasmic spines and Schwann sheath covered by single or multiple layers of the basal lamina. Rounded cells in the vicinity Ruffini-endings-IR S-100- kidney-shaped nucleus and enveloped the axoplasmic spines with their cytoplasmic processes.

Authors/year	Sample	Methodology	Results	Observations	Receptors Features
Sato et al 1989	Five Rodents upper incisors-Guinea pig			Lingual PDL: IR NFP Ruffini-like corpuscles (middle region)	✓ IR S-100 distributed in the periodontal ligament and dental pulp of all the rodent species examined, showing a distribution pattern similar to the IR NFP.
	Hamster, Mongolian gerbil (Meriones unguicularis) Mouse Squirrel (Tamias sibiricus)	NFP S-100	fundamentally identical to that in the rat	Labial periodontal ligament: < IR NFP (N)-terminating among collagen fibres as free endings.	
Maeda et al 1990b	Rat incisors	nonspecific cholinesterase activity light and electron microscopic levels (terminal Schwann cells)	Terminal Schwann cells positive for nonspecific cholinesterase Ordinary Schwann cells associated with more proximal nerve fibres reacted negatively	Schwann cells-well-developed Golgi apparatus and rough endoplasmic reticulum	---
Maeda et al 1990a	HUMANS	NFP S-100	free and specialized nerve endings (immunoreactive NFO and S100)	No lamellated nerve terminals were found in the human periodontal ligament	<ul style="list-style-type: none"> ✓ Free endings-tree like ramification/all tooth length ✓ Specialized nerve endings-ruffini endings (expanded nerve endings in a dendritic fashion around the root apex/coiled endings-located at the mid-region/spindle-shaped/expanded nerve endings-both rarely found around tooth apex)
Kannari 1990	Hamster incisors	immunohistochemistry for nervous-specific proteins and electron microscopy	electron microscopy: the Ruffini endings displayed expanded axon terminals filled with large-sized mitochondria	3D reconstructions of the Ruffini endings at the electron microscopic level revealed complicated shapes for the axon terminals and a characteristic relation with tSC	<ul style="list-style-type: none"> ✓ lingual PDL- exclusively innervated by Ruffini endings - alveolar half intertwined with transverse collagen fibres ✓ labial periodontal ligament lacked them

Rapidly adapting mechanoreceptors fire only a few nerve impulses when a stimulus is applied or withdrawn, while slowly adapting one fires throughout the stimulus application, but generally with a decreasing frequency. The very slowly adapting mechanoreceptors fire throughout the stimulus application, even if it is maintained for hours (*van Steenberghe 1979*).

“Like the slow-adapting type II (SAII) mechanoreceptors in the skin, most human periodontal mechanoreceptors (about 70%) are active spontaneously and discharge regularly in response to forces applied to the teeth.”

Trulsson 2006

Rapidly adapting mechanoreceptors have a higher threshold level than slowly adapting ones (*van Steenberghe 1979; Linden 1990b*). This has been shown in cats, dogs and men (*Linden 1990b*) and could result from a more remote localization of the rapidly adapting mechanoreceptors in the periodontal ligament (*van Steenberghe 1979*). Indeed, Linden (1990a) has reported that this difference in adapting properties might be related to the relation with adjacent structures and position of mechanoreceptor in the ligament, rather than represent different morphological types of receptors. In turn, PDL nerve fibre distribution and spatial arrangement might influence PDL mechanoreceptor characteristics. The receptors with higher threshold were located near the fulcrum portion of the tooth and those with low threshold near the apex (*Cash and Linden 1982b*). This relation between the position of a mechanoreceptor in the ligament and its response characteristics was explained by the larger displacements at apical levels compared to the fulcrum level. In general, a few receptors have been observed above the fulcrum (*Hildebrand et al 1995, Loescher and Robinson 1989a; Linden 1990a*).

The spontaneously firing ones are actually considered a variant of slowly adapting receptors (*van Steenberghe 1979*). These are units which fire action potentials even when the tooth is not being moved. It was proved that this is not injury discharge since the recordings last for hours. Actually, Linden (1990a) reported that the cause of this spontaneous activity was unknown, and no clarification has been found in the recent literature.

Hannam, in 1982, suggested that the spontaneous activity may be a species difference in that it appeared to be more common in studies in rabbits and dogs than in cats. In those last animals, spontaneous activity has been recorded in the

trigeminal ganglion and the mesencephalic nucleus only after cutting the cervical sympathetic trunk. Later, this spontaneous activity was abolished by cervical sympathetic nerve stimulations (*Linden 1990b*). Therefore, spontaneous activity was in part attributed to cutting of the sympathetic nerve supply to the teeth and supporting structures during the peripheral nerve studies in cats. Another suggestion was that the spontaneous activity was due to a constant stretch imposed by the enviroing tissues on the receptor (*van Steenberghe 1979*).

Those neurophysiological findings were hyphothetically correlated to histological findings (*van Steenberghe 1979*). Conduction velocities have been reported in the range of respectively between 24-60 m/second (slowly adapting) and 28-83m/second (rapidly adapting). and corresponded to the fibre diameters found in histological studies (*van Steenberghe 1979*). Linden, in 1990b, reported that the PDL mechanoreceptors have a conduction velocity range from 26-87m/second, placing them within the A-beta group of fibres. Hildebrand et al (1995) reported that the cat periodontal axons have conduction velocities of 25-85m/sec, with a mean of 55m/sec.

It was suggested that the slowly adapting mechanoreceptors would correspond to organized nerve endings, while free nerve endings would be rapidly adapting ones. Yet, the exact periodontal structures within which these receptors were located has not been elucidated till the early 80's (*van Steenberghe 1979*). Hannam in his review in 1982 pointed out that there was no direct evidence about receptor morphology, either for the slowly adapting or the rapidly adapting mechanoreceptors (*Linden 1990a*). He suggested that a better clue to the morphological and functional correlations could be provided by developing a complete picture of the receptor behaviour using features such as their response to sustained and dynamic stimuli, directional sensitivities, tonic or resting discharge and neuronal conduction velocities. Later, several studies affirmed that all human periodontal afferents are in fact slowly adapting receptors (*Trulsson 2006; Lobbezoo et al 2002; Maeda et al 1999; Trulsson and Johansson 1996*).

Hannam (1982) compared the response of the slowly adapting receptor to that of the type II skin receptor (Ruffini terminal) and the rapidly adapting units to Meissner corpuscles and other corpuscular lamellated receptors described previously

in the PDL of the cat and caiman. Until the exact site of the receptor was known the idea that the two groups of physiological characteristics represented two morphologically distinct groups of receptors was pure speculation. This speculation was confused still further by the descriptions of putative end-organs in the periodontal ligament as well as the possibility of species differences. According to Hannam (1982), differences in technique and standards of preparation, as well as the natural enthusiasm for describing detail, undoubtedly contributed to this impressive array of descriptive terms, making comparison ever difficult (*van Steenberghe 1979*).

If the tooth is considered to rotate about a fulcrum when force is applied to its crown, then varying degrees of displacement of the tooth root relative to the surrounding alveolar bone will occur. This graded displacement is greatest at the apex and reduces towards the fulcrum for any given force. The receptors at the apex would receive the greatest displacement and consequently the greatest stimulus. Hence, they would appear to have a lower force threshold and would adapt slowly if at all (*Linden 1990a*). The receptors near the fulcrum would receive less stimulus, that is less displacement, for the same applied force. This could explain why they have the higher threshold and adapt rapidly. It has been shown that slowly adapting receptors behave more like rapidly adapting receptors if a reduced force is applied to the tooth. This would be consistent with the displacement hypothesis. From their studies, Linden and co-workers concluded that the response characteristics of a receptor depend on the position of the receptor and on the rate and magnitude of forces applied to the tooth crown.

Studying receptors located in the labial region in cats, Cash and Linden (1982b) reported that all receptors responded maximally when the crown of the tooth was pushed so as to stretch the labial side of the ligament. From this came the conclusion that PDL mechanoreceptors respond maximally when that part of the ligament in which they lie is put under tension. In this same study, the receptors were all located between the fulcrum and the apex of the tooth. The slowly adapting receptors appeared to be situated in the apical third of the ligament, and the rapidly adapting receptors situated below the fulcrum of the tooth but closer to the fulcrum than to the apex. It was suggested that there may be only one type of PDL mechanoreceptor and that the rate of adaptation of a particular receptor might be dependent on its location within the ligament.

It appears that between 0.01N and 0.02N (approx.1-2g) is sufficient to evoke a response from the majority of slowly adapting neurons (*Linden 1990b*). According to Linden (1990b), Pfaffman in the cat, Hannam in the dog and Fujita in man noted that the more rapidly adapting neurons tended to have higher thresholds than did the slowly adapting neurons (*Linden 1990b*). The threshold of the more rapidly adapting neurons were reported to be in terms of tens of grams instead of a few grams. It was suggested that this could be due to both a morphological and a functional difference between the two types of endings, but equally it could be due to differences in the receptor sites (*Linden 1990b*).

There is a general agreement in attributing directional sensitivity to periodontal neural receptors. To explain the concept of directional sensitivity, the response to a given mechanical stimulus is maximal in a particular direction and it falls progressively to zero as the force moves away from this optimal direction. Besides, it has been suggested that the rate of force application also influences the discharge frequency of slowly and rapidly adapting units in the periodontal ligament. Increasing the rate of force application shortens the latency time of the first action potential.

In experimental animals, most nerve fibres involved in PDL mechanoreception had their receptive field in one tooth. A few fibres responded to stimulation of two or three teeth (*Trulsson 1993*). In humans, on the other hand, a high proportion of individual fibre giving rise to the PDL mechanoreceptors responded to stimuli applied to more than one tooth. This occurred more often in adjacent teeth; and up to three-five adjacent teeth could provoke action potentials in isolated fibres of the inferior alveolar nerve. They are considered as multiple-tooth receptive fields (*van Steenberghe 1979*). This seems to be due to mechanical interactions between adjacent teeth rather than to fibre branching (*Hildebrand et al 1995*). It should be noted that a force of less than 0.5Newton applied to a tooth causes a deformation of the alveolar bone, which means that even lower forces could stimulate receptors of neighbouring teeth through the transseptal fibre plexus, tooth contact or liquid movement, according to van Steenberghe (1979).

In the view of the directional sensitivity of the mechanoreceptors and the multiple-tooth character of the receptive field in humans, the periodontal message reaching the CNS during mastication must be highly complex (*Hildebrand et al 1995*).

Studies on human mandibular teeth show that even though individual periodontal mechanoreceptive afferents do not provide exact information regarding the direction of a force applied to a tooth, populations of such afferents are well suited to give detailed directional information (*Trulsson et al 1992*).

According to the current knowledge, the majority of the periodontal mechanoreceptive units in man adapt slowly with low force thresholds (*Trulsson et al 1992*). This is in agreement with other studies in animals (*Tabata and Karita 1986; Loescher and Robinson 1989*). Periodontal mechanoreceptors of posterior teeth also exhibit directional sensitivity which implies that they respond maximally to forces applied in a particular direction. Furthermore, rate and magnitude of the force applied to a tooth may modify the response characteristics of the mechanoreceptors. These characteristics can be explained on the basis of an intimate relationship between neural endings and the envioning collagen fibre bundle network (*Jacobs and van Steenberghe 1994*).

According to microneurographic experiments in humans, most periodontal mechanoreceptors (about 70%) are active spontaneously and discharge regularly during sustained tooth loads (*Trulsson 2007; Trulsson 2006*) like the mechanoreceptors in the skin, the slow-adapting type II (SA II). Due to this electrophysiological behaviour, those receptors have been classified as slowly adapting receptors. About half of those receptors responded to forces applied to more than one tooth and their receptive fields were broadly tuned to the direction of force application. However, their highest response rate occurred when stimulating one particular tooth, named the receptor-bearing tooth by Trulsson (2007) .

From observation in humans, this author concluded that the receptor-bearing tooth is most often an incisor or a canine, indicating a decreasing in number of receptors in the periodontal ligaments distally along the dental arch. Byers and Dong (1989) have previously described this characteristic in periodontal receptors of monkey, cat and rat by means of histological techniques. This fact suggested a well-developed mechanoreceptive innervation of the anterior part of the mouth.

Moreover, the periodontal receptors supplying the anterior and posterior teeth differed in their capacity to signal the horizontal and vertical forces, respectively (*Trulsson 2007*). There is a shift from a high sensitivity to most directions at the

anterior teeth to the distal-lingual direction at the molars meeting the functional demands of anterior versus posterior teeth. In other words, the periodontal receptors supplying the lower molar teeth were well suited to encode information about the forces that normally imposed to the molars during mastication. Considering the relation between discharge curve and force amplitude, normally those receptors showed the highest sensitivity to changes in force at forces below 1N in the anterior teeth and 4N for posterior teeth (*Trulsson 2007*). They were classified as saturating receptors and represented the large majority of periodontal receptors (80-85%). Saturating receptors become progressively less sensitive to both the magnitude and rate of rapid changes in force, as contact force grows in amplitude (*Trulsson 2006*).

Trulsson (2007) reported that most receptors efficiently encode food contact during chewing, but due to saturation at higher forces, these receptors poorly encode the magnitude of strong chewing forces and force changes. In contrast, the non-saturating receptors, which exhibited a nearly linear relationship between discharge rate and force amplitude, represented the minority among receptors found and had the capacity to encode force and force changes at quite high forces levels (*Trulsson 2007*).

II.III Connections to Central Nervous System:

Anatomical studies in animals have shown that the periodontal ligament is richly innervated by mechanoreceptors whose cell bodies are located either in the trigeminal ganglion (TG) or in the mesencephalic (MS) trigeminal nucleus (*Trulsson 2006; Linden 1990a*). Both were suggested to be sensitive to stretch of the ligament induced by tooth movement (*Linden and Scott 1989a*), but their thresholds, central connections, and functional significance differ (*Byers and Dong 1989*).

The primary afferent neurons in the trigeminal ganglion are pseudounipolar. Their central processes pass to the main sensory trigeminal nucleus (MSTN) while others pass to the spinal tract of the trigeminal nucleus (STTN). The trigeminal ganglion contains the cell bodies of a representative sample of all periodontal mechanoreceptors ranging from the most slowly adapting to the most rapidly adapting receptors. The mesencephalic nucleus contains the only known group of primary afferent neurons with their cell bodies located within the CNS. Those

receptors respond to forces applied to tooth alone, nose, hard palate (type P) and to opening of the mouth (muscle spindles) (*Linden 1990b and van Steenberghe 1979*). No very slowly adapting mechanoreceptors were observed with cell bodies located at MS (*Linden and Scott 1989a*).

The functional significance, if any, of the two distinct cell body populations of PDL receptors is unknown (*Linden 1990b*). The different sites and intensity of the stretch forces occurring during the use of different types of teeth may determine the variations in the size and location of the TG mechanoreceptors. The different distribution of MS receptors may contribute to their response thresholds and static properties, which differ from those of TG receptors (*Byers and Dong 1989; Trulsson 2006; Linden 1990b*).

In the trigeminal ganglion, mechanoreceptors were reported to be distributed over a much wider area of the periodontal ligament between the fulcrum and the apex than those in the mesencephalic nucleus (*Linden and Scott 1989a*). The MS mechanoreceptors were located in a discrete area of the periodontal ligament between the fulcrum and the apex of the tooth. None was found in the apical part of the ligament. When recording in the mesencephalic nucleus the direction of maximum sensitivity of the mechanoreceptors were unilaterally distributed around the tooth root. The majority of neurones (over 70%) responded maximally when the area extending from labial to mesial was under tension strains (*Linden and Scott 1989a*) suggesting that most of those receptors were located at this region. On the other hand, no predominant directional sensitivity was observed in the trigeminal ganglion. This suggested that the mechanoreceptors with cell bodies in the trigeminal ganglion are distributed in the periodontal ligament much more evenly around the tooth root in the periodontal ligament.

In studies from 1988 and 1989, Linden and co-workers have shown that populations of PDL mechanoreceptor neurons represented in the mesencephalic nucleus do not all degenerate following tooth extraction. But since the majority of those present do not appear to reinnervate new tissues in which they can be mechanically stimulated, it was suggested that it was unlikely that they had any functional role following tooth loss (*Linden 1990a*).

Neurons of the MS and TG innervating the periodontium of incisor, canine and molar teeth in monkeys and baboons were counted and mapped using the horseradish peroxidase (Hrp), retrograde axonal transport method (*Hassanali 1997*). Periodontal afferent neurons of all of these teeth were well represented in the MS, although the incisors had a significantly higher number of labelled neurons than the canines or molars. The periodontal MS neurons may be favourably located to make collateral connections with the trigeminal motor nucleus for jaw reflexes. Incisors and canines had a large and predominantly ipsilateral representation in the TG. In contrast, molar representation in the ganglion was sparse and all labelled neurons supplied ipsilateral teeth. The maxillary and mandibular teeth had a somatotopic distribution within the respective maxillary (middle) and mandibular (posterolateral) compartments of the TG. It is suggested that the anterior teeth with greater connections to the MS and TG may impart greater sensory perception and be involved in jaw reflexes to ensure a good occlusal relation during mastication, while the afferent connections of the molars may initiate complex jaw reflexes during the occlusal phase of mastication (*Hassanali 1997*).

In the mesencephalic trigeminal nucleus of rabbits, Passatore et al (1983) found two types of units, namely primary afferents supplying jaw raising muscle spindles and periodontal or gingival mechanoreceptors (*Trulsson 2006*). These two groups of neurons exhibited a rostrocaudal somatotopy. Similar to the study of Hassanali (1997), the incisors were also the most widely represented, followed by interalveolar gingiva and molars; the axonal conduction velocity ranged between 9 and 40 m/sec and between 8 and 16 m/sec for ipsilaterally and contra laterally projecting neurons, respectively.

The motor responses obtained by electrical stimulation of discrete areas of the MS confirmed the presence of a high degree of segregation between the two different populations of neurons. In fact, jaw raising movements were obtained when stimulating the area containing the somata of spindle afferent neurons, while only jaw opening movements were elicited by stimulation of the caudal levels of the nucleus, where the somata of periodontal and gingival afferent neurons were located. These data also show that the periodontal neurons whose somata are located in the MS participate in the jaw opening reflex, just as the more numerous periodontal

mechanoreceptors whose somata are located in the TG. Soma-somatic and soma-axon hillock gap junctions were found among the neurons of the MS, particularly in the caudal third of the nucleus (*Passatore et al 1983; Trulsson 2006*).

II. IV Functional significance of nerve fibres and endings in the PDL:

The main functional significance of PDL mechanoreceptors is found in the masticatory function. The neurophysiological aspects of posterior and anterior teeth together with the presence of two connections to the CNS uncover the role of those receptors in the modulation of the trigeminal sensory input during mastication. Masticatory function is performed by jaw muscles that can generate large forces across very short distances and apply them via rigid teeth (*Türker et al 2007*). To avoid any damage to teeth and surroundings tissues, masticatory forces need to be controlled precisely by peripheral feedback and these forces must change from bite-to-bite depending on the properties of the bolus. The physiological significance of PDL nerve fibres in this context have been reviewed by *Türker et al (2007)*, *Trulsson (2007)*, *Sessle (2006)*, *Lund and Kolta (2006)*, *Lobbezoo et al (2006)* and *Türker (2002)*. In general, those fibres play a role during oral somatosensory and motor function. A comprehensive report on this role and its functional consequences is found in the mentioned reviews.

"Mastication is a repetitive feeding behaviour typical of mammals. It is produced by a brainstem central pattern generator that is subject to conscious control and to sensory feedback."

Lund and Kolta 2006

Lund and Kolta (2006) reviewed two fundamental features of mastication: its centrally generated core motor program and the sensory feedback, which is responsible for adapting the program to food properties. As described by the authors, mastication requires the coordinated action of the muscles of the jaws, tongue, lips, and cheeks. This coordinated action results from the interaction of an intrinsic rhythmical neural pattern and sensory feedback generated by the interaction of the effector system (muscles, bones, joints, teeth, soft tissues) with food.

Just as individual muscles are represented at specific locations within the motor cortex, so are the various patterns of mastication. The movements elicited by

stimulation of anterior and posterior sites are clearly distinct, and movements evoked from left and right cortices are mirror images of one another. The activity of most neurons in the masticatory cortex is higher during ingestion than during mastication, suggesting that it plays a major role in setting parameters of the first bite. It may also contribute to the continuous modulation of the masticatory pattern, through its extensive projections to all of the cell groups in the brainstem that are thought to compose the central pattern generator (CPG) (Lund and Kolta 2006). This 'masticatory area' (CPG) partly overlaps the representation of individual jaw, tongue and facial muscles. To produce mastication, this region of the cortex has to be stimulated by a long-lasting, medium frequency trains of shocks (approximately 10-100Hz) (Sessle 2006). Inputs from sensory receptors in the mouth and muscle spindles can also activate the CPG. The frequency of mastication does depend on the average stimulus frequency and voltage. In addition, many interneurons have axons that cross the midline and these are probably responsible for the coordination between the two halves of the CPG.

When food is taken into the mouth, it will be split into smaller pieces by the front teeth before being moved to posterior parts of the dentition. In the initial stages of food intake, forces are applied to the incisors in all directions. The molars, on the other hand, grind food substances only during more forceful chewing. During the final phase of the chewing cycle, when the lower molars on the working side approach the intercuspal position from a posterior and lateral position, they are likely to experience distal and lingually directed forces upon contact with the opposing upper molar teeth. Given their directional preference for distal-lingual loading, the mechanoreceptors supplying the lower molar teeth are well suited to encode information about the forces that normally act on the posterior teeth during mastication (Trulsson 2006). The lower static and dynamic sensitivity of periodontal receptors at posterior teeth may reflect a functional adaptation to the faster and stronger forces that are developed during motor activities involving the posterior teeth (Trulsson 2006).

“Among many morphologically different periodontal mechanoreceptors, Ruffini ending receptor is the primary mechanoreceptor in humans and other mammals“

Maeda et al 1999

These observations indicate that subjects use periodontal afferent information to specify the level of force during the hold phase of a hold-and-split task of masticatory function. This periodontal afferent information is generated thanks to the tactile and reflex function of PDL mechanoreceptors (*Lobbezzo et al 2006*). Scientific evidence related to the modulation of trigeminal sensory input during mastication is also collected from studies on oral tactile function and muscular reflexes.

II.IV a *Contribution of periodontal receptors to the oral tactile function*

Jacobs and van Steenberghe (1994) report that the PDL nerve endings, mainly PDL mechanoreceptors, may contribute to the exteroceptive function. Yet, they call attention for the misinterpretation of this function as “tooth proprioception”. Proprioceptors, such as muscle spindles or joint receptors, would be activated by stimuli inside the body, giving information about the relative positions and movements of the limbs (*Jacobs and van Steenberghe 1994*). The diameter of the afferent fibres and their conduction velocity also argue against proprioception. Periodontal mechanoreceptors are actually very sensitive to external forces applied to the tooth, they have a tactile function.

Tactile function seems more or less related to PDL mechanoreceptors, depending on the degree of mouth opening (*Jacobs and van Steenberghe 1994*). The interocclusal detection of small objects, the active threshold level, is very much dependent on the activity of PDL mechanoreceptors, while for larger interocclusal distances, muscle and articular receptors seem to take over. In agreement to the conclusions of Trulsson and Johanson (1996), during functional mouth openings, such as during food comminution, periodontal mechanoreceptors play a prominent role.

The predominant role of periodontal receptors in detecting and discriminating forces acting on a tooth has been proven in previous studies (*van Steenberghe 1979*). According to Jacobs and van Steenberghe (1994), a clear distinction should be made between “passive” and “active” threshold in the psychophysical approach. The first is the detection of forces applied to the teeth, and the second one, the interocclusal detection of small objects such as strips. The active detection task is further divided into a static and a functional threshold determination. While active threshold determination provides means to observe a parameter of jaw motor control, the

passive threshold determination evaluates more precisely the role of periodontal mechanoreceptors although not in a physiological situation. In psychophysical threshold determinations, a threshold range, rather than an absolute value exists. A subject uses his own criteria to discriminate between stimulus and noise. The reliability of the response is affected by the subject's attention and psychological attitude. Unfortunately, tactile threshold determinations are often performed without using an appropriate psychophysical methodology. A summary of previous studies about threshold determination of teeth is provided by Jacobs and van Steenberghe (1994).

Human teeth are sensitive to very small forces applied to the teeth. Pfaffmann noted that 0.01-0.02 Newton force is sufficient to evoke a response from the majority of mechanoreceptors of the cat's dental nerve (*Linden 1990b*). Although the removal of the pulp did not change the response, an advanced periodontal breakdown is associated with a higher threshold (*Jacobs and van Steenberghe 1994*). This could be related to an increased mobility or to a partial loss of receptors. In edentulous jaws, the performance of detection or discrimination tasks is even worse, although edentulous patients still keep mechanoreceptors in the mucosa and the periosteum of the jaw bone. These receptors only differ from periodontal ligament mechanoreceptors in their receptive fields.

Thus, the "periodontal feedback" and its exteroceptive function is not completely lost in edentulism. When patients are rehabilitated with oral implants, the active absolute threshold level increases compared to the natural dentition, but remains below the threshold noted in denture wearers. The passive threshold is about 10 to 100 times larger for edentulous patients with implant-supported prostheses and 50 to 100 times larger for denture wearers when compared to patients with natural teeth. The rapid elastic bone deformation during implant loading may trigger periosteal receptors, which however remain less sensitive than periodontal ligament receptors (*Jacobs and van Steenberghe 1994*).

Studies on passive threshold of teeth have made several characteristics of periodontal mechanoreceptors become obvious. Teeth are more sensitive to lateral than to axial forces, which might be part of a protective mechanism. Loading a tooth labiolingually indeed results in a more pronounced deformation of the

mechanoreceptors and a lower threshold. Furthermore, posterior teeth have higher passive threshold values than anterior ones, which may be explained by the less intense stimulation of individual mechanoreceptors due to anatomical and visco-elastic differences. For the active threshold, results are quite different since the periodontal mechanoreceptor characteristics can be masked by the activation of non-periodontal receptors. This explains the lack of difference between active threshold level of anterior and posterior teeth. Since the insertion of a foil between the distal teeth is associated with a larger mouth opening, a stronger activation of muscular and/or articular receptors occurs. This probably compensates for higher threshold values normally observed for posterior teeth (*Jacobs and van Steenberghe 1994*).

II.IV b *Brain stem reflexes and periodontal receptors*

It is worth to note that the central connections of the PDL mechanoreceptors are quite unique in that most of these receptors have their cell bodies in the trigeminal mesencephalic nucleus along with the spindle cell bodies. Therefore, it has been suggested that in the trigeminal mesencephalic nucleus, an electrical link may exist between the cell bodies of muscle spindles and periodontal receptors (*Türker 2002*). The importance of peripheral feedback in controlling masticatory muscle activity has been illustrated by the greatly reduced facilitation of the masseter muscle after removing sensory feedback from PDL receptors (*Türker 2002*). When spindle bodies were also destroyed, facilitation of jaw closing muscles disappeared almost completely (*Türker 2002*).

The spinal cord functions primarily in the transmission of neural signals between the brain and the rest of the body but also contains neural circuits that can independently control numerous reflexes and central pattern generators (*Sessle 2006*). By analogy, it is supposed that the same occurs during the oral motor function. The spinal cord would be the trigeminal ganglion and the trigeminal mesencephalic nucleus from where the neural signals between the brain and the rest of the oral region would be transmitted. Furthermore, the trigeminal mesencephalic nucleus would contain neural circuits that could independently control muscular reflexes and the masticatory central pattern generator.

Linden (1990) reported that intra-oral mechanoreceptors contribute to reflexes involving the muscles of mastication and the masticatory-salivary reflex. The latter, of course, in addition to the gustatory input from the facial and glossopharyngeal nerves that have been shown to provide a greater stimulus than that provided by mechanical stimulus alone (*Linden 1990b*). For a comprehensive account of the inhibitory and excitatory reflex responses that may be evoked in the jaw-closing muscles in humans when periodontal receptors are stimulated, the reader is referred to the review by Türker (2002).

The mandible has some unique characteristics. It is the only limb to cross the anatomic sagittal plane and articulates with the skull base by means of 2 parallel joints. According to Lobbezoo et al (2006), those features imply that the human trigeminal neuromotor system involves homonymous bilateral reflexes. Since high forces can be exerted by the jaw-closing muscles versus the rather weak jaw-opening muscles, these must be balanced by a fast cybernetic modulation. In turn, the trigeminal reflexes demonstrate two neurophysiological particularities. Their primary afferents have their cell bodies in the brain (nucleus mesencephalicus), which contrasts with other limbs and they have a bilateral symmetric reflex function, since the mandible is the only limb that crosses the midline. Another interesting feature is that just as walking, chewing relies on a central pattern generator for chewing, in between the supracollicular and midpontine level (*van Steenberghe 1998*).

Studies in monkeys have revealed that each muscle or movement is represented multiple times within the face primary motor cortex (MI), leading to the current view that each output zone of MI controls one of the many contextual functions in which a muscle participates (*Sessle 2006*). Mastication and swallowing in the monkey could be evoked by intra-cortical microstimulation (ICMS) not only from the classical 'masticatory area' lateral to face MI but also from within the face primary somatosensory cortex (SI). Furthermore, each of these regions disrupts chewing and swallowing to varying degrees, indicating that each may be involved differentially in the production and patterning of chewing and swallowing, and underscoring why cortical damage can lead to severe clinical problems with eating and speaking in stroke patients.

They also underscore the importance of the somatosensory cortex as well as motor cortex in the fine motor control of oro-facial movements. The convergence of various inputs to cortical areas may contribute to mandibular kinaesthesia, and the substantial number of face MI neurons receiving bilateral inputs from oro-facial tissues is probably related to the need for bilateral sensorimotor coordination in orofacial muscle function. Thus, both face MI and SI may use oro-facial afferent inputs to guide, correct and control movement by the use of sensory cues prior to movement and by using sensory information generated during movement.

van Steenberghe (1979) has concluded that the clinical implications of the periodontal-jaw muscle reflex were questionable. They seemed to play a role in some dysfunction syndromes. The role of periodontal receptors in the control of jaw muscles activity, according to the author, has been overemphasized by some. Most reflexes can be elicited by several afferent pathways, so that when one falls off, the other take over without any major functional deficiency. This can be illustrated by the fact that the monosynaptic reflex followed by a silent period has also been described in edentulous subjects. The role of central neural programming in masticatory function should also not be underrated (*van Steenberghe 1979*).

Concerning the functional significance of periodontal receptors, jaw-opening reflex and silent period are interrelated (*van Steenberghe 1979*). Although much work has been accomplished on the silent period, the concurrent monosynaptic reflex has been mostly neglected. It could not be shown that periodontal receptors are the solely origin of these reflexes. Periodontal receptors not only influence jaw muscles activity through reflex mechanisms, but also modulate jaw muscles control through interaction with other afferents, such as laryngeal input at the brain stem level and muscle afferents at the cortical level (*van Steenberghe 1979*). The periodontal input seems to influence the gammadotoneurons through afferents in the mesencephalic nucleus although no coupling between cells of periodontal and muscle spindle origin could be demonstrated in the mesencephalic nucleus (*van Steenberghe 1979*). It is perhaps through one of these interactions that periodontal receptors regulate the maximal clenching. This regulation was shown by applying local anaesthesia to the two antagonistic teeth, seven out of nine subjects developed increased clenching forces. Although this experiment did not allow to differentiate between the periodontal

and pulpal receptors, it substantiates the hypothesis that these receptors have a negative feedback on jaw closing muscles activity during maximal clenching efforts. Visual display of the forces reached, had a stimulating effect when the periodontal receptors were eliminated (*van Steenberghe 1979*).

Earlier studies on the possible involvement of high threshold periodontal receptors in protective reflexes, preventing too strong biting forces during mastication, have yielded conflicting results according to Hildebrand et al (1995). Mechanical tooth stimulation in humans, cats, rabbits and rats can induce both excitatory and inhibitory jaw-closing muscle responses. While brisk taps applied to human incisors elicit short-latency inhibitory reflex responses in the masseter muscle, slow pushes evoke a long-latency primarily excitatory reaction. Hence, different types of mechanical stimuli may activate different reflex mechanisms. For example, periodontal receptors seem to be directly involved both in reflexes of salivary secretion and in the “jaw-opening reflex” (*Hildebrand et al 1995; Linden 1990b*). In humans and rats the masseter muscle is more active than the temporal muscle during occlusion of the incisors, but both muscles are equally active during molar occlusion. This shows that the muscular reflexes elicited by periodontal stimuli also depend on the type of tooth stimulated. Moreover, the reflex responses of dental stimulation vary with the background activity – in rats, excitatory effects prevail at low levels of background activity (*Hildebrand et al 1995*).

Hildebrand and coworkers (1995) continue by stating that the innervated periodontium is most probably not the only sense organ underlying oral kinaesthesia. Forces applied to teeth may also stimulate receptors in dentin, pulp, periosteum, gingival mucosa and fibrous sutures, as well as in the temporomandibular joint related muscles. The view that jaw muscle receptors may be involved is supported by the markedly reduced acuity of oral kinaesthesia in patients with Duchene’s muscle dystrophia. Further, the degree of jaw opening influences the excitability of cortical neurons sensitive to tooth pressure, as observed in the cat. A corresponding observation in humans is that the experienced hardness of a piece of rubber increases with its size (*Hildebrand et al 1995*).

II.IV c *Lacking PDL mechanoreceptors - other evidence on physiological significance of PDL mechanoreceptors*

To efficiently handle the food during chewing, activation of the jaw muscles must be coordinated to produce jaw actions that are spatially adapted to the food's distribution in relation to the teeth (*Trulsson 2007*). Although PDL receptors poorly encode the magnitude of tooth loads during strong chewing forces (*Johnsen and Trulsson 2005*), their responses are still dependent on the direction of the force (*Johnsen and Trulsson 2003*). As a consequence, they can continuously encode spatial information about tooth loads and most likely contribute to the spatial control of jaw actions (*Trulsson 2007*). Indeed, the lack of coordination in chewing has been observed following denervation of intraoral receptors including the PDL receptors. The absence of sensory input resulted in reduced masticatory force and distorted spatial control of jaw movements during chewing (*Inoue et al 1989*).

From studies in humans, it was concluded that PDL receptors of anterior and posterior teeth contribute differently to chewing control (*Trulsson 2007*). The PDL receptors of anterior teeth are crucial for the regulation of precise manipulative actions involving application of low forces by the incisors. Thus, those PDL receptors efficiently encode tooth load when subjects contact and gently manipulate the food using the teeth (*Trulsson 2006*). On the other hand, PDL receptors of posterior teeth are important to inform about mechanical properties of the food during chewing. Those receptors are well suited to encode in detail the jaw movement and the temporal changes in the chewing force that occur during the early contact phase of each chewing cycle (*Trulsson 2007*). Thus, periodontal receptors may contribute to the selection of the most appropriate motor signals, given the existent mechanical food properties. In rabbits, blocking the information from periodontal receptors significantly reduced the build-up speed of the masticatory force during chewing (*Hidaka et al 1997*).

Lund and Kolta (2006) discussed the adaptation of the central pattern generator (CPG) output to changes in food hardness. They reported that the increase in electromyographic (EMG) burst is proportional to the hardness of an object. If the nerve supplying the PDL receptors are cut, the increase in EMG activity is much less, suggesting that periodontal afferents are responsible for some adaptation to food

hardness. Both periodontal and muscle spindles send important inputs to the CPG. It seems that the two inputs may have differential effects on burst-generating neurons because some neurons firing during jaw opening receives periodontal feedback, while those that fire during closing are excited by spindle afferents.

In this way, it has been demonstrated that signals from PDL receptors are used in the fine motor control of the jaw and it became clear from studies of various patient groups that important sensory-motor functions are lost and impaired when these receptors are removed during extraction of the teeth (*Trulsson 2006; Veyrune et al 2007*). Dentate subjects choose to use hold forces large enough to achieve a stable clasp (on average 0.6 N), but automatically avoid higher forces (>1 N) at which the sensitivity of most receptors (the saturating receptors) to force changes is compromised. Patients lacking periodontal receptors, such as patients using dental prostheses supported by the oral mucosa or dental implants showed high hold force levels. During anaesthesia of the periodontal tissues, the hold forces are considerably increased and show greater variability (*Trulsson 2006*). These higher hold forces provided a greater level of security in maintaining the clasp on the morsel and probably stimulate alternative, less sensitive mechanoreceptors in the tissues that are able to signal its engagement by the teeth. Furthermore, in anaesthetised subjects, and in patients lacking periodontal receptors, the morsel frequently escaped from the incisor edges during the biting task, indicating an impaired spatial control of the jaw-action vector. Thus, when periodontal afferent information is lacking, patients show a marked disturbance in the control of precisely directed, low biting forces, suggesting that periodontal receptors play an important role in the specification of the level, direction and point of attack of forces used to hold and manipulate food between the teeth (*Trulsson 2006*).

Veyrune et al (2007) showed that preparing the same food bolus for swallowing required a greater number of masticatory cycles and a longer duration of mastication for complete denture wearers than for dentate subjects. In addition, complete denture wearers failed to increase EMG activity per cycle in response to food hardness. In general, complete denture wearers have shown greater number of masticatory cycles, longer duration of mastication and higher total and average muscular activities. In opposition, the masticating rate in complete denture wearers was slightly lower than in dentate patients, and this feature remained unchanged

independently of food hardness. Depending of food hardness, the parameters for number of cycles, durations of mastication, total muscular activity, average muscular activity and masticating rate ranged from 28-40 cycles in dentates and 36-57 cycles in denture wearers; 22-31s of mastication in dentate and 30-44s for denture wearers; 18-35mVs of total muscular activity for dentate and 28-54mVs in denture wearers; 0.67-0.89 mVs average muscular activity of dentate and 0.82-1.02 mVs for denture wearers; 1.33-1.31Hz of masticating rate in dentate and 1.21-1.30Hz in denture wearers. Interestingly, complete denture wearer showed a higher interindividual variability for total muscular activity than dentate subjects, suggesting that other individual factors may explain muscular function during mastication in patients lacking periodontal mechanoreceptors.

Animal research showed that applying force to an implant in the cat's jaw did not lead to action potentials in the afferent nerve while this was the case in the canine tooth on the other side (*Bonte et al. 1993*). But tapping the same implant was able to induce an inhibitory reflex in the jaw closing muscles.

In man, during clenching, tapping with a well-defined force an implant in the upper jaw also leads to an inhibitory reflex in the jaw closing muscle as observed through electromyography. This could not be elicited in subjects with implant-supported bridges in both opposing jaws but clearly when periodontal ligaments remained in the antagonistic jaw (*Bonte and van Steenberghe 1991*). In subjects with single implants, masseter muscle reflexes were observed although with a higher threshold than for teeth (*Stuge et al. 1993*).

Silent periods following tapping teeth together or the elicitation of the jaw jerk reflex were not different for implant-supported bridges or for natural teeth (*Haraldson and Ingervall 1979*). Also for the unloading reflex no differences were noted between patients with implant-supported bridges or natural teeth or dentures. Indeed, it is well established that the input for such reflexes does not originate from periodontal mechanoreceptors (*Duncan et al. 1992*). The fixations of prostheses on implants hardly influences jaw function as reflected in maximum bite force and EMG activity (*van Kampen et al. 2002; Mericske- Stern et al. 2000*).

The reflex effect on jaw closing muscles was investigated in three patient groups involving fully edentulous subjects with dentures or implant-supported fixed

prostheses in both jaws, vs. partially edentulous subjects. Each time an upper jaw implant was stimulated in a standardized manner while the EMG activity of the masseter muscles was recorded. Post-stimulus EMG complexes were very dependent on the presence of periodontal neural receptors, either in the ligament or the gingiva (*Jacobs and van Steenberghe 1995*).

Indeed, to understand the muscular function during mastication is a complex task surrounded by many hypotheses still needing to be tested. It was suggested that due to the atrophic state of the masticatory muscles of edentulous subjects, inside a given muscle, the active fraction of motor units may be greater in complete denture wearers, and the muscles of denture wearers may work nearer to the maximal bite force during mastication (*Veyrune et al 2007*). Therefore, this greater number of active motor units and total EMG activity may not be necessarily associated with the intensity of bite force. In the same way, it has been shown that edentulous subjects have to use higher potentials of muscle activity, the percentage of maximal voluntary contraction, than age-matched dentate subjects (*Alajbeg et al 2005 and 2006*). It is important to note that studying the EMG parameters did not give any indication about crushing of food, and masticatory efficiency needs to be known before an overall understanding of mastication process can be achieved, as stated by Veyrune et al (2007).

Complete denture wearers, thus patients lacking periodontal ligament, presented both lower masticatory efficiency and lower bite force than dentate subjects. Therefore, the increased chewing activity does not lead to a better comminution of food bolus. Finally, the closing phase appears to be the critical kinematic parameter differentiating denture wearers from dentate subjects. Simulated chewing experiments in anesthetized rabbits has shown that the contribution from the PDL mechanoreceptors stands out as the most important feedback source, since they generated the major part of closing muscle activity (*Türker 2002*). In humans, the importance of PDL mechanoreceptors can be illustrated in patients treated with implant-supported prosthesis. Unlike subjects with healthy teeth who display bite-to-bite variation in muscular activity, these patients chew with approximately the same pattern of muscle activity during the whole masticatory sequence (*Haraldson 1983*). The dependence of total jaw-closer muscle activity on the performance of the peripheral receptors ensures that, should resistance between the jaws suddenly

yield, this positive feedback would immediately cease, hence reducing the jaw-closing muscle activity and helping to stop the jaws from forcefully coming together (*Türker 2002*). Interestingly, experiments both in animals and man indicate that the impact forces on osseointegrated implants lead to reflex inhibition of jaw closing muscles (*van Steenberghe 1998*).

Finally, the role of PDL innervation in the etiology behind the eruption has been proposed in the literature (*Kjaer and Nolting 2009*). However this discussion was considered out of the scope of this review. A summary of the main characteristics of PDL mechanoreceptors in humans and its functional significance is presented in table 2.6.

II.V Periodontal neuropeptides and neural growth factors:

As it can be observed from the studies of Maeda and collaborators (table 2.5), immunohistochemical researches frequently use neuropeptides to identify the presence of nerve fibres and, most useful, to understand how those fibres function. Nerve fibres immunoreactive to some neuropeptides have been found in the PDL and could confirm observations from other studies on PDL innervation using morphological and eletrophysiological techniques. For example, Sato et al (1988) reported in rats that “the restricted location of the stretch receptor, Ruffini-like corpuscle, in the lingual periodontal ligament appears to be an essential element, because this region is regularly extended during mastication. The nervous elements were restricted to the alveolar half of the periodontal ligament in every region; they avoided the dental half of the periodontal ligament, which presumably moves continuously with the tooth”. These observations are in line with eletrophysiological studies of Linden and Scott (1989) in cats; Byers (1985) in rats; Loescher and Holland (1991) in cats.

Table 2.6: Summary of main characteristics of PDL mechanoreceptors in humans and its functional significance.

Subjects	Receptor characteristics	author	methods	Functional significance
humans	<ul style="list-style-type: none"> - Slowly adapting - non-saturating receptors (15-20%) and saturating receptors (80-85%) - Encode forces from more than 1 tooth - Highest response rate when stimulating one specific tooth (receptor-bearing tooth) - Tuned to direction of force (\neqant/post teeth) - Highest sensitivity < 1N (anterior teeth) and 4N (posterior teeth). - Dynamic sensitivity reduced at high forces (saturation tendency) - Poorly encode magnitude and force changes at higher loads 	Trulsson 2007	<p>Microneurographic recordings from single nerve fibres</p> <p>Disadvantage: no info nerve ending position</p>	<p>At low forces:</p> <ul style="list-style-type: none"> - Control of manipulative forces (positioning the food between teeth and prepare for chewing). <p>At high forces:</p> <ul style="list-style-type: none"> - Mechanical properties of food - Spatial contact dentition and food
humans	<p>-sensitivity to static forces and rapidly changing forces (dynamic sensitivity)</p> <ul style="list-style-type: none"> - saturating receptors become progressively less sensitive to both the magnitude and rate of rapid changes in force, as contact force grows in amplitude. 	Trulsson 2006	Microneurographic	<p>periodontal mechanoreceptive information</p> <p>to regulate the level of jaw force during the hold phase of the 'hold-and-split' task</p>
humans	Functional characteristics of periodontal receptors at threshold level are set by the visco-elastic properties of the surrounding tissues.	Jacobs and van Steenberghe 1994	<p>Psychophysical threshold assessment (tactile function)</p> <p>Disadvantage: activation other receptors/method variability (stimulus/set up) active threshold: interincisor distance of 5mm or more –non periodontal receptor play a predominant role</p>	<p>PDL receptors- essential for accurate interdental microthickness discrimination</p> <p>Absolute threshold is remarkably increased during chewing because of the progressive intrusion of the tooth in its alveolus after each chewing cycle. In the passive discrimination tasks teeth are more sensitive than implants, at chewing forces, implants and teeth seem equally sensitive</p>

Immunostaining for S-100 has been shown to be useful for demonstration of neural elements in the periodontal ligament, it demonstrates the Schwann sheaths of nerves (*Maeda 1987*). Moreover, S-100-immunoreactive neural elements were more numerous in incisors than in molars (*Maeda et al 1987*), confirming the more densely innervation in the anterior teeth (*Trulsson 2007*). Maeda et al (1989) found rounded cells in the vicinity of Ruffini endings. Morphologically, those cells presented a kidney-shaped nucleus and enveloped the axoplasmic spines with their cytoplasmic processes. From morphological features, the cells in question were identified as the K-cells described by Everts et al. (1977), as cited by the authors.

These K-cells developed Golgi apparatus and rough endoplasmic reticulum, suggesting active synthesis of proteins. Immunohistochemistry at the electron microscopic level revealed an intense immunoreactivity for S-100 protein in the cytoplasm of the K-cell and led to a conclusion that the K-cells were terminal Schwann cells associated with Ruffini endings, presumably corresponding to the lamellar cells in the inner bulb of sensory corpuscles (*Maeda et al 1989*). However, immunohistochemical studies have found no lamellated nerve endings in the human periodontal ligament (*Maeda et al 1990a*).

In the PDL of rats and cats, sensory fibres were observed expressing calcitonin gene related peptide (CGRP) and substance P (SP) receptors (*Hildebrand et al 1995*), the former being more frequent than the latter. Some proportion of the periodontal CGRP-fibres may be destined to the gingiva. In this same way, free periodontal endings with CGRP and SP receptors can be found, but these peptides do not seem to be present in the Ruffini-like endings. Both CGRP and SP immunoreactive fibres usually occurs in relation to blood vessels and can be also located near the cementum or associated with the epithelial rest of Malassez (*Hildebrand et al 1995*). A few fibres containing vasoactive intestinal peptide (VIP) and occasional neuropeptide Y immunoreactive (NPY-IR) fibres were found in the periodontal ligament as well. The presence of such units in association with intraligamental blood vessels indicates that peptidergic sensory fibres may control periodontal blood flow (*Hildebrand et al 1995*).

Persistent expression of GAP-43 has also been observed in fibres of free nerve endings and Schwann sheaths around axon terminals of Ruffini endings in the

periodontal ligament of normal adult rat molars (*Maeda and Byers 1996*). It is believed that continual appearance of GAP-43 in mature animals is related to the remodelling activity of periodontal nerves associated with dynamic reconstruction of periodontal fibres (*Jayawardena and Takano 2006*). Glia-specific S-100 protein and non-specific cholinesterase enzyme are known to be good markers for the identification of Schwann elements of nerves. The findings of Maeda et al (1990) indicated that nonspecific cholinesterase is a useful marker to distinguish terminal Schwann cells from ordinary Schwann cells and that the enzyme may be synthesized in the rough endoplasmic reticulum and conveyed toward the nerve endings. Since this enzyme has been known to be shared by the inner bulb of Pacinian corpuscles and the lamellar cells of Meissner's corpuscles, they are likely to have a mechanoreceptive function in these specialized Schwann cells. Absence of staining for S100 protein immunohistochemistry and cholinesterase reactivity of the nerve elements in the tooth related part of the guinea pig periodontal ligament infers a lack of Schwann elements in those endings (*Jayawardena and Takano 2006*). It was suggested that Ruffini endings in guinea pig periodontal tissues have variable spatial correlation to the surrounding fibres, implicating their diverse mechanoreceptive properties depending on the anatomical location (*Jayawardena et al 2002*).

Regarding the neural growth factors, immunohistochemical analysis indicated that axonal terminal Schwann cell components of Ruffini-like periodontal mechanoreceptors are sensitive to members of the neurotrophin family growth factors (*Matsuo et al 2002; Hildebrand et al 1995*). Whether growth factors and their receptors are present in relation to periodontal fibres during normal maintenance remained largely unknown (*Hildebrand et al 1995*). On the other hand, several studies have shown that multiple neurotrophins such as glial cell line-derived neurotrophic factor (GDNF), neurotrophin-4/5 (NT- 4/5) and brain derived neurotrophic factor (BDNF) might play roles in the development and/or maturation of the periodontal Ruffini endings (*Ohishi et al 2009; Igarashi et al 2007; Maruyama et al 2005; Alkhamrah et al 2003; Harada et al 2003; Hoshino et al 2003*).

III - INFLUENCE OF ORAL TREATMENTS AND FUTURE APPROACHES IN PDL INNERVATION

III.I Influence of oral treatments:

Some occlusal changes and nerve injury or trauma may occur during oral treatments as such orthognatic surgery, orthodontic treatment and tooth reimplantation and transplantation. Previous studies have reported on peculiar changes in the morphology and the distribution of nerve elements in the periodontal ligament in association with altered tooth loads, resection of inferior alveolar nerve and regeneration of the PDL (see: *Jayawardena and Takano 2006*).

The loss of function after extraction of antagonist tooth may also be take into consideration as Shi et al (2005) and Muramoto et al (2000) showed that mechanical stimulation is required for morphological maintenance of the Ruffini endings in the periodontal ligament of the rat incisors and molars. A reduction in the occlusal force has induced morphological changes in the terminal morphology of the periodontal Ruffini endings: they became smooth, unlike the irregular profiles observed in the control group receiving normal loads. The reduced size and number of axon terminals of periodontal Ruffini endings following reduced occlusal force and the restoration of the morphological alteration after the re-establishment of incisor occlusion indicated that proper mechanical stimulation is an important factor for maintaining the morphology of mechanoreceptors (*Shi et al 2005*).

Using the protein gene product 9.5 (PGP 9.5) and S-100 protein immunohistochemistry, Imai et al (2003) showed that that parts of periodontal Ruffini endings can regenerate following inferior alveolar nerve (IAN) cross-anastomosis with mental nerve. Hayashi et al (2000) suggested that the terminal Schwann cell is important in the development and maturation of the periodontal Ruffini endings. Indeed, alterations in the behaviour and distribution of Schwann cells were reported following transection of the IAN (*Atsumi et al 2000; Atsumi et al 1999*). In the PDL of the rat lower incisor, the terminal Schwann cells migrates into the tooth related-part of the ligament during the regeneration of the PDL nerve fibres (*Atsumi et al 2000*).

Orthodontic movement

Anomalies of sensation are often associated with orthodontic tooth movement. It is frequently reported that the pain is elicited from teeth when a normal (non-noxious) biting force is applied to a tooth that is being moved orthodontically, particularly in the first few days following commencement of treatment or adjustment of orthodontic arches (*Linden 1990a*). Despite these common clinical observations there have been few, if any, studies on alteration in the periodontal mechanoreceptor response during or following orthodontic treatment. There are considerable data concerning the degenerative and regenerative changes that occur when orthodontic forces are applied to the teeth. However, these studies have concentrated on histological changes occurring in the collagen, bone and gingivae. In 1990 (*see: Linden 1990a*), a few studies showed that when a tooth is moved through the bone changes take place in the innervation. Later, it has been speculated that the periodontal nerves are involved in the inflammatory process, and release various neuropeptides during orthodontic tooth movement (*Jayawardena and Takano 2006, Vandevska-radunovic 1999*).

A transient injury-related sprouting of vessel-related CGRP immunoreactive axons has been found in the periodontal ligament of rat and cat teeth subjected to orthodontic treatment (*Hildebrand et al 1995*). Similarly, application of orthodontic forces to cat canines induces an increased occurrence of SP immunoreactive pulpal and periodontal axons – there is an early peak in the pulp, and a later increase in the periodontium, the latter being most evident on the compression side. These workers suggested that mechanical load of the periodontal ligament elicits a local SP-release, which “activates” periodontal cells. Certainly, cellular responses in the periodontium to mechanical forces in vivo deserve further study (*Hildebrand et al 1995*).

It has been reported that all the periodontal nerve elements are confined to the alveolar related part in the periodontal ligament of continuously erupting incisors of various rodents such as rat, mouse, guinea pig, squirrel, hamster and Mongolian gerbil (*Jayawardena and Takano 2006*). However, Jayawardena and Takano (2006) found thin nerve fibres in the tooth related part of guinea pig incisors. It raised an intriguing question regarding how these nerves exist despite rapid remodelling and drastic movement of the surrounding tissues associated with the eruptive movement

of the tooth. Besides, Piyapattamin et al (1999) reported that changing the direction of the force applied to the PDL results in rapid and prolonged changes in the morphology of Ruffini-like mechanoreceptors.

Reinnervation of replaced and transplanted teeth

Tooth replantation has been a subject of interest for centuries. Already Hunter (1773) and Younger (1886) found that a vital periodontal ligament is necessary for successful replantation (*see: Hildebrand et al 1995*). Based on experimental studies in animals, some workers concluded that ankylosis and root resorption, major problems after replantation, can be prevented if the tooth is replanted with the periodontal ligament. Studies in monkey, dog and man clearly showed that the success of replantation depends critically on the presence of a vital periodontal ligament. In the case of a young teeth epithelial root sheath of Hertwig must be included. The fact that a grossly normal periodontal membrane can be re-established after replantation evoked the question if the periodontium and the pulp become reinnervated (*Hildebrand et al 1995*).

Tooth autotransplantation or replantation is a routine procedure, that is used for treatment of tooth agenesis or traumatic tooth loss (*Hildebrand et al 1995*). Both in experimental animals and in man, tooth removal and replantation is followed by pulpal revascularization and reinnervation. The success rate is highest if the donor tooth has not completed its root formation. In general, replanted human teeth regain sensitivity within months after surgery. In experimental animals, axonal regeneration regularly takes place to autotransplanted or replanted teeth. The density of pulpal axons in autotransplanted monkey incisor teeth is similar to that in normal teeth, but it does not necessarily mean that a normal function has been reestablished. Axons regrowing toward a replanted tooth do not show the abnormal sprouting seen after other types of tooth injury. The replanted teeth exhibit a marked divergence in pulpal healing, and the pulpal nerve density never reaches the normal levels (*Hildebrand et al 1995*). Replanted cat canines redevelop functional periodontal axons, but their response properties remain subnormal, even 1 year after surgery (*Loescher and Robinson 1991a*).

Electrophysiological investigations on cats have shown that the periodontal mechanoreceptors supplying the lower canine are reinnervated within 12 weeks of

sectioning the inferior alveolar nerve but have altered discharge characteristics (Loescher and Holland 1991b; Loescher and Robinson 1989b). The mechanoreceptors responded with raised mean force thresholds and reduced maximum discharge frequencies, and they adapted more rapidly. These changes may have arisen from alterations in the structure of the receptor or from an alteration in the distribution of the receptors within the ligament (Loescher and Holland 1991a).

Wakisaka et al (2000) reviewed the morphological and cytochemical characteristics of periodontal Ruffini ending under normal and regeneration processes. Following nerve injury, the periodontal Ruffini endings of the rat incisor ligament can regenerate more rapidly than Ruffini endings in other tissues. During regeneration, terminal Schwann cells associated with the periodontal Ruffini endings migrate into regions where they are not found under normal conditions. Also during regeneration, alterations in the expression level of various bioactive substances occur in both axonal and Schwann cell elements in the periodontal Ruffini endings. Neuropeptide Y, which is not detected in intact periodontal Ruffini endings, is transiently expressed in their regenerating axons. Growth-associated protein-43 (GAP-43) is expressed transiently in both axonal and Schwann cell elements during regeneration, while this protein is localized in the Schwann sheath of periodontal Ruffini endings under normal conditions (Wakisaka et al 2000).

As the importance of axon-Schwann cell interactions has been proposed, further investigations are needed to elucidate their molecular mechanism particularly the contribution of growth factors during the regeneration as well as development of the periodontal Ruffini endings. Takahashi-Iwanaga et al (1997) described that the tips of the axon branches-together with their Schwann sheaths-became attenuated and projected into tight bundles of collagen, indicating their susceptibility to mechanical deformations of the surrounding tissue. Margins of the axon terminals were conspicuously ruffled with long tongue-like projections of Schwann cells. The Schwann cell tongues twined around collagen bundles in their distal portions, and associated closely with fine axon projections in their proximal portions, suggesting their involvement in the mechanical transmission of stimuli to axon terminals (Takahashi-Iwanaga et al 1997).

III.II Future research approaches in the PDL studies:

From previous studies, one can conclude that mechanoreceptors have their morphology, location, distribution and neurophysiological characteristics directly related to the biomechanical environment within they are located. van Steenberghe (1979) suggested that the tactile threshold characteristics of mechanoreceptors are set by their binding with the surrounding visco-elastic tissues. The interrelation between structures inside the PDL has been cited several times as an important feature to understand the transduction of mechanical stimuli by the periodontal ligament mechanoreceptors. The mechanotransduction might not be a function of sensory nerve fibres alone, but rather a function which many other cells in the PDL may take part.

To understand and identify the co-adjuvants of this special oral function, the spatial arrangement of PDL has been further investigated (*Naveh et al 2013; Lin et al 2013; Naveh et al 2012a*). Better understanding of the PDL's biomechanical behavior under physiologic and traumatic loading conditions might enhance the understanding of the PDL's biologic reaction in health and disease. As commented by Jayawardena and Takano (2006), exploring the distribution pattern of nerves in relation to other structures within the periodontal ligament of various species should be important to understand their roles within the ligament.

Fill et al (2011) explain that from a biomaterials perspective, the PDL is a complex, fibre-reinforced substance that responds to force in a viscoelastic and nonlinear manner. The PDL consists of 53–74% collagen fibres and 1-2% blood vessels and nerve endings that are embedded into an amorphous mucopolysaccharide matrix. Fibrous collagen elements resist tensile forces and the highly hydrated viscous ground substance into which fibrous proteins are embedded forms the extracellular matrix. The ground substance is responsible for the PDL's viscoelastic properties when subject to loading. Also, the PDL's cellular response to mechanical loading results in a metabolic response (remodeling of the ground substance and fibrous tissue). This tissue responds rigidly to rapid deformations (mastication) while deforming elastoplastically when subjected to low-grade continuous forces (orthodontic movements). These PDL's mechanical properties are

essential parameters for understanding the mechanical behavior of a tooth root and surrounding tissues (*Fill et al 2011*).

Several factors may affect the mechanical properties of the PDL (*Fill et al 2011*). To cite some, the geometric configuration of the periodontium, size and shape of tooth root, the regional differences and thickness of PDL, age, ethnicity, race, gender, genetics, dental environment, overall physical health, diet, type of loading and material mechanics. There is such variability in these parameters that it may be a possibility that each individual PDL (i.e., from every single tooth) has its own distinct biomechanical behaviour—much like the uniqueness of a fingerprint, as suggested by *Fill et al (2011)*. Therefore, to reproduce or predict the biomechanical behaviour of the PDL remains a complex task.

For understanding the stress and strains acting in the PDL, the spatial arrangement should be studied in order to find if there is any pattern in this geometric characteristic of the PDL. Several functional characteristics of PDL mechanoreceptors do not have to be properties of the receptor itself, but could be due to their connection with the adjacent tissues. For example, the PDL mechanoreceptors are able to sense loads through its intimate contact with the surrounding collagen fibres (*Lambrichts et al 1992*). As the properties of the collagen fibres alters within the PDL regions, it supports the idea that their adaptation properties depend on the location of the mechanoreceptors within this ligament (*Jacobs and van Steenberghe 1994, Linden and Millar 1988*).

Knowledge on the basic structure-function relations of tooth-PDL-bone system have a direct implications for better understanding pathological and therapeutic processes in orthodontics, periodontics and jaw bone regeneration (*Naveh et al 2012b*). According to *Naveh et al (2012a)*, much still remains to be learned about the responses to load and the factors that control them in the teeth-PDL-bone system. Such knowledge is relevant to study phenomena such as abfraction, the manner in which dental implants function even in the absence of PDL-like tissue and the implications to bone remodelling of the movements imposed during orthodontics interventions (*Naveh et al 2012a*).

To conclude, future knowledge in the mechanosensory function of the PDL may be derived from researches related to mechanosensing and

mechanotransduction functions of cells (*Rahman et al 2011; Hitomi et al 2009; Page et al 2004; Welsh et al 2002; Gillespie and Walker 2001*). It is known that many cellular reactions are controlled or mediated by mechanical forces (*in: <http://www.mechanobiology.nl/>*). Cells probe the mechanical properties of their environment and subsequently transduce this information accurately into a specific molecular response: mechanical cues can determine the fate of stem cells, modulate the function of entire tissues and play a key role in various pathologies. Cells also alter their motility and metabolic functions depending on the mechanics of their surroundings. Strikingly, cells are not passive observers of the mechanical properties – many cells actively manipulate their surroundings either by the generation of new extracellular or pericellular materials or, even by exerting forces on the outside world (*in: <http://www.mechanobiology.nl/>*).

Treatment involving regeneration of periodontal tissues should consider the role of mechanical loads in the molecular systems of those tissues. The molecular systems might be controlled by macroscopic mechanical stimuli (*Ariga et al 2011*). Application of mechanical loads is known to affect some molecular association and chemical reactions, causing variation of optical properties, sometimes resulting in self-healing functions or capture and release of molecules under macroscopic mechanical motions. The use of macroscopic mechanical stimuli to drive molecular systems has been considered to control of nanosystems at the nanoscale on demand. According to Ariga et al (2011), accessing nanoscience and nanotechnology from the macroscopic world might reveal the great potential of nanoscale and molecular systems. The ability of cells to convert a mechanical stimulus into a electrical signal (mechanotransduction) is a example of how evolution has built sophisticated mechanisms which bridge the nano and macro scales (*Ariga et al 2011*).

In several mechanosensory systems, a transduction channel can detect deflection of an external structure relative to an internal structure such as deformation of the skin, oscillation of a hair cell bundle (*Ariga et al 2011*). The probability of a channel opening varies depending on tensional perturbations of the corresponding elements caused by the deflection. To be able to predict those tensional perturbations the biomechanical environment should be first macroscopically represented. In this way, the next research searched for 3D reconstructions of

histological slices in the literature. In addition, a 3D reconstruction of the the PDL is presented in an attempt to better visualize the PDL neurovascularization.

IV - Three Dimensional Reconstruction of Human Periodontal Ligament Structures using Light Microscopy Imaging

Three dimensional images make it easier to comprehend the complicated structures, having an influence on Anatomical and Physiological approach for teaching, learning and researching. Three dimensional models are constantly used to study effects of mechanical loading on anatomical structures in vitro (*Rahimi et al 2005*). Anatomy and physiology have been frequently revisited through the lens of 3D imaging and modelling techniques (*Cifor et al 2011; Cifor et al 2009*), hence the periodontal ligament, a relevant structure for dental research, might also appear under those spotlights (*Naveh et al 2012b*). Revealing the spatial arrangement of structures within the periodontal ligament can further our understand of its normal as well as abnormal function (*Naveh et al 2012a*). In addition, it can help to unveil its biomechanical behaviour which is of special interest for several research areas in dentistry (*Naveh et al 2013*).

Knowledge about the periodontal ligament is to be applied in most of dental specialities. To cite a few examples, the PDL response to loads is a key player in the study of tooth movement during eruption and orthodontic treatment, PDL regeneration is one of the main goals of any periodontological treatment, tooth reimplantation or transplantation, and finally, the local distribution of forces through the PDL might influence prosthetic design (*Naveh et al 2013; Archangelo et al 2012; Naveh et al 2012a and b*). Besides, in edentulous patients, the PDL is missing and the oral function of those individuals must be interpreted as a novel physiological situation. It means that the occlusal loads, before transmitted to the bone via the teeth supported by the PDL, are now transmitted via the dental prostheses supported by mucosa or osseointegrated implants directly to the bone.

Untangling the periodontal ligament by 3D modelling techniques - Is the 3D modelling of the periodontal ligament possible?

Three-dimensional (3D) reconstruction of anatomical structures can give additional insight into the morphology, interrelation and function of these structures (Hofman *et al* 2009). Histological tissue samples can be stained to show tissue composition and imaged with high spatial resolution. However, many of these studies have also been limited since observations on 2D histological sections are susceptible to artefacts, e.g. related to the direction and location of the histological slices (Sigal *et al* 2010). Histological three dimensional (3D) knowledge is commonly an extrapolation of two dimensional (2D) observations. This knowledge is relevant to understand how structures are distributed around in the PDL and as such to reveal how loads act on and are sensed by the PDL. This section aims to develop 3D reconstruction technique using histological slices, encouraging the application of 3D histological reconstruction on further studies as a new approach to understand the biomechanical behaviour of the PDL. This 3D histological visualization can overcome the drawbacks of limited cross-sectional planes on conventional 2D histological techniques.

Note that standard 2D image processing techniques will hardly provide 3D information from sections, except for the volume fraction value (figure 2.3).

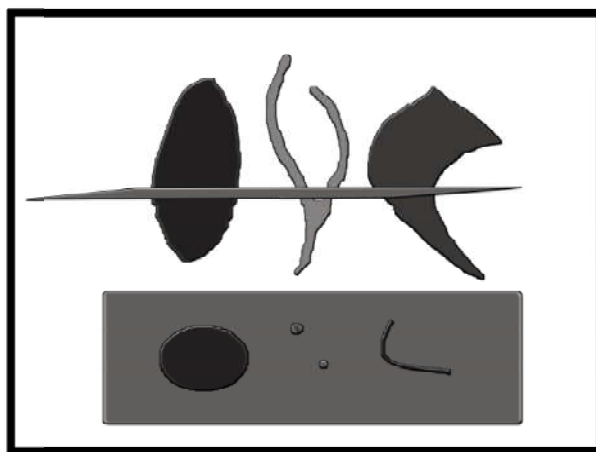


Figure 2.3: 3D true dimension X 2D representation in histological slices.

The figure below shows serial slices of the same region within the PDL (figure 2.4). After analysing those slices it becomes clear that structures composing the PDL changes constantly along the histological slices, e.g. in position, size, shape and how they are intermingled within the collagen fibres.

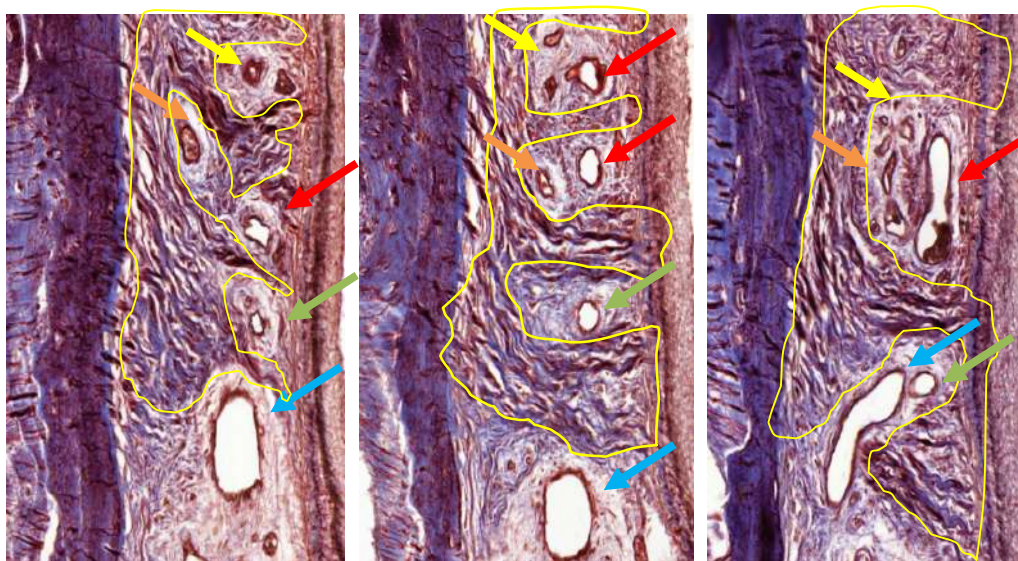


Figure 2.4: Histological slice of human PDL (thricome Masson) in the axial plane. Arrows in the same color represents similar structures observed in the different slices. The yellow contour shows the area containing collagen fibres.

The aim of this article is to describe the possible applications and limitations of a 3D imaging technique in the study of the periodontal ligament.

Material and Methods:

Using light microscopy, 3D reconstructions of human periodontal ligament were performed from digitized 2D histological images. The data sample included human material obtained from cadaver (3 anterior teeth). These specimens were fixed in formaldehyde, decalcified, dehydrated and embedded in paraffine. Thin histological slices (6 μm) were obtained and stained with Trichrome staining of Masson.

Thin sections (6 μm) were used for the analysis of fibres distribution presented at chapter 3 and for the 3D reconstruction in the last part of chapter 2. Ultra-thin sections (0.5 μm) were used for the image analysis using transmission electron microscopy to confirm the presence of myelinated nerve fibres (MNF). Only a few slices were prepared for it. Because of this, I now removed the ultra-thin from the thesis since they were not used in the 3D reconstruction, but actually done in order to confirm the appearance of MNF on light microscopy.

Digitizing:

Using a Mirax Scan (Carl Zeiss Micro imaging GmbH, Germany), high-resolution digital data records were produced (figure 2.5). First, all images were analysed at 50x using a software image analysis (Mirax Viewer) in order to identify myelinated nerve fibres, epithelial rests of malassez (ERM), cementicles and their morphology and interrelation. In total 300 slices were scanned and analysed at Mirax Viewer to identify myelinated nerve fibres, epithelial rests of Malassez (ERM), cementicles, their morphology and interrelation.

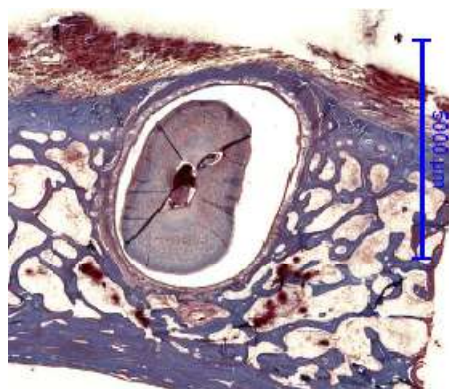


Figure 2.5: Axial slice of canine tooth and its support tissues. High-resolution digital data (MRXS extension) records were produced using Mirax Scan (Carl Zeiss Micro imaging GmbH, Germany).

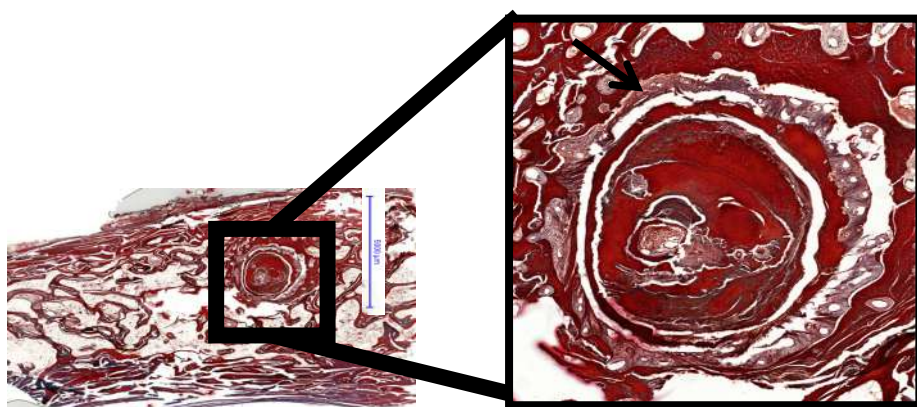


Figure 2.6: The region of interest (ROI) was selected and exported in tiff extension from MiraxViewer in order to align the slices on Adobe Photoshop. Image size and resolution (11655X9140 pixels/50dpi /304MB) were change to 8000 X8370 pixels/ 300dpi/196MB. Arrow - periodontal ligament (PDL).

After digitizing images, these were open on Mirax Viewer and the region of interest was select and exported as tiff images generating files of ~ 400MB (figure 2.6).

Those images were observed on Photoshop, and the follow steps were done: **STEP 1** - Image size, changed to 300dpi and 8000 pixels; **STEP 2** - Load a stack of those images for further alignment ; **STEP 3** - Image registration : using scale and

rotation – scaling was needed to be able to align the images as the inherent deformation from histological technique do not allow for registration using only rotation and translation; **STEP 4** - Images saved as tiff, generating files of ~168MB.

Then, images were prepared to be visualized for 3 different goals. First for image sequence visualization, second for image observation and measurements of number of nerve fibres (chapter 3) and the third for segmentation and 3D model reconstruction. As it is described below:

1. Image sequence:

STEP 1 - Image size changed to 5MB to allow visualization on Image J (National Institutes of Health)

STEP 2 - Import image sequence on Image J

2. Image observation and measurements:

STEP 1 - PDL delimitation (segmentation). **STEP 2** - Demarcation and labelling of observed structures in layers at photoshop, allow comparison with other images (figure 2.7).

3. Segmentation and 3D model

STEP 1 - After segmentation of PDL, bone and tooth root were segmented generating images illustrated in figure 2.8.

STEP 2 - Registration: After selecting and exporting the ROI, a global alignment was done using Adobe Photoshop CS4 (*Adobe Systems, USA*). A stack of slices were loaded using several layers and the alignment were executed using rotation and scale tools. This scale tool performed an elastic transformation on the slices.

STEP 3 - 3D Model: Six types of structures were segmented on 15 slices : blood vessels, isolated fibres and group fibres in the PDL, root and pulp. The segmentation was done on each image separately by drawing with a pen in a tablet PC and then saved in a lower resolution (1322X1322/300dpi/5MB). Each structure type at the low resolution images were labelled by colours (figure 2.9) using Reconstruct software (*Synapse Web, KristenM. Harris, PI, <http://synapses.clm.utexas.edu/>*) before using the 3D Model reconstruction tool.

The segmentation on Reconstruct software was done by tracing lines within the sections to specify the structure profiles on each slice. Each structure profile received a label, and all profiles which shared the same label belong to the same 3D object. This allowed the 3D objects to be extracted from section files by grouping together all the profiles with the same label.

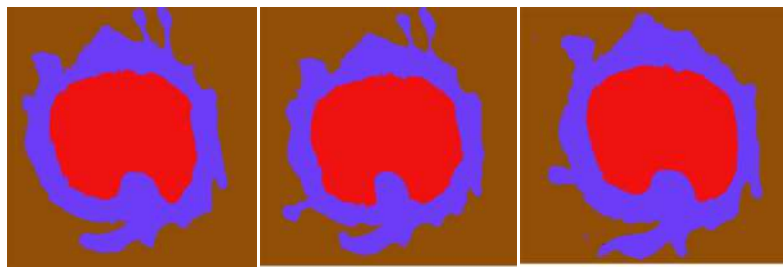


Figure 2.7: Three histological slices after segmentation of tooth root, represented in red, PDL (purple) and alveolar bone (brown).

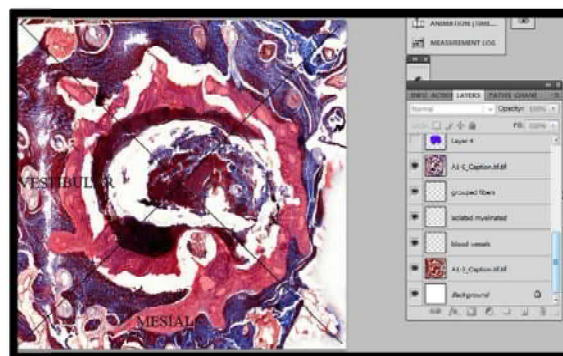


Figure 2.8: Axial slice of canine tooth and its support tissues. Segmentation of PDL in red, arrows indicate the layers created at Adobe Photoshop.

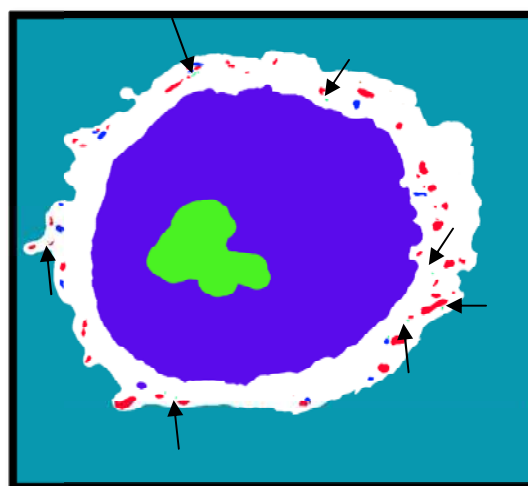


Figure 2.9: Segmented image prepared for 3D reconstruction. Pulp is represented in green, root in purple; PDL-white; Blood vessels-red; grouped myelinated nerve fibres - blue; isolated nerve fibres – in green (black arrows).

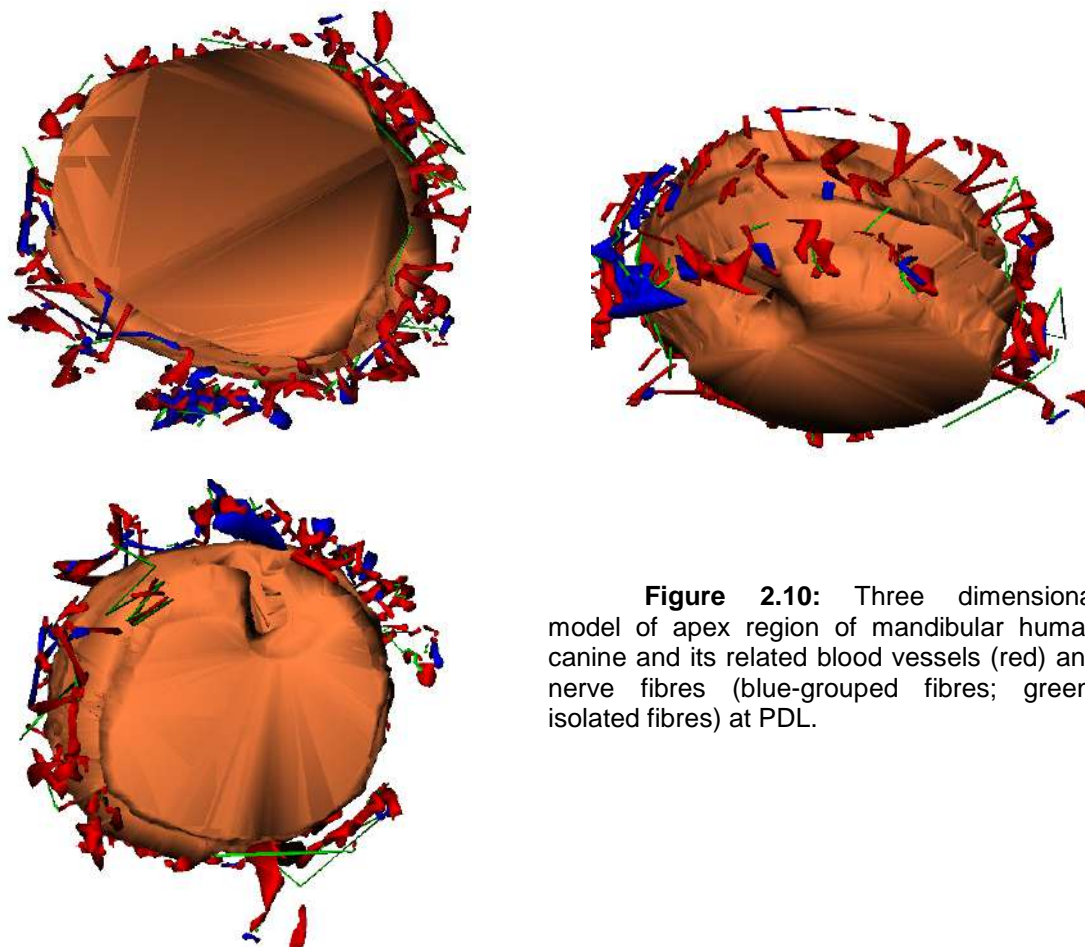


Figure 2.10: Three dimensional model of apex region of mandibular human canine and its related blood vessels (red) and nerve fibres (blue-grouped fibres; green-isolated fibres) at PDL.

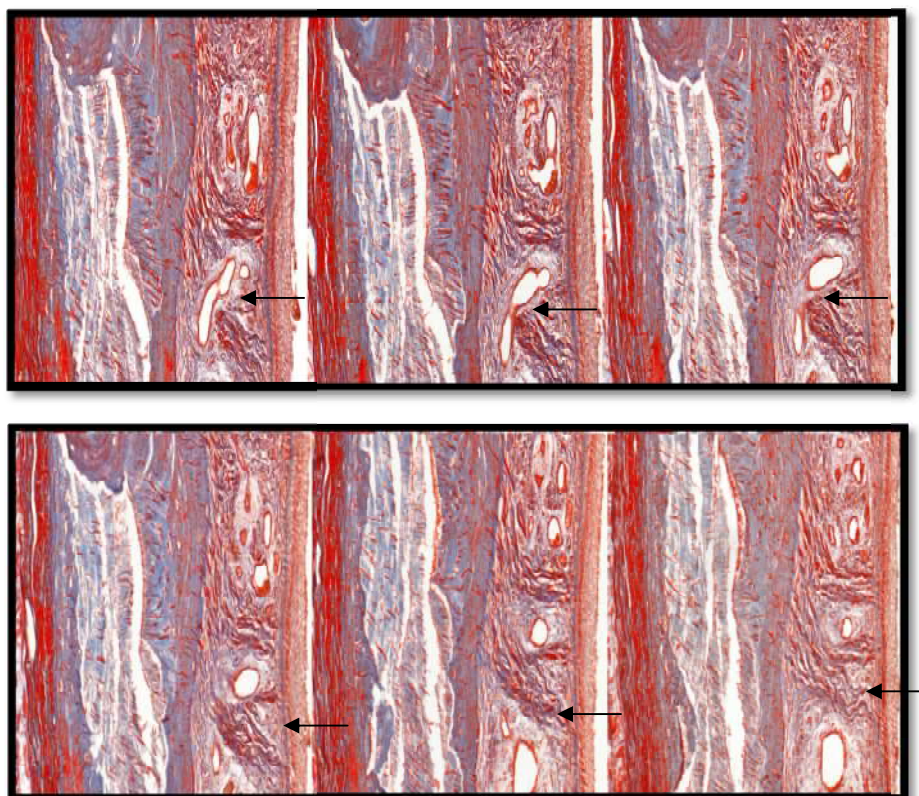


Figure 2.11: Image sequence after registering digital histological slices. Note that nerve and vessels branches and take several direction along the slices. Some collagen fibres can be seen crossing a branching blood vessel (black arrows).

Results

Three-dimensional models and image sequence visualization of some PDL structures could be obtained with light microscopic 2D images of a PDL from a human canine tooth (figure 2.10).

The 3D model showed numerous blood vessels and a number of myelinated nerve fibres around the tooth apex. Grouped and myelinated nerve fibres could be detected together with numerous blood vessels. Yet, isolated nerve fibres were seen in less amount and having a more tortuous trajectory compared to grouped myelinated nerve fibres. The image sequence visualization allow to scroll easily through out the histological slices and to follow the structures within the tissue as well as its alterations along its length, facilitating 3D extrapolations (figure 2.11).

Discussion

Although 2D histological slices have a great impact on quantification and visualization of data, 3D volume reconstruction from these 2D slices is required in order to fully appreciate anatomical structures (*Bagci and Bai 2008*). Three dimensional images make it easier to comprehend complex structures and can influence teaching, learning and researching approaches related to Anatomy and Physiology. Several research fields have been involved in the development of new imaging techniques which can provide three dimensional descriptions of anatomical structures and biological tissues (*Thiele et al 2013; Lidke and Lidke 2012; Cifor et al 2011*). In addition, the knowledge of the structure of biological specimens is critical to understanding their functions at all scales and is crucial in biosciences to complement biomechanical and biochemical studies (*Thiele et al 2013; Jayo and Parsons 2012; Rahimi et al 2005*).

Substantial progress has been made in the medical field, yet a detailed description of some oral structures are still lacking a 3D characterization. Those oral structures include the periodontal ligament, a soft tissue mainly composed by connective tissue and some other particular components. This tissue, which is highly responsible for tooth support and mechanosensory function, has a complex spatial arrangement important to be determined. This spatial arrangement is relevant to identify the loads acting on this tissue during oral function (*Naveh et al 2012a*).

In this study, continuous and non-continuous blood vessels, as well as grouped and isolated myelinated nerve fibres were reconstructed around the tooth apex. The

lack of continuity between the same structures in the different sections may be caused by an alteration in the running direction avoiding the structure to be depicted in all histological sections. This creates a gap between sections illustrated by the absence of connection of vessels or fibres at same position in different sections. Yet, this gap may be also consequence of a space between section due to the loss of material during histological preparation. Besides, although the complete tooth was cut into consecutive slices, not all consecutive slices could be used for analysis and reconstruction. Some slices did not show a good image quality due to inherent limitations to the histological preparation (e.g.: slice deformation; over-staining and other artifacts). In turn, this has influenced in the discontinuity of some structures, and is one of limitations that are needed to overcome to be able to obtain better 3D reconstructions from histological slices.

The more tortuous trajectory of isolated nerve fibres illustrated by our 3D model illustrates the typical description of 2D morphological studies which reported that these fibres are more frequently in the cemental related part of the PDL than the grouped nerve fibres. Thus, those fibres may run from the alveolar related part, probably branching from grouped myelinated fibres and acquiring a more commonly a tortuous trajectory.

Computer-based 3D visualizations reconstructed from sectional images represent a valuable tool in biomedical research and medical diagnosis. Particularly with those imaging technique that provide virtual sections, such as CT and MRI, 3D reconstructions have become routine (*Feuerstein et al 2011; Dauguet et al 2007*). Reconstructions from physical sections, such as those used in histological preparations, have not experienced an equivalent breakthrough, due to inherent shortcomings in sectional preparation that impede automated image-processing and reconstruction (*Cifor et al 2011; Streicher et al 1997*).

Three major obstacles are noticed to automated 3D reconstruction from serial physical sections: misalignment, distortion and staining variation. In our study, the dimensional distortion and the heterogenous pigmentation were the main challenges since they considerably increased the time spent on registration and segmentation of images. Since histological slices changed smoothly from slice to slice and the section distortions induced by the preparation process were local in nature, accurate alignment of these slices could only be achieved by using elastic registration methods, similarly to Bagci and Bai (2008).

To understand the arrangement and distribution of intra-epithelial vessels and their function, Cerri et al (2004) used light microscopy to create a computer 3D reconstruction of the blood capillaries of the enamel organ of rat molar. Besides light microscopy, other images techniques have been applied on 3D reconstruction of physical slices, such as orthogonal plane fluorescence optical sectioning microscopy (*Hofman et al 2009*), scanning transmission electron microscopy (*de Jonge et al 2010*) and confocal scanning laser microscopy (*Buda et al 2009*).

Kannari (1990) has presented a computerized 3D reconstruction of PDL Ruffini endings of hamster incisors. They used 20 electron micrographs at 1.0 μ m intervals which were enlarged and printed on glossy papers. Several fibre terminals of Ruffini endings were serially traced on a graph paper. Information on the outline of the fibre terminals and their Schwann sheaths was serially input into a 3D graphic analytic system based on three fiducial points for reconstruction. A surface-model from this system showed the shape of the fibre terminals and their relationship to the terminal Schwann cells. Two types of fibre terminals were mingled in one Ruffini ending, the plate-like terminals, more numerous, and the knob-type.

Streicher et al (1997) proposed a new method for 3D reconstruction using external markers for realignment of the sectional images and for geometric correction of distortion. Besides, a self-adapting dynamic thresholding technique was used to compensate for artifactual staining variation. It is important to highlight that the images used in our study were not prepared to be used in computerized approach. Those were data collected for conventional 2D observations. As the acquisition processes of different 2D histological images are performed independently, slice misalignment and deformation is often unavoidable. The deformation varies from section to section and non-coherent distortions may exist in consecutive sections. Therefore, our data only allowed us to give the first steps on this technique and identify the main drawbacks needed to be overcome in future histological preparations for a computerized approach.

Simulations based on finite elements methods are in part replacing biomechanical measurements of loading of biological tissues, such as bone, teeth and ligaments by certain force systems (*Rahimi et al 2005*). Finite elements models are used to calculate force/deflection diagram and are applied in the dental field to study the biomechanics of oral implants, orthodontic tooth movements, or design and

verification of mechanical properties of prosthetic partial dentures and bridges (*Rahimi et al 2005*).

A critical review revealed that significant variations exist, some of six orders of magnitude, in the PDL's elastic constant and mechanical properties (*Fill et al 2011*). One key factor to realistic and validated simulations is the precise reconstruction of a specimen and its segmentation into the materials it is composed of (*Rahimi et al 2005*). *Rahimi et al (2005)* presented a FE model generation based on different imaging modalities including microscopic images of histological serial sections, μ CT scans as well as CT- and MRI-images of different specimens. The contours of the different structures were determined using interactively specified interpolation points.

In this way, future researches should use mutual information from histological and other image modalities for 3D reconstruction aimed to generate high quality finite element meshes of PDL. Furthermore, to depict the real 3D arrangement of PDL might improve the knowledge about this structure, as well as it may facilitate to visualise and understand PDL function and importance to the oral system.

Conclusions:

Mechanoreceptors in the PDL have been described according to their morphology, neurophysiological aspects, spatial arrangement and functional significance and as such to permit the understanding of the mechanosensory function in teeth. Similar efforts should be made to describe mechanoreception around implants. It has been confirmed that most functions regarded as those of the mechanoreceptors in the PDL are partially restored after implant treatment. Psychophysical tests, masticatory efficiency, as well as bite force assessments showed the appropriate scientific evidence for such observation.

Three-dimensional volume reconstruction from 2D histological slices may have great potential in visualising the complex PDL anatomy, spatial arrangement and interrelationship among the different PDL structures. The present study is the first to histologically visualise 3D human periodontal ligament structures. Further research is needed to adapt histological slicing for refined 3D histological imaging. Future approaches should combine information from different imaging techniques, such as histological and radiological 3D reconstructions.

These factors can limit our understanding of periodontal, peri-implant and newly formed bone at biomechanical level. Further improvement on periodontal, peri-implant and bone tissue researches should allow a more objective and standardized analysis of these tissues. Focus should also be put on human bone and tissue innervation.

References:

- Archangelo CM, Rocha EP, Pereira JA, Martin Junior M, Anchieta RB, Freitas Júnior AC. Periodontal ligament influence on the stress distribution in a removable partial denture supported by implant: a finite element analysis. *J Appl Oral Sci* 2012;20:362-8.
- Alajbeg IZ, Valentic-Peruzovic M, Alajbeg I, Illes D, Celebic A. The influence of dental status on masticatory muscle activity in elderly patients. *Int J Prosthodont* 2005; 18:333-8.
- Alajbeg IZ, Valentic-Peruzovic M, Alajbeg I, Cifrek M. The influence of age and dental status on elevator and depressor muscle activity. *J Oral Rehabil* 2006; 33:94-101.
- Alkhamrah BA, Hoshino N, Kawano Y, Harada F, Hanada K, Maeda T. The periodontal Ruffini endings in brain derived neurotrophic factor (BDNF) deficient mice. *Arch Histol Cytol* 2003; 66:73-81.
- Ariga K, Mori T and Jonathan P. Hill. Control of nano/molecular systems by application of macroscopic mechanical stimuli. *Chem Sci* 2011; 2:195–203.
- Atsumi Y, Imai T, Matsumoto K, Sakuda M, Maeda T, Kurisu K, Wakisaka S. Effects of different types of injury to the inferior alveolar nerve on the behaviour of Schwann cells during the regeneration of periodontal nerve fibres of rat incisor. *Arch Histol Cytol* 2000; 63:43-54.
- Atsumi Y, Matsumoto K, Sakuda M, Maeda T, Kurisu K, Wakisaka S. Altered distribution of Schwann cells in the periodontal ligament of the rat incisor following resection of the inferior alveolar nerve: an immunohistochemical study on S-100 proteins. *Brain Res* 1999; 849:187-95.
- Bagci U, Bai L. Fully automatic 3D reconstruction of histological images. *Biomedical Imaging: From Nano to Macro. ISBI 2008. 5th IEEE International Symposium May 2008: 991 – 994.*
- Boggio V, Ladizesky MG, Cutrera RA, Cardinali DP. Autonomic neural signals in bone: physiological implications for mandible and dental growth. *Life Sci* 2004; 75:383-95.
- Bonte B, Linden RW, Scott BJ, van Steenberghe D. Role of periodontal mechanoreceptors in evoking reflexes in the jaw-closing muscles of the cat. *J Physiol* 1993; 465:581-94.
- Bonte B, van Steenberghe D. Masseteric post-stimulus EMG complex following mechanical stimulation of osseointegrated oral implants. *J Oral Rehabil* 1991; 18:221-9.
- Buda GJ, Isaacson T, Matas AJ, Paolillo DJ, Rose JK. Three-dimensional imaging of plant cuticle architecture using confocal scanning laser microscopy. *Plant J* 2009; 60:378-85.

- Byers MR. Sensory innervation of periodontal ligament of rat molars consists of unencapsulated Ruffini-like mechanoreceptors and free nerve endings. *J Comp Neurol* 1985; 231:500-18.
- Byers MR, Dong WK. Comparison of trigeminal receptor location and structure in the periodontal ligament of different types of teeth from the rat, cat, and monkey. *J Comp Neurol* 1989; 279:117-27.
- Byers MR, Holland GR. Trigeminal nerve endings in gingiva, junctional epithelium and periodontal ligament of rat molars as demonstrated by autoradiography. *Anat Rec* 1977; 188:509-23.
- Byers MR, O'Connor TA, Martin RF, Dong WK. Mesencephalic trigeminal sensory neurons of cat: axon pathways and structure of mechanoreceptive endings in periodontal ligament. *J Comp Neurol* 1986; 250:181-91.
- Cash RM, Linden RW. The distribution of mechanoreceptors in the periodontal ligament of the mandibular canine tooth of the cat. *J Physiol* 1982; 330:439-47.a
- Cash RM, Linden RW. Effects of sympathetic nerve stimulation on intra-oral mechanoreceptor activity in the cat. *J Physiol* 1982; 329:451-63.b
- Cerri PS, de Faria FP, Villa RG, Katchburian E. Light microscopy and computer three-dimensional reconstruction of the blood capillaries of the enamel organ of rat molar tooth germs. *J Anat* 2004; 204:191-5.
- Cifor A, Bai L, Pitiot A. Smoothness-guided 3-D reconstruction of 2-D histological images. *Neuroimage* 2011; 56:197-211.
- Cifor A, Pridmore T, Pitiot A. Smooth 3-D reconstruction for 2-D histological images. *Inf Process Med Imaging* 2009; 21:350-61.
- Dauguet J, Delzescaux T, Condé F, Mangin JF, Ayache N, Hantraye P, Frouin V. Three-dimensional reconstruction of stained histological slices and 3D non-linear registration with in-vivo MRI for whole baboon brain. *J Neurosci Methods* 2007; 164:191-204.
- de Jonge N, Sougrat R, Northan BM, Pennycook SJ. Three-dimensional scanning transmission electron microscopy of biological specimens. *Microsc Microanal* 2010; 16:54-63.
- Duncan RC, Storey AT, Rugh JD, Parel SM. Electromyographic activity of the jaw-closing muscles in patients with osseointegrated implant fixed partial dentures. *J Prosthet Dent* 1992; 67:544-9.
- Everts V, Beertsen W, van den Hooff A. Fine structure of an end organ in the periodontal ligament of the mouse incisor. *Anat Rec* 1977; 189:73-89.
- Feuerstein M, Heibel H, Gardiazabal J, Navab N, Groher M. Reconstruction of 3-D histology images by simultaneous deformable registration. *Med Image Comput Assist Interv* 2011; 14:582-9.
- Fill TS, Carey JP, Toogood RW, Major PW. Experimentally determined mechanical properties of, and models for, the periodontal ligament: critical review of current literature. *J Dent Biomech* 2011; 2011:312980.
- Gillespie PG, Walker RG. Molecular basis of mechanosensory transduction. *Nature* 2001; 413:194-202.
- Griffin CJ, Spain H. Organization and vasculature of human periodontal ligament mechanoreceptors. *Arch Oral Biol* 1972; 17:913-21.
- Halata Z, Munger BL. Sensory nerve endings in rhesus monkey sinus hairs. *J Comp Neurol* 1980; 192:645-63.
- Harada F, Hoshino N, Hanada K, Kawano Y, Atsumi Y, Wakisaka S, Maeda T. The involvement of brain-derived neurotrophic factor (BDNF) in the

- regeneration of periodontal Ruffini endings following transection of the inferior alveolar nerve. *Arch Histol Cytol* 2003; 66:183-94.
- Haraldson T. Comparisons of chewing patterns in patients with bridges supported on osseointegrated implants and subjects with natural dentitions. *Acta Odontol Scand* 1983; 41:203-8.
- Haraldson T, Ingervall B. Silent period and jaw jerk reflex in patients with osseointegrated oral implant bridges. *Scand J Dent Res* 1979; 87:365-72.
- Hassanali J. Quantitative and somatotopic mapping of neurones in the trigeminal mesencephalic nucleus and ganglion innervating teeth in monkey and baboon. *Arch Oral Biol* 1997; 42:673-82.
- Heasman PA. The myelinated fibre content of human inferior alveolar nerves from dentate and edentulous subjects. *J Dent* 1984; 12:283-6.
- Heasman PA, Beynon AD. Myelinated fibre diameters of human inferior alveolar nerves. *Arch Oral Biol* 1986; 31:785-7.
- Hidaka O, Morimoto T, Masuda Y, Kato T, Matsuo R, Inoue T, Kobayashi M, Takada K. Regulation of masticatory force during cortically induced rhythmic jaw movements in the anesthetized rabbit. *J Neurophysiol* 1997; 77:3168-79.
- Hildebrand C, Fried K, Tuisku F, Johansson CS. Teeth and tooth nerves. *Prog Neurobiol* 1995 ; 45:165-222.
- Hitomi Y, Suzuki A, Kawano Y, Nozawa-Inoue K, Inoue M, Maeda T. Immunohistochemical detection of ENaC β in the terminal Schwann cells associated with the periodontal Ruffini endings of the rat incisor. *Biomed Res* 2009; 30:113-9.
- Hofman R, Segenhout JM, Wit HP. Three-dimensional reconstruction of the guinea pig inner ear, comparison of OPFOS and light microscopy, applications of 3D reconstruction. *J Microsc* 2009; 233:251-7.
- Hoshino N, Harada F, Alkhamrah BA, Aita M, Kawano Y, Hanada K, Maeda T. Involvement of brain-derived neurotrophic factor (BDNF) in the development of periodontal Ruffini endings. *Anat Rec A Discov Mol Cell Evol Biol* 2003; 274:807-16.
- Igarashi Y, Aita M, Suzuki A, Nandasena T, Kawano Y, Nozawa-Inoue K, Maeda T. Involvement of GDNF and its receptors in the maturation of the periodontal Ruffini endings. *Neurosci Lett* 2007; 412:222-6.
- Imai T, Atsumi Y, Matsumoto K, Yura Y, Wakisaka S. Regeneration of periodontal Ruffini endings of rat lower incisors following nerve cross-anastomosis with mental nerve. *Brain Res* 2003; 992:20-9.
- Inoue T, Kato T, Masuda Y, Nakamura T, Kawamura Y, Morimoto T. Modifications of masticatory behavior after trigeminal deafferentation in the rabbit. *Exp Brain Res* 1989; 74:579-91.
- Jacobs R, van Steenberghe D. Qualitative evaluation of the masseteric poststimulus EMG complex following mechanical or acoustic stimulation of osseointegrated oral implants. *Int J Oral Maxillofac Implants* 1995; 10:175-82.
- Jacobs R, van Steenberghe D. Role of periodontal ligament receptors in the tactile function of teeth: a review. *J Periodontal Res* 1994; 29:153-67.
- Jayawardena CK, Takahashi N, Takano Y. A unique localization of mechanoreceptors in the periodontal tissue of guinea pig teeth. *Arch Histol Cytol* 2002; 65:233-44.
- Jayawardena CK, Takano Y. Nerve-epithelium association in the periodontal ligament of guinea pig teeth. *Arch Oral Biol* 2006; 51:587-95.

- Jayo A, Parsons M. Imaging of cell adhesion events in 3D matrix environments. *Eur J Cell Biol* 2012; 91:824-33.
- Johnsen SE, Trulsson M. Encoding of amplitude and rate of tooth loads by human periodontal afferents from premolar and molar teeth. *J Neurophysiol* 2005; 93:1889-97.
- Johnsen SE, Trulsson M. Receptive field properties of human periodontal afferents responding to loading of premolar and molar teeth. *J Neurophysiol* 2003; 89:1478-87.
- Jyväsjärvi E, Kniffki KD, Mengel MK. Functional characteristics of afferent C fibres from tooth pulp and periodontal ligament. *Prog Brain Res.* 1988;74:237-45.
- Kannari K. Sensory receptors in the periodontal ligament of hamster incisors with special reference to the distribution, ultrastructure and three-dimensional reconstruction of Ruffini endings. *Arch Histol Cytol* 1990; 53:559-73.
- Kjaer I, Nolting D. The human periodontal membrane: focusing on the spatial interrelation between the epithelial layer of Malassez, fibres, and innervation. *Acta Odontol Scand* 2009; 67:134-8.
- Kubota K, Osanai K (1977). Periodontal sensory innervation of the dentition of the Japanese shrew-mole. *J Dent Res* 56:531-537.
- Lambrichts I, Creemers J, Vansteenbergh D. Morphology of neural endings in the human periodontal ligament: an electron microscopic study. *Journal of Periodontal Research* 1992; 27:191-196.
- Lewinsky W, Stewart D. The Innervation of the Periodontal Membrane of the Cat, with some Observations on the Function of the End-Organs found in that Structure. *J Anat* 1937; 71:232-5.
- Lidke DS, Lidke KA. Advances in high-resolution imaging--techniques for three-dimensional imaging of cellular structures. *J Cell Sci* 2012; 125:2571-80.
- Lin JD, Özcoban H, Greene JP, Jang AT, Djomehri SI, Fahey KP, Hunter LL, Schneider GA, Ho SP. Biomechanics of a bone-periodontal ligament-tooth fibrous joint. *J Biomech* 2013; 46:443-9.
- Linden RW. An update on the innervation of the periodontal ligament. *Eur J Orthod* 1990; 12:91-100.a
- Linden RW. Periodontal mechanoreceptors and their function. In: Taylor A (ed) *Neurophysiology of the jaws and teeth.* The Macmillan press 1990: 52-95.b
- Linden RW, Millar BJ. The response characteristics of mechanoreceptors related to their position in the cat canine periodontal ligament. *Arch Oral Biol* 1988; 33:51-6.
- Linden RW, Scott BJ. The site and distribution of mechanoreceptors in the periodontal ligament of the cat represented in the mesencephalic nucleus and their possible regeneration following tooth extraction. *Prog Brain Res* 1988; 74:231-6.
- Linden RW, Scott BJ. Distribution of mesencephalic nucleus and trigeminal ganglion mechanoreceptors in the periodontal ligament of the cat. *J Physiol* 1989; 410:35-44.a
- Linden RW, Scott BJ. The effect of tooth extraction on periodontal ligament mechanoreceptors represented in the mesencephalic nucleus of the cat. *Arch Oral Biol* 1989; 34:937-4. b
- Lobbezoo F, Trulsson M, Jacobs R, Svensson P, Cadden SW, van Steenberghe D. Topical review: modulation of trigeminal sensory input in humans: mechanisms and clinical implications. *J Orofac Pain* 2002; 16:9-21.

- Loescher AR, Robinson PP. Properties of periodontal mechanoreceptors supplying the cat's lower canine at short and long periods after reinnervation. *J Physiol* 1991; 444:85-9.a
- Loescher AR, Robinson PP. Characteristics of periodontal mechanoreceptors supplying reimplanted canine teeth in cats. *Arch Oral Biol* 1991; 36:33-40. b
- Loescher AR, Robinson PP. Receptor characteristics of periodontal mechanosensitive units supplying the cat's lower canine. *J Neurophysiol* 1989; 62:971-8.a
- Loescher AR, Robinson PP. Properties of reinnervated periodontal mechanoreceptors after inferior alveolar nerve injuries in cats. *J Neurophysiol*. 1989; 62:979-83.b
- Loescher AR, Holland GR. Distribution and morphological characteristics of axons in the periodontal ligament of cat canine teeth and the changes observed after reinnervation. *Anat Rec* 1991; 230:57-72.
- Long A, Loescher AR, Robinson PP. A quantitative study on the myelinated fibre innervation of the periodontal ligament of cat canine teeth. *J Dent Res* 1995; 74:1310-7.
- Lumpkin EA, Bautista DM. Feeling the pressure in mammalian somatosensation. *Curr Opin Neurobiol* 2005; 15:382-8.
- Lund JP, Kolta A. Generation of the central masticatory pattern and its modification by sensory feedback. *Dysphagia* 2006; 21:167-74.
- Maeda T, Ochi K, Nakakura-Ohshima K, Youn SH, Wakisaka S. The Ruffini ending as the primary mechanoreceptor in the periodontal ligament: its morphology, cytochemical features, regeneration, and development. *Crit Rev Oral Biol Med* 1999; 10:307-27.
- Maeda T, Byers MR. Different localizations of growth-associated protein (GAP-43) in mechanoreceptors and free nerve endings of adult rat periodontal ligament, dental pulp and skin. *Arch Histol Cytol* 1996; 59:291-304.
- Maeda T, Kannari K, Sato O, Iwanaga T. Nerve terminals in human periodontal ligament as demonstrated by immunohistochemistry for neurofilament protein (NFP) and S-100 protein. *Arch Histol Cytol* 1990;53:259-65.a
- Maeda T, Kannari K, Sato O, Kobayashi S, Iwanaga T, Fujita T. Cholinesterase activity in terminal Schwann cells associated with Ruffini endings in the periodontal ligament of rat incisors. *Anat Rec* 1990; 228:339-44.b
- Maeda T, Sato O, Kobayashi S, Iwanaga T, Fujita T. The ultrastructure of Ruffini endings in the periodontal ligament of rat incisors with special reference to the terminal Schwann cells (K-cells). *Anat Rec* 1989; 223:95-103.
- Maeda T. Sensory innervation of the periodontal ligament in the incisor and molar of the monkey, *Macaca fuscata*. An immunohistochemical study for neurofilament protein and glia-specific S-100 protein. *Arch Histol Jpn* 1987;50:437-54.
- Maeda T, Iwanaga T, Fujita T, Takahashi Y, Kobayashi S. Distribution of nerve fibres immunoreactive to neurofilament protein in rat molars and periodontium. *Cell Tissue Res* 1987; 294:13-23.
- Maruyama Y, Harada F, Jabbar S, Saito I, Aita M, Kawano Y, Suzuki A, Nozawa-Inoue K, Maeda T. Neurotrophin-4/5-depletion induces a delay in maturation of the periodontal Ruffini endings in mice. *Arch Histol Cytol* 2005; 68:267-88.
- Matsuo S, Ichikawa H, Silos-Santiago I, Kiyomiya K, Kurebe M, Arends JJ, Jacquin MF. Ruffini endings are absent from the periodontal ligament of *trkB* knockout mice. *Somatosens Mot Res* 2002;19:213-7.

- Mengel MK, Jyväsjärvi E, Kniffki KD. Identification and characterization of afferent periodontal C fibres in the cat. *Pain* 1992; 48:413-20.
- Mericske-Stern R, Venetz E, Fahrländer F, Bürgin W. In vivo force measurements on maxillary implants supporting a fixed prosthesis or an overdenture: a pilot study. *J Prosthet Dent* 2000; 84:535-47.
- Millar BJ, Halata Z, Linden RW. The structure of physiologically located periodontal ligament mechanoreceptors of the cat canine tooth. *J Anat* 1989; 167:117-27.
- Muramoto T, Takano Y, Soma K. Time-related changes in periodontal mechanoreceptors in rat molars after the loss of occlusal stimuli. *Arch Histol Cytol* 2000; 63:369-80.
- Nakakura-Ohshima K, Maeda T, Ohshima H, Noda T, Takano Y. Postnatal development of periodontal ruffini endings in rat incisors: an immunoelectron microscopic study using protein gene product 9.5 (PGP 9.5) antibody. *J Comp Neurol* 1995; 362:551-64.
- Nasution FH, Toda K, Soma K. Functional maturation of periodontal mechanoreceptors during development in rats. *Brain Res Dev Brain Res* 2002; 139:307-12.
- Naveh GR, Brumfeld V, Shahar R, Weiner S. Tooth periodontal ligament: Direct 3D microCT visualization of the collagen network and how the network changes when the tooth is loaded. *J Struct Biol* 2013; 181:108-15.
- Naveh GR, Lev-Tov Chattah N, Zaslansky P, Shahar R, Weiner S. Tooth-PDL-bone complex: response to compressive loads encountered during mastication - a review. *Arch Oral Biol* 2012 a; 57:1575-84.
- Naveh GR, Shahar R, Brumfeld V, Weiner S. Tooth movements are guided by specific contact areas between the tooth root and the jaw bone: A dynamic 3D microCT study of the rat molar. *J Struct Biol* 2012 b; 177:477-83.
- Ohishi M, Harada F, Rahman F, Saito I, Kawano Y, Nozawa-Inoue K, Maeda T. GDNF expression in terminal schwann cells associated with the periodontal Ruffini endings of the rat incisors during nerve regeneration. *Anat Rec (Hoboken)* 2009; 292:1185-91.
- Page AJ, Brierley SM, Martin CM, Martinez-Salgado C, Wemmie JA, Brennan TJ, Symonds E, Omari T, Lewin GR, Welsh MJ, Blackshaw LA. The ion channel ASIC1 contributes to visceral but not cutaneous mechanoreceptor function. *Gastroenterology* 2004; 127:1739-47.
- Passatore M, Filippi GM. Sympathetic modulation of periodontal mechanoreceptors. *Arch Ital Biol* 1983; 121:55-65.
- Piyapattamin T, Takano Y, Eto K, Soma K. Morphological changes in periodontal mechanoreceptors of mouse maxillary incisors after the experimental induction of anterior crossbite: a light and electron microscopic observation using immunohistochemistry for PGP 9.5. *Eur J Orthod* 1999; 21:15-29.
- Rahimi A, Keilig L, Bendels G, Klein R, Buzug TM, Abdelgader I, Abboud M, Bourauel C. 3D reconstruction of dental specimens from 2D histological images and microCT-scans. *Comput Methods Biomech Biomed Engin* 2005; 8:167-76.
- Rahman F, Harada F, Saito I, Suzuki A, Kawano Y, Izumi K, Nozawa-Inoue K, Maeda T. Detection of acid-sensing ion channel 3 (ASIC3) in periodontal Ruffini endings of mouse incisors. *Neurosci Lett* 2011; 488:173-7.
- Rood JP. The diameters and internodal lengths of the myelinated fibres in human inferior alveolar nerve. *J Dent* 1978; 6:311-5.

- Sato O, Maeda T, Kobayashi S, Iwanaga T, Fujita T, Takahashi Y. Innervation of periodontal ligament and dental pulp in the rat incisor: an immunohistochemical investigation of neurofilament protein and glia-specific S-100 protein. *Cell Tissue Res* 1988; 251:13-21.
- Sato O, Maeda T, Iwanaga T, Kobayashi S. Innervation of the incisors and periodontal ligament in several rodents: an immunohistochemical study of neurofilament protein and glia-specific S-100 protein. *Acta Anat (Basel)* 1989; 134:94-9.
- Sessle BJ. Mechanisms of oral somatosensory and motor functions and their clinical correlates. *J Oral Rehabil* 2006; 33:243-61.
- Schroeder H E, *The Periodontium-Handboek of microscopy anatomy-Springer* 1986: 208-221
- Shi L, Kodama Y, Atsumi Y, Honma S, Wakisaka S. Requirement of occlusal force for maintenance of the terminal morphology of the periodontal Ruffini endings. *Arch Histol Cytol* 2005; 68:289-99.
- Sigal IA, Flanagan JG, Tertinegg I, Ethier CR. 3D morphometry of the human optic nerve head. *Exp Eye Res* 2010; 90:70-80.
- Streicher J, Weninger WJ, Müller GB. External marker-based automatic congruencing: a new method of 3D reconstruction from serial sections. *Anat Rec* 1997; 248:583-602.
- Stuge U, Brodin P, Bjørnland T. Masseter muscle reflex evoked by tapping on osseointegrated Frialit implants. *Int J Oral Maxillofac Implants* 1993; 8:650-4.
- Svensson KG, Trulsson M. Regulation of bite force increase during splitting of food. *Eur J Oral Sci* 2009; 117:704-10.
- Svensson KG, Trulsson M. Impaired force control during food holding and biting in subjects with tooth- or implant-supported fixed prostheses. *J Clin Periodontol* 2011; 38:1137-46.
- Svensson KG, Grigoriadis J, Trulsson M. Alterations in intraoral manipulation and splitting of food by subjects with tooth- or implant-supported fixed prostheses. *Clin Oral Implants Res* 2013; 24:549-55.
- Tabata T, Karita K. Response properties of periodontal mechanosensitive fibres in the superior dental nerve of the cat. *Exp Neurol* 1986; 94:469-78.
- Takahashi-Iwanaga H. Three-dimensional microanatomy of mechanoreceptors and their possible mechanism of sensory transduction. *Ital J Anat Embryol* 2001; 106:481-7.
- Thiele H, Heldmann S, Trede D, Strehlow J, Wirtz S, Dreher W, Berger J, Oetjen J, Kobarg JH, Fischer B, Maass P. 2D and 3D MALDI-imaging: Conceptual strategies for visualization and data mining. *Biochim Biophys Acta* 2013 [Epub ahead of print].
- Trulsson M. Force encoding by human periodontal mechanoreceptors during mastication. *Arch Oral Bio.* 2007; 52:357-60.
- Trulsson M. Sensory-motor function of human periodontal mechanoreceptors. *J Oral Rehabil* 2006; 33:262-73.
- Trulsson M, Johansson RS. Encoding of tooth loads by human periodontal afferents and their role in jaw motor control. *Prog Neurobiol* 1996; 49:267-84.
- Trulsson M. Multiple-tooth receptive fields of single human periodontal mechanoreceptive afferents. *J Neurophysiol* 1993; 69:474-81.
- Trulsson M, Johansson RS, Olsson KA. Directional sensitivity of human periodontal mechanoreceptive afferents to forces applied to the teeth. *J Physiol* 1992; 447:373-89.

- Türker KS, Sowman PF, Tuncer M, Tucker KJ, Brinkworth RS. The role of periodontal mechanoreceptors in mastication. *Arch Oral Biol* 2007; 52:361-4.
- Türker KS. Reflex control of human jaw muscles. *Crit Rev Oral Biol Med* 2002; 13:85-104.
- Umemura T, Yasuda K, Ishihama K, Yamada H, Okayama M, Hasumi-Nakayama Y, Furusawa K. A comparison of the postnatal development of muscle-spindle and periodontal-ligament neurons in the mesencephalic trigeminal nucleus of the rat. *Neurosci Lett* 2010 ; 473:155-7.
- van Kampen FM, van der Bilt A, Cune MS, Bosman F. The influence of various attachment types in mandibular implant-retained overdentures on maximum bite force and EMG. *J Dent Res* 2002; 81:170-3.
- van Steenberghe D. The structure and function of periodontal innervation. A review of the literature. *J Periodontal Res* 1979; 143:185-203.
- van Steenberghe D; Trigeminal reflexes elicited by means of endosseous implants. In: Jacobs R. (ed) *Osseoperception*. Leuven KU Leuven. 1998:157-67.
- Vandevska-Radunovic V. Neural modulation of inflammatory reactions in dental tissues incident to orthodontic tooth movement. A review of the literature *Eur J Orthod* 1999; 213: 231-47.
- Veyrone JL, Lassauzay C, Nicolas E, Peyron MA, Woda A. Mastication of model products in complete denture wearers. *Arch Oral Biol* 2007; 52:1180-5.
- Wakisaka S, Atsumi Y, Youn SH, Maeda T. Morphological and cytochemical characteristics of periodontal Ruffini ending under normal and regeneration processes. *Arch Histol Cytol* 2000; 63:91-113.
- Welsh MJ, Price MP, Xie J. Biochemical basis of touch perception: mechanosensory function of degenerin/epithelial Na⁺ channels. *J Biol Chem* 2002; 277:2369-72.

Chapter 3

Distribution of nerve fibres in the periodontal ligament

Publication related to this chapter:

Huang Y, Corpas LS, Martens W, Jacobs R, Lambrichts I. Histomorphological study of myelinated nerve fibres in the periodontal ligament of human canine. *Acta Odontol Scand* 2011; 69:279-86.

Histomorphological study of myelinated nerve fibres in the periodontal ligament of human canine

Abstract

Objective: The aim of this study was to compare the distribution of myelinated nerve fibres in the PDL around human canine tooth to the distribution previously described in animals. **Material and Methods:** A human mandibular canine was donated with the surrounding PDL and alveolar bone to the Department of Anatomy (University Hasselt). After embedding into paraffin block, the canine was horizontally cut in 6µm thin serial sections. At root levels of 0.3, 1.5, 3, 4.5 and 6 mm from apex, five slices at each level were selected and then, the number of myelinated nerve fibres was evaluated at each slice. Some slices were selected to perform immunocytochemistry enabling the ultrastructural description of the neural structures. **Results:** The distribution of myelinated fibres varied not significantly from apical to coronal level, with a total number of 38 at 0.3 mm from the apex, 25 at 1.5 mm, 25 at 3 mm, 31 at 4.5 mm and 32 at 6 mm. Mesial and buccal regions were typically more densely innervated ($P < 0.01$) except at the 3mm level. The average density of myelinated nerve fibres increased closer to the apex. However, the average diameter did not show any significant differences among quadrants or root levels ($P > 0.05$). The average diameter of myelinated fibres ranged from 5.3 to 8.0 µm. No linear correlation between average diameter and average density was found ($P = 0.1$). Grouped myelinated axons were twice as common as isolated ones, with the innervation being rather close to the alveolar bone. Isolated myelinated axons were observed to group around large blood vessels. Furthermore, other special structures such as cementicles and epithelial rests of Malassez were identified in close relation to the nerve fibres. **Conclusion:** The present results in humans confirmed previous observations in animals indicating a denser innervation by grouped myelinated nerve fibres at tooth apex intertwined with transverse collagen fibres and closer to the alveolar bone than to the cemental part of the PDL. It also revealed more densely innervated mesial and buccal sites of the human canine.

Introduction

The periodontal ligament (PDL) is part of the complex supporting structures around the tooth being highly involved in oral physiological actions, such as tooth support, protection, load distribution to bone and sensory feedback. This periodontal sensory feedback is strongly related to the existence of myelinated nerve fibres owing specialized terminals, such as Ruffini endings in the PDL (*Jacobs et al 1992; Jacobs and van Steenberghe 1994; Lobbezoo et al 2002; Byers 1985; Byers et al 1986; Millar et al 1994*). The rich PDL innervation guarantees a rapid and efficient conduction of action potentials along axons (*Nave and Trapp 2008*). Morphological investigations with various histological techniques have revealed that specialized endings, such as Ruffini-like endings, are the primary mechanoreceptor in the PDL. In general, they were classified as a low-threshold type II stretch mechanoreceptor, though its development, distribution and morphology vary among species, tissue and tooth types (*Maeda et al 1999*).

Contrary to cutaneous Ruffini endings, PDL Ruffini endings lack a distinct fibrous capsule (*Byers 1985 and Maeda et al 1989*). Other common features of PDL Ruffini endings were: 1. their concentration in the region where PDL fibres are most stretched when during tooth function and 2. their morphology was related to the location within the ligament, e.g. in dense collagenous tissue they showed extensive arborisation, while it was rarely seen in loose connective tissue near the blood vessels (*Maeda et al 1999*). Ultrastructurally, two types of Ruffini endings were usually present in the PDL: type 1 are Ruffini endings which possess a lamellar Schwann cells and expanded nerve endings equipped with extensions penetrating surrounding tissues and type 2 which are thinner, less branched Ruffini endings with a fewer extensions, less elaborate Schwann cells, and less basal lamina (*Byers 1985*).

The location of PDL mechanoreceptors is believed to be related to the load distribution within this ligament (*Linden 1990, Cash and Linden 1982*) and is of functional significance (*Long et al 1995*). Considering the region between the tooth fulcrum and apex, the highest displacement during tooth loading occurs at the region closer to the tooth apex (*Cash and Linden 1982*). Therefore, this would be a better location for a more efficient function of PDL mechanoreceptors. In this location the

mechanoreceptors can be activated during lower force application than if they are located near the fulcrum. Indeed, the apical third of the tooth root was found to be the most densely innervated in several studies (*Loescher and Holland 1991; Long et al 1995; Sato et al 1992; Maeda et al 1987*), mainly by slowly-adapting low-threshold mechanoreceptors (*Trulsson 2006; Trulsson and Johansson 1996; Trulsson et al 1992; Loescher and Robinson 1989*). According to Maeda et al (1999), the region around the tooth apex receives a rich innervation of both types 1 and 2 Ruffini endings, while the middle region appears to contain abundant type 2 periodontal Ruffini endings.

The distribution of myelinated nerve fibres may reflect the distribution of PDL mechanoreceptors along the tooth root. This hypothesis is based on two considerations about the PDL Ruffini endings in animals. Firstly, since PDL Ruffini endings are actually terminal parts of myelinated nerve fibres (*Long et al 1995; Loescher and Holland 1991*), the highest number of these fibres are to be expected near to the tooth apex than to its fulcrum. Secondly, the more extensive arborisation seen in type 1 Ruffini endings, mostly located near the tooth apex than in the middle region, would allow those fibres to be more frequently seen at this region. Indeed, it has been reported in several animals that the majority of mechanoreceptors are located nearer to the tooth apex (*Cash and Linden 1982*) than to its fulcrum. It has been postulated that these receptors are subjected to some form of viscous coupling to the stimulus and that the variation in the nature of PDL mechanoreceptors activity may be due to the spatial location of the receptors within the periodontal tissues (*Cash and Linden 1982*).

However contradictory results have been reported in the literature (*for review Linden 1990; Maeda et al 1999*). By immunohistochemistry, nerve fibres were found to be densely distributed in the apical third of the PDL of dog incisors and canines (*Sato et al 1992*). Nevertheless, the nerve fibre endings have been also described evenly around the tooth root (*Cash and Linden 1982*) or concentrated in the mid-way between the tooth apex and the cervical margin (*Loescher and Holland 1991*), similarly to electrophysiological studies in cats. Cash and Linden (1982) reported that PDL mechanoreceptors equally distributed along the tooth root of cat canines. On the other hand, Linden and Scott (1989) described most of mechanoreceptors located in the whole area of the ligament between the fulcrum and the canine apex in cats

(Linden and Scott 1989). Differences in distribution along the tooth root have been found regarding the adaptation features of those fibres, being slowly adapting more densely found at the tooth apex (Cash and Linden 1982) or to the origin of the cell bodies of those nerve fibres in the trigeminal ganglion or mesencephalic nucleus (Linden and Scoot 1989).

In humans, similar contradictory observations have been done, since most of mechanoreceptors have been described in the apical third of the ligament, as well as in the intermediate area between apex and cervical region (Fukuda and Tazaki 1994; Cash and Linden 1982). It is evident that human studies are more unlikely to produce true physiological records than animal studies. Thus, it is more complex to correlate morphological and functional characteristics of mechanoreceptors found in humans. To date, the knowledge on the distribution of the myelinated nerve fibres in the human PDL is far from complete. The purpose of the present study was to unravel the number and distribution of myelinated nerve fibres in the PDL of a human canine.

Material and Methods

The following experiment was carried out according to the local ethical guidelines, on a patient who had donated his body to the Department of Anatomy (University Hasselt). One periodontally healthy permanent mandibular canine with its surrounding PDL and alveolar bone tissues was collected 5 days post-mortem from a Caucasian 73- year's man.

Light Microscopy Observation

The specimens were fixed in 10% formalin solution for 3 days and decalcified in 5% nitric acid, followed by dehydration through a graded concentration of ethanol and embedded in paraffin. In total 2003 thin serial sections with a thickness of 6 µm were horizontally sectioned using a Reichert microtome (Reichert, Wien, Austria), then mounted, cleared in xylol, stained with the Masson trichrome stain and finally digitized by a high resolution Mirax Scan (Carl Zeiss Micro imaging GmbH, Germany). Observations were performed by two previously trained observers using a dedicated image software package (Mirax Viewer 1.1, Göttingen, Germany). The magnification used was of 50x and the visualization was performed in a 30 inch LCD monitor (Apple Inc., Cupertino, USA). Within all the digitized sections scanned for

observations, five sections at five root levels (0.3, 1.5, 3, 4.5 and 6 mm from the apex respectively) were randomly selected and averaged to quantify the diameter, number and density (number/area) of myelinated nerve fibres in the human PDL of a canine tooth.

To determine the number and diameter of myelinated axons around the tooth circumference, at each root level, the PDL was divided into four quadrants, named buccal, distal, lingual and mesial (Figure 1a). The area of each region and the lesser diameter of myelinated nerve fibres were manually selected and measured with a dedicated image software package (Mirax Viewer 1.1, Göttingen, Germany). To prevent the distortion which occurs when a nerve fibre is cut obliquely during the biopsy, the lesser diameter was considered as a better parameter which can represent the diameter of non-circular fibres. The fibres partially at the borderline between two regions were excluded.

Besides, sections from different levels were used to compare apical (sections at 0.3mm from the apex), intermediate (1.5mm, 3.0mm and 4.5mm) and fulcrum (6.0mm) regions regarding to diameter range and distribution by quadrants (mesial, distal, buccal and lingual regions). Similarly to Heasman and Beynon (1986) in the IAN, the diameter distribution was determined among the different root levels and quadrants.

Finally, the myelinated axons were classified into two groups (Figure 3.1b-c) as described by Loescher and Holland (1991) and Long et al (1995): grouped axons, which were those either adjacent to blood vessels or in a bundle with 3 or more other nerve fibres and isolated axons, which existed more than 20µm from a blood vessel and not in a bundle with more than 3 other fibres.

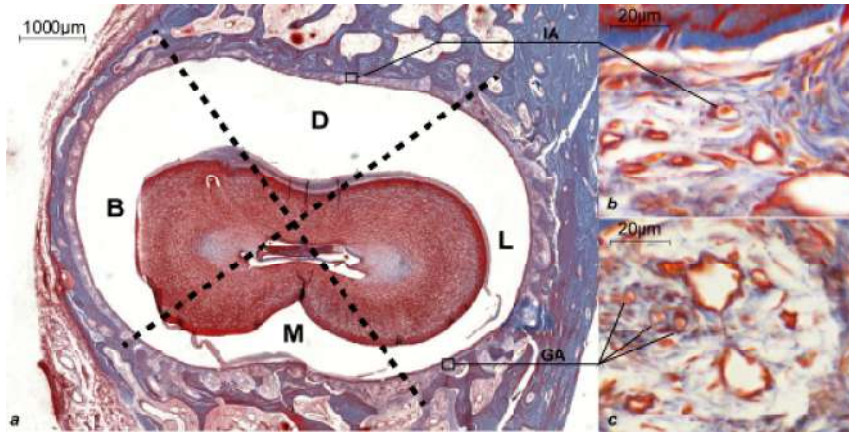


Figure 3.1. Horizontal section of the canine root with the projected line used for histomorphometrical evaluation of four quadrants of the periodontal ligament (B=buccal; D=distal; L=lingual; M=mesial; IA=isolated myelinated axons; GA=grouped myelinated axons).

Immunocytochemistry

Immunocytochemical stainings were performed using the peroxidase-based EnVision System (DakoCytomation, Glostrup, Denmark). The sections were deparaffinised and washed for 30 min at 4°C in 0.01 M phosphate buffered saline (PBS). Non-specific binding sites were blocked with 3% normal goat serum in PBS. After washing in PBS, the sections were incubated with the primary mouse monoclonal antibody against the neurofilament protein (Abcam, Cambridge, UK) for 1 hour, washed again, and incubated for 30 min with goat anti-mouse horseradish peroxidase-conjugated secondary antibodies. A highly sensitive diaminobenzidine chromogenic substrate system was used to visualize the peroxidase. After mounting in an aqueous mounting medium (Aquatex, Merck, Darmstadt, Germany), the tissue was examined using a photomicroscopy equipped with an automated camera (Nikon Eclipse 80i, Nikon Co., Japan). Control tissues were subjected to the same immunoperoxidase staining, with omission of the primary antibody.

Statistical Analysis

The distribution of nerve fibres diameters in the different root regions was observed through graphics created using JMP stats-software. A statistical software R package (version 2.8.1) was used for statistical analysis. Data were analyzed by descriptive statistics and presented as mean (SD). The two-way ANOVA test ($\alpha =$

0.05) allowed multiple comparisons between the five root levels and four quadrants. Pearson's correlation was used to compare the average density and average diameter of myelinated nerve fibres at five root levels.

Results

The PDL tissue examined around the canine sample was healthy and normal. The tooth, from the tip of the crown to the root apex, measured 22 mm in length, and the tooth root, from the apex to the alveolar crest, measured approximately 13 mm (Figure 3.2). Thus, considering the fulcrum of this tooth being situated in the mid-way of its alveolar support, our study has considered for investigation the tooth area between the fulcrum and the apex of the tooth as the histological sections observed were located maximum at 6mm from the apex.

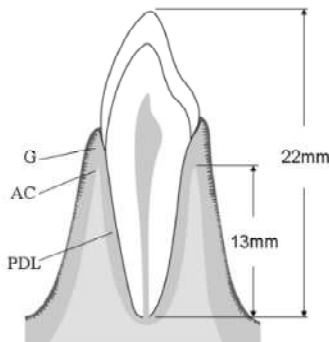


Figure 3.2. Schematic diagram of the canine sample measurement (G=gingiva; AC=alveolar crest; PDL=periodontal ligament).

The average number of myelinated axons in the PDL at level of 0.3 mm from apex was 38, sharing approximately 25.2% of five root levels, followed by 6 mm from apex with 21.2%, 4.5 mm from apex 20.5% , 3 mm and 1.5 mm with the same 16.6% (figure 3.3).

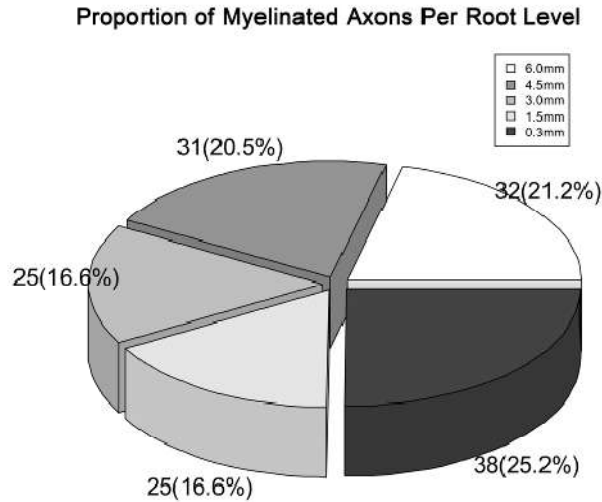


Figure 3.3. Pie chart of average number of myelinated axons in the periodontal ligament of the human canine sample at five root levels.

The average density (mm^2) of myelinated axons was highest at a 0.3 mm distance from the apex, while the lowest value occurred at a distance of 6mm from apex (figure 3.4). Furthermore, there were buccal peaks and mesial peaks of density distribution at all levels ($P < 0.01$) except at 3 mm level

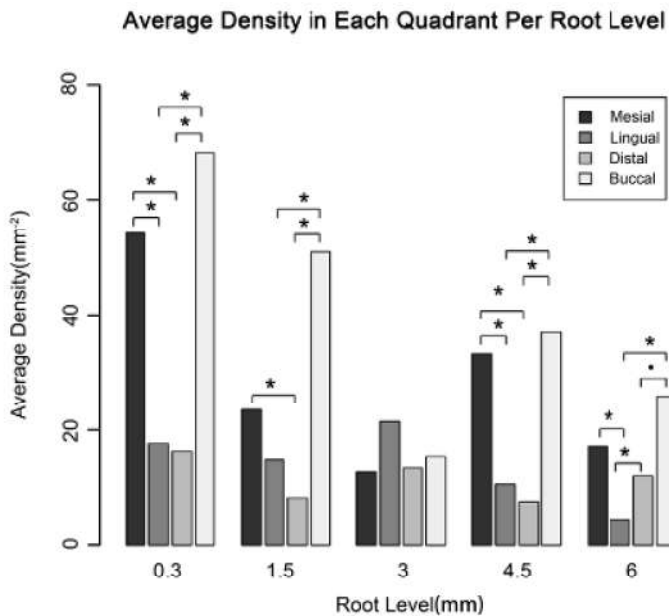


Figure 3.4. Average density of myelinated axons in different quadrants per level. Asterisks indicate the statistical difference ($\alpha < 0.05$) of density within each level. At 0.3mm and 4.5mm level, both the buccal and mesial density were significantly higher than the lingual and distal density; at 1.5mm level, the buccal density was significantly higher than the lingual and distal density, while the mesial density was only significantly higher than the distal density; at 3mm level, no significant differences in density were found within four quadrants; at 6mm level, both the buccal and mesial density showed significant differences compared with the lingual density. Significant codes: * $P < 0.01$, ' $0.05 < P < 0.1$

As shown in Table 3.1, the mean diameter of myelinated axons in the PDL of this canine ranged from 5.3 to 8.0 μm . The mean diameter did not show any significant difference in four quadrants or at five root levels ($P > 0.05$). Pearson's correlation indicated that there was no linear correlation between average diameter and average density ($r^2 = 0.12$).

Table 3.1. Average diameter of myelinated axons in the periodontal ligament of the human canine sample (μm)

Quadrants	0.3mm		1.5mm		3mm		4.5mm		6mm	
	Mean	S.D.	Mean	S.D.	Mean	S.D.	Mean	S.D.	Mean	S.D.
Mesial	6.1	2.0	7.0	2.2	7.5	2.4	7.3	2.4	6.9	2.5
Lingual	5.9	2.1	5.3	1.7	8.0	1.8	6.1	1.8	7.4	3.5
Distal	6.6	1.9	5.6	1.5	7.8	2.1	6.8	1.7	5.9	1.8
Buccal	6.3	2.0	5.9	2.2	7.1	2.1	6.3	2.3	6.4	2.5

No statistical differences were found in four quadrants per level ($\alpha = 0.05$)

The graphics on figure 3.5 shows diameter range and distribution by quadrants sections from different levels used to compare apical, intermediate and fulcrum regions. The fibre diameters ranged between 2-15 μm . The diameter distribution presented a unimodal distribution with peaks frequently found around 5-6 μm , except for the lingual side which peak was found between 8-9 μm (figure 3.6).

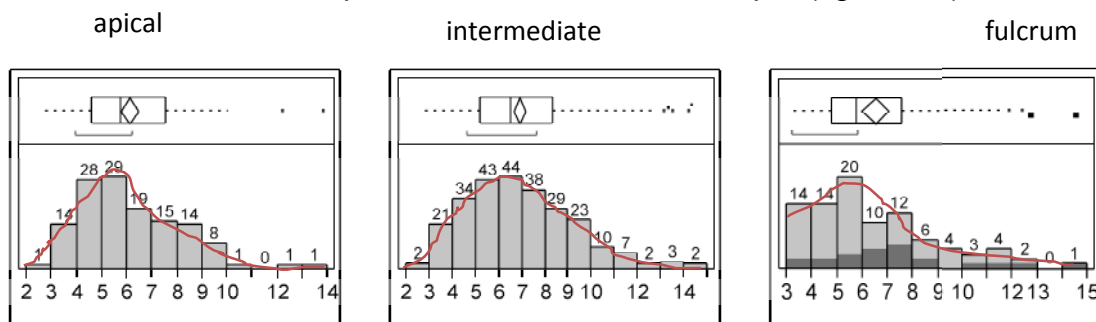


Figure 3.5. Number of nerve per diameter between the fulcrum and the apical region of the tooth root.

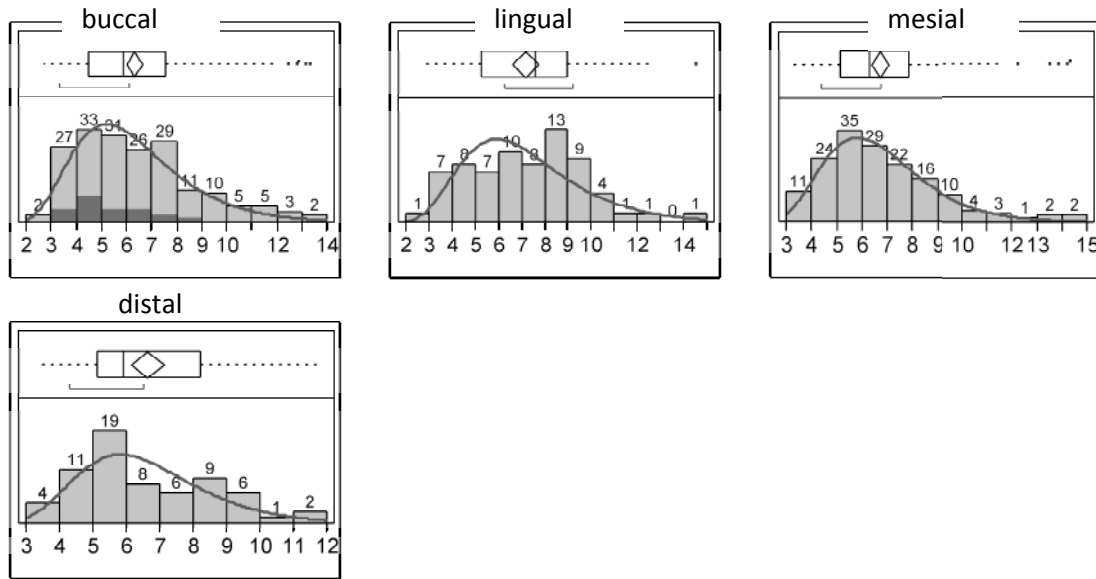


Figure 3.6. Number of nerve per diameter in the buccal, lingual, mesial and distal regions between the fulcrum and the apical region of the tooth root.

Although the diameter range was between 2-15μm, the graphics in the figure 3.7 illustrate that the highest concentration of fibres was between 3μm and 10μm, with a few number of nerve fibres larger than 10μm.

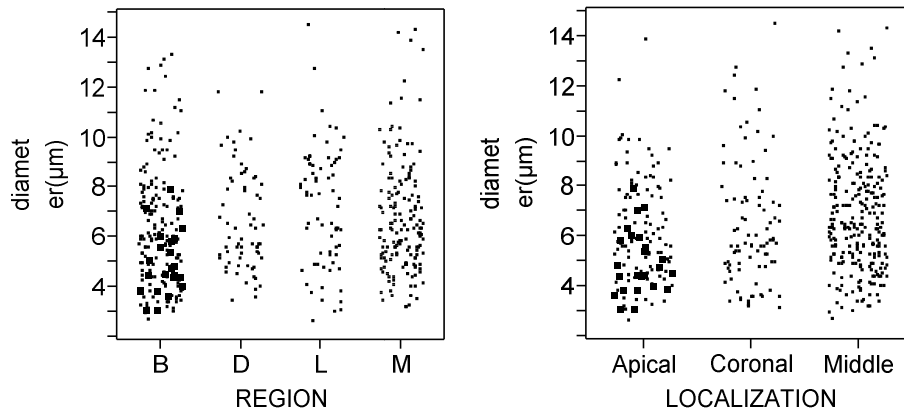


Figure 3.7. Distribution of nerve fibre diameter in the buccal, lingual, mesial and distal regions between the fulcrum and the apical region of the tooth root.

Grouped nerve fibres composing coarse nerve bundles were mostly found in the vicinity of blood vessels (figure 3.8) and seemed to branch frequently originating isolated nerve fibres. Neurovascular structures appeared to enter and/or leave the alveolar bone creating an inter-digitising relationship between PDL structures and alveolar bone.

The number of isolated myelinated axons was only half as many as that of grouped ones (table 3.2). The grouped myelinated axons were frequently observed at the alveolar-related part of the PDL, with a proportion of 83%, while the rest were present in the vicinity of the cementum. The isolated axons at alveolar-related part held 61%, though the number of isolated myelinated axons was still less than that of the grouped ones.

Table 3.2. Average number of grouped and isolated myelinated axons in the periodontal ligament (PDL) of the human canine sample at five root levels

Groups	0.3mm		1.5mm		3mm		4.5mm		6mm		Total	
	ARP		ARP		ARP		ARP		ARP		ARP	
	CRP		CRP		CRP		CRP		CRP		CRP	
GA	25	6	14	3	10	1	21	4	19	4	89	18
IA	5	2	5	3	8	6	3	3	6	3	27	17
Total	30	8	19	6	18	7	24	7	25	7	116	35

ARP=alveolar related part of PDL; CRP=cementum related part of the PDL; GA=grouped axons;

IA=isolated axons

Three histological sections presented a relationship between myelinated axons and blood vessels in the buccal PDL at the coronal level (level of 10 mm from apex) (figure 3.8). The isolated myelinated fibre showed a tendency to move towards grouped fibres around large blood vessels from the bottom upwards.

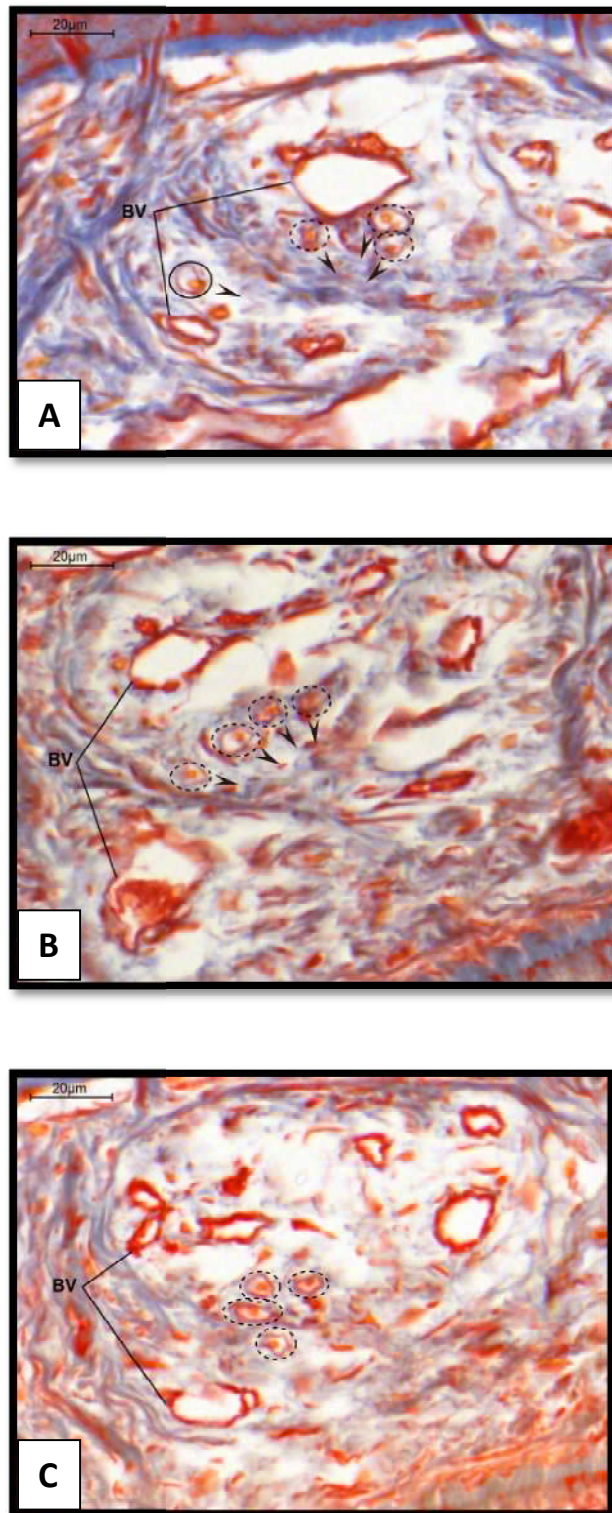


Figure 3.8. One bundle of grouped myelinated nerve fibres distributed in the mesial quadrant at coronal level of the canine root. Dotted circles indicate examples of grouped myelinated axons, and solid circles indicate examples of isolated myelinated axons (BV=blood vessel; from a to c=from bottom upward). (a) A group of three myelinated fibres were accompanied by a larger blood vessel, while an isolated myelinated axon was accompanied by a smaller blood vessel. (b) When the smaller blood vessel concoured with a distant blood vessel, the isolated myelinated axon gradually joined the previous grouped ones. (c) Finally the isolated myelinated axon became a large bundle of one grouped myelinated axons, achieving a new innervation.

Neurofilament immunoreactivity was demonstrated by the immunocytochemistry (figure 3.9). The myelinated nerve fibres around a blood vessel were clearly visualized in the section stained for neurofilament protein.

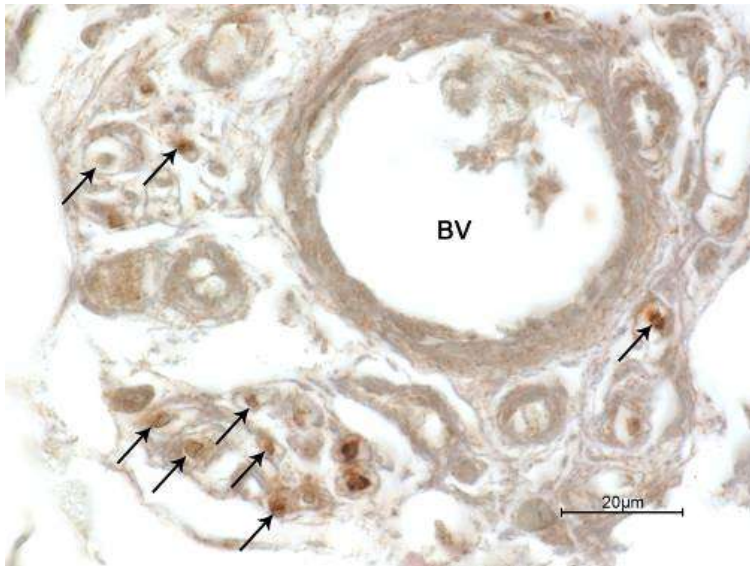


Figure 3.9. Immunocytochemical image of myelinated nerve fibres (as indicated by arrows) labelled with an antibody against the neurofiment protein. The brown colour is caused by the diaminobenzidine staining via the secondary antibody (BV=blood vessels).

Discussion

The PDL innervation plays a primary role in oral tactile function, allowing one to feel a 1-gram loading or to detect interocclusal strips of 20 μm (Jacobs *et al* 1992). This extremely sensitive system may thus allow modulating motor function or even refining the central masticatory pattern (Lund and Kolta 2006).

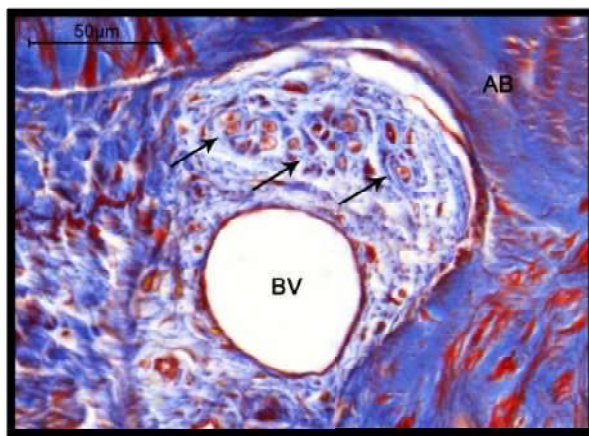


Figure 3.10. Richly innervated area in the periodontal ligament (PDL): grouped and isolated myelinated nerve fibres related or not with a blood vessel were present in the PDL, mainly in the apical region. Arrows identify grouped myelinated axons in the vicinity of blood vessels (BV=blood vessels; AB=alveolar bone).

Literature on a description of PDL innervation mainly covers papers on small animal PDL (*Byers 1985; Byers et al 1986; Kizior 1968; Kannari 1990; Sato et al 1992; Loescher and Holland 1991; Loescher et al 1993; Long et al 1995; Maeda et al 1989*). Three types of nerve endings were identified under electron microscopy, including free nerve endings (originating from myelinated and unmyelinated nerve fibres), Ruffini-like endings (mostly found at apical part of the PDL) and lamellate corpuscles (*Lambrichts et al 1992; Fukuda and Tazaki 1994; Byers and Maeda 1997*).

In our study, coarse nerve fibre bundles were mostly found in the vicinity of blood vessels (figure 3.10), branching frequently (figure 3.8). This finding has been reported in previous studies by Lambrichts et al. (1992) and Fukuda & Tazaki (1994) in humans. It is important, however, to stress that only the tooth related parts of human PDL were observed. The present study confirmed this finding by serial sections on a complete human PDL.

The number and density of myelinated axons at the apical region was the highest among the five different root levels. From the 151 myelinated nerve fibres identified in the study, 38 (25%) were found at 0.3mm distance from the tooth apex. This is in agreement with previous studies in humans showing that the tooth apical third is more innervated by nerve fibres and specialized endings (*Fukuda and Tazaki 1994, Lambrichts et al 1992, Maeda et al 1999*) than other two thirds.

However previous studies in cats (*Long et al 1995, Loescher and Holland 1991*), rats and monkeys (*Byers and Dong 1989*) have found a larger number of nerve fibres than the present investigation. This may be explained by difference in the histological techniques and samples used. In our study, nerve fibres were identified and included in the analysis when it had a clear appearance of myelinated nerve fibres for the histological technique applied. It means a blue line forming the outside rounded structure, an inside rounded brown structure representing the nucleus and a white area in between those two rounded structures. Any doubt in considering the structure seen as a nerve fibre was discussed between the two trained observers.

While two previous studies on the innervation of cat canines (*Kizior et al 1968; Loescher and Holland 1991*) and other in rat molars (*Byers 1985*) pointed out that apical fibres were generally larger than the coronal ones. The present study did not find

significant difference on the diameter between the evaluated levels and quadrants. Whether this discrepancy reflects differences on the diameter distribution in the PDL of animals and humans or not remains to be determined on larger samples and controlled studies.

Similarly to our results, Long et al (1995) have found the distribution of nerve fibres around the tooth circumference to be non-uniform. In agreement with the study of Linden and Scott (1989) in cats, the highest number of fibres in our study was found in the buccal and mesial region, whereas Long et al (1995) found it to be at distal and mesial regions at the tooth apex. The lingual region was the most sparsely innervated region in cats (*Long et al 1995*), whereas in humans this region showed higher concentration of nerve fibres of larger diameter (8-9 μ m) than the other regions (5-6 μ m). Nevertheless, no linear relationship between the average diameter and the average density was observed.

The diameter range (2-15 μ m) found in this study is in agreement with previous studies on the distribution of myelinated nerve fibres in the inferior alveolar nerve by Heasman and Beynon (1986) and Rood (1978), also in humans. Heasman and Beynon reported a bimodal curve with peaks of 2-4 μ m and 8-9 μ m. It shows that myelinated nerve fibres within these diameter range are more frequent in the alveolar inferior nerve, clearly representing two groups of fibres in a physiological classification; the first range represents fibres involved in pain and temperature sensory function (fibres A δ – 1-5 μ m) and the second, touch and pressure (fibres A β – 5-12 μ m) (*Manzano et al 2008*). Yet, we found a unimodal curve with peaks mostly found within the 5-6 μ m range in the PDL of all tooth regions and quadrants, except by the lingual. In this way, the myelinated fibres in the range of 5-6 μ m are not the most frequently seen in the alveolar inferior nerve, whereas they are the ones which innervate the PDL. Fibres larger than 12 μ m are considered A α associated to afferent nerves from muscle and from Golgi tendons organs. It is interesting to note that although fibres ranging from 2-15 μ m have been reported in the literature no report is made about the function of fibres > 12 μ m in the PDL.

Regarding the classification of grouped and isolated fibres proposed by Loescher and Holland (1991), the number of grouped axons was twice as large as that of isolated ones. Both grouped and isolated myelinated axons were frequently observed

in the alveolar related part of the PDL (table 3.2), unlike the previous findings in cats (*Loescher and Holland 1991*). In those animals, isolated fibres were situated predominantly in the cemental half of the ligament. It is probable that the alveolar half of the PDL is more prone to have a denser innervation than the cemental half due to the more extensive nutrient supply coming from alveolar bone. The function of these myelinated axons may be directly or indirectly related to the remodelling of periodontal tissue. The image sequence (figure 3.8) shows a dynamic relationship between neural structures and blood vessels suggesting that the isolated myelinated axon had a tendency to move towards large-diameter blood vessels.

Interestingly, the number of isolated fibres was greatest at 3mm from root apex, similarly to Long et al (1995). From all fibres observed at this level, 56% were isolated, being 24% found in the cemental half. It was suggested that this highest number of isolated fibres at this level may reflect the distribution of mechanoreceptors (*Long et al 1995*). Indeed, electrophysiological recordings located the majority of the receptors at 3mm and 4mm from the root apex (*Loescher and Robinson 1989*). The percentage of myelinated fibres designated as isolated in our study was 29%, thus higher than the 15-16% previously reported by Loescher and Holland (1991) and Long et al (1995).

Conclusions:

Although limited to the lower canine, the present study is the first serial section approaching at the light microscopy level performed in humans. In this study most of myelinated nerve fibres in the PDL of human canine tooth was found grouped in the vicinity of blood vessels. Those fibres were mostly seen at the alveolar part of the PDL and the highest density was found at the apical third. No functional distinction could be made from the size of those fibres since the diameter range presented may be related to several sensory functions. In all levels and quadrant, fibres larger than 10µm were found, although in a few number. The function of those fibres in the PDL has not been found in the literature.

Interesting observations could be made regarding the 3mm level which was considered the intermediate region between apex and tooth fulcrum. Firstly, isolated fibres were found in higher concentration than the grouped ones at this level.

Secondly, it showed the highest concentration of isolated fibres in the cemental half of the PDL than the other levels. Moreover, this level presented a more uniform density distribution among quadrants, whereas in all the other levels buccal and mesial quadrants were the most densely innervated. Further information should be acquired to find any potential links between morphological characters and physiological functions of myelinated nerve fibres in humans.

References

- Byers MR. Sensory innervation of periodontal ligament of rat molars consists of unencapsulate Ruffini-like mechanoreceptors and free nerve endings. *J Comp Neurol* 1985; 231:500-18.
- Byers MR, Dong WK. Comparison of trigeminal receptor location and structure in the periodontal ligament of different types of teeth from the rat, cat, and monkey. *J Comp Neurol* 1989; 279:117-27.
- Byers MR, Maeda T. Periodontal innervation: regional specializations, ultrastructure, cytochemistry and tissue interactions. *Acta Med Dent Helv* 1997; 2:116-33.
- Byers MR, O'Connor TA, Martin RF, Dong WK. Mesencephalic trigeminal sensory neurons of cat: axon pathways and structure of mechanoreceptive endings in periodontal ligament. *J Comp Neurol* 1986; 250:181-91.
- Cash RM, Linden RW. The distribution of mechanoreceptors in the periodontal ligament of the mandibular canine tooth of the cat. *J Physiol* 1982; 330:439-47.
- Fukuda M, Tazaki M. Distribution of organized sensory nerve endings in the human periodontal ligament. *Bull Tokyo Dent Coll* 1994; 35:133-7.
- Heasman PA, Beynon AD. Myelinated fibre diameters of human inferior alveolar nerves. *Arch Oral Biol* 1986; 31:785-7.
- Jacobs R, Schotte A, van Steenberghe D. Influence of temperature and foil hardness on interocclusal tactile threshold. *J Periodontal Res* 1992; 27:581-7.
- Jacobs R, van Steenberghe D. Role of periodontal ligament receptors in the tactile function of teeth: a review. *J Periodontal Res* 1994; 29:153-67.
- Kannari K. Sensory receptors in the periodontal ligament of hamster incisors with special reference to the distribution, ultrastructure and three-dimensional reconstruction of Ruffini endings. *Arch Histol Cytol* 1990; 53:559-73.
- Kizior JE, Cuozzo JW, Bowman DC. Functional and histologic assessment of the sensory innervation of the periodontal ligament of the cat. *J Dent Res* 1968; 47:59-64.
- Lambrichts I, Creemers J, van Steenberghe D. Morphology of neural endings in the human periodontal-ligament- an electron-microscopic study. *J Periodontal Res* 1992; 27:191-6.
- Linden RW. An update on the innervation of the periodontal ligament. *Eur J Orthod* 1990; 12:91-100.
- Linden RW, Scott BJ. Distribution of mesencephalic nucleus and trigeminal ganglion mechanoreceptors in the periodontal ligament of the cat. *J Physiol* 1989; 410:35-44.

- Lobbezoo F, Trulsson M, Jacobs R, Svensson P, Cadden S, van Steenberghe D. Topical review: modulation of trigeminal sensory input in humans: mechanisms and clinical implications. *J Orofac Pain* 2002; 16:9-21.
- Loescher AR, Holland GR. Distribution and morphological characteristics of axons in the periodontal ligament of cat canine teeth and the changes observed after reinnervation. *Anat Rec* 1991; 230:57-72.
- Loescher AR, Robinson PP. Receptor characteristics of periodontal mechanosensitive units supplying the cat's lower canine. *J Neurophysiol* 1989; 62:971-8.
- Loescher AR, Holland GR, Robinson PP. The distribution and morphological characteristics of axons innervating the periodontal ligament of reimplanted teeth in cats. *Arch Oral Biol* 1993; 38:813-22.
- Long A, Loescher AR, Robinson PP. A quantitative study on the myelinated fibre innervation of the periodontal ligament of cat canine teeth. *J Dent Res* 1995; 74:1310-7.
- Lund J, Kolta A. Generation of the central masticatory pattern and its modification by sensory feedback. *Dysphagia* 2006; 21:167-74.
- Maeda T, Sato O, Kobayashi S, Iwanaga T, Fujita T. The ultrastructure of Ruffini endings in the periodontal ligament of rat incisors with special reference to the terminal Schwann cells (K-cells). *Anat Rec* 1989; 223:95-103.
- Maeda T, Ochi K, Nakakura-Ohshima K, Youn SH, Wakisaka S. The Ruffini ending as the primary mechanoreceptor in the periodontal ligament: Its morphology, cytochemical features, regeneration, and development. *Crit Rev Oral Biol Med* 1999; 10:307-27.
- Manzano GM, Giuliano LM, Nóbrega JA. A brief historical note on the classification of nerve fibres. *Arq Neuropsiquiatr* 2008; 66:117-9.
- Millar BJ, Halata Z, Linden RW. A possible explanation for the response characteristics of multi-tooth periodontal ligament mechanoreceptors in the cat. *Anat Embryol (Berl)* 1994; 190:445-52.
- Nave KA, Trapp BD. Axon-glia signaling and the glial support of axon function. *Annu Rev Neurosci* 2008; 31:535-61.
- Sato O, Maeda T, Kannari K, Kawahara I, Iwanaga T, Takano Y. Innervation of the periodontal ligament in the dog with special reference to the morphology of Ruffini endings. *Arch Histol Cytol* 1992; 55:21-30.
- Rood JP. The diameters and internodal lengths of the myelinated fibres in human inferior alveolar nerve. *J Dent* 1978; 6:311-5.
- Trulsson M. Sensory-motor function of human periodontal mechanoreceptors. *J Oral Rehabil* 2006; 33:262-73.
- Trulsson M, Johansson RS, Olsson KA. Directional sensitivity of human periodontal mechanoreceptive afferents to forces applied to the teeth. *J Physiol* 1992; 447:373-89.
- Trulsson M, Johansson RS. Encoding of tooth loads by human periodontal afferents and their role in jaw motor control. *Prog Neurobiol* 1996; 49:267-84.

Chapter 4

Other PDL special structures: Epithelial Rests of Malassez and Cementicles

Publication related to this chapter:

Struys T, Schuermans J, Corpas L, Politis C, Vrielinck L, Schepers S, Jacobs R, Lambrichts I. Proliferation of epithelial rests of Malassez following auto-transplantation of third molars: a case report. *J Med Case Rep.* 2010; 19;4:328.

Introduction

The epithelial rests of Malassez (ERM) are development residues of epithelial root sheath of Hertwig (ERSH) in the PDL (*Becktor et al 2007*). ERM are histologically described as a fold of outer and inner enamel epithelium formed during tooth development (*Korkmaz et al 2011*). It is found in the inner zone of the PDL near the root cementum. Once root formation is completed, the ERSH become penetrated by several collagen bundles of PDL, resulting in a fenestrated ERM network that surrounds the tooth (*Haku et al 2011*). In this way, those structures should not be seen as isolated groups of cells, but rather as a network, similar to a fishnet surrounding the root (*Rincon et al 2006*).

The reason why ERM persist in the periodontal ligament years after the completion of the dentition is unknown (*Hildebrand et al 1995*). These cells are part of the normal structures within the periodontal ligament and it is believed that they play an important functional role that needs further investigation (*Rincon et al 2006*). It was demonstrated that the ERM cells were distributed in the PDL in a network-shaped manner along the root surface and in the furcation region. The distribution of ERM was observed to be more prominent in teeth with incomplete root formation (*Becktor et al 2007*).

Cementicles are mineralized structures that either freely reside in the periodontal ligament or adhere to the root surface (*Schroeder 1986*). True cementicles consist of a collagenous matrix intermixed with a non-collagenous ground substance. The presence of cementicles and ectopic enamel deposits on the root may compromise plaque and calculus removal. Despite the relative frequency and clinical relevance of radicular enamel deposits and cementicles, their etiology and nature are unknown (*Bosshardt and Nanci 2003*).

In the first part of this chapter, the morphology and function of ERM and cementicles (figure 4.1) is discussed based in the existing literature. In the second

part, a case report is presented about ERM structure after tooth autotransplantation.

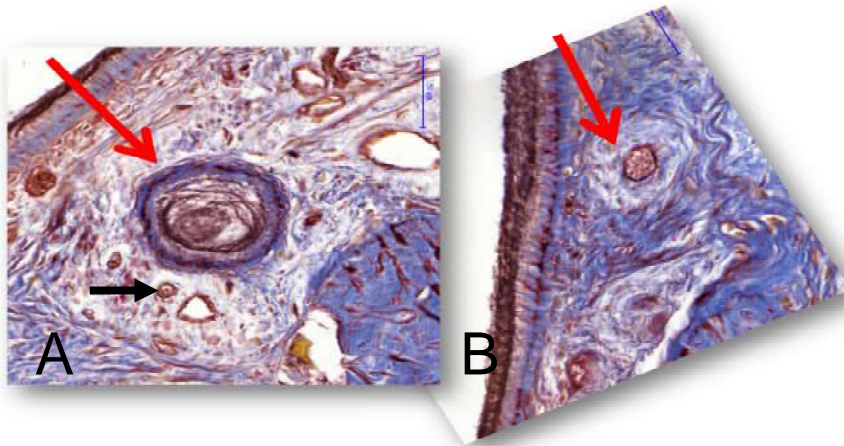


Figure 4.1: The red arrow indicates a cementicle in (A) and ERM in (B). Black arrow in (A) shows a myelinated nerve fibre in the surroundings of the cementicles.

Part I - Literature review

Epithelial Rests of Malassez

The ERM can be identified easily as small clumps of epithelial cells within the periodontal ligament, closely to the radicular cementum surface (*Rincon et al 2006*). It has been assumed that these islands of epithelial cells are important for the formation and resorption of cementum and for the prevention of ankylosis. Their main function would be to prevent root resorption and to maintain the width of the PDL, thereby preventing ankylosis (*Fujiyama et al 2004*). It was reported that proliferation of ERM occurs during experimental tooth movement (*Talic et al 2003*). In porcine, ERM cells produce prostaglandin E2 (*Brunette et al 1979*) which is capable of activating osteoclasts which stimulate bone breakdown and bone remodelling (*Kale et al 2004*). The role of ERM in preventing calcification and ankylosis of has been illustrated in a study comparing vertebrate ankylosis-type attachment and mammalian “true” periodontium (*McIntosh et al 2002*). That study demonstrated that the root of a gecko was free of ERM and at the same time connected to bone via ankylosis. Whereas in the crocodilian and mouse, root size and shape were developed from ERM, and in connection with disintegration of the ERM into ERM the periodontal ligament was established (*McIntosh et al 2002*).

Fujiyama et al (2004) found that denervation led to dento-alveolar ankylosis with a decrease in the width of the periodontal spaces. Interestingly, with regeneration of the Malassez epithelium 10 weeks after the denervation, the periodontal space width showed a correspondingly significant increase. These findings suggested that the Malassez epithelium may be involved in the maintenance of periodontal space and that it might be indirectly associated to the sensory innervation. In addition, the denervation activated root resorption of the coronal root surface and the consequently resorbed lacunae were repaired by cellular cementum. It was suggested that Malassez epithelium may negatively regulate root resorption and also induce acellular cementum formation (*Fujiyama et al 2004*). Additionally, orthodontic root resorption has been regarded as an exaggerated response to loss of PDL homeostatic control, possibly mediated by the epithelial rests of Malassez (*Kat et al 2003*).

The general morphological characteristics of the ERM have been previously described by Rincon et al (2006). They suggested that one of the functional roles of the ERM may lie not only in maintaining the normal periodontal function and cellular elements, but also contributing to the periodontal regeneration. In agreement with previous observations in animals (*Rincon et al 2006, Peters et al 1995*), a later investigation in humans (*Becktor et al 2007*) showed that the ERM were not randomly distributed cell clusters in the PDM, but appeared as an almost continuous chain of epithelial cells with regular breaks forming a network around the root. However, the ERM were described as a heterogeneous population of cells, in both cats and humans (*Tadokoro et al 2002; Kvinnsland et al 2000*). The epithelial cells seems to be intimately associated with non-epithelial, immunocompetent cells, e.g. macrophages and/or dendritic like cells. It has been suggested that epithelial and non-epithelial cell probably communicate with each other, as well as with the surrounding fibroblasts (*Tadokoro et al 2008*).

Under transmission electron microscopy (TEM) analysis, the ERM demonstrated the presence of tonofilaments and desmosomes. The tonofilaments were bound together into bundles called tonofibrils. These did not appear to be in direct contact with the cementum. The presence of tonofilaments, desmosomes and a basal lamina, with hemidesmosomes surrounding the cell rests, confirmed the epithelial nature of these cells. The average distance from the cementum to the

epithelial cells was measured in three regions – apical (21 μm), middle radicular (33 μm), and cervical (41 μm) – indicating a coronal migration away from the root surface (Valderhaug et al 1967; Rincon et al 2006). The ultrastructural characteristics differentiated the epithelial nature of these cells from fibroblasts and cementoblasts of the periodontium (Rincon et al 2006). Regarding differences between species, the ultrastructure of ERM from rat periodontal ligament sections resembles that of humans and other animals (Hamamoto et al 1989).

The ERM have a propensity to differentiate (Yamasaki and Pinero 1989) and to proliferate upon various kinds of stimuli (Tadokoro et al 2002) and they have been implicated in a number of dental pathologies (Cerri et al 2009; Ten Cate 1972). They have been observed to be associated with inflammatory developmental or neoplastic stimuli, developmental cyst formation, such as the gingival or lateral periodontal cyst (Ten Cate 1972), inflammatory cysts, odontogenic tumors and apical migration of the pocket epithelium (Spoughe 1980). The continued tooth eruption is dependent on remodelling activity in the PDL, and ERM might participate in this process (Becktor et al 2007). However, the exact factors responsible for this phase of tooth eruption are unknown. In order to contribute to this phase of tooth eruption, the periodontal membrane must be provided with two types of regulatory mechanisms: one is a calcification mechanism for differentiation of osteogenic cells for bone production and the other is a non-calcification mechanism for maintaining a fixed space. Recently, an investigation reported that ERM modulate cell proliferation and apoptosis, and inhibit differentiation by reducing the expression of specific proteins under mechanical stretching (Haku et al 2011). Further description of the protein expression, neuropeptides, extracellular matrix and cell surface proteins in ERM are provided by Haku et al (2011) and Rincon et al (2006).

Furthermore, ERM play an important role in the distribution of fibrous and neural elements in the PDL (Kjaer and Nolting 2009). Ruffini-like receptors and free nerve endings were reported closely apposed to those epithelial rests (Lambrichts et al 1993). Lambrichts et al (1993) suggested that the epithelial rests may function as targets for developing periodontal axons, and that the periodontal axonal/epithelial cells complexes might have a mechanoreceptive function. Similarly Heyeraas et al (1993) reported that protein gene product 9.5 (PGP-9.5) and calcitonin gene related peptide (CGRP) immunoreactive axon terminals are associated with periodontal

epithelial rests of Malassez (*Hildebrand et al 1995*). The PGP-9.5 is a marker for mature nerve fibres, considered as a general neurochemical marker. CGRP is a neuropeptide (*Fristad et al 1994; Gunjigake et al 2006*) widely expressed in sensory neurons. This neurochemical marker plays also important roles in nerve function (*Fristad et al 1994*) and repair when axons are severed (*Li et al 2004, Sample et al 2011*).

In humans, Lambrichts et al (1993) described that the ERM appeared as oval and round clusters of cells in sections cut perpendicular to the root axis. In longitudinal sections the epithelial cells were arranged in strands. Myelinated nerve fibres with average diameter of 5µm, lost their myelin sheaths in the vicinity of the ERM and reached them as unmyelinated preterminal axons (figures 4.2-4.3). These neural structures sometimes surrounded the ERM. A more complete ultrastructural information is provided for the myelinated and unmyelinated fibres found in the vicinity of ERM in Lambrichts et al (1993). The axons mostly faced the epithelial cells while Schwann cells were usually located towards the outer connective tissue. A dramatic decrease in the number of ERM is reported after the second decade of life, resulting in a low incidence of ERM in adult periodontal ligament (*Reeve and Wetz 1962*). In line with this, Gonçalves et al (2008) and Cerri et al (2009) suggested that epithelial cell death by apoptosis may be, at least in part, responsible for the reduction in the number of rests of Malassez according to age. Furthermore, the intracellular calcium ion concentration was found to be differently regulated during tooth development and in adult PDL (*Korkmaz et al 2011*). On the other hand, Lambrichts et al (1993) did not had a significantly higher density of ERM in the sample obtained from patients younger than 20 years old.

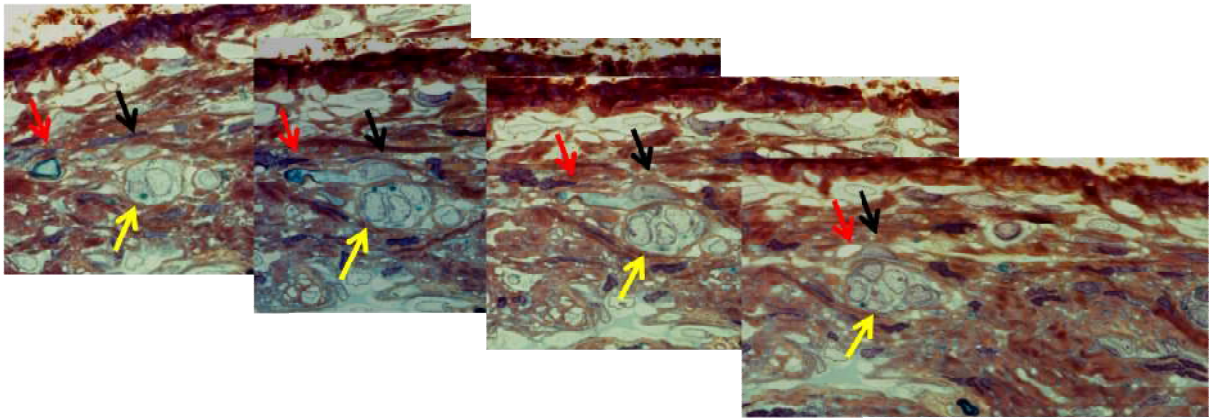


Figure 4.2 : Relationship between myelinated nerve fibre (red arrows) and epithelial rests malassez (yellow arrows). In this sequence, myelinated nerve fibre gradually loses its myelin sheets and become in close contact with ERM. Black arrows indicates de nucleus of Schwann cell. (courtesy of Prof.Ivo Lambrichts, Hasselt University).

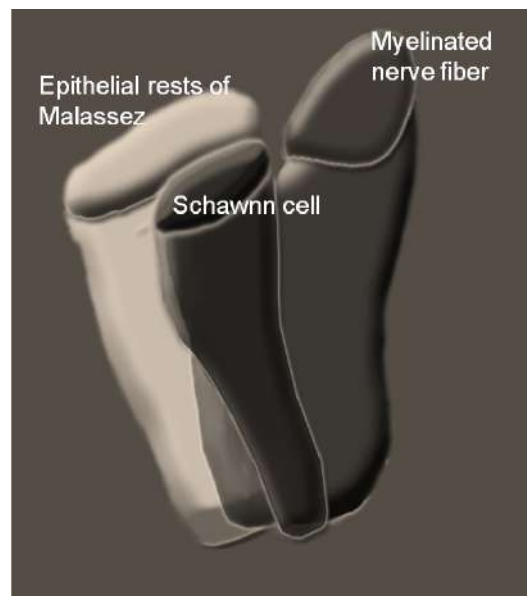


Figure 4.3: A further 3D reconstruction allowed a morphologic assessment of the nerve fibres in relation to other periodontal ligament structures.

Later, in an attempt to gain insight into clinical questions on tooth eruption, alveolar bone formation, tooth movement, and tooth resorption in humans, Kjaer and Nolting (2009) have studied this spatial interrelation between what they called epithelial layer of Malassez and nerve fibres in areas close to the root surface. They suggested that the genetic composition of the epithelial layer of Malassez in the periodontal membrane may be the key to understanding the different functions (table 4.1) of the periodontal membrane and also the individual differences of these

functions. For them, different factors should be discussed to clarify the etiology behind eruption: influence from innervation of the periodontal membrane; influence from the epithelial layer of Malassez; the periodontal fibres, cells, and the surrounding alveolar bone. In the other hand, they describe that tooth resorption is a normal process in the primary dentition, but a pathological process in the permanent dentition. Differences between periodontal membranes surrounding primary root surfaces and permanent root surfaces may be important in our understanding differences in resorption patterns.

Table 4.1: Summary reported ERM functions from Kjael and Nolting (2009).

Functions ERM
Protect root surface from resorption processes
Healing after reimplantation
Prevent dento-alveolar ankylosis
Reorganization of the membrane during eruption and tooth movement
Related to cementum repair

The association between neural and ectodermal structures has been related to mechanoreception and target function for nerve growing (*Lambrichts et al 1993*). During growth the budding nerve fibre seeks its target epithelial cell either by chemotropism or random searching and recognition (*Lambrichts et al 1993*). Nerve growth factor receptors were observed in the epithelial rests of dental follicle of unerupted human third molars (*Lambrichts et al 1993*). Nerve growth factor receptors were also observed in pinocytotic vesicles in the membrane of Schwann cells ensheathing Ruffini-like endings in the PDL of rats (*Byers 1990*). In guinea pigs PDL, this association was found to be site specific and only seen in the presence of cementum (*Jayawardena and Takano 2006*).

Recent studies involving experimental denervation have reported that the distribution of the cell rests of Malassez is regulated by sensory innervation of the periodontal ligament (*Fujiyama et al 2004; Yamashiro et al 2000*). Yamashiro et al.

(2000) and Fujiyama et al (2004) claimed that the cell rests of Malassez may play a role in maintenance of the width of the periodontal space by preventing root resorption and ankylosis, based on the observations that denervation of the inferior alveolar nerve resulted in decreased cell rests of Malassez followed by dento-alveolar ankylosis in the molar periodontal ligament of rats. They also observed a significant retrieval of the width of the periodontal ligament with restoration of epithelium cell clusters associated with nerve regeneration.

Awareness of such a relationship within the periodontal ligament is important for the success of regeneration therapy in the periodontium. Further research is needed to clarify the nature of interactions and the bioactive molecules involved. Several studies have investigated the expression of different types of proteins by the ERM (*Shimonishi et al 2007; Mizuno et al 2005; Rincon et al 2005; Mouri et al 2003*). These proteins can be broadly classified into a number of groups, such as cytokeratins and neuropeptides, as well as extracellular matrix and cell-surface proteins including a variety of growth factors, cytokines and extracellular matrix-degrading proteinases. Observations from studies using cytokeratins confirmed the epithelial phenotype of those cells (*Rincon et al 2006*). A number of neuropeptides, including calcitonin gene-related peptide (CGRP), protein gene product 9.5 (PGP 9.5), substance P (SP), vasoactive intestinal peptide (VIP), tyrosine receptor kinase A (TrkA) – a high-affinity receptor of nerve growth factor – and parathyroid hormone-related protein (PTHrP) may be expressed by the ERM (*Tadokoro et al 2002*). Using PGP 9.5, Tadokoro et al (2002) demonstrated that Malassez epithelium not only exhibits neuroendocrine cells, but additionally that the neuroendocrine cells represent Merkel-like cells.

Extracellular matrix and cell-surface proteins such as growth factors and cytokines were also expressed by the ERM (*Rincon et al 2005; Hasegawa et al 2003*). Some of matrix macromolecules expressed by ERM include amelogenin and enamelin, glycosaminoglycans, hyaluronic acid, dermatan sulphate, chondroitin sulphate and type IV collagen fibronectin, laminin and laminin-5. Interestingly, these cells also synthesize several proteins more commonly associated with mesenchymal tissues rather than epithelial tissues, such as osteopontin, bone sialoprotein and osteoprotegerin. Other proteins expressed by the ERM include cell-surface molecules, such as calbindin D28 (which are vitamin D-dependent calcium-binding proteins) and epidermal growth factor receptor, growth factors such as epidermal

growth factor and bone morphogenetic proteins 2 and 4, various cytokines, including interleukin-1 α , interleukin-6, interleukin-8 and granulocyte–macrophage colony-stimulating factor (GM-CSF), β defensin (BD-1) and prostaglandins E and F. It is noteworthy that the ERM can express a number of bone/cementum-related proteins which could implicate them in a regenerative role of the PDL (*Rincon et al 2006*).

Rincon et al (2006) suggests 4 putative functions of the epithelial cell rests of Malassez in periodontal regeneration. 1. Maintenance of PDL space (synthesis of hyaluronate, proteoglycans and type IV collagen); 2. Osteopontin synthesis acting as an aid for cementum repair, and mineralized tissue formation on root surface; 3. Bone sialoproteinsynthesis acting as adhesion molecule and initiator of mineralization of root surface and 4. Absence of these cells in regeneration of tissues may account for some lack of predictable functional outcomes. It is important to highlight that both bone sialoprotein (BSP) and osteopontin (OPN) may have a role in recruiting and maintaining selective cells at the root surface, an equally important role may be related to the control of mineralization along the root surface.

Cementicles

True cementicles consists of a collagenous matrix intermixed with a noncollagenous ground substance (*Bosshardt and Nanci 2003*). Despite the relative frequency and clinical relevance of cementicles, their etiology and nature are still unknown. The literature about this PDL structure is scarce and just a few studies were found discussing cementicles distribution and function. Holton et al (1986) determined the prevalence and distribution of attached cementicles on different root surfaces in 415 extracted human incisors, canines, premolars and molars. Cementicles were seen on approximately 50% of the canines and molars and on fewer than 50% of the other teeth. These structures were most frequently found in the middle and apical thirds of canine roots and in furcation region of molars.

Although epithelial rests of Malassez have been implicated in the formation of cementicles (*Schroeder et al 1986*), the characterization of the cells that initially are involved in cementicle formation is poor. Structurally, there is a close resemblance of cementicles with root cementum suggesting an involvement of cementoblasts in their formation. Although morphologically resembling their normal tissue counterparts,

biochemical compositions of the cementicles are entirely unknown. Bone sialoprotein (BSP) and osteopontin (OPN) were detected in the cementicles, mainly associated with the interfibrillar ground substance (*Bosshardt and Nanci 2003*). These two NCPs are typically found in bone and cementum and may, like in their normal tissue counterparts, play a role in the mineralization (*Bosshardt and Nanci 2003*).

Two types of matrix deposit have been described: a cementicle like structure and the “true” cementicles. The first is represented by a round and concentrically arranged lamellae and a more homogeneously structured matrix deposit in the connective tissue. On the other hand, in the second type, lamellation is less prominent and smaller coalesced matrix subunits were seen. Common to both matrix structures is that they lack collagen fibrils. However, the surrounding matrix is collagenous in nature. Bosshardt and Nanci (2003) suggested that cementicles-like are associated to the ectopic deposition of enamel. Collagen-free cementum-like and enamel-like calcifications were consistently present in the periodontal ligament adjacent to ectopic enamel deposits. Their coexistence suggests a causal connection. True cementicles occurred independently of ectopic enamel formation and resembled acellular extrinsic fibre cementum in structure and composition.

Kodaka and Debari (2002) examined afibrillar cementum (AFC) and cementicle-like structures (CLS) in human teeth by scanning electron microscopy and energy-dispersive X-ray microanalysis. They described that the large masses of afibrillar cementum in the enamel fissures often enclosed cementicle-like structures with concentric appositional rings, while some of the independent cementicle-like structures contained cell- or ameloblast-like remnants in the core surrounded by a few or many concentric appositional rings. They suggested that some or many of the calcified epithelial cells will grow into cementicles and cementicle-like structure (CLS) surrounded by concentric appositional rings and then become their cores.

Part II - Proliferation of epithelial rests of Malassez following auto-transplantation of third molars: a case report

The periodontal ligament (PDL) is the dense fibrous connective tissue which connects the cementum-covered surface of the root with the alveolar bone (*Berkovitz 2004*). Its main function lies in preventing damage to the dental tissues during mastication. It consists, in part, of thick collagen bundles, called Sharpey's fibres that run from the alveolar wall into the cementum and are responsible for resisting the displacing masticatory forces. Other functions which are addressed to the cells in the PDL are the formation, maintenance and repair of the alveolar bone and cementum. It has already been described that the alveolar bone can adapt its shape according to the needs during root development (*Yamashiro et al 2003*). This is an important feature when looking at auto-transplantation where this process will be responsible for remodelling the new alveolar socket to the shape of the transplanted tooth. Furthermore, the periodontal ligament has rich sensory innervations (*Heyeraas et al 1993*) and a close relationship with the mechanoreceptors and the epithelial rests of Malassez (ERM) has been detected (*Lambrichts et al 1993*). ERM are the remnants of the epithelial root sheath of Hertwig (ERSH), a fold of the outer and inner enamel epithelium formed during tooth development. Once root formation is completed, the ERSH becomes penetrated by several collagen bundles of the PDL, resulting in a fenestrated network that surrounds the tooth. The precise function of the ERM is not known yet, but it is believed that they are involved in preventing root resorption and maintaining the width of the periodontal ligament, thereby preventing ankylosis (*Fujiyama et al 2004*). As it is reported that proliferation of ERM occurs during experimental tooth movement (*Talic et al 2003*), the aim of this study was to investigate whether an auto-transplantation could also act as a trigger for this epithelial proliferation.

Case presentation

A 21-year-old Caucasian woman presented multiple caries and inflammatory parodontal cysts (IPCs). One of the IPCs was located in the lower jaw near molar 37. A histopathological examination revealed that the cyst was predominantly surrounded

by granulation tissue although the local presence of Malpighian epithelium could be found. On the periphery it was surrounded by an inflammatory infiltrate which consisted mainly of lymphocytes, plasmocytes and neutrophilic polymorphonuclear cells. The outermost lining consisted of a dense compact connective tissue and no signs of malignant degeneration could be detected.

Two weeks later, the IPCs were enucleated after incision and trepanation of the bone. We decided to extract teeth 15, 37, 45 and 47 because of multiple and severe carious lesions. As the patient had a substantial loss of molars, the intra-osseous teeth 18 and 48 were extracted carefully and transplanted into position 36 and 47, respectively. The procedure was done as atraumatically as possible with no visible damage to the periodontal ligament of the extracted teeth. No problems were encountered during surgery and the auto-transplantation was a success. After four months, an X-ray was taken of the upper and lower jaw (figure 4.4) with a Siemens Orthoceph 10E operated at 70 kV and 15 s of irradiation.

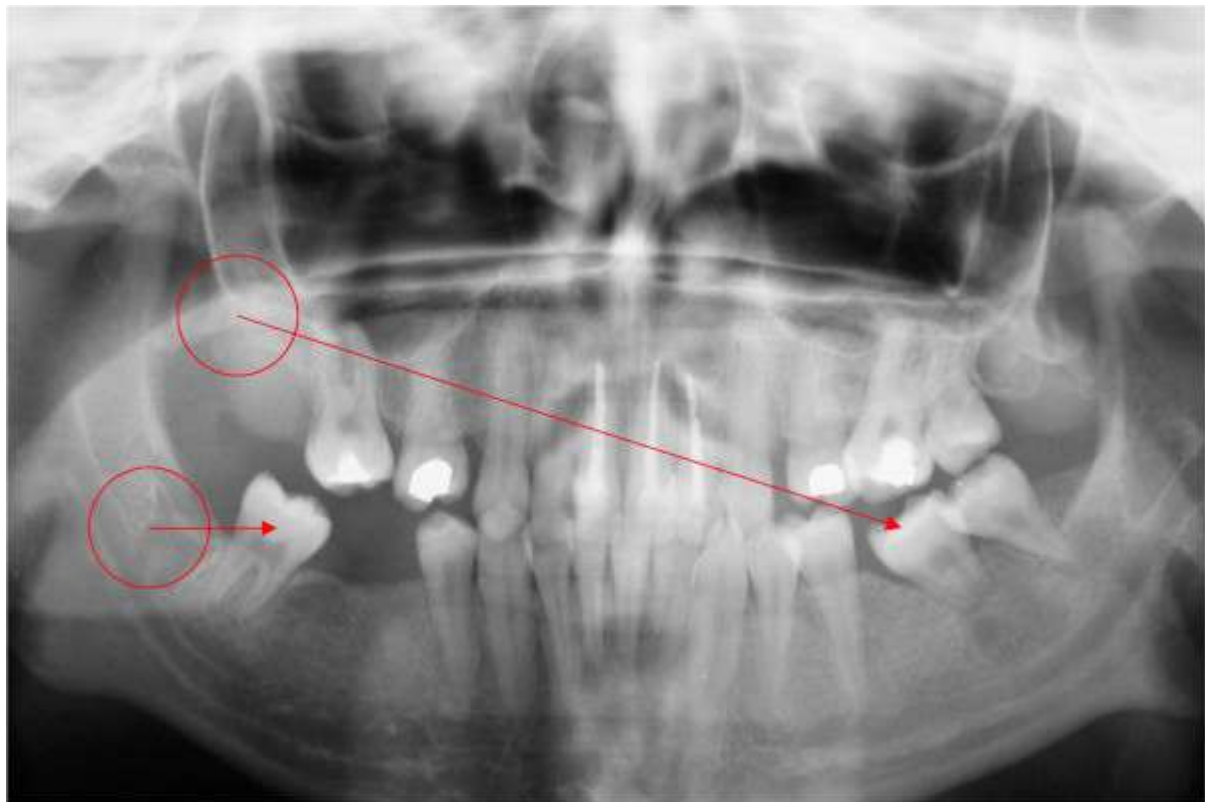


Figure 4.4: X-ray of the upper and lower jaw four months after surgery. Teeth 18 and 48 were extracted carefully and transplanted into position 36 and 47, respectively (marked by circles and arrows).

Two years later, the patient requested a partial extraction of the lower jaw teeth because of recurrent infections. As a result of renewed progressive caries of the two auto-transplanted teeth, she agreed with the removal of the auto-transplanted elements. The teeth were collected with her informed consent and the approval of the ethical board.

The extracted auto-transplanted teeth were immediately immersed and conserved in formol. The tissue of interest was collected by removing the PDL from the mid-cervical part of the teeth and it was fixed a second time in 2% glutaraldehyde in 0.05 M cacodylate buffer (pH 7.3). The fixative was gently aspirated with a glass pipette and the specimens were post-fixed in 2% osmium tetroxide, put through a dehydrating series of graded concentrations of acetone and embedded in araldite according to the conventional method. Semi-thin sections (0.5 μm) were stained with a solution of thionin and methylene blue (0.1 aqueous solution) for light microscopy. Ultra-thin sections (0.06 μm) were mounted on 0.7% formvar-coated grids, stained with uranyl acetate and lead citrate and examined in a Philips EM 208 transmission electron microscope operated at 80 kV.

From a light microscopic examination of the semi-thin sections, we concluded that the ERM of the transplanted teeth were slightly larger than in normal PDL. A mean value of 20 cells was counted in the transplanted tissue in contrast to a mean value of 10 cells in normal/control PDL (figure 4.5). We also noted compartmentalization of collagen bundles in the PDL (arrows in figure 4.6).

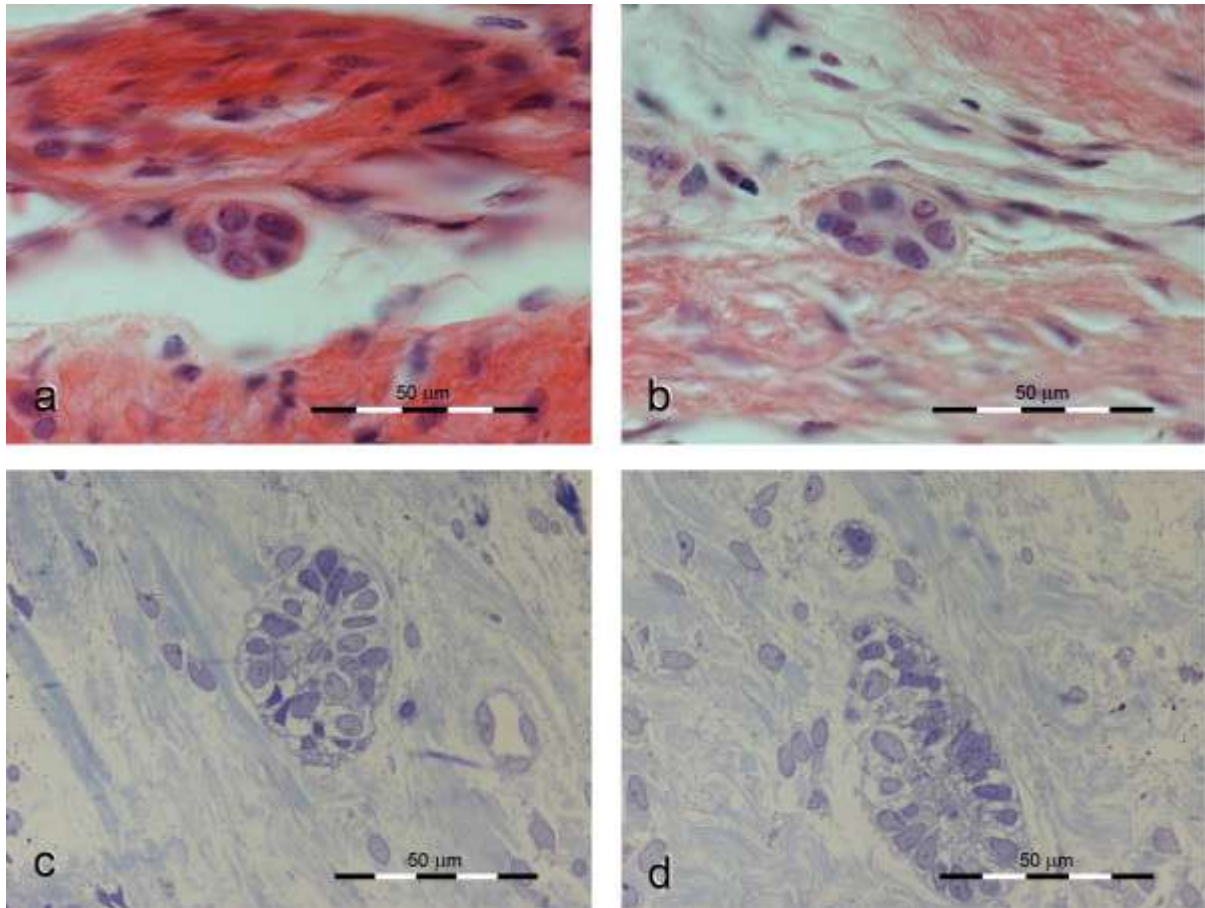


Figure 4.5: Light microscopic images of epithelial rests of Malassez (ERM). (a-b) ERM of a normal human periodontal ligament with an average of 10 cells to 1 ERM. (c-d) ERM of a transplanted human periodontal ligament with an average of 20 cells to 1 ERM.

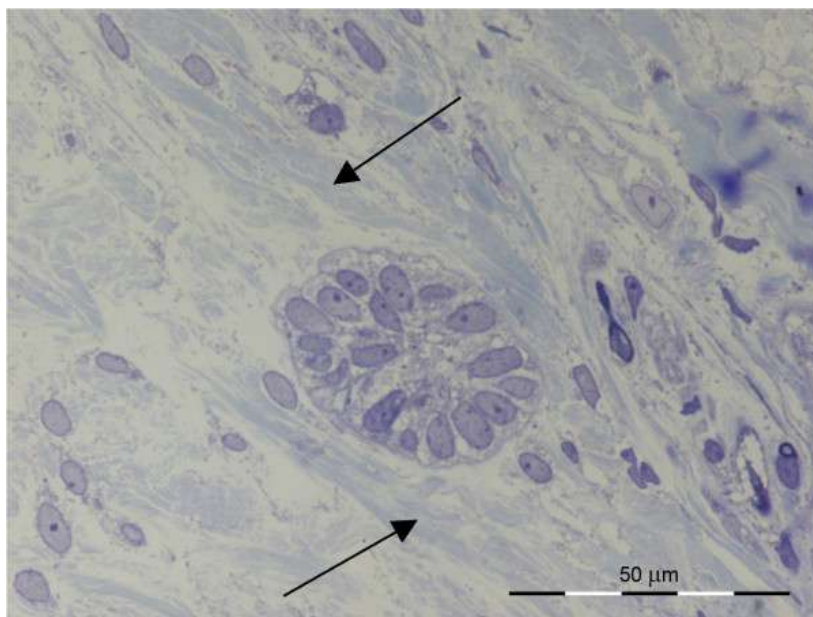


Figure 4.6: Light microscopic image of the compartmentalization of collagen fibres that occurs after autotransplantation (arrow).

From transmission electron microscope (TEM) analysis we concluded that the auto-transplantation was successful because fully developed blood vessels appeared in the PDL (figure 4.7a). The lumen was surrounded by mature endothelial cells which were firmly connected to each other with tight junctions (arrows in figure 4.7a). In the periphery, the blood vessels were supported by smooth muscle cells (asterisks in figure 4.7a). The enlargement of the ERM seen with the light microscope was confirmed by the TEM images (figure 4.7b). The epithelial cells formed typical clusters which were separated by bundles of collagen fibres. The epithelial nuclei were large, predominantly euchromatic and irregular in shape. The ERM were lined by a basal lamina (arrow in figure 4.7b). Another interesting feature was the innervation of the ERM. Some fine neurites made contact with the ERM (figure 4.8). These were characterized by the presence of neurofilaments in the cytoplasm (asterisks in figure 4.8). Apart from these neurites, fully matured myelinated nerve fibres (arrow in figure 4.8) accompanied by their Schwann cells were another feature of the successful regeneration of the PDL.

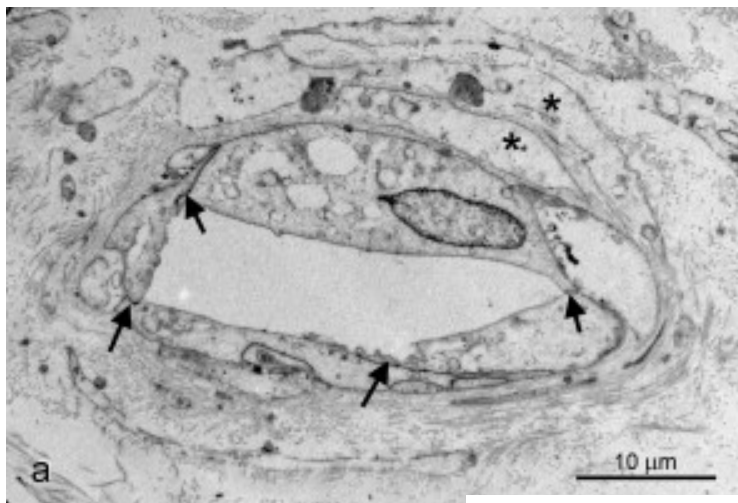
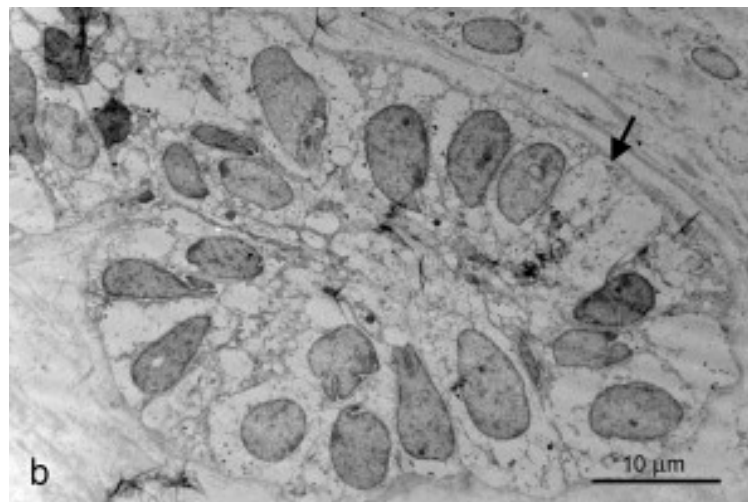


Figure 4.7: Electron microscopic images of the transplanted PDL. (a) Shows fully developed blood vessels. (b) Shows the electron microscopic aspect of the enlarged ERM.



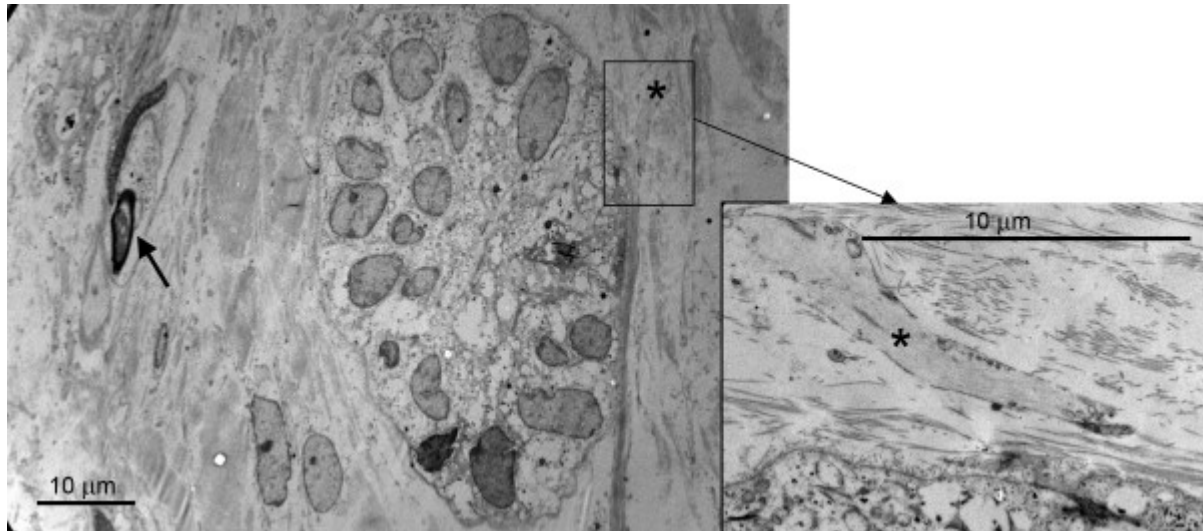


Figure 4.8: Electron microscopic image of the re-innervation of the ERM in the autotransplanted PDL.

Discussion

The specific morphological features which could be detected on the ultrastructural level can be regarded as typical for ERM and are confirmed in the recent literature (*Tadokoro 2009; Cerri et al 2009; Tadokoro et al 2002*). ERM cells produce prostaglandin E2 (*Brunette et al 1979*) and prostaglandin E2 is capable of activating osteoclasts which stimulate bone breakdown and bone remodelling (*Kale et al 2004*).

In auto-transplantation, the alveolar bone around the implantation-site normally has to be remodelled to provide a good fit for the implanted tooth. Bone breakdown is a process involved in this remodeling and it can be stimulated by increased prostaglandin E2 secretion by the ERM. This could explain why the ERM in the PDL of transplanted teeth are enlarged. It is also possible that the ERM in PDL of transplanted teeth remain enlarged when the remodeling process has finished. This implies that transplanted teeth will always have more mobility in the jaw than normal teeth because of the increased prostaglandin E2 secretion.

In addition to the expected bone remodeling, the PDL also needs to be remodelled. The compartmentalization of the collagen bundles can be seen as a consequence of this process. Furthermore, following auto-transplantation, the need for re-innervation of the PDL is of significant value. As ERM play an important role in

the distribution of the fibrous and neural elements in the PDL (*Kjaer and Nolting 2009*), the enlargement of ERM detected after auto-transplantation could be seen as an attempt to direct PDL remodeling and re-innervation. The innervation of the ERM suggests that this whole process is directed by the nervous system.

Conclusion

Since this case report has shown that an enlargement of ERM in case of tooth auto-transplantation, it is suggested that the ERM might be involved in the remodelling and re-innervation process of PDL. In turn, one of the key elements necessary for a successful auto-transplantation might be the conservation of the periodontal ligament.

References

- Becktor KB, Nolting D, Becktor JP, Kjaer I. Immunohistochemical localization of epithelial rests of Malassez in human periodontal membrane. *Eur J Orthod* 2007; 29:350-3.
- Berkovitz BK. Periodontal ligament: structural and clinical correlates. *Dental Update* 2004; 31:46–50.
- Bosshardt DD, Nanci A. Immunocytochemical characterization of ectopic enamel deposits and cementicles in human teeth. *Eur J Oral Sci* 2003; 111:51-9.
- Brunette DM, Heersche JN, Purdon AD, Sodek J, Moe HK, Assuras JN. In-vitro cultural parameters and protein and prostaglandin secretion of epithelial cells derived from porcine rests of Malassez. *Arch Oral Biol* 1979; 24:199–203.
- Byers MR. Segregation of NGF receptor in sensory receptors, nerves and local cells of teeth and periodontium demonstrated by EM immunocytochemistry. *J Neurocytol* 1990; 19:765-75.
- Cerri PS, Gonçalves Jde S, Sasso-Cerri E. Area of rests of Malassez in young and adult rat molars: evidences in the formation of large rests. *Anat Rec (Hoboken)* 2009; 292:285-91.
- Fristad I, Heyeraas KJ, Kvinnsland I. Nerve fibres and cells immunoreactive to neurochemical markers in developing rat molars and supporting tissues. *Arch Oral Biol* 1994; 39:633-46.
- Fujiyama K, Yamashiro T, Fukunaga T, Balam TA, Zheng L, Takano-Yamamoto T. Denervation resulting in dento-alveolar ankylosis associated with decreased Malassez epithelium. *J Dent Res* 2004; 83:625-9.
- Gonçalves JS, Sasso-Cerri E, Cerri PS. Cell death and quantitative reduction of rests of Malassez according to age. *J Periodontal Res* 2008; 43:478-81.
- Gunjigake KK, Goto T, Nakao K, Konoo T, Kobayashi S, Yamaguchi K. Correlation between the appearance of neuropeptides in the rat trigeminal

- ganglion and reinnervation of the healing root socket after tooth extraction. *Acta Histochem Cytochem* 2006; 39:69-77.
- Haku K, Muramatsu T, Hara A, Kikuchi A, Hashimoto S, Inoue T, Shimono M. Epithelial cell rests of Malassez modulate cell proliferation, differentiation and apoptosis via gap junctional communication under mechanical stretching in vitro. *Bull Tokyo Dent Coll* 2011; 52:173-82.
- Hamamoto Y, Nakajima T, Ozawa H. Ultrastructural and histochemical study on the morphogenesis of epithelial rests of Malassez. *Arch Histol Cytol* 1989; 52:61-70.
- Hasegawa N, Kawaguchi H, Ogawa T, Uchida T, Kurihara H. Immunohistochemical characteristics of epithelial cell rests of Malassez during cementum repair. *J Periodontal Res* 2003; 38:51-6.
- Heyeraas KJ, Kvinnsland I, Byers MR, Jacobsen EB. Nerve fibres immunoreactive to protein gene product 9.5, calcitonin gene-related peptide, substance P, and neuropeptide Y in the dental pulp, periodontal ligament, and gingiva in cats. *Acta Odontol Scand* 1993; 51:207-21.
- Hildebrand C, Fried K, Tuisku F, Johansson CS. Teeth and tooth nerves. *Prog Neurobiol* 1995; 45:165-222.
- Holton WL, Hancock EB, Pelleu GB Jr. Prevalence and distribution of attached cementicles on human root surfaces. *J Periodontol* 1986; 57:321-4.
- Jayawardena CK, Takano Y. Nerve-epithelium association in the periodontal ligament of guinea pig teeth. *Arch Oral Biol* 2006; 51:587-95.
- Kale S, Kocadereli I, Atilla P, Asan E. Comparison of the effects of 1,25 dihydroxycholecalciferol and prostaglandin E2 on orthodontic tooth movement. *Am J Orthod Dentofacial Orthop* 2004; 125:607-14.
- Kat PS, Sampson WJ, Wilson DF, Wiebkin OW. Distribution of the epithelial rests of Malassez and their relationship to blood vessels of the periodontal ligament during rat tooth development. *Aust Orthod J* 2003; 19:77-86.
- Kjaer I, Nolting D. The human periodontal membrane: focusing on the spatial interrelation between the epithelial layer of Malassez, fibres, and innervation. *Acta Odontol Scand* 2009; 67:134-8.
- Kodaka T, Debari K. Scanning electron microscopy and energy-dispersive X-ray microanalysis studies of afibrillar cementum and cementicle-like structures in human teeth. *J Electron Microsc (Tokyo)* 2002; 51:327-35
- Korkmaz Y, Klinz FJ, Beikler T, Blauhut T, Schneider K, Addicks K, Bloch W, Raab WH. The Ca(2+)-binding protein calretinin is selectively enriched in a subpopulation of the epithelial rests of Malassez. *Cell Tissue Res* 2010; 342:391-400.
- Kvinnsland IH, Tadokoro O, Heyeraas KJ, Kozawa Y, Vandevska-Radunovic V. Neuroendocrine cells in Malassez epithelium and gingiva of the cat. *Acta Odontol Scand* 2000; 58:107-12.
- Lambrichts I, Creemers J, van Steenberghe D. Periodontal neural endings intimately relate to epithelial rests of Malassez in humans. A light and electron microscope study. *J Anat* 1993; 182:153-62.

- Li XQ, Verge VM, Johnston JM, Zochodne DW. CGRP peptide and regenerating sensory axons. *J Neuropathol Exp Neurol* 2004; 63:1092-103.
- McIntosh JE, Anderton X, Flores-De-Jacoby L, Carlson DS, Shuler CF, Diekwisch TG. Caiman periodontium as an intermediate between basal vertebrate ankylosis-type attachment and mammalian "true" periodontium. *Microsc Res Tech* 2002; 59:449-59.
- Mizuno N, Shiba H, Mouri Y, Xu W, Kudoh S, Kawaguchi H, Kurihara H. Characterization of epithelial cells derived from periodontal ligament by gene expression patterns of bone-related and enamel proteins. *Cell Biol Int* 2005; 29:111-7.
- Mouri Y, Shiba H, Mizuno N, Noguchi T, Ogawa T, Kurihara H. Differential gene expression of bone-related proteins in epithelial and fibroblastic cells derived from human periodontal ligament. *Cell Biol Int* 2003; 27:519-24.
- Peters BH, Peters JM, Kuhn C, Zöller J, Franke WW. Maintenance of cell-type-specific cytoskeletal character in epithelial cells out of epithelial context: cytokeratins and other cytoskeletal proteins in the rests of Malassez of the periodontal ligament. *Differentiation* 1995; 59:113-26.
- Reeve CM, Wentz FM. The prevalence, morphology, and distribution of epithelial rests in the human periodontal ligament. *Oral Surg Oral Med Oral Pathol* 1962; 15:785-93.
- Rincon JC, Young WG, Bartold PM. The epithelial cell rests of Malassez--a role in periodontal regeneration? *J Periodontal Res* 2006; 41:245-52.
- Rincon JC, Xiao Y, Young WG, Bartold PM. Production of osteopontin by cultured porcine epithelial cell rests of Malassez. *J Periodontal Res* 2005; 40:417-26.
- Sample SJ, Hao Z, Wilson AP, Muir P. Role of calcitonin gene-related peptide in bone repair after cyclic fatigue loading. *PLoS One* 2011;6:e20386.
- Schroeder H E, *The Periodontium-Handboek of microscopy anatomy-Springer* 1986: 208-221.
- Shimonishi M, Hatakeyama J, Sasano Y, Takahashi N, Uchida T, Kikuchi M, Komatsu M. In vitro differentiation of epithelial cells cultured from human periodontal ligament. *J Periodontal Res* 2007; 42:456-65.
- Spouge JD. A new look at the rests of Malassez. A review of their embryological origin, anatomy, and possible role in periodontal health and disease. *J Periodontol* 1980;51:437-444.
- Tadokoro O. Epithelial and PGP9.5-immunoreactive cells of Malassez epithelium in the periodontal ligament of cats: a transmission electron microscopic study. *Acta Odontol Scandinavica* 2009; 1-5:1502-3850.
- Tadokoro O, Vandevska-Randunovic V, Inoue K. Epithelial cell rests of Malassez and OX6-immunopositive cells in the periodontal ligament of rat molars: a light and transmission electron microscope study. *Anat Rec (Hoboken)* 2008; 291:242-53.
- Tadokoro O, Maeda T, Heyeraas KJ, Vandevska-Radunovic V, Kozawa Y, Hals Kvinnsland I. Merkel-like cells in Malassez epithelium in the periodontal ligament of cats: an immunohistochemical, confocal-laser scanning and

- immuno electron-microscopic investigation. *J Periodontal Res* 2002; 37:456–463.
- Talic NF, Evans CA, Daniel JC, Zaki AE. Proliferation of epithelial rests of Malassez during experimental tooth movement. *Am J Orthod Dentofacial Orthop* 2003; 123:527-33.
- Ten Cate AR. The epithelial cell rests of Malassez and the genesis of the dental cyst. *Oral Surg Oral Med Oral Pathol* 1972; 34:956-64.
- Valderhaug J, Zander HA. Relationship of "epithelial rests of Malassez" to other periodontal structures. *Periodontics* 1967; 5:254-8.
- Yamasaki A, Pinero GJ. An ultrastructural study of human epithelial rests of Malassez maintained in a differentiated state in vitro. *Arch Oral Biol* 1989; 34:443-51.
- Yamashiro T, Fujiyama K, Fukunaga T, Wang Y, Takano-Yamamoto T. Epithelial rests of Malassez express immunoreactivity of TrkA and its distribution is regulated by sensory nerve innervation. *J Histochem Cytochem* 2000; 48:979-84.
- Yamashiro T, Tummers M, Thesleff I. Expression of bone morphogenetic proteins and Msx genes during root formation. *J Dental Res*. 2003;82:172–6.

Chapter 5

The peri-implant innervation:

Literature review and histological findings in humans

Publication related to this chapter:

Corpas LS, Lambrichts I, Quirynen M, Collaert B, Politis C, Vrielinck L, Martens W, Struys T, Jacobs R. Bone innervation around osseointegrated implants: literature review and report of histological findings in humans. (submitted)

Bone innervation around osseointegrated implants: literature review and report of histological findings in humans

Abstract

Objective: The aim of the present study was to review the literature about peri-implant innervation and to describe nerve fibres around osseointegrated implants in humans. **Material and Methods:** Twelve mechanically failed-implants, partially or fully osseointegrated, retrieved from 10 patients were collected from 3 dental centers over a period of 5 years. The implants were removed with a trephine bur and immediately immersed in 2% glutaraldehyde or 10% formalin solution. Semi-thin sections (0.5 μ m) were stained with thionin methylene blue for light microscopical analysis and digitized using a high resolution scan. Observations were done by a trained observer at a magnification of 50X. In addition, an ultrastructural analysis was performed on serial ultra-thin sections (0.06 μ m) using transmission electron microscopy. **Results:** Both myelinated and unmyelinated nerve fibres could be identified inside the Haversian canals of the osteonal bone near the implant threads. Myelinated fibres were also located at the woven bone around the implant. However, no nerve endings could be observed around the implants. **Conclusions:** This study showed for the first time the presence of nerve fibres in the peri-implant bone. Previous studies in animals showed that those fibres participate in the process of bone modeling and remodeling. Nevertheless, the role of peri-implant bone innervation in the osseoperception phenomenon cannot be ruled out since the mechanism of mechanoreception in bone is not fully understood.

Introduction

Osseointegration is a well-documented phenomenon responsible for the biological integration between bone tissue and titanium implants (*Albrektsson et al 1986*). Apart from integrating biologically, osseointegrated implants are at the same time physiologically incorporated (*Hagberg et al 2008; van Steenberghe 2000*). Studies on physiological integration of oral and skeletal osseointegrated implants (*Jacobs 1998; Gallagher et al 2008*) claim the existence of a peri-implant innervation influencing the oral function. However, reviewing the literature, it can be concluded that the role of this innervation in the physiological integration of implants remains only partially understood (*Jacobs 1998; Jacobs and van Steenberghe 2006*).

It is commonly known that an extensive nerve supply is present throughout the bone tissue (*Mach et al 2002; Serre et al 1999; Buma et al 1995; Herskovits et al 1990; Martin and Burr 1989*). Both myelinated and unmyelinated nerve fibres have been found in the periosteum, bone cortex, Haversian systems, Volkmann's canals, marrow spaces (*Mach et al 2002; Buma et al 1995; Lambrichts 1998*), and in healed bone after tooth extraction (*Gunjigake et al 2006; Mason and Holland 1993; Hansen 1980*). Moreover, some studies have shown that both sympathetic and sensory fibres are involved in the innervation of the skeleton (*Mach et al 2002; Sample et al 2008; Rubin and Rubin 2008*). Understanding the sympathetic and sensory components of bone innervation might contribute to unravel their influence on bone dynamics and sensory function (*Buma et al 1995*). It is clear that the innervation of bone has a functional role in bone physiology; e.g. bone growth, bone remodeling and bone repair (*Sample et al 2008; Herskovits et al 1990*). Previous studies involving sensory bone innervation have focused on bone pain in injury and disease (*Mach et al 2002; Castaneda-Corral et al 2011*) and stimulus perception via osseointegrated implants (*Jacobs and van Steenberghe 2006*). Nevertheless, the physiological role of bone innervation remains a matter of debate. Further clarification about bone innervation can be found in the review by McCredie (2007).

Regarding osseointegrated implants, the changes in bone innervation patterns, associated with implant placement have been firstly reported by Sawada et al (1993) and Buma et al (1995). The presence of nerve fibres involved in bone remodeling and growth at the interface between living and necrotic bone tissue has

shown that nerve fibres can regenerate after implant placement (*Sawada et al 1993; Buma et al 1995*). Whether there are sensory receptors, acting as peri-implant mechanoreceptors, remains to be determined. Yet any potential indication in that direction might help to understand the osseoperception phenomenon after implant rehabilitation. Indeed, osseoperception refers to the recovery of sensory function in implant rehabilitated patients (*Jacobs and van Steenberghe 2006; Trulsson 2005; Klineberg et al 2005*), which accounts for a better physiological integration of prostheses. In this way, patients rehabilitated with osseointegrated implants seem subjectively not much impaired in their masticatory and other oral functions (*Abarca et al 2006*), notwithstanding their lack of information from periodontal mechanoreceptors impairing fine motor control (*Trulsson 2007; Trulsson 2006; Trulsson 2005*).

Several studies confirm the improved oral function of those patients compared to conventional prosthetic rehabilitation (*Jacobs and van Steenberghe 2006; van der Bilt 2011; Lundqvist and Haraldson 1992; Lundqvist and Haraldson 1990; Haraldson and Ingervall 1979; Haraldson et al 1979; Haraldson and Carlsson 1977*). However, the physiological mechanisms for the osseoperception phenomenon remain to be elucidated. While electrical stimulation of implants resulted in a clear sensory response (*Zhu et al 2009; Van Loven et al 2000; Bonte et al 1993*), evidence on perception after mechanical implant stimulation is scarce. Only very recently, Habre-Hallage et al (2012) proved that pure mechanical stimulation of an implant could be perceived at the sensory cortex using functional magnetic resonance imaging (fMRI). Previous studies on peri-implant innervation (see tables 5.1 and 5.2) may help to explain this osseoperception phenomenon (*Wada et al 2001; Ysander 2001; Wang et al 1998; Buma et al 1995; Weiner et al 1995; Sawada et al 1993*). Nerve fibres could be detected using different implant surfaces and loading approaches in different animals. Although those studies indicated some factors that might influence the peri-implant innervation, so far no study has been reported in humans. Therefore, the overall aim of the present study was to identify and describe nerve fibers found around osseointegrated implants in humans by means of light and transmission electron microscopy. In addition, a literature review on peri-implant innervation was carried out to position the present findings.

Table 5.1: Summary of previous animal studies on peri-implant bone innervation.

Authors	Year	Aim	Sample	Methods
Sawada et al	1993	Identify tissue reactions and responses of nerve fibres to implantation (chronological alternations in pattern of innervation in the healing socket X implant sites)	<ul style="list-style-type: none"> • Dog mandibles • unloaded 	<ul style="list-style-type: none"> • Immunohistochemistry-neurofilament protein (NFP) • Stain: haematoxylin-eosin
Buma et al	1995	Describe the distribution of the fibres that contain calcitonin gene-related protein peptide (CGRP) in normal bones and in bones that are remodelling after insertion of implant	<ul style="list-style-type: none"> • Goat tibias • Loaded after 3 weeks 	<ul style="list-style-type: none"> • Routine histology • Stain: hematoxylin and eosin • Fluorescence microscopy • Immunocytochemistry – CGRP and B-50/GAP-43 • Analysis: at 1 ; 6 and 12 weeks healing
Weiner et al	1995	Survey peri-implant region for axonal elements	<ul style="list-style-type: none"> • 12 implants (hydroxyapatite coated) - 3 dog mandibles • Loaded and unloaded 	<ul style="list-style-type: none"> • Immunohistochemistry-NFP • Stain: hematoxylin
Wang et al	1998	Investigate the characteristics, quantity and the chronological changes of nerve tissues around 3 kinds of implant materials	<ul style="list-style-type: none"> • 10 mongrel dogs • Single-crystal sapphire, TiO₂ and HA-coated implant • Control: not implanted, (analysis: 3 months after extraction) • Unloaded? (not specified in the article) 	<ul style="list-style-type: none"> • Analysis: 3 days, 1 week, 1 month and 3 months after implantation • Light microscopy and histomorphometry • Nerve tissue (histological slices) was reconstructed • Stain: Urea-silver nitrate
Wada et al	2001	Examine the effects of occlusal forces on the distribution of NFP-positive nerve fibres in the tissue of peri-implant bone	<ul style="list-style-type: none"> • 3 mongrel dogs • Bilateral 2nd/3rd/4th mandibular premolars and the 1st molar • 4 screw type implants • Load and unload implants • Two types of surfaces: Anode Oxidized Titanium Alloy (AOT)] surface or a Ti-6Al-4V [Hydroxyapatite-coating (HAC) 	<ul style="list-style-type: none"> • Loaded 3 months after implantation • Analysis: 6 months after implantation • Immunohistochemistry –NFP • Stain: labelled-streptavidin-biotin method
Ysander et al	2001	Describe a model and the results of histological and neuropeptide investigation in remodelled bone incorporating osseointegrated intramedullary titanium fixtures.	<ul style="list-style-type: none"> • 18 rat femurs • Commercially pure titanium rods • Unloaded implants 	<ul style="list-style-type: none"> • 8 weeks after implantation • Microscopic and immunohistochemical (CGRP) observations • confocal, fluorescent, bright-field, and phase microscopy • Light and fluorescent photomicroscopy • Stain: Avidin-Biotin Complex (ABC) and chromagen/ hematoxylin or methyl green

Table 5.2: Summary of main findings in previous animal studies on peri-implant bone innervation.

Author	Main findings	Remains unclear
Sawada et al	<ul style="list-style-type: none"> • 1 and 2 weeks after implantation - NFP-immunopositive nerve fibres (granulation tissue) • 4 weeks after the implantation - distribution and number of nerve fibres - almost identical to bone marrow of the edentulous area 	<p>After osseointegration:</p> <ul style="list-style-type: none"> • no significant changes in the distribution pattern of NFP-positive nerves • no incidence of regeneration of sensory receptors <p>After fibro-osseointegration:</p> <ul style="list-style-type: none"> • a number of nerve fibres NFP-immunopositive penetrated into a thick layer of fibrous connective tissue
Buma et al	<ul style="list-style-type: none"> • 2 types of fibres : fairly thick fibres in nerves showing no varicose structures / free running fibres with varicose appearance • Fibres CGRP-positive in all nerves • Small branches enter the cortical bone • Associated with blood vessels located at the Volkmann's canals • Fairly thick nerve or thick branch enter the medullary space through the nutrient canals • At 1 week: no positive staining with CGRP in the endosteal necrotic bone/ no immunostaining for B50/GAP43 antibody/ stained nerves outside necrotic bone • At 6 weeks: immunoreactivity where vascularisation was restored • CGRP-positive fibres at the transition between necrotic and revascularizing areas • Control bone occasionally found CGRP-positive fibres • Bone with implant showed many varicose fibres in almost all remodeling cavities • Blindly endings with thick parts of the structures directed towards the implant • At 12 weeks: proliferated nerve fibres disappeared/ pre-operative situation restored – bone innervated with sparse CGRP-positive fibres 	<ul style="list-style-type: none"> • Exact nature and function of nerve fibres observed in bone tissue • Nature of chemical factors involved in the regulatory process of cellular activity during bone remodeling
Weiner et al	<ul style="list-style-type: none"> • Two to three labelled sites per section in the peri-implant region were commonly found • No particular distribution • More common in connective tissue • In larger Haversian systems • No label in the lamellar bone or smaller Haversian systems 	<ul style="list-style-type: none"> • Role of axons in proprioception* • Clinical and functional significance of findings
Wang et al	<ul style="list-style-type: none"> • After 3 days: nerve fibre degeneration 	<ul style="list-style-type: none"> • Nerve fibres might originate from what innervated the

*although mechanoreception would be a more suitable term –for further clarification see Jacobs and van Steenberghe 1994 (Jacobs R, van Steenberghe D. Role of periodontal ligament receptors in the tactile function of teeth: a review. J Periodontal Res. 1994 May;29(3):153-67.) Review.

Table 5.2: Summary of main findings in previous animal studies on peri-implant bone innervation.

	<ul style="list-style-type: none"> • After 1 week: nerve fibre regeneration • After 1 week and 1 month: different pattern of bone formation around different materials • After 1 week and 3 months: different distribution of nerve tissue around different materials (reconstructed image) • 3 months after extraction: bone marrow shows fatty changes • Negative correlation bone contact ration and nerve density 	<p>PDL before tooth extraction</p> <ul style="list-style-type: none"> • Osteoblasts may influence secondarily the distribution of nerve fibres in the peri-implant area • Relation between quantitative difference of nerve fibres detected around different implant materials and sensation differences
Wada et al	<ul style="list-style-type: none"> • NFP-positive nerve fibres did not come into direct contact with the surface of the implant • No differences between load and unload or between implant surfaces material • NFP-positive fibres more frequently observed at 200µm from implant interfaces in the loaded implants • Free nerve endings and tree-like ramification • Present under the screw-threaded region or in the bone marrow space 	<ul style="list-style-type: none"> • Origin and role of nerve fibres in the peri-implant tissue
Ysander et al	<ul style="list-style-type: none"> • Upregulation of CGRP during bone remodelling –no significant inflammatory reaction • Cellular concentration of CGRP increased in association with osseointegration • Bone marrow cells resembling osteoclast and activated monocytes or macrophages were CGRP-positive in higher density in osseointegrated specimens (neuropeptide activity of activated bone marrow cells participating in the remodelling of bone around the implant threads) • New and normal bone adjacent to and fully occupying the space between fixture threads • Normal innervation in remodelled bone – small nerve fibres with the antibody Protein Gene Product 9.5 (PGP 9.5) • No difference in the neural density of operated bone when compared to the contralateral unoperated bone • Changes outside the time period of the study/ methods not sensitive enough to reveal small changes in nerve density and/or activity 	<ul style="list-style-type: none"> • Exact functional relationship between neuropeptides and bone remodelling • Influence of loading of implants on nerve density and/or activity

Material and Methods

A. Sample

The total sample of this study consisted of 12 partially or fully osseointegrated implants of 10 patients, collected in 3 dental centers in Belgium (UZLeuven (University Leuven and University Hospitals Leuven), Leuven, Belgium; ZOL (East Limburg Hospital), Genk, Belgium; Private Clinic, Leuven, Belgium) over a period of 5 years.

To guarantee histological observations of peri-implant tissues with healthy osseointegration, the majority of implants were retrieved because of mechanical failure. Yet, as mechanical failure is not frequently observed, implants retrieved as a result of extensive bone loss were also included and subjected to the histological analysis if a sufficient amount of healthy osseointegration was observed in the apical part of the implant. The study protocol was approved by the Ethical Committees of UZLeuven (protocol: S55446) and ZOL (protocol: 08/052L) and all patients gave their informed consent allowing the failed implant to be included in the study.

More information about the type of implants retrieved and the clinical information is provided in table 5.3. The amount of bone tissue was in the range of 0.5 to 1.0mm around implant retrieved. Those implants presented a surface roughness in the range of 0.68 μ m to 1.4 μ m (*Wennenberg and Albrektsson 2009*).

B. Specimen processing and histological analysis

To examine peri-implant bony tissues with healthy osseointegration, a histological analysis was performed. The implants were removed with a trephine bur and immediately immersed in 2% glutaraldehyde in 0.05 M cacodylate buffer (pH 7.3) or formaldehyde (10% formalin solution).

Table 5.3: Information patients, clinical status, type of prostheses, surgery and implant retrieved. Conv=conventional; M=male; F=female.

implant	age	gender	date removed	type	Additional information	site (jaw and location)	reason failure	surgery type	load	time in function	Rehabilitation Type
1	65	M	10 01 2008	osseotite	Nobel 3.75/10mm	13	FRACTURE	conv	conv	10 YEARS	fixed prosthesis
2	65	M	10 01 2008	osseotite	Nobel 3.75/10mm	14	FRACTURE	conv	conv	10 YEARS	fixed prosthesis
3	65	M	10 01 2008	osseotite	Nobel 3.75/10mm	SINUS REGION 15	FRACTURE	conv	conv	10 YEARS	fixed prosthesis
4	56	F	07 01 2008	NSGroovy	Nobel 3.75/13mm	35	Bone loss	conv	conv	6 months	crown
5	71		18 12 2007	NSGroovy	Nobel 5.0/10mm	35	Bone loss	conv	conv	6 months	crown
6	-	-	nov/08	-	-	-	FRACTURE	conv	conv	-	fixed prosthesis
7	73	M	nov/08	branemark	15mm	14	FRACTURE	conv	conv	14 years	fixed prosthesis
8	76	M	28 09 2009	branemark	13 e 8mm	14/15	Bone loss	conv	conv	17 years	fixed prosthesis
9	77	M	mei-2011	branemark	15mm	16 or 14 or 12	Bone loss	conv	conv	16 years	fixed prosthesis
10	-	-	09 11 2009	OSSEOSPEED	ASTRA 4.0/11mm	-	FRACTURE	-	-	-	-
11	79	F	mrt/10	OSSEOSPEED	ASTRA	31	Bone loss	-	IMMEDIATE	10 YEARS	fixed
12	56	M	jun/10	OSSEOSPEED	-	12	Bone loss	IMMEDIATE	IMMEDIATE	~10 Years	fixed

After fixation, the specimens were decalcified in 10% EDTA, dehydrated through a graded concentration of acetone and embedded in araldite. Subsequently, the specimens were sectioned, using a bone microtome (Reichert Ultracut E microtome (Reichert, Wien, Austria)) and further processed for light microscopical and ultrastructural analysis. Semi-thin sections (0.5 μ m) were stained with thionin methylene blue (0.1% aqueous solution) for light microscopy, and finally digitized using a high resolution Mirax Scan (Carl Zeiss Micro imaging GmbH, Germany). Observations were done by a trained observer at a magnification of 20X, 40X and 100X with a 30 inch LCD monitor (Apple Inc., Cupertino, USA), using a dedicated image software (Mirax Viewer 1.1, Göttingen, Germany). To assess the ultrastructural characteristics, serial ultra-thin sections (0.06 μ m) were mounted on

0.7% formvar-coated grids, contrasted with uranyl acetate and lead citrate and subsequently examined in an EM 208 S® transmission electron microscope (Philips, Eindhoven, The Netherlands) operated at 80 kV.

The diameter of 24 myelinated nerve fibres were measured in order to estimate the mean diameter of nerve fibres observed in the study sample. Bearing in mind the limited sample size and the diversity in human bone material, from which implants were retrieved, inferential statistics were considered irrelevant. Instead, only descriptive data reporting was carried out.

Results

In all specimens, bone tissue formation near the implant interface was observed. The areas with no direct bone contained either bone marrow or fibrous tissue. Woven bone, lamellar bone and marrow could be found in our study sample (figure 5.1). Bone tissue around implants presented osteons, Haversian canals and osteocytes, all of this being similar to cortical bone (figures 5.2 and 5.3).

Only few nerve fibres could be identified, most of them being myelinated and located in the Haversian systems near the implant threads (figures 5.4 and 5.5). Myelinated and unmyelinated nerve fibres could be identified inside the Haversian canals of the osteonal bone around the implants. Although those fibres were in close proximity to the implant interface (figure 5.4), no direct contact was observed between the nerve fibres and the implant interface. Myelinated fibres were identified by a thick blue envelop in the vicinity of Schwann cells. The thick and thin myelinated nerve fibres observed in the present study had an average diameter of 5.13µm (values ranging from 2.49-9.14µm and sd=1.84).

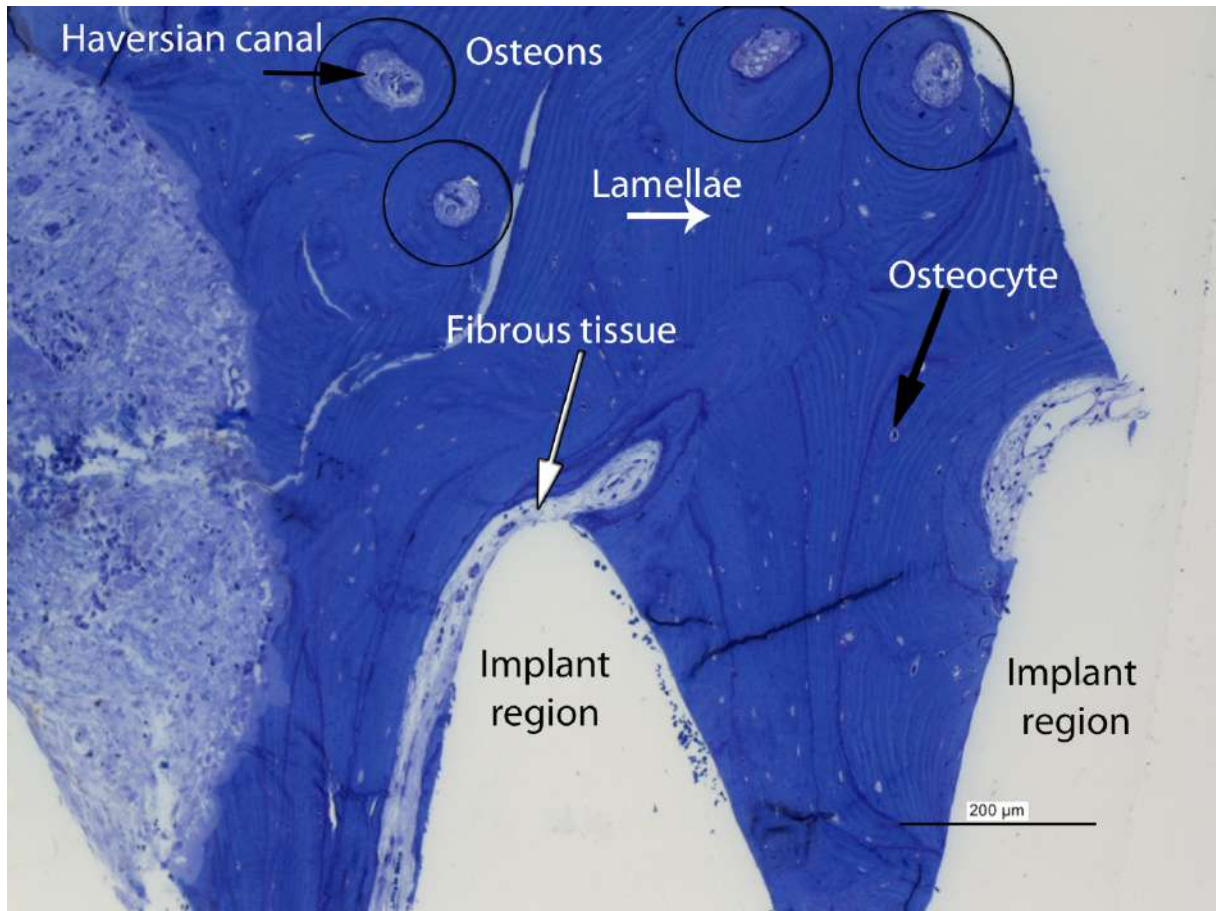


Figure 5.1: Photomicrograph of human peri-implant bone showing the presence of fibrous tissue, osteocytes, bone lamellae, osteons and Haversian canals (stain: thionin methylene blue).

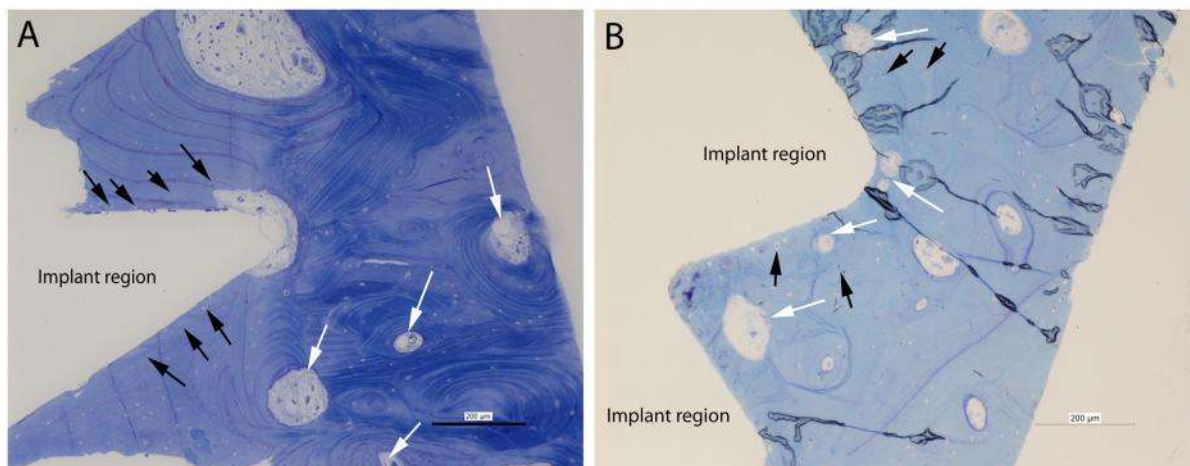


Figure 5.2: Photomicrographs (A) and (B) showing the presence of osteons (white arrows) and osteocytes (black arrows) close to the implant region (stain: thionin methylene blue).

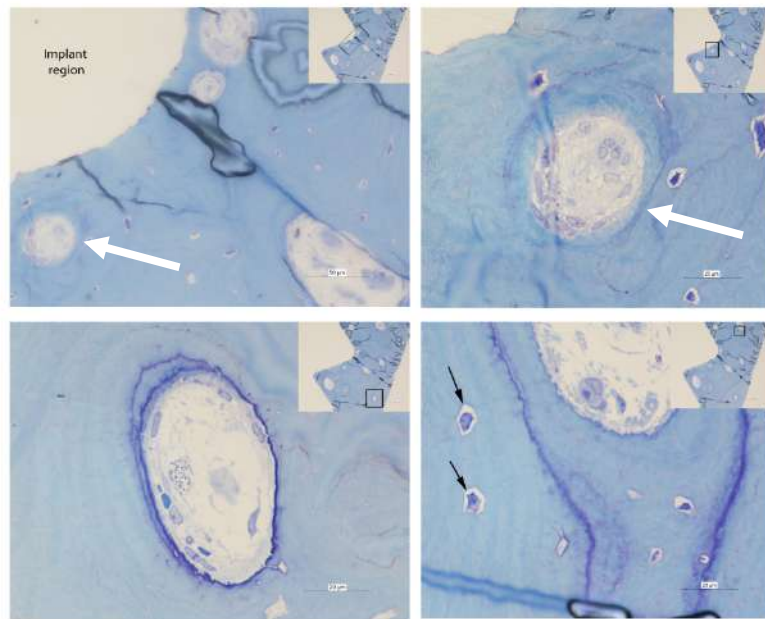


Figure 5.3: Higher magnification of osteons (white arrow) and osteocytes (black arrows) observed in figure 5.2B. Top right image indicates the region selected for the higher magnification (stain: thionin methylene blue).

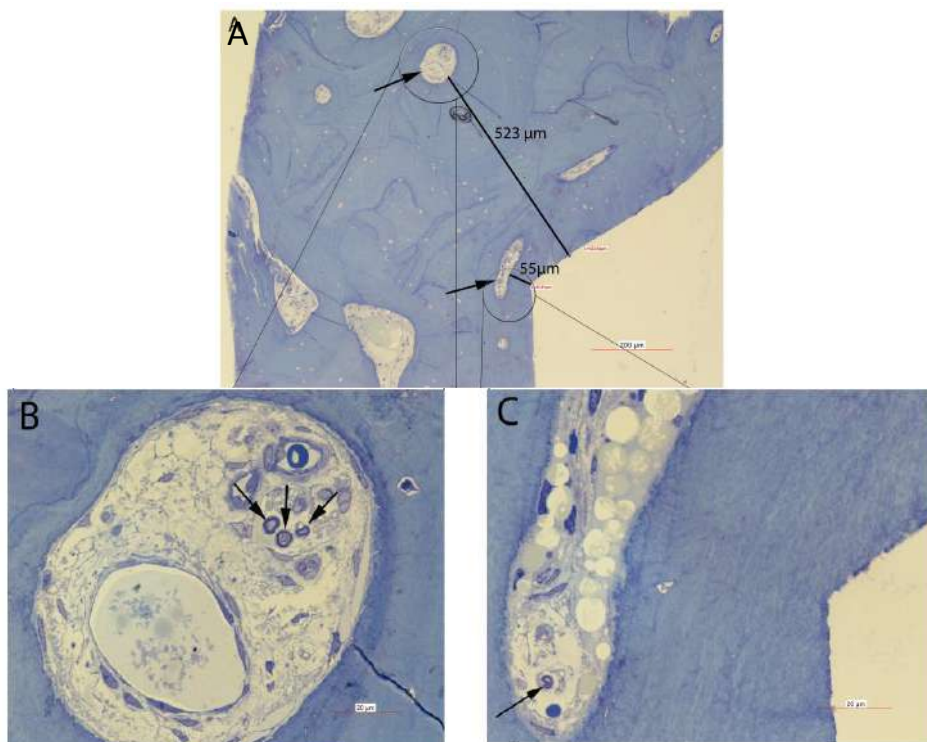


Figure 5.4: (A) Photomicrographs of osteonal bone around implant showing the proximity of the Haversian canals (black arrows) to the implant surface (stain: thionin methylene blue). (B) and (C) Myelinated fibres (black arrows) observed at the higher magnification image of Haversian canals in A (stain: thionin methylene blue). Those fibres are observed as rounded structures with dark-blue color at the periphery and light-blue at the center

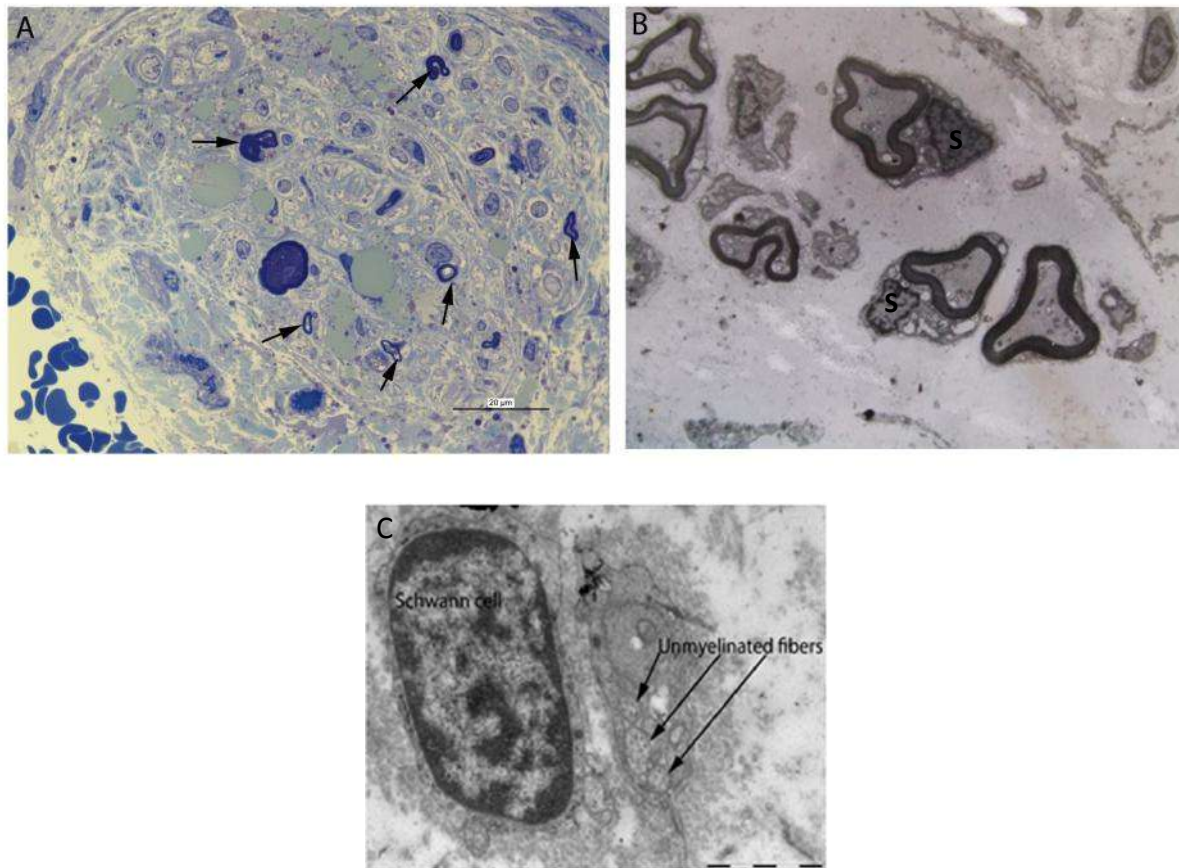


Figure 5.5: Light (A) and transmission electron microscopy (B) of human peri-implant bone tissue showing myelinated fibres (black arrows) embedded within the extracellular matrix. Schwann's cells (S) were found surrounding the axons with associated collagen fibres. (C)Transmission electron microscopic image of an unmyelinated nerve fiber adjacent to a Schwann cell (A) Stain: thionin methylene blue and (B) and (C) contrasted with: uranyl acetate and lead citrate.

Discussion

This study showed the presence of both myelinated and unmyelinated nerve fibres in human bone around titanium implants. Similar to previous studies conducted in dog mandibles (*Wada et al 2001; Weiner et al 1995*), nerve fibres were found in the Haversian canals which were located in the vicinity of the implant cavity. A minimum distance of 55µm between the Haversian canal containing nerve fibres and the implant cavity was observed in our study. These results correspond to the 60µm distance previously described by Weiner et al (1995). As reported by Wada et al (2001), these nerve fibres did not reach the implant. Although a connective tissue lacuna has been found adjacent to the implant, the presence of nerve fibres at this location could not be confirmed, similar to findings of Weiner et al (1995).

Previous studies already reported the presence of nerve fibres in the peri-implant bone in animals (*Wada et al 2001; Ysander 2001; Wang et al 1998; Buma et al 1995; Weiner et al 1995; Sawada et al 1993*). Those studies suggest that peri-implant innervation is similar to that found in an unoperated bone or in the healed extraction socket (*Ysander 2001; Buma et al 1995; Sawada et al 1993*). In addition, similar events, associated with changes in the nerve fibre density during bone modeling, are described for both extraction socket healing and osseointegration process (*Gunjigake et al 2007; Wang et al 1998; Mason and Holland 1993; Sawada et al 1993; Hansen 1980*). The low occurrence of nerve fibres, observed in this study, is further supported by the low density of nerve fibres (0.03% to 0.07%) found 6 months after implant placement, reported by *Wada et al (2001)*.

Wang et al (1998) suggest that loaded implants present higher density of nerve fibres when compared to unloaded implants. Furthermore, these implants presented more fatty changes in the peri-implant bone than the loaded ones. Hence, both nerve fibre density and loading approach would influence bone modeling, as suggested by the authors. However, more research is necessary to draw clear conclusions about the influence of loading on peri-implant innervation. Such a comparison was not possible in our sample since all implants were already loaded for more than 6 months.

According to *Wang et al (1998)* and *Wada et al (2001)*, implant surfaces influence at the same time nerve fibre density and bone-to-implant contact ratio. However, nerve fibre density shows a negative correlation with bone contact ratio in unloaded implants. The highest nerve density ($1.87\mu\text{m}/\text{mm}^2$) has been found in implant surfaces with a bone contact ratio around 8.40%. On the other hand, the lowest nerve density ($0.83\mu\text{m}/\text{mm}^2$) was associated with implant surfaces where bone contact ratio was around 78.09% (*Wang et al 1998*). Yet, more researches are needed to further study the influence of different implant-related variables, namely loading protocols or implant surfaces, on the bone modeling and innervation.

In our study, thick and thin myelinated nerve fibres were identified with a general mean diameter around $5.13\mu\text{m}$ (values ranging from $2.49\text{--}9.14\mu\text{m}$). Within this diameter range, they may represent fibres of type A β , A γ , A δ or B, according to

the Erlanger-Gasser classification, or type II or III, in the Lloyd's classification (Manzano *et al* 2008). As such, their function can be related to that of afferent and efferent autonomic nerve fibres, as well as of the afferent somatic nerve fibres, e.g. touch perception and pressure. The morphology of Ruffini-like mechanoreceptors as described in mammal and human in the periodontal ligament (Maeda *et al* 1999; Lambrichts *et al* 1992; Kannari 1990) could not be shown in the present histological study on human peri-implant bone. Nevertheless, the presence of some nerve fibres structurally resembling mechanoreceptors has been previously shown in animal bone (Lambrichts 1998). One hypothesis would be that the morphology of mechanoreceptors varies amongst species, whereas, most importantly, the mechanoreception mechanism may vary according to the tissues in which those nerve fibres are confined.

While tactile function becomes impaired after tooth extraction, the improved oral function of edentulous patients after implant rehabilitation has been supported by numerous evidences (Lundqvist and Haraldson 1992; Lundqvist and Haraldson 1990; Lundqvist and Haraldson 1984). The possible role of inferred PDL remnants and of other nerve fibres/receptors located in the bone or surrounding tissues has been discussed in previous studies (Jacobs and van Steenberghe 2006; Trulsson 2005; Jacobs *et al* 2002; Jacobs 1998; Jacobs and van Steenberghe 1995; Bonte *et al* 1993; Bonte and van Steenberghe 1991; Linden and Scott 1989b). However, depending on the stimulus and the design of the animal or human study, several conclusions, and mainly hypotheses, can be drawn. Using electrophysiological records after tooth extraction in cats, the study of Linden and Scott (1989b) showed that at least some mechanoreceptors which originally innervated the periodontal ligament are still present in the edentulous bone. This is shown by electrical stimulation of the edentulous ridge yielding an activation of nerve fibres with cell bodies in the mesencephalic nucleus. Yet, no activation was found in the mesencephalic nucleus or in the trigeminal ganglion after mechanical stimulation of the edentulous ridge (Linden and Scott 1989b) or implants (Bonte *et al* 1993). However osseointegrated implants influenced the reflex effects of jaw-closing muscles in cats. Bonte *et al* (1993) report inhibition of electrical activity if sufficient forces are applied either to the tooth or to the implant. On the other hand, no similar inhibitory reflex has been found

in humans in the absence of teeth (*Jacobs and van Steenberghe 1995; Bonte and van Steenberghe 1991*).

In the natural dentition, periodontal ligament nerve fibres having their cell bodies located at the mesencephalic nucleus are associated with specialized mechanosensory feedback during oral function (*Linden and Scott 1989a*). Since those fibres do not respond to mechanical stimulation, even though still present after tooth extraction, this function is expected to remain impaired after oral implant rehabilitation. Indeed, studies evaluating load perception threshold on implants and teeth found that this function, although better than in a fully edentulous condition, remains impaired on osseointegrated implants (*Jacobs and van Steenberghe 1993*). However, very important is the recent observation of Habre-Hallage et al. (2012). This group was the first to demonstrate a sensory cortical response in humans after pure mechanical implant stimulation. They underlined the role of central plasticity occurring after tooth extraction and implant rehabilitation, which may allow some functional adaptation controlled by other areas in the central nervous system.

Although the present study could not identify specialized sensory receptors in the peri-implant tissues, the diameter of myelinated nerve fibres observed in the present research suggested that these fibres might be involved in the transmission of pressure and touch stimuli (*Manzano et al 2008*). Knowledge derived from studies about mechanoreceptors located in the human periodontal ligament should be applied in future immunohistochemical studies to unravel sensory function in bone tissue after implant placement. Indeed, studies in periodontal ligament have shown that immunoreactivity to neurofilament protein (NFP), S-100 antibody and unspecific cholinesterase acetylcholinase are related to Ruffini-like mechanoreceptors in the periodontal ligament (*Maeda et al 1999; Kannari 1990*). Up till now, studies on bone innervation are more advanced in describing the function of nerve fibres in the bone remodeling and in transmission of nociceptive stimuli. Future studies should focus on the molecular process taking place during mechanical stimuli in mandible rehabilitated with implants, as well as in the dentate and edentulous jaw bone.

Peri-implant tissue has been investigated from several aspects; e.g. density of nerve fibres (*Wada et al 2001; Buma et al 1995; Weiner et al 1995; Sawada et al 1993*),

collagen fibre and osteon orientation (*Traini et al 2009; Neugebauer et al 2006*), bone-implant contact and effects of implant materials in nerve conduction (*Onur et al 2006*). Nevertheless, the innervation patterns for sensory nerve fibres involved in the tactile function have never been demonstrated after implant placement. From psychophysical studies, it is known that an improved tactile function can be expected in edentulous patients after implant rehabilitation (*Jacobs and van Steenberghe 2006; Lundqvist and Haraldson 1984*). Furthermore, evidence related to masticatory function and central stimulation reinforces the role of peri-implant bone innervation in the physiological integration of implants (*Habre-Hallage et al 2012; van der Bilt 2011; Kimoto et al 2008; Yan et al 2008*).

The present study describes for the first time peri-implant innervation in humans. This implies that the present discussion has to oppose the human findings to the state-of-the-art on animal findings. After implant insertion into the tibia of the goat, Buma et al (1995) described necrosis and subsequent dynamic neural sprouting and reinnervation associated with the process of bone formation. The remodeled bone became reinnervated 6 weeks after implant placement with nerve distribution becoming similar to the normal bone after 12 weeks. This study supported the close relationship between vascularization and innervation, once nerve regeneration was observed in areas where vascularization has been restored.

In a dog model, Wang et al (1998) have reported nerve fibre degeneration 3 days after implant installation, followed by regeneration at day 7. Immunohistochemical studies using NFP have shown the presence of NFP-positive nerves in the bone marrow, Haversian canals or associated with fibrous connective tissue (*Wada et al 2001; Weiner et al 1995; Sawada et al 1993*), although with no particular distribution (*Weiner et al 1995*). By using protein gene product 9.5 (PGP 9.5) in rat femurs, Ysander et al (2001) have reported no significant difference in the neural density between the osseointegrated site and the unoperated contralateral bone. Similarly, Sawada et al (1993) have observed no significant changes in the distribution pattern of NFP-positive nerves or incidence of regeneration of sensory receptors after osseointegration.

Nevertheless, Ysander et al (2001) have reported changes in the neuropeptide activity of bone marrow cells participating in bone remodelling around the implant threads. According to the authors, the cellular concentration of calcitonin gene related peptide (CGRP) increases in association with osseointegration. CGRP is a widely expressed constituent of sensory neurons which plays an important role in nerve function and repair when axons are severed. In addition, CGRP seems also involved in bone remodelling (*Li et al 2004; Konttinen et al 1996*). Compared to the contralateral control side, bone marrow cells resembling osteoclast and activated monocytes or macrophages were CGRP-positive in higher density in osseointegrated specimens, mainly where the remodeling process had not yet been finalized (*Ysander et al 2001*). Those findings may indicate a true relationship between nervous system, bone remodeling and osseointegration process, also reported by other authors (*Konttinen et al 1996; Buma et al 1995*). Yet, no study has been found discussing differences in nerve fibre morphology, distribution pattern or molecular processes related to the several aspects involved in implant rehabilitation.

Irrespective of all those evidences, it has to be admitted that from all vertebrate senses, touch/tactile function is the least understood at the molecular level (*Welsh et al 2002*) making the connection between morphology and function a complex matter to unravel using the histological techniques available. It has been postulated that the core components of mechanosensors are ion channels. Such channels could convert mechanical energy directly into an electrical signal; this could account for the very high speed response of mechanosensors (*Welsh et al 2002*). The understanding of tactile function at the molecular level might help to identify nerve fibres involved in the osseoperception phenomenon. The exact origin of nerve fibres identified in the present study could not be determined. Therefore, in line with the conclusion by Buma et al (1995), detailed tracer studies are needed to evaluate the exact nature of the fibres demonstrated in the present study.

The debate on peri-implant bone innervation is stimulated by the technical difficulties inherent in the application of neurohistological techniques to hard tissue such as bone. One should keep in mind that the osseoperception phenomenon, in implants and normal bone needs further exploration. Future studies should approach

the perspectives on improving bone innervation around implants, its applicability and advantage over the current techniques.

Conclusions

The present report is the first to describe the presence, size and location of peri-implant bone innervation in human jaw bone. Nerve fibres could be detected inside newly formed bone. Both myelinated and unmyelinated nerve fibres were observed in the peri-implant bone, localized in the Haversian canals, also those close to the bone-implant interface.

References

- Abarca M, van Steenberghe D, Malevez C, Jacobs R. The neurophysiology of osseointegrated oral implants. A clinically underestimated aspect. *J Oral Rehabil* 2006; 33:161-9.
- Albrektsson T, Jansson T, Lekholm U. Osseointegrated dental implants. *Dent Clin North Am* 1986; 30:151-74.
- Bonte B, Linden RW, Scott BJ, van Steenberghe D. Role of periodontal mechanoreceptors in evoking reflexes in the jaw-closing muscles of the cat. *J Physiol* 1993; 465:581-94.
- Bonte B, van Steenberghe D. Masseteric post-stimulus EMG complex following mechanical stimulation of osseointegrated oral implants. *J Oral Rehabil* 1991; 18:221-9.
- Buma P, Elmans L, Oestreicher AB. Changes in innervation of long bones after insertion of an implant: immunocytochemical study in goats with antibodies to calcitonin gene-related peptide and B-50/GAP-43. *J Orthop Res* 1995;13:570-7.
- Castaneda-Corral G, Jimenez-Andrade JM, Bloom AP, Taylor RN, Mantyh WG, Kaczmarek MJ, et al. The majority of myelinated and unmyelinated sensory nerve fibres that innervate bone express the tropomyosin receptor kinase A. *Neuroscience* 2011; 178:196-207.
- Gallagher P, Desmond D and MacLachlan M. *Psychoprosthetics*. London: Springer 2008.
- Gunjigake KK, Goto T, Nakao K, Konoo T, Kobayashi S, Yamaguchi K. Correlation between the appearance of neuropeptides in the rat trigeminal ganglion and reinnervation of the healing root socket after tooth extraction. *Acta Histochem Cytochem* 2006; 39:69-77.
- Habre-Hallage P, Dricot L, Jacobs R, van Steenberghe D, Reyckler H, Grandin CB. Brain plasticity and cortical correlates of osseoperception revealed by punctate mechanical stimulation of osseointegrated oral implants during fMRI. *Eur J Oral Implantol* 2012; 5:175-90.
- Hagberg k, Häggström E, Jönsson S, Rydevik B and Brånemark R. Osseoperception and Osseointegrated Prosthetic Limbs. In: Gallagher P, Desmond D and MacLachlan M. *Psychoprosthetics*. London: Springer 2008: 131-140.

- Hansen HJ. Neuro-histological reactions following tooth extractions. *Int J Oral Surg* 1980; 9:411-26.
- Haraldson T, Carlsson GE. Bite force and oral function in patients with osseointegrated oral implants. *Scand J Dent Res* 1977; 85:200-8.
- Haraldson T, Carlsson GE, Ingervall B. Functional state, bite force and postural muscle activity in patients with osseointegrated oral implant bridges. *Acta Odontol Scand* 1979; 37:195-206.
- Haraldson T, Ingervall B. Muscle function during chewing and swallowing in patients with osseointegrated oral implant bridges. An electromyographic study. *Acta Odontol Scand* 1979; 37:207-16.
- Herskovits MS, Singh IJ, Sandhu HS. Innervation of Bone. In: Hall BK, editor. *Bone. Vol 3: Bone matrix and bone specific products.* Boca Raton: CRC Press Inc. p 1990:166-185.
- Jacobs R, van Steenberghe D. From osseoperception to implant-mediated sensory-motor interactions and related clinical implications. *J Oral Rehabil* 2006; 33:282-92.
- Jacobs R, Wu CH, Goossens K, Van Loven K, Van Hees J, van Steenberghe D. Oral mucosal versus cutaneous sensory testing: a review of the literature. *J Oral Rehabil* 2002; 29:923-50.
- Jacobs R. *Osseoperception.* Leuven: KULeuven, 1998.
- Jacobs R, van Steenberghe D. Qualitative evaluation of the masseteric poststimulus EMG complex following mechanical or acoustic stimulation of osseointegrated oral implants. *Int J Oral Maxillofac Implants* 1995;10:175-82.
- Jacobs R, van Steenberghe D. Comparison between implant-supported prostheses and teeth regarding passive threshold level. *Int J Oral Maxillofac Implants* 1993; 8:549-54.
- Kannari K. Sensory receptors in the periodontal ligament of hamster incisors with special reference to the distribution, ultrastructure and three-dimensional reconstruction of Ruffini endings. *Arch Histol Cytol* 1990; 53:559-73.
- Kimoto K, Ono Y, Tachibana A, Hirano Y, Otsuka T, Ohno A, et al. Chewing-induced regional brain activity in edentulous patients who received mandibular implant-supported overdentures: a preliminary report. *J Prosthodont Res* 2011; 55:89-97.
- Klineberg I, Calford MB, Dreher B, Henry P, Macefield V, Miles T, et al. A consensus statement on osseoperception. *Clin Exp Pharmacol Physiol* 2005; 32:145-6.
- Kontinen Y, Imai S, Suda A. Neuropeptides and the puzzle of bone remodeling. State of the art. *Acta Orthop Scand* 1996; 67:632-9.
- Lambrichts I. Histological and ultrastructural aspects of bone innervation. In: Jacobs R. (ed) *Osseoperception.* Leuven: KULeuven 1998:13-20.
- Lambrichts I, Creemers J, van Steenberghe D. Morphology of neural endings in the human periodontal-ligament- an electron-microscopic study. *J Periodontal Res* 1992; 27:191-6.
- Li XQ, Verge VM, Johnston JM, Zochodne DW. CGRP peptide and regenerating sensory axons. *J Neuropathol Exp Neurol* 2004; 63:1092-103.
- Linden RW, Scott BJ. Distribution of mesencephalic nucleus and trigeminal ganglion mechanoreceptors in the periodontal ligament of the cat. *J Physiol* 1989 a; 410:35-44.
- Linden RW, Scott BJ. The effect of tooth extraction on periodontal ligament mechanoreceptors represented in the mesencephalic nucleus of the cat. *Arch Oral Biol* 1989 b; 34:937-41

- Lundqvist S, Haraldson T. Oral function in patients wearing fixed prosthesis on osseointegrated implants in the maxilla. *Scand J Dent Res* 1990; 98:544-9.
- Lundqvist S, Haraldson T. Oral function in patients wearing fixed prosthesis on osseointegrated implants in the maxilla: 3-year follow-up study. *Scand J Dent Res* 1992; 100:279-83
- Lundqvist S, Haraldson T. Occlusal perception of thickness in patients with bridges on osseointegrated oral implants. *Scand J Dent Res* 1984; 92:88-92.
- Mach DB, Rogers SD, Sabino MC, Luger NM, Schwei MJ, Pomonis JD, et al. Origins of skeletal pain: sensory and sympathetic innervation of the mouse femur. *Neuroscience* 2002; 113:155-66.
- Manzano GM, Giuliano LM, Nobrega JA. A brief historical note on the classification of nerve fibres. *Arq Neuropsiquiatr* 2008; 66:117-9.
- Maeda T, Ochi K, Nakakura-Ohshima K, Youn SH, Wakisaka S. The Ruffini ending as the primary mechanoreceptor in the periodontal ligament: its morphology, cytochemical features, regeneration, and development. *Crit Rev Oral Biol Med* 1999; 10:307-27.
- Martin RB, Burr DB.. Structure, function, and adaptation of compact bone. New York: Raven Press, 1989.
- Mason AG, Holland GR. The reinnervation of healing extraction sockets in the ferret. *J Dent Res* 1993; 72:1215-21.
- McCredie J. Nerves in bone: the silent partners. *Skeletal Radiol* 2007; 36:473-5.
- Neugebauer J, Traini T, Thams U, Piattelli A, Zoller JE. Peri-implant bone organization under immediate loading state. Circularly polarized light analyses: a minipig study. *J Periodontol* 2006; 77:152-60.
- Onur MA, Sezgin A, Gurpinar A, Sommer A, Akca K, Cehreli M. Neural response to sandblasted/acid-etched, TiO₂-blasted, polished, and mechanochemically polished/nanostructured titanium implant surfaces. *Clin Oral Implants Res* 2006; 17:541-7.
- Rubin J, Rubin C. Functional adaptation to loading of a single bone is neuronally regulated and involves multiple bones. *J Bone Miner Res* 2008; 23:1369-71.
- Sample SJ, Behan M, Smith L, Oldenhoff WE, Markel MD, Kalscheur VL, et al. Functional adaptation to loading of a single bone is neuronally regulated and involves multiple bones. *J Bone Miner Res* 2008; 23:1372-81.
- Sawada, M., Kusakari, H., Sato, O., Maeda, T. & Takano, Y. Histological investigation on chronological changes in peri-implant tissues, with special reference to response of nerve fibres to implantation. *J Jap Prost Soc* 1993; 37:144–158.
- Serre CM, Farlay D, Delmas PD, Chenu C. Evidence for a dense and intimate innervation of the bone tissue, including glutamate-containing fibres. *Bone* 1999; 25:623-9.
- Traini T, Neugebauer J, Thams U, Zoller JE, Caputi S, Piattelli A. Peri-implant bone organization under immediate loading conditions: collagen fibre orientation and mineral density analyses in the minipig model. *Clin Implant Dent Relat Res* 2009; 11:41-51.
- Trulsson M. Sensory and motor function of teeth and dental implants: a basis for osseoperception. *Clin Exp Pharmacol Physiol* 2005; 32:119-22.
- Trulsson M. Sensory-motor function of human periodontal mechanoreceptors. *J Oral Rehabil* 2006; 33:262-73.

- Trulsson M. Force encoding by human periodontal mechanoreceptors during mastication. *Arch Oral Biol* 2007; 52:357-60.
- van der Bilt A. Assessment of mastication with implications for oral rehabilitation: a review. *J Oral Rehabil* 2011; 38:754-80.
- Van Loven K, Jacobs R, Swinnen A, Van Huffel S, Van Hees J, van Steenberghe D. Sensations and trigeminal somatosensory-evoked potentials elicited by electrical stimulation of endosseous oral implants in humans. *Arch Oral Biol* 2000; 45:1083-90.
- van Steenberghe D. From osseointegration to osseoperception. *J Dent Res* 2000; 79:1833-7.
- Wada S, Kojo T, Wang YH, Ando H, Nakanishi E, Zhang M, et al. Effect of loading on the development of nerve fibres around oral implants in the dog mandible. *Clin Oral Implants Res* 2001; 12:219-24.
- Wang, Y.-H., Kojo, T., Ando, H., Nakanishi, E., Yoshizawa, H., Zhang, M., Fukuyama, H., Wada, S., Uchida, Y. Nerve regeneration after implantation in peri-implant area. A histological study on different implant materials in dogs. In: Jacobs R. (ed) *Osseoperception*. Leuven KULeuven 1998:3-11
- Weiner S, Klein M, Doyle JL, Brunner M. Identification of axons in the peri-implant region by immunohistochemistry. *Int J Oral Maxillofac Implants* 1995; 10:689-95.
- Welsh MJ, Price MP, Xie J. Biochemical basis of touch perception: mechanosensory function of degenerin/epithelial Na⁺ channels. *J Biol Chem* 2002; 277:2369-72.
- Wennerberg A, Albrektsson T. On implant surfaces: A review of current knowledge and opinions. *Int J Oral Maxillofac Implants* 2009; 24:63-74.
- Yan C, Ye L, Zhen J, Ke L, Gang L. Neuroplasticity of edentulous patients with implant-supported full dentures. *Eur J Oral Sci* 2008; 116:387-93.
- Ysander M, Brånemark R, Olmarker K, Myers RR. Intramedullary osseointegration: development of a rodent model and study of histology and neuropeptide changes around titanium implants. *J Rehabil Res Dev* 2001; 38:183-90.
- Zhu YB, Lin Y, Qiu LX, Wang Y. [An animal study of peripheral neurophysiologic mechanism in osseoperception phenomena of dental implant]. *Zhonghua Kou Qiang Yi Xue Za Zhi* 2009; 44:460-3.



PART II

Radio-anatomical assessment

Chapter 6

Peri-implant bone characterization

Bone structure and density

Publication related to this chapter:

Corpas LS, Jacobs R, Quirynen M, Huang Y, Naert I, Duyck J. Peri-implant bone tissue assessment by comparing the outcome of intra-oral radiograph and cone beam computed tomography analyses to the histological standard. Clin Oral Implants Res 2011; 22:492-9.

Peri-implant bone tissue assessment by comparing the outcome of intra-oral radiograph and cone beam computed tomography analyses to the histological standard.

Abstract:

Objectives: The present study aims to identify radiographic methods revealing data that are most representative for the true peri-implant bone as assessed by histology.

Materials and methods: Eighty implants were placed in 10 minipigs. To assess matching between different images modalities, measurements conducted on intra-oral digital radiographs (IO), cone beam (CBCT) and histological images were correlated using Spearman's correlation. Paired tests (Wilcoxon test) were used to check changes on bone parameters after 2 and 3 months healing.

Results: Significant correlations were found between bone defect depth on IO and histological slices ($r=+0.70$, $p<0.01$), as well as on CBCT images and histological slices ($r=+0.61$, $p<0.01$). CBCT and IO images deviate respectively 1.20 and 1.17mm from the histology regarding the bone defect. No significant correlations were detected between fractal analysis on CBCT, intra-oral radiography and histology. For bone density assessment, significant but weak correlations ($r=+0.50$, $p<0.01$) were found for intra-oral radiography versus histology. Significant marginal bone level changes could be observed after 3 months of healing using intra-oral radiography.

Conclusions: This study allowed linking radiographic bone defect depth to the histological observations of the peri-implant bone. Minute bone changes during a short-term period could be followed up using digital intra-oral radiography. Radiographic fractal analysis did not seem to match histological fractal analysis. CBCT was not found reliable for bone density measures, but might hold potential with regard to structural analysis of the trabecular bone.

Introduction

Radiographic analyses are commonly used in implant dentistry as an important diagnostic tool for treatment planning and follow-up (*Laurell & Lundgren 2009; Misch et al 2008; Vercrijssen et al 2008; Ribeiro-Rotta et al 2007; Parel et al 2004; BouSerhal et al 2002; Floyd et al 1999; Brånemark et al 1997*). During treatment planning, bone quantity and quality need to be determined (*Song et al 2009; Turkyilmaz et al 2007; Turkyilmaz et al 2006*), whereas for treatment follow-up, analysis of implant stability, marginal bone level and bone implant contact are applied (*Alsaadi et al 2007; Aranyarachkul et al 2005; Atsumi et al 2007; Friberg et al 2000; Meredith 1998*). Follow-up analysis aims to assess osseointegration and detect signs of failing integration at an early stage. Marginal bone loss and loss of bone-to-implant contact (e.g. by marsupialisation) may indeed negatively influence implant success (*Qian et al 2012; Snauwaert et al. 2000; Isidor 1997; Misch 1990*). Several criteria to analyze oral implants radiologically have been proposed by different authors (*Thoma et al 2013; Pikner 2008; Albrektsson et al. 1986; Schnitman and Shulman 1979*). In general, radiological success criteria are defined by a minimum marginal bone loss and absence of peri-implant radiolucency (*Qian et al 2012; Pikner 2008*).

Intra-oral radiography have been widely used to reveal changes around implants, mainly due to its considerable advantages, e.g. low costs, readily availability, good patient tolerance, user friendliness and ability to provide high-resolution images for accurate measures at the implant sites (*Jacobs & van Steenberghe 1997; Tyndall and Brooks 2000; Pikner 2008; Hermann et al 2001; Isidor 1997*). Nevertheless, to detect a continuous bone loss, it is important that changes in the bone level can be reliably measured by radiological assessment. Intra-oral radiographic measures have proven to estimate the marginal bone level closer to reality (gold standard histological assessment) when compared to clinical probing in an animal study (*Isidor 1997b*).

Despite their widespread use, intra-oral radiographs may also suffer from the inherent 2D nature, with anatomical superposition and geometric distortion, limiting the visibility of intraosseous defects and their changes over time (*Patel et al 2009a; Tyndall & Brooks 2000*). On 2D images, unfavorable marginal bone level or absence of osseointegration can be hidden by superimposition (*Isidor 1997 b*). Furthermore, to

detect non-osseointegration, the presence of a soft tissue layer adjacent to the implant surface should be made visible radiologically. Yet, intra-oral radiographs cannot always achieve this considering limits in spatial and contrast resolution (*Jacobs & van Steenberghe 1997; Pikner 2008*). Furthermore, the 2D nature prevents evaluating the buccal and lingual bone levels.

Cone beam computer tomography (CBCT) might overcome some of the limitations of intra-oral radiographs (*Patel et al 2009a; Patel 2009b; Patel et al 2009 c*). Indeed, three-dimensional imaging may allow examining the implant and its surrounding tissues in several orthogonal planes, while having the possibility to scroll through the slices to visualize the 3D anatomy. However, marginal bone level measurements on CBCT images have never been validated. This is necessary, considering that CBCT images can indeed contribute to an increased spatial resolution, yet the accuracy and precision of technique might be hampered by image resolution and artifacts generated by implant material.

It is important to note that an appropriate radiological examination not only aims to follow marginal bone level changes, but also monitor other modifications in the marginal bone. Thanks to development of digital image processing, some minute changes in the bone, which up till now remained radiologically invisible, became noticeable. Bone density (*Nackaerts et al 2006; Lee et al 2007; Nackaerts et al 2008*) and structure (*Huang et al 2013; Couture et al 2003; Dougherty & Henebry 2001; Lindh et al 1996; Mish et al 1999; Wilding et al 1995*) can be cited as two other features helping to measure objectively morphological and physical changes in the bone. Hence, other methods should become clinically available to allow radiologists and surgeons to determine precisely bone changes by means of radiological images. However, the application of these new technologies (digital intra-oral radiography and CBCT) and the clinical validity of new bone parameters still need to be tested.

Therefore, this study aims to analyze the marginal bone level measured on CBCT images and to evaluate some bone characteristics (bone density and fractal features) on CBCT and intra-oral radiograph images using histological slices as gold standard. Furthermore, it will be evaluated if those analyses can radiologically detect bone remodelling. This will be approached using intra-oral radiography by comparing

bone level, density and structure at implant placement and 2 and 3 months after implant healing in an animal model. Thus, the following hypotheses were formulated:

1) tissue parameters assessed on intra-oral radiographs and cone beam computer tomograms match those found in histomorphometric analyses of the same sites. (Part I: Matching);

2) radiographic changes in peri-implant tissue parameters are noticeable after 3 months of healing (Part II: Short follow up).

3) IO radiographic density of peri-implant bone varies among implant neck, threads and apical regions (Part III: Intra-oral radiographic density)

4) IO radiographic density of bone before implant placement can predict marginal bone loss after 3 months healing (Part III: Intra-oral radiographic density)

Material & Methods:

Material:

Ten Göttingen male mini-pigs were used as experimental animals. Ethical approval was obtained from the local ethical committee for laboratory animal science (Biomedical Science Group, KU Leuven). A total of 80 implants were placed in upper and lower jaw. In each of the 4 quadrants, the last premolar and first molar were extracted 3 months prior to the start of the study. At baseline, 2 implants were placed in each jaw, and four additional implants were placed 2 months after the first implant installation. The animals were then sacrificed one month later. Surgical procedures were performed under general anaesthesia following a standardized protocol (crestal incision, progressive widening osteotomy site, tapping, and submerged healing). Eighty implants were used to conduct the correlation between radiological and histological images and forty implants were observed at the follow up part of the study (figure 6.1).

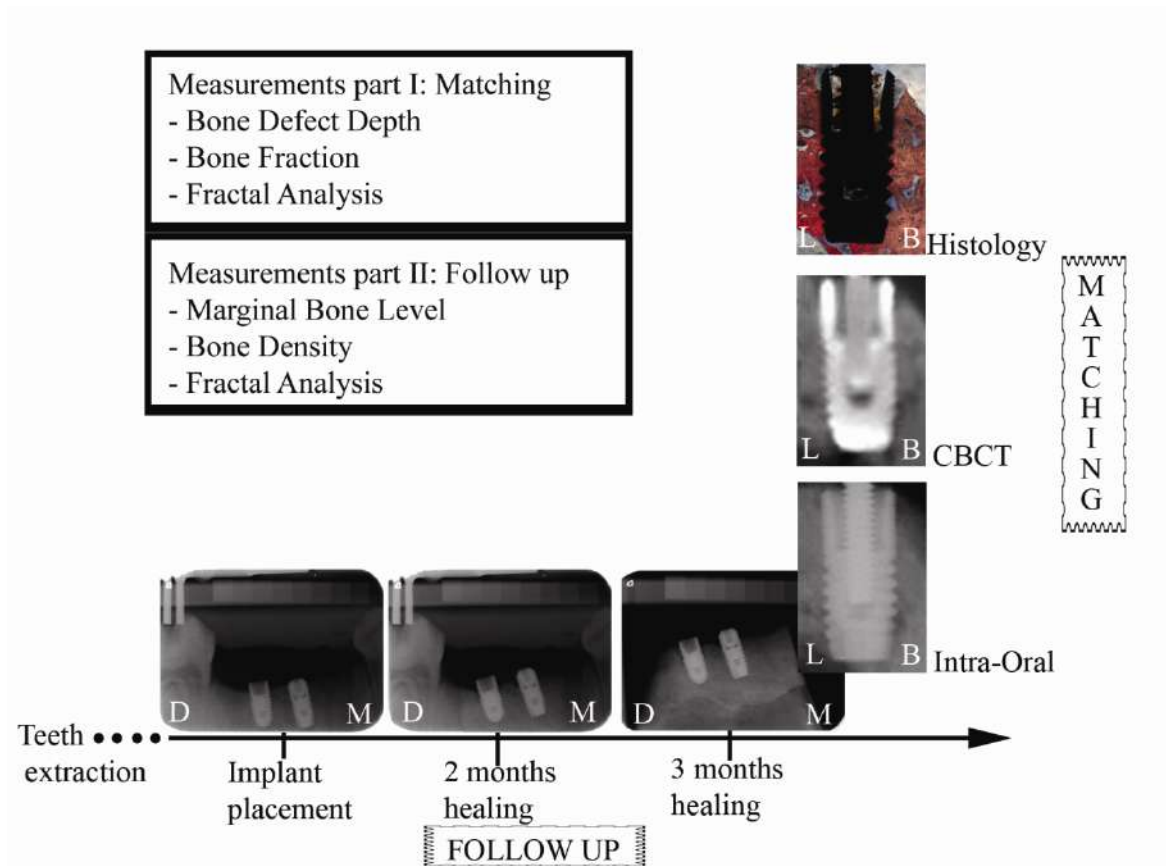


Figure 6.1: Study design overview. M (mesial side); D (distal side); B (buccal side); L (lingual side). Images on BL (bucco-lingual) direction were used to check matching between different image modalities while images on MD (mesio-distal) direction were used to proceed follow-up measurements.

Methods:

Part I: Matching

In this part of the study, measurements on intra-oral radiographs and on CBCT were compared to the same measurement on histological images derived from the same sections of the same specimen using similar orientation and region of interest (ROI) (figure 6.2).

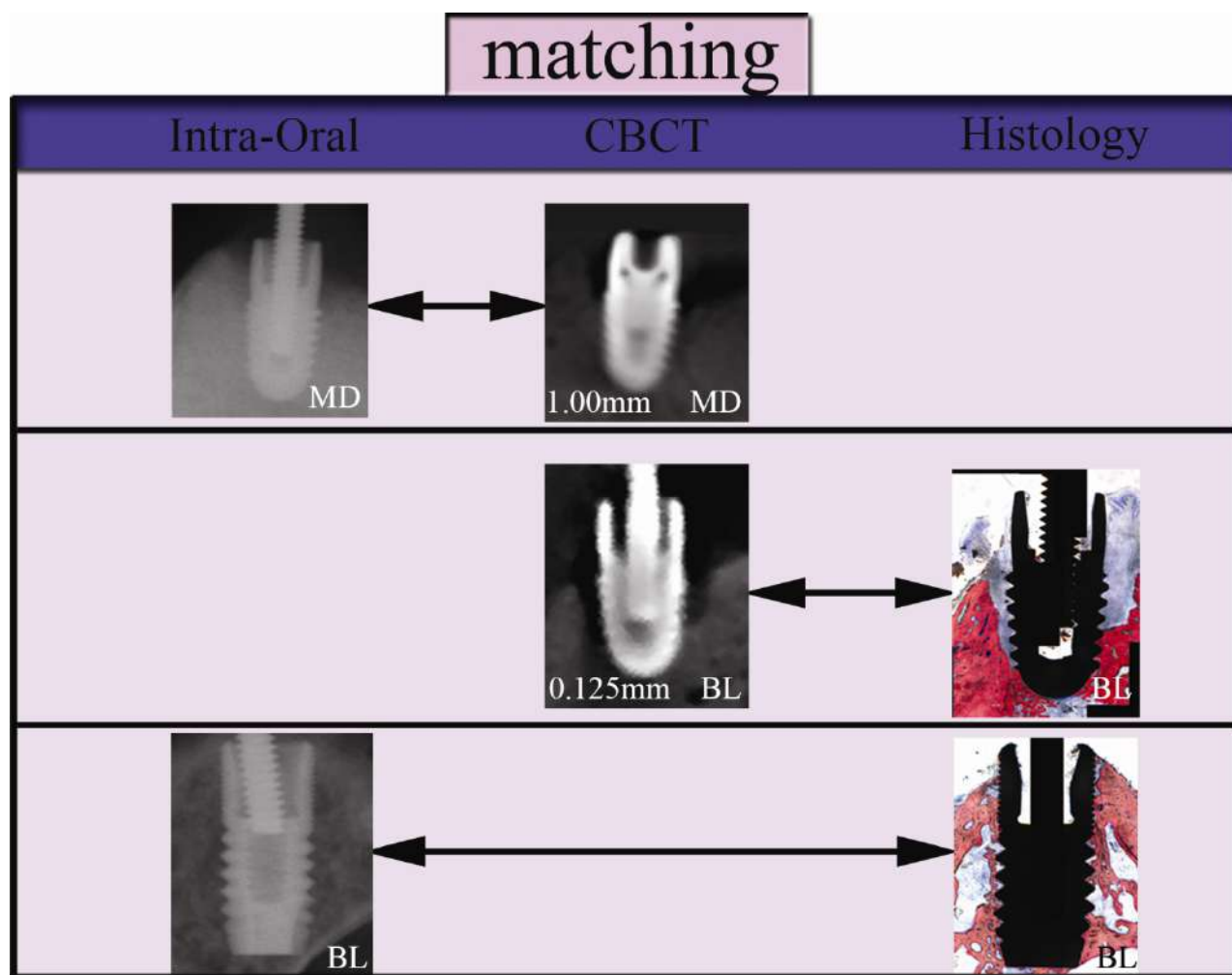


Figure 6.2: Methodological design (Part I: Matching). Image direction is indicated by letters on the right bottom of the images. MD= mesio-distal direction; BL= bucco-lingual direction. Only images taken on the same direction were used for matching purposes. Numbers on the left top indicate the slice thickness. Histological slices thickness had a slice thickness ranging from 20 to 30 μm .

Digital Intra-oral radiography

After a pilot testing with dry pig jaws in water as a soft tissue simulator, radiographic images were taken using the Planmeca Prostyle Intra[®] radiation tube (Planmeca, Helsinki, Finland) at 70kV, 8mA and 0.16s. Intra-oral digital radiography was performed on all samples after animal sacrifice with the VistaScan[®] phosphorplate technique (Dürr Dental, Bietigheim-Bissingen, Germany) related DBSwin[®] software (Dürr Dental). Jaw bone segments including the implants were inserted in a wooden box for standard projection geometry (figure 6.3). This box was designed including an aluminium step wedge, a film holder and an opening to fit a rectangular collimator, as described in detail previously (Nackaerts et al 2006). The

wedge consisted of nine steps, gradually increasing with 1.3mm and it was included to standardize radiographs and to allow densitometric analysis.

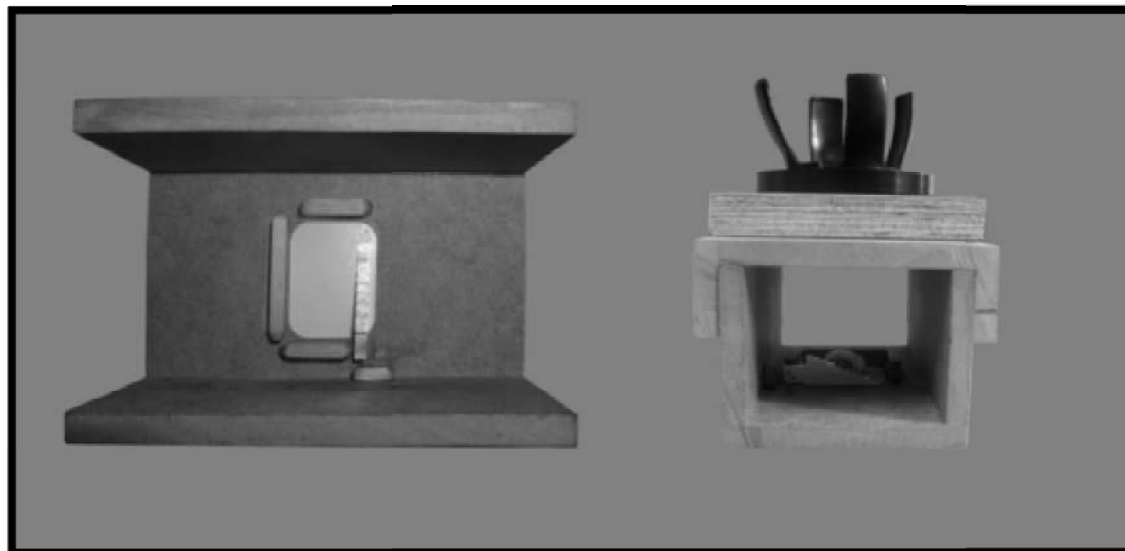


Figure 6.3: Wooden box for standardized radiography. Left image: Aluminium wedge is included in all radiographs . Right image: Collimator fits cover box.

Intra-oral digital radiographs of each specimen were taken after animal sacrifice in two different cutting directions revealing the bucco-lingual and mesio-distal regions around the implants. These images could be correlated to histological images (bucco-lingual direction of view) and also used at the follow up section of the study (mesio-distal of view). Images accepted to further analysis should clearly show threads on both implant surfaces.

Cone Beam Computed Tomography

The same sample obtained after the animal sacrifice was used to obtain the CBCT images using the Accuitomo 3D (Morita, Kyoto, Japan). The exposure parameter settings selected after a pilot test included: 65kV, 1.5mA, 17.5 s and a 360° turn. Images were reconstructed with a slice thickness of 0.125mm and a cutting direction for histological matching (figure 6.2).

The DICOM images from the CBCT were exported and saved to be analyzed using dedicated software (**Image J**, US National Institutes of Health, Bethesda, Maryland, USA; **Axiovision**, Carl Zeiss MicroImaging GmbH, Jena, Germany).

Histological images

The tissue samples with the implants were fixed in a CaCO₃-buffered formalin solution and dehydrated in an ascending series of ethanol concentrations over 18 days. Embedding was performed by infiltration and polymerisation of methylmetacrylate. Sectioning of the samples was done with a diamond saw (Leica SP1600, Wetzlar, Germany) in the mesio-distal direction. The sections were reduced to a final thickness of 20 to 30 µm by grinding and polishing (Exakt 400 CS grinding device, Exakt Technologies Inc., Germany). Up to 10 sections were prepared per sample and the middle one was selected. These sections were stained with a combination of Stevenel's blue and Von Gieson's picrofuchsin, visualising mineralised bone tissue (red) and non-mineralised tissue (blue-green).

Histological examinations were performed under the light microscope (Leitz Laborlux S, Wetzlar, Germany) at a magnification of x40. The assessments of the histomorphometrical proportions were performed by means of a high-sensitivity colour video camera (AxioCam MRc5, Zeiss, Göttingen, Germany) mounted on the light microscope and by means of a colour image analyzing software package (Axiovision 4.0, Zeiss, Göttingen, Germany).

Due to technical limitations, histological sections were made in the mesio-distal direction providing bucco-lingual view of bone and implant, whereas the initial intra-oral radiographic views (*in vivo*) showed these structures in a mesio-distal view. At sacrifice intra-oral radiographs were taken in both directions, as such to enable matching with histology and comparison over time. For CBCT, reconstructions in both directions also guaranteed a perfect match with histological and intra-oral radiographs

Measurements

First, the corresponding cross-sectional CBCT image to be used selected: one sectional image to correspond to the histological image and the other to correspond to the intra-oral radiograph (figure 6.4).

1. Bone defect depth

Bone defect depth is the distance (mm) of the crater-shaped marginal bone defect. The Axiovision software was used to evaluate intra-oral radiographs, CBCT and histological images (figure 6.4).

2. Peri-implant bone fraction

By means of the Axiovision software, the bone fraction (percentage of bone) around the implant could be measured on histological images, CBCT and intra-oral radiographs. This bone fraction was measured in a zone of 100 μm around the implant (figure 4).

3. Fractal analysis

Fractal Analysis was used to detect changes in the bone structure or geometry. Image J software using the box-count function was applied to all 3 image modalities. The region of interest (ROI, 4x1 mm²) consisted of the bone around the implant from the first thread to the last thread.

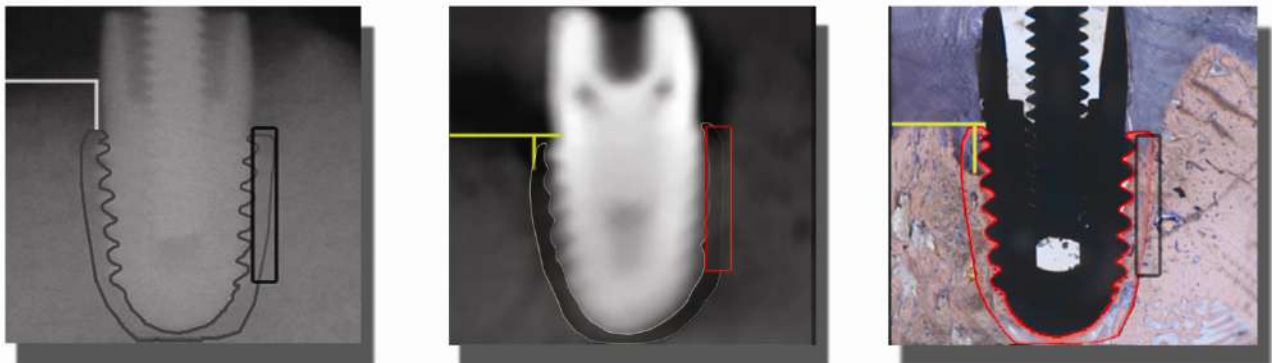


Figure 6.4: Regions of interest (ROI) at matching part: on intra-oral (A), CBCT (B) and histological (C) images. Bone defect depth (lines); Bone fraction (contour line around implant) and Fractal analysis (rectangle).

After selecting the ROI, this area was transformed in a binary image and noise was removed applying a despeckle tool on Image J. After this the fractal box count function was used on the same software. A graphic and a fractal dimension number were automatically generated and the latter was used as fractal dimension result for further statistical analysis.

Part II: Follow up

At this part of the study, some bone parameters were analysed to detect possible changes over the time (baseline, 2 months and 3 months healing) using standardized digital intra-oral radiographs.

Digital Intra-oral radiography

At baseline, the intra-oral digital radiography was performed on all samples with the VistaScan[®] phosphorplate technique (Dürr Dental, Bietigheim-Bissingen, Germany) with related DBSwin[®] software (Dürr Dental). Right and left premolar region of upper and lower jaws were radiographed. Rinn XCP[®] (Dentsply Rinn, Elgin, Illinois, USA) film-holding instruments were adapted to contain an aluminium step wedge to standardize radiographs and to allow densitometric analysis. The wedge consisted of nine steps, gradually increasing by 1.3mm. At the time of implant surgery, individualized impression moulds (Kerr Compound Sticks, Kerr Corporation, Paris, France) were made for each minipig and attached to a bite block to standardize the geometrical conditions of the radiographs (figure 6.5).



Figure 6.5: Individualized positioning device (adapted from the Rinn XCP position device, see Nackaerts et al 2006) for standardized follow-up radiography, using a film-holder with aluminum step wedge and occlusal key in green stent. Left image: Film-holder with occlusal green stent and phosphorplate positioned; Right image: Tube view of the device showing the occlusal stent, step wedge and phosphor plate.

The use of the paralleling technique, complemented with a positioning holder, minimized image enlargement and geometric distortion of the radiographs.

Radiographs were taken at implant placement, after 2 months and 3 months healing (figure 6.6).

Measurements

1. Marginal bone level

Marginal bone level analysis was conducted using DBSWIN (Dürr Dental, Bietigheim-Bissingen, Germany). After scanning, the perio filter was used and the distance between implant top and the first implant-bone contact was measured at the baseline and after 2 and 3 months of healing (figure 6.6).

2. Bone density

Custom-made software which converts grey values into millimetre aluminium equivalent (mm Al eq) values was used. This software was previously described and thoroughly tested in vitro (see: Sun et al 2009; Nackaerts et al 2006). This measurement was conducted only on intra-oral radiographs as these were the images taken with aluminium step wedge. The region of interest (2.0mm^2) was the bone around the implant neck (figure 6.6). This result generated aluminium equivalent density (AED) values of the bone as showed in intra-oral images.

3. Fractal analysis

The same approach as described earlier was used (figure 6.6). A smaller ROI (2.0mm^2) was chosen as not all follow-up clinical images revealed the entire length of the implant.

Part III: Intra-oral radiographic density 1

The main objective of this part was to determine aluminum equivalent density (AED) values of peri-implant bone at implant neck, threads and apical regions, and evaluate whether AED values at baseline could predict bone loss after 3 months healing. The intra-oral radiographic images analyzed were taken at baseline and 3 months after healing as explained before. Bone density was measured as mentioned at follow up section. The region of interest was the bone around the implant neck, threads and apex (figure 6.7). Those measurements were conducted on images

taken at 3 months healing. This result generated aluminium equivalent density (AED) values of the bone as showed in Intra-oral images.

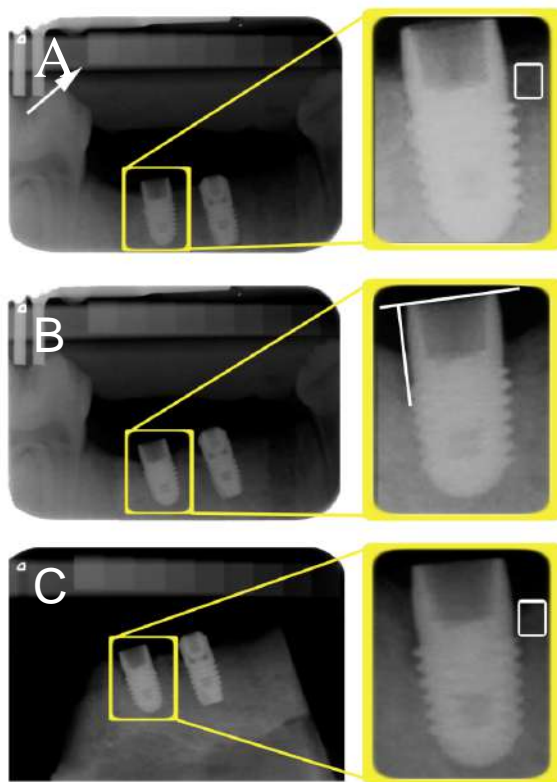


Figure 6.6: Part II (follow-up) measurements. **A:** close-up shows ROI for bone density method. Aluminium wedge (white arrow) was used as a reference for bone density measurements. **B:** close-up shows marginal bone level method. Notice implant top was used as reference point. **C:** close-up shows ROI for fractal analysis.

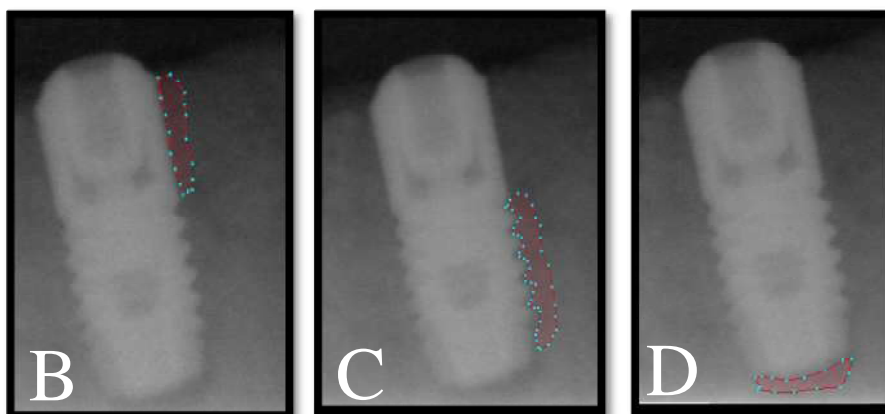


Figure 6.7: Part III measurements. **A:** Aluminium wedge was used as a reference for bone density measurements. **B-D:** ROI implant neck (B), threads (C) and apical (D).

To evaluate whether AED values at baseline could predict bone loss after 3 months healing, the mean bone density at the three levels was used to calculate total bone density at baseline. Bone loss after 3 months healing was calculated in IO radiographs by subtracting the marginal bone level after 3 months from the marginal bone level at baseline.

Statistics

For statistical analysis, Statistica software (Statistica version 6, StatSoft Inc., Tulsa, OK, USA) was applied with the level of significance set at 0.05. Nonparametric Spearman's tests allowed comparing radiographic methods to the histological standard. Friedman test for comparison of dependent data and Wilcoxon matched pairs test was applied to search for significant differences among baseline, 2 and 3 months healing period. Furthermore, Kruskal-Wallis with Bonferoni correction were used to compare the radiographic density among implant regions, Pearson correlation tests were used to check the correlation between bone losses after 3 months healing to the AED values at the baseline. In addition, a linear regression analysis was used to verify if AED at baseline could explain the bone loss after 3 months healing.

Results

Part I: Matching

Results showed statistically significant correlations in bone defect depth between intra-oral radiographic images and histological slices ($r=0.70$, $p<0.01$) as well as between CBCT images and histological slices ($r=0.61$, $p<0.01$) (table 6.1). However, intra-oral radiographs and CBCT images yielded a bone defect depth mean underestimation of 1.17mm and 1.20mm, respectively, compared to the histological slices. Higher marginal bone levels ($>1.5\text{mm}$) on histological images accounted for higher mean deviations on intra-oral (2.27mm) and CBCT images (2.16mm) when compared with lower ($<1.5\text{mm}$) marginal bone levels (-0.002mm and 0.04mm deviation on intra-oral and CBCT images, respectively). For the peri-implant bone fraction, a weak and not significant correlation was found between mean results

obtained on CBCT and on histological images. Furthermore, no significant correlations were detected between fractal analysis as evaluated on CBCT, intra-oral radiography and histology.

Table 6.1: Correlation coefficients between different methods.

Measurement	Correlation	Correlation coefficient
Bone Defect Depth	CBCT x Histology	0.61*
	CBCT x Intra-oral	0.64*
	Histology x Intra-oral	0.70*
Bone Fraction	CBCT x Histology	0.28
Fractal analysis	CBCT x Histology	0.34
	CBCT x Intra-oral	-0.04
	Histology x Intra-oral	-0.19

*Statistically significant ($p < 0.05$)

Part II: Follow up

When monitoring changes over time using intra-oral radiography, 2 and 3 months evaluation period allowed visualising peri-implant marginal bone level and density changes, with a significant peri-implant bone loss as established by a more apical position of marginal bone level after 2 months (1,20mm) and 3 months (1,75mm) of healing compared to the baseline bone level (0 mm) (table 6.2).

Table 6.2: Follow-up measurements (baseline, 2 months and 3 months healing). Number of cases, mean, confidence interval, standard deviation (SD), minimum and maximum is described below.

BASELINE							
METHODS	N	Mean	95% CI	SD	Minimum	Maximum	
Marginal Bone Level (mm)	40	0.00 ^a	0,09 - 0,42	0.50	0	2.45	
Bone Density (mmAl eq)	39	5.25	4,51 - 6,21	2.61	0.30	11.55	
Fractal Analysis (D)	39	1.72 ^b	1,69 - 1,74	0.07	1.47	1.82	
2 MONTHS							
Marginal Bone Level (mm)	38	1.20 ^a	1,09 - 1,89	1.21	0	4.55	
Bone Density (mmAl eq)	36	5.92	5,04 - 6,85	2.68	0.60	10.80	
Fractal Analysis (D)	36	1.71	1,67 - 1,72	0.06	1.53	1.84	
3 MONTHS							
METHODS	N	Mean	95% CI	SD	Minimum	Maximum	
Marginal Bone Level (mm)	37	1.75 ^a	1,37 - 2,25	1.37	0	4.75	
Bone Density (mmAl eq)	37	5.62	5,25 - 6,45	1.88	2.80	9.85	
Fractal Analysis (D)	37	1.67 ^b	1,63 - 1,68	0.09	1.39	1.84	

^{a, b} difference between means marked with same letter were statistically significant ($p < 0.01$)

No significant changes of AED were found after 3 months, despite the higher values compared to baseline. Although not statistically significant, an increase of bone density and decrease fractal dimension could be detected after 3 months of osseointegration (table 6.2).

AED was significantly, although weakly, correlated to bone defect depth and marginal bone level changes. No correlation was found with peri-implant bone volume. AED values lower than 5mmAeq at baseline showed marginal bone level changes greater than 2.0mm after 3 months healing (figure 6.8).

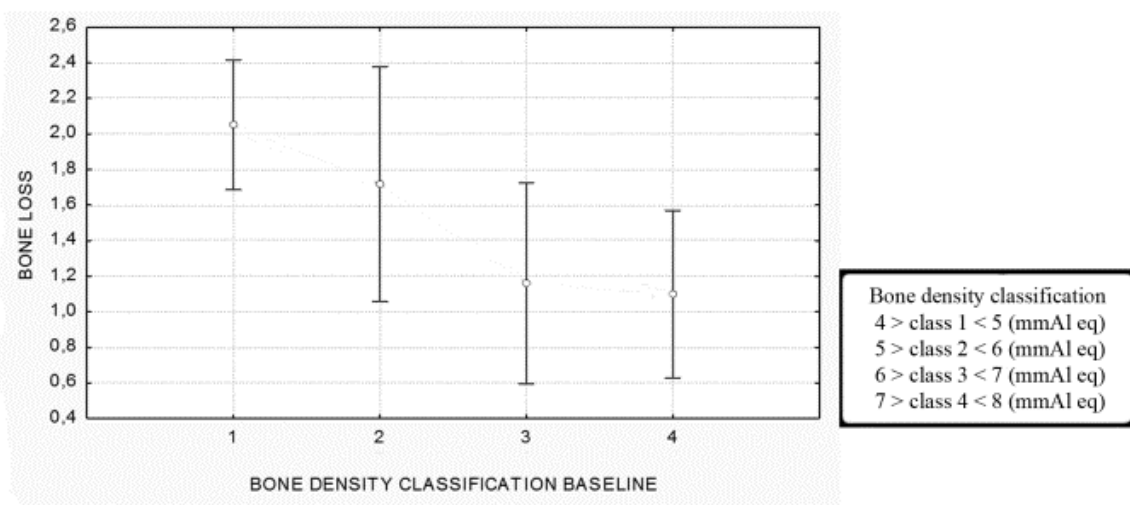


Figure 6.8: Graphic showing mean (SD) bone loss (in mm) after 3 months healing with the sample classified according to baseline bone density.

Part III: Intra-oral radiographic density

The bone tissue around implant threads and apical region showed a significantly higher radiographic density (AED) than around implant neck (figure 6.9 and table 6.3).

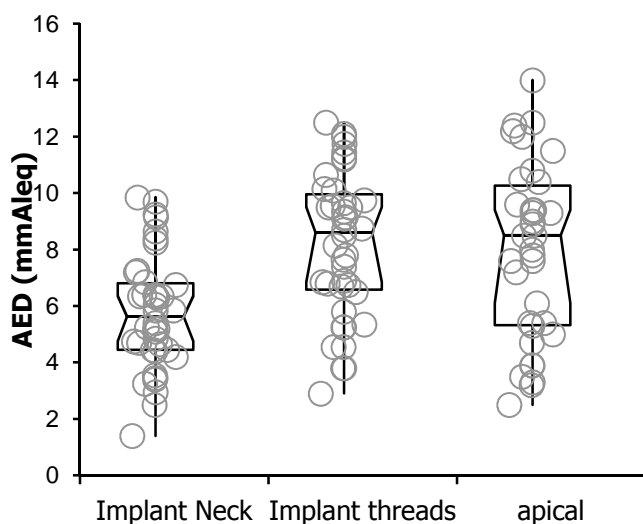


Figure 6.9: Box-plot showing the mean, sample distribution and 95%CI of AED at different implant levels.

Table 6.3: Aluminum density equivalent values of peri-implant bone at implant neck, threads and apical regions ($p=0,0001$)

Groups	Mean	95% CI	SE	SD
Implant Neck	5,76	5,11 to 6,40	0,32	2,02
Implant threads	8,19	7,37 to 9,00	0,40	2,56
apical	7,96	6,89 to 9,03	0,53	3,11

AED was significantly, although weakly, correlated to bone loss. AED values lower than 5mmAleg at baseline showed a bone loss greater than 2.0mm after 3 months healing (figure 6.10 and table 6.4).

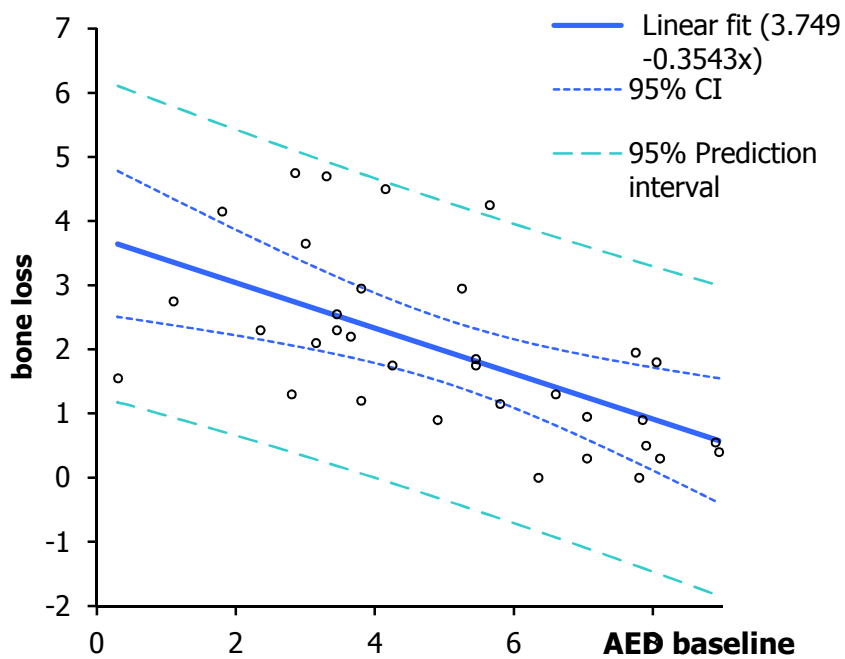
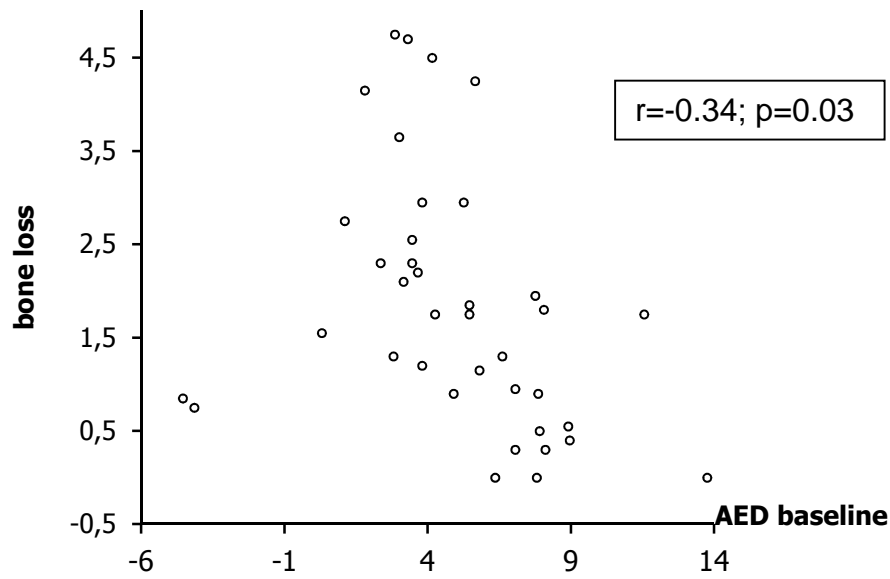


Figure 6.10: The graphic (A) indicates a cutting value of AED at the baseline to predict the bone loss after 3 months healing. The linear regression analysis, represented in graphic (B), was used to verify this observation.

Table 6.4: Linear regression analysis bone loss X AED baseline.

Term	Coefficient	95% CI	SE	p
Intercept	3,749	2,80 to 4,70	0,47	<0.0001
Slope	-0,3543	-0,53 to -0,18	0,08	0,0002
bone loss = 3.749 - 0.3543AED baseline				

Discussion

This study compared changes in bone parameters measured on histological and radiological images obtained after 3 months of implant placement. Variables considered in the study were: bone defect depth, peri-implant bone fraction, marginal bone level, bone density and bone structure (fractal analysis). The study design allowed comparing these variables to verify the possible link of various radiographic analyses to the true histological standard of the peri-implant bone tissues, as well as to evaluate changes over time.

Marginal bone level and bone defect depth values obtained on intra-oral radiography and CBCT images were lower than the values obtained on histological images. Caulier et al (1997) concluded that histological marginal bone level measurements are 0.85 mm more apical than on intra-oral radiographs. Zybutz et al (2000) reported that intra-oral radiographs underestimate the marginal bone level around teeth by approximately 1.4 mm compared to direct bone measurements during surgical procedures. In the present study, this underestimation varied from 1.17 mm (bone defect depth intra-oral radiograph) to 1.20 mm (bone defect depth CBCT). However, fifty percent of the deviations were smaller than 0.5mm, being not considered clinically significant. Besides, CBCT images were more reliable to identify some cases of extensive bone loss (figure 6.11).

Marginal bone level greater than 1.5mm was considered the “cut off point” of this research (boundary between “problematic” and “non-problematic” cases). Both image modalities achieved high specificity and an average sensitivity (table 6.5) using histological measurements as true results. However, more than marginal bone

level should be observed when evaluating implant failure or success (*Esposito et al 2009; Esposito et al 2009b; Esposito et al 1997*).

Table 6.5: Sensitivity and specificity IO and CBCT tests. Table shows number of positive and negative cases on IO and CBCT images considering marginal bone level greater than 1.5mm as positive result.

IMAGE S	<1.5mm (test negative) (n° cases)	> 1.5mm (test positive) (n° cases)	False positive	False negative	Sensitivity	Specificity
IO	48	29	6	22	67%	84%
CBCT	44	33	7	20	69%	82%
HISTO	32	45	-	-	-	-



Figure 6.11: Examples of intra-oral (A), histological (B) and CBCT (C) images of same specimen.

It is important to consider the shortcomings in the present study design, e.g. differences in slices thickness & orientation, when the final goal is to try to match intra-oral radiographs with histological standards. Nevertheless, it is worthy to be noted that histological bone defect depth measurements were significantly correlated with all radiographic measures (table 6.1). Interestingly, total marginal bone loss after 3months were significantly higher for lower density bones at baseline, indicating that more bone loss occurred for lower density bone (figure 6.8). This observation corresponds well to those reported by Nackaerts et al (2008), who observed a tendency towards bone loss when having a lower bone quality. The finding also confirms the outcome of 5 other studies (*Mohammad et al 2003; Payne et al 1999; Taguchi et al 2005; Takaishi et al 2005; Yoshihara et al 2004*).

Several methods have been used to determine the radiographic density of bone tissue, e.g. direct use of gray values, linear transformation of the attenuation coefficient (Hounsfield units), digital image subtraction and the use of an aluminum step wedge. The step wedge is used as an image internal reference to calculate the aluminum equivalent density of the bone. This method has shown a high precision, accuracy and diagnostic specificity in previous studies (*Sun et al 2009; Nackaerts et al 2008*).

The bone density range obtained with the custom-made software (5.13 –7.28 mmAl eq) is in agreement with the mean values (5.7 mmAl eq) found in a previous study (*Nackaerts et al 2008*) using the same custom-made software. A significant correlation was found between the bone density measured on 2D radiographic images and peri-implant bone fraction assessment on histological slices ($r=+0.50$). The significant correlation between the radiographic bone density and peri-implant bone fraction on histological slices and the corresponding changes in density and bone level over time, may suggest that the use of a dedicated bone density tool with Al wedge, may be advocated to detect bone changes. Furthermore, a previous study (*Nackaerts et al 2006*) reports that this custom-made software was able to detect an actual change in bone mineralization of 6.6%. This is a crucial value to consider, as previous studies reported that 30-53% of the bone needed to be removed before a difference could be noted radiographically (*Dreyer 1993*).

AED might be a promising diagnostic tool to predict bone tissue response to titanium implants. An increased bone loss (>2mm) seems more likely to occur at low density bones(<5mmAl eq). Distinct bone densities were found around the implant neck, threads and apical levels. Radiographic bone density was found lower at implant neck than in the other two levels. This difference may be explained by the more intense bone remodeling around implant neck since this region has a higher stress/strain concentration. Yet, for a more precise analysis of osseointegration, further studies are needed to better diagnose the absence of bone formation around implants by means of radiographic images.

In the present study, the fractal analysis method was unable to detect significant changes or to provide a result matching among histological, intra-oral radiograph and CBCT images. Although this method has been developed and has

prove to show some correlation with the actual bone status (*Benhamou et al 2001; Caligiuri et al 1994; Chung et al 1994; Faulkner & Pocock 2001; Fazzalari & Parkinson 1996; Feltrin et al 2004; Geraets & van der Stelt 2000; Heo et al 2002; Jolley et al 2006; Majumdar et al 1999; Parkinson & Fazzalari 2000; Updike & Nowzari 2008; Wagle et al 2005*), it remains a mathematical process with plenty of outcome measure points. This latter presume creates a big gap between this high end fractal analysis and the true histological gold standard. Indeed, according to our knowledge no study could ever prove a true matching. One could however think of this method as a kind of structural analysis, especially when CBCT imaging comes into play. Indeed, as density values of CBCT are unstable, a three-dimensional structural analysis method might be considered as a valid alternative to measure bone quality (*Hua et al 2009*). There is indeed a tendency towards a matching bone structural pattern, even when simply matching histological and cone beam CT slices, which might be objectified and automated by advanced image analysis methods (figure 6.12).

In this perspective, there is a need to develop new dedicated analysis methods for bone quality assessment using CBCT. The results of the present study may have applications for implant follow-up in daily dental practice as well as in animal research designs to allow for refined non-invasive monitoring of the peri-implant bone level during healing and osseointegration.

Conclusions

Within the limits of an animal study it can be concluded that:

1. Significant correlations could be observed between the bone level histologically assessed and the bone level measured on IO radiographs, and CBCT images.
2. On average CBCT and IO images deviated respectively 1,20 and 1,17mm from the histological bone level, with 50% having a deviation of less than 0.5mm on both images modalities.
3. Tissue parameters as measured on intra-oral radiographs correlate significantly with some histomorphometric parameters. However, such correlation could not be established for CBCT images.
4. An increased bone loss (>2mm) seemed more likely to occur at low density bones(<5mmAeq).
5. Radiographic fractal analysis did not seem to match histological fractal analysis.
6. CBCT was not found reliable for bone density measures, but might hold potential with regard to structural analysis of the trabecular bone

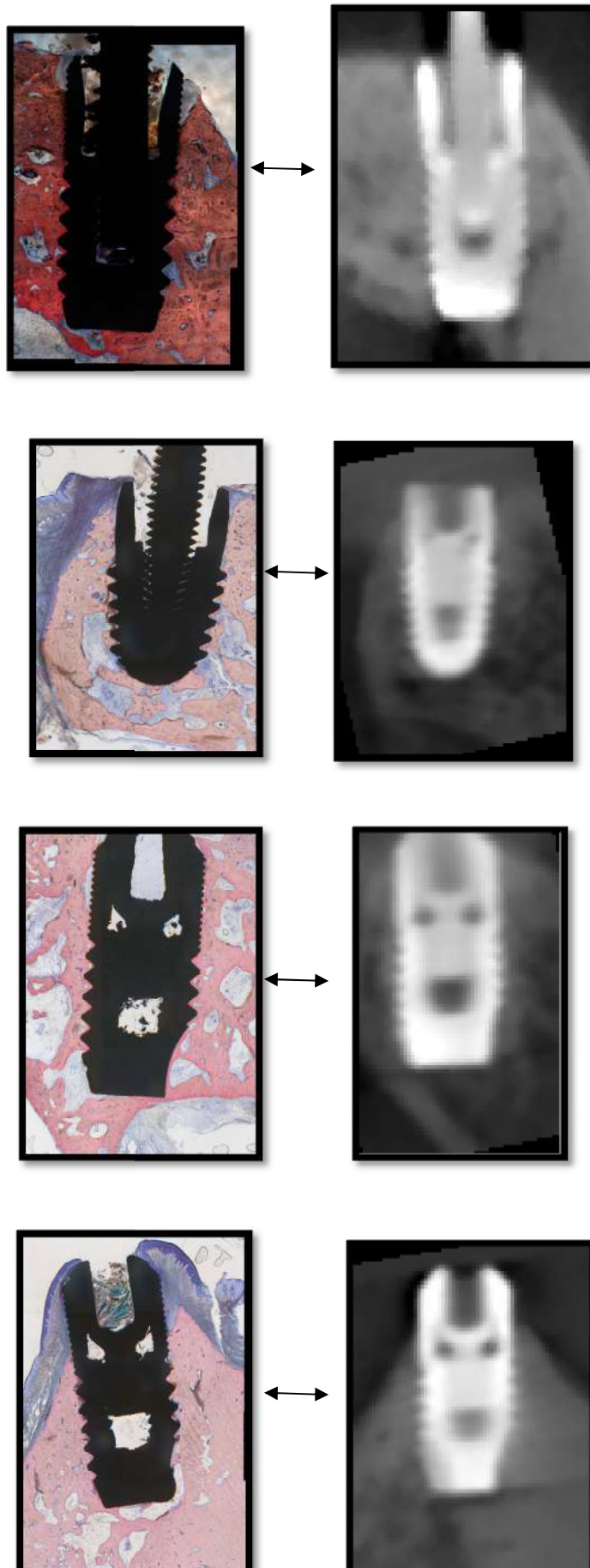


Figure 6.12: Examples of CBCT slices corresponding to the histological slice of the same specimen.

References

- Albrektsson T, Zarb G, Worthington P, Eriksson AR. The long-term efficacy of currently used dental implants: a review and proposed criteria of success. *Int J Oral Maxillofac Implants* 1986; 1:11-25.
- Alsaadi G, Quirynen M, Michiels K, Jacobs R, van Steenberghe D. A biomechanical assessment of the relation between the oral implant stability at insertion and subjective bone quality assessment. *J Clin Periodontol* 2007; 34:359-66.
- Aranyarachkul P, Caruso J, Gantes B, Schulz E, Riggs M, Dus I, Yamada JM, Crigger M. Bone density assessments of dental implant sites: 2. Quantitative cone-beam computerized tomography. *Int J Oral Maxillofac Implants* 2005; 20:416-24.
- Atsumi M, Park SH, Wang HL. Methods used to assess implant stability: current status. *Int J Oral Maxillofac Implants* 2007; 22:743-54.
- Bahrami G, Isidor F, Wenzel A, Vaeth M. Correspondence Between Conventional and Digitised Radiographs for Assessment of Marginal Bone. *Oral Health Prev Dent* 2013 Mar 15. [Epub ahead of print]
- Benhamou CL, Poupon S, Lespessailles E, Loiseau S, Jennane R, Siroux V, Ohley W, Pothuau L. Fractal analysis of radiographic trabecular bone texture and bone mineral density: two complementary parameters related to osteoporotic fractures. *J Bone Miner Res* 2001; 16:697-704.
- BouSerhal C, Jacobs R, Quirynen M, van Steenberghe D. Imaging technique selection for the preoperative planning of oral implants: a review of the literature. *Clin Implant Dent Relat Res* 2002; 4:156-72.
- Brånemark PI, Hansson BO, Adell R, Breine U, Lindström J, Hallén O, Ohman A. Osseointegrated implants in the treatment of the edentulous jaw. Experience from a 10-year period. *Scand J Plast Reconstr Surg Suppl* 1977; 16:1-132.
- Caligiuri P, Giger ML, Favus M. Multifractal radiographic analysis of osteoporosis. *Med Phys* 1994; 21:503-8.
- Caulier H, Naert I, Kalk W, Jansen JA. The relationship of some histologic parameters, radiographic evaluations, and Periotest measurements of oral implants: an experimental animal study. *Int J Oral Maxillofac Implants* 1997; 12:380-6.
- Chung HW, Chu CC, Underweiser M, Wehrli FW. On the fractal nature of trabecular structure. *Med Phys* 1994; 21:1535-40.
- Couture RA, Whiting BR, Hildebolt CF, Dixon DA. Visibility of trabecular structures in oral radiographs. *Oral Surg Oral Med Oral Pathol Oral Radiol Endod* 2003; 96:764-71.
- Dougherty G, Henebry GM. Fractal signature and lacunarity in the measurement of the texture of trabecular bone in clinical CT images. *Med Eng Phys* 2001; 23:369-80.
- Dreyer WP. Technological advances in the clinical diagnosis of periodontal diseases. *Int Dent J* 1993; 43:557-66.
- Esposito M, Worthington HV, Thomsen P, Coulthard P. Interventions for replacing missing teeth: different times for loading dental implants. *Cochrane Database Syst Rev* 2004;(3):CD003878. Review. Update in: *Cochrane Database Syst Rev*. 2007;(2):CD003878.
- Esposito M, Hirsch JM, Lekholm U, Thomsen P. Failure patterns of four osseointegrated oral implant systems. *J Mater Sci Mater Med* 1997; 8:843-7.

- Esposito M, Coulthard P, Thomsen P, Worthington HV. Interventions for replacing missing teeth: different types of dental implants. *Cochrane Database Syst Rev*. 2005 Jan 25;(1):CD003815. Review. Update in: *Cochrane Database Syst Rev*. 2007;(4):CD003815.
- Faulkner KG, Pocock N. Future methods in the assessment of bone mass and structure. *Best Pract Res Clin Rheumatol* 2001; 15:359-83.
- Feltrin GP, Stramare R, Miotto D, Giacomini D, Saccavini C. Bone fractal analysis. *Curr Osteoporos Rep* 2004; 2:53-8.
- Floyd P, Palmer P, Palmer R. Radiographic techniques. *Br Dent J* 1999 9; 187:359-65.
- Friberg B, Gröndahl K, Lekholm U, Brånemark PI. Long-term follow-up of severely atrophic edentulous mandibles reconstructed with short Brånemark implants. *Clin Implant Dent Relat Res* 2000; 2:184-9.
- Geraets WG, van der Stelt PF. Fractal properties of bone. *Dentomaxillofac Radiol* 2000; 29:144-53.
- Heo MS, Park KS, Lee SS, Choi SC, Koak JY, Heo SJ, Han CH, Kim JD. Fractal analysis of mandibular bony healing after orthognathic surgery. *Oral Surg Oral Med Oral Pathol Oral Radiol Endod* 2002; 94:763-7.
- Hermann JS, Schoolfield JD, Nummikoski PV, Buser D, Schenk RK, Cochran DL. Crestal bone changes around titanium implants: a methodologic study comparing linear radiographic with histometric measurements. *Int J Oral Maxillofac Implants*. 2001; 16:475-85.
- Hua Y, Nackaerts O, Duyck J, Maes F, Jacobs R. Bone quality assessment based on cone beam computed tomography imaging. *Clin Oral Implants Res* 2009; 20:767-71.
- Huang Y, Van Dessel J, Liang X, Depypere M, Zhong W, Ma G, Lambrechts I, Maes F, Jacobs R. Effects of Immediate and Delayed Loading on Peri-Implant Trabecular Structures: A Cone Beam CT Evaluation. *Clin Implant Dent Relat Res* 2013 Apr 2. [Epub ahead of print]
- Isidor F. Histological evaluation of peri-implant bone at implants subjected to occlusal overload or plaque accumulation. *Clin Oral Implants Res* 1997; 8:1-9.
- Isidor F. Clinical probing and radiographic assessment in relation to the histologic bone level at oral implants in monkeys. *Clin Oral Implants Res* 1997; 8:255-64.
- Jacobs, R. & van Steenberghe, D. Radiographic planning and assessment of endosseous oral implants. Springer, Berlin 1997.
- Jolley L, Majumdar S, Kapila S. Technical factors in fractal analysis of periapical radiographs. *Dentomaxillofac Radiol* 2006; 35:393-7.
- Laurell L, Lundgren D. Marginal bone level changes at dental implants after 5 years in function: a meta-analysis. *Clin Implant Dent Relat Res* 2011; 13:19-28.
- Lee S, Gantes B, Riggs M, Crigger M. Bone density assessments of dental implant sites: 3. Bone quality evaluation during osteotomy and implant placement. *Int J Oral Maxillofac Implants* 2007; 22:208-12.
- Lindh C, Petersson A, Rohlin M. Assessment of the trabecular pattern before endosseous implant treatment: diagnostic outcome of periapical radiography in the mandible. *Oral Surg Oral Med Oral Pathol Oral Radiol Endod* 1996; 82:335-43.
- Majumdar S, Lin J, Link T, Millard J, Augat P, Ouyang X, Newitt D, Gould R, Kothari M, Genant H. Fractal analysis of radiographs: assessment of trabecular bone structure and prediction of elastic modulus and strength. *Med Phys* 1999; 26:1330-40.

- Meredith N. Assessment of implant stability as a prognostic determinant. *Int J Prosthodont* 1998; 11:491-501.
- Misch CE. Divisions of available bone in implant dentistry. *Int J Oral Implantol* 1990; 7:9-17.
- Misch CE, Perel ML, Wang HL, Sammartino G, Galindo-Moreno P, Trisi P, Steigmann M, Rebaudi A, Palti A, Pikos MA, Schwartz-Arad D, Choukroun J, Gutierrez-Perez JL, Marenzi G, Valavanis DK. Implant success, survival, and failure: the International Congress of Oral Implantologists (ICOI) Pisa Consensus Conference. *Implant Dent* 2008; 17:5-15.
- Mohammad AR, Hooper DA, Vermilyea SG, Mariotti A, Preshaw PM. An investigation of the relationship between systemic bone density and clinical periodontal status in post-menopausal Asian-American women. *Int Dent J* 2003; 53:121-5.
- Nackaerts O, Jacobs R, Pillen M, Engelen L, Gijbels F, Devlin H, Lindh C, Nicopoulou-Karayianni K, van der Stelt P, Pavitt S, Horner K. Accuracy and precision of a densitometric tool for jaw bone. *Dentomaxillofac Radiol* 2006; 35:244-8.
- Nackaerts O, Gijbels F, Sanna AM, Jacobs R. Is there a relation between local bone quality as assessed on panoramic radiographs and alveolar bone level? *Clin Oral Investig* 2008; 12:31-5.
- Nackaerts O, Jacobs R, Quirynen M, Rober M, Sun Y, Teughels W. Replacement therapy for periodontitis: pilot radiographic evaluation in a dog model. *J Clin Periodontol* 2008; 35:1048-52.
- Parel SM, Triplett RG. Interactive imaging for implant planning, placement, and prosthesis construction. *J Oral Maxillofac Surg* 2004; 62:41-7.
- Parkinson IH, Fazzalari NL. Methodological principles for fractal analysis of trabecular bone. *J Microsc*. 2000; 198:134-42.
- Patel S, Dawood A, Whaites E, Pitt Ford T. New dimensions in endodontic imaging: part 1. Conventional and alternative radiographic systems. *Int Endod J* 2009; 42:447-62.
- Patel S, Dawood A, Mannocci F, Wilson R, Pitt Ford T. Detection of periapical bone defects in human jaws using cone beam computed tomography and intraoral radiography. *Int Endod J* 2009; 42:507-15.
- Patel S. New dimensions in endodontic imaging: Part 2. Cone beam computed tomography. *Int Endod J* 2009; 42:463-75.
- Payne JB, Reinhardt RA, Nummikoski PV, Patil KD. Longitudinal alveolar bone loss in postmenopausal osteoporotic/osteopenic women. *Osteoporos Int* 1999; 10:34-40.
- Pikner SS. Radiographic follow-up analysis of Brånemark dental implants. *Swed Dent J Suppl* 2008; 194:5-69.
- Qian J, Wennerberg A, Albrektsson T. Reasons for marginal bone loss around oral implants. *Clin Implant Dent Relat Res* 2012; 14:792-807.
- Ribeiro-Rotta RF, Lindh C, Rohlin M. Efficacy of clinical methods to assess jawbone tissue prior to and during endosseous dental implant placement: a systematic literature review. *Int J Oral Maxillofac Implants* 2007; 22:289-300.
- Schnitman PA, Shulman LB. Recommendations of the consensus development conference on dental implants. *J Am Dent Assoc* 1979; 98:373-7.
- Schropp L, Kostopoulos L, Wenzel A, Isidor F. Clinical and radiographic performance of delayed-immediate single-tooth implant placement associated

- with peri-implant bone defects. A 2-year prospective, controlled, randomized follow-up report. *J Clin Periodontol* 2005; 32:480-7.
- Snauwaert K, Duyck J, van Steenberghe D, Quirynen M, Naert I. Time dependent failure rate and marginal bone loss of implant supported prostheses: a 15-year follow-up study. *Clin Oral Investig* 2000; 4:13-20.
- Song YD, Jun SH, Kwon JJ. Correlation between bone quality evaluated by cone-beam computerized tomography and implant primary stability. *Int J Oral Maxillofac Implants* 2009; 24:59-64.
- Sun Y, De Dobbelaer B, Nackaerts O, Loubele M, Yan B, Suetens P, Politis C, Vrielinck L, Schepers S, Lambrichts I, Horner K, Devlin H, Jacobs R. Development of a clinically applicable tool for bone density assessment. *Int J Comput Assist Radiol Surg* 2009; 4:163-8.
- Taguchi A, Suei Y, Ohtsuka M, Nakamoto T, Lee K, Sanada M, Tsuda M, Ohama K, Tanimoto K, Bollen AM. Relationship between self-reported periodontal status and skeletal bone mineral density in Japanese postmenopausal women. *Menopause* 2005; 12:144-8.
- Takaishi Y, Okamoto Y, Ikeo T, Morii H, Takeda M, Hide K, Arai T, Nonaka K. Correlations between periodontitis and loss of mandibular bone in relation to systemic bone changes in postmenopausal Japanese women. *Osteoporos Int*. 2005; 16:1875-82.
- Thoma DS, Sanz Martin I, Benic GI, Roos M, Hämmerle CH. Prospective randomized controlled clinical study comparing two dental implant systems: demographic and radiographic results at one year of loading. *Clin Oral Implants Res*. 2013;19. [Epub ahead of print]
- Turkyilmaz I, Tözüm TF, Tumer C, Ozbek EN. Assessment of correlation between computerized tomography values of the bone, and maximum torque and resonance frequency values at dental implant placement. *J Oral Rehabil* 2006; 33:881-8.
- Turkyilmaz I, Tumer C, Ozbek EN, Tözüm TF. Relations between the bone density values from computerized tomography, and implant stability parameters: a clinical study of 230 regular platform implants. *J Clin Periodontol* 2007; 34:716-22.
- Tyndall DA, Brooks SL. Selection criteria for dental implant site imaging: a position paper of the American Academy of Oral and Maxillofacial radiology. *Oral Surg Oral Med Oral Pathol Oral Radiol Endod*. 2000; 89:630-7.
- Udike SX, Nowzari H. Fractal analysis of dental radiographs to detect periodontitis-induced trabecular changes. *J Periodontal Res* 2008; 43:658-64.
- Vercruyssen M, Jacobs R, Van Assche N, van Steenberghe D. The use of CT scan based planning for oral rehabilitation by means of implants and its transfer to the surgical field: a critical review on accuracy. *J Oral Rehabil* 2008; 35:454-74.
- Wagle N, Do NN, Yu J, Borke JL. Fractal analysis of the PDL-bone interface and implications for orthodontic tooth movement. *Am J Orthod Dentofacial Orthop* 2005 ;127:655-61.
- Wilding RJ, Slabbert JC, Kathree H, Owen CP, Crombie K, Delpont P. The use of fractal analysis to reveal remodelling in human alveolar bone following the placement of dental implants. *Arch Oral Biol* 1995; 40:61-72.
- Yoshihara A, Seida Y, Hanada N, Miyazaki H. A longitudinal study of the relationship between periodontal disease and bone mineral density in community-dwelling older adults. *J Clin Periodontol* 2004; 31:680-4.

Chapter 7

Mandibular neurovascular canals

Influence of inter-specific, temporal and geographical variability

Publication related to this chapter:

Corpas LS, Liang X, Oliveira C, Lambrichts I, Semal P, Gilissen E; Raymundo Junior R, Jacobs R. Comparative anatomy of neurovascular canals and tooth roots in mandibles of modern humans and great apes. (in prep)

Comparative anatomy of neurovascular canals and tooth roots in mandibles of modern humans and great apes

ABSTRACT

Objectives: Mandibular anatomy has been constantly revisited by means of state-of-the-art imaging technologies such as Cone Beam Computed Tomography (CBCT). Yet, neurovascular canals located inside the mandible, together with the roots of the teeth supported by this jaw bone, have scarcely been discussed regarding their average dimensions and variability within the human and non-human primate populations. **Materials and methods:** The present paper reported on the anatomical variability of mandibular neurovascular canals (mandibular, incisive and lingual canals) and tooth roots of 160 modern humans and great apes (Homo, Pan and Gorilla). The Kruskal–Wallis Non-Parametric test and Dunn’s All Pairs for Joint Ranks were applied to compare the variability of mandibular canals and root lengths among the different groups. Multivariate analysis searched for redundant information, any patterning in the sample, and whether groups could be differentiated by the studied variables. **Results and conclusions:** The anatomical variability within mandibles of anatomically modern humans from different period of time and regions, besides within mandibles of human and non-human primates, contributed to an overview about neurovascular canal anatomy and the relation with adjacent tooth roots. The longer root length was not associated to smaller distances to neurovascular canals. Geographically, anatomical features which characterize some populations could be related to potential surgical and pathological risks. After comparing to mandibles of great apes, the incisive canal is suggested to be a feature unique to the human mandibles.

INTRODUCTION

The anatomy of the mandible and lower teeth has been extensively studied in several research fields. Nevertheless, little has been discussed about the neurovascular canals located inside the mandible and the roots of teeth supported by this jaw bone. Knowledge is scarce about their average dimensions and variability within human and non-human primate population. Apart of its multidisciplinary application, this knowledge may also add relevant considerations of clinical applicability.

Mandibular anatomy has been extensively revisited by means of advanced imaging technologies such as Cone Beam Computed Tomography (CBCT) (*Oliveira-Santos et al 2011; De Vos et al 2009; Greenstein et al 2008; Spoor et al 2000*). This image technique generates high quality image with a three dimensional (3D) visualization (*Liang et al 2010*) leading to a more complete anatomical information (*Vandenbergh et al 2010; Jacobs et al 2002*). In this way, maxillary and mandibular anatomy has been carefully addressed in the recent literature adding better descriptions of neurovascular structures (*for review Jacobs et al 2007*). Mandibular anatomy has been revisited by 3D imaging with a focus on the mental foramen (*Greenstein et al., 2006*), mandibular canal (*Oliveira-Santos et al 2012; Kim et al 2009; Levine et al 2007*), incisive canal (*Jacobs et al. 2002; Romanos et al. 2009*), lingual canal (*Liang et al 2006; Liang et al 2007; Katakami et al 2009*), as well as to other less frequently observed anatomical variations such as bifid canals (*Oliveira-Santos et al 2011b; Kuribayashi et al 2010; Naitoh et al 2009a; Rouas et al 2007; Clayes and Wackens 2005*), double mental foramina (*Oliveira-Santos et al., 2011; Orhan et al., 2011*), anterior loop (*Kuzmanovic et al 2003; Mraiwa et al., 2003*), lateral canal (*Katakami et al 2009*) and buccal canals (*Fuakami et al 2011*).

The position of those canals is of paramount importance since they harbour nerves and vessels and any damage induced through surgery or implantology might lead to permanent impairment of those neurovascular structures (*Morris et al 2010; Colella et al 2007; Renton et al 2010; Liang et al 2008*). For instance, any nerve damage during mandibular surgery can result in sensory disturbances (*Juodzbaly et al 2011; Tay and Zuniga 2007; Walton 2000; Poort et al 2009; Abarca et al 2006; Dao et al 1998*), expressed by a variety of symptoms ranging from altered sensation to pain

(Sessle 2006). As long term sensory disturbances are unlikely to be successfully treated (Bagheri et al 2010; Ziccardi et al 2007), they have a negative impact on the patient's morbidity and quality of life (Venta et al 1998; Abarca et al 2006). Prevention is obviously the better approach to avoid such perioperative complication (Froum et al 2011; Hegedus et al 2006); therefore, knowledge on mandibular canal anatomy and its variability (for review: Liang et al 2008; Gintaras et al 2010 ; Kingsmill et al 1999) is crucial for a precise and safe surgical planning (Quevedo et al 2011; Rosano et al 2009; Guerrero et al 2006. Van Assche et al 2007).

Although the mandibular form may reflect functional adaptation to forces experienced during mastication (Plavcan and Daegling 2006), the mandibular neurovascular canal has been considered the most stable structure guiding mandibular development (Curien et al 2011; Captier et al 2006) and as such, it may be a relevant structure to indicate intra and interspecific patterning related to mandibular anatomy. However, the variations related to nerves are considered cranial discrete traits of the human skull (Hanihara and Ishida 2001a). This means that they may result from a process of adaptation to various environmental and subsistence patterns as well as random drift by population size, network and isolation, resulting in the development of regional frequency patterns (reviewed and discussed by Hanihara and Ishida 2001b,c,d). Dimension variability such as canal diameter and proximity to root apices can be cited as relevant features to the surgical planning, e.g. larger canals closer to root apices are high risk factors for inferior alveolar nerve injuries (Kovisto et al 2011). However, whether there is a regional or any other trend on this canal trait is still to be determined and can certainly be useful for successful clinical diagnosis and treatment prognosis in the dental practice.

This study investigated the anatomical variability of mandibular neurovascular canals and root lengths of humans and great apes (Homo, Pan and Gorilla). In this chapter, it is reported the anatomical variability of mandibular neurovascular canals and tooth roots from a geographically distributed sample of contemporary humans compared to medieval and prehistoric humans, likewise compared to gorillas and chimpanzees. The crossing of information generated by an intra and interspecific approaches may yield useful outcomes for clinical and research applications.

MATERIAL AND METHODS

Material

The study sample consisted of 160 mandibular radiological images from modern humans (*Homo sapiens sapiens*), chimpanzees (*Pan paniscus*) and gorillas (*Gorilla gorilla graueri*). Modern human group comprised of adult mandibles from three periods of time: prehistory, the middle ages and contemporary times. The contemporary sample was composed of adult mandibles from 7 geographical locations: Brazil, China, Congo, Greenland, India, Indonesia, and Belgium. The sample size is showed in table 7.4.

The mandibular data sets of Brazilian and Belgian populations were patients' CBCT images taken for preoperative treatment planning. All the patients gave their informed consent for this examination while consulting the Department of Periodontology of University Hospitals (KULeuven, Belgium) and the private clinic Dental Radiology Rubens Raymundo (Rio de Janeiro, Brazil). The remaining mandibular datasets consisted of dry adult mandibles provided by the Royal Belgian Institute of Natural Sciences (Brussels, Belgium), from the department of Basic Medical Sciences (University Hasselt, Belgium) and from the Royal Museum for Central Africa (Tervuren, Belgium).

Methods

The CBCT images of Belgian and Brazilian groups were taken using i-CAT CBCT scanner (I-CAT[®], Imaging Sciences International, Hatfield, PA, USA) and NewTom CBCT scanner (NewTom 3G[®], Quantitative Radiology, Verona, Italy), respectively. As for the dry mandibles, images were acquired by means of 3D Accuitomo CBCT (J.Morita, Kyoto, Japan). All axial, sagittal and coronal images were carefully examined under standardized viewing conditions. Linear measurements were performed using i-Dixel (J.Morita, Kyoto, Japan) and MVE (Dr. Jürgen Abel, Neuss, Germany) software tools. The characteristics of each CBCT system used are shown in table 7.1. The smallest voxel size of each system was used in this study.

Table 7.1: Characteristics of CBCT systems.

	3D Accuitomo®	iCAT®	NewTom 3G®
Company	J. Morita, Japan	Imaging Sciences Int., USA	QR, Italy
Dimensions (mm)	2080h x 1600w x 850d	1830h x 910w x 1120d	1890w x 2500d
kV	60-80	120	110
mA	1 – 10	3 - 8	1.8-3.4mAs
Scan Time (s)	18	10,20,40	32
Voxel (mm)	0,125	0,4 (0,2)	0,16-0,42
Reconstruction Time	< 5'	2-10'	/
Object size (mm)	40x40,60x60	160x130(220)	100, 150, 200 (dia)
Detector type	FPD	Am Si FPD	/
Focal Spot (mm)	0,5x0,5	0,5x0,5	/
Gray Scale (bit)	12	14	/
Patient Position	Seated	Seated	Laying

The measurements applied were related to neurovascular canals- mandibular, incisive and lingual canals - and to tooth roots, e.g. root length of mandibular canine, second premolar and third molar. The linear measurements using CBCT images have been reported as accurate and reliable in previous studies (*Liang et al 2010; Loubele et al 2008; Loubele et al 2007*). In addition, the interobserver agreement expressed by the correlation coefficient, was higher than 95% ($r=0.98$, $p<0.0001$) in our pilot study.

Lingual canals were considered those bony canals found at the middle anterior region of the mandible, lateral canals were those located to right or left side of this middle region. Mandibular canal was the bony canal running from mental foramen till mandibular foramen at the mandibular ramus. Incisive canal was considered the anterior extension of the mandibular canal after passing the mental foramen.

The continuous measurements related to mandibular canal were: canal diameter (MC), mental foramen diameter (MF), vertical distance from the canal to root apex of third molar (DA38) and premolar (DA35) and their root lengths (RL38/ RL35), from cement-enamel junction to the apex (figure 7.1).

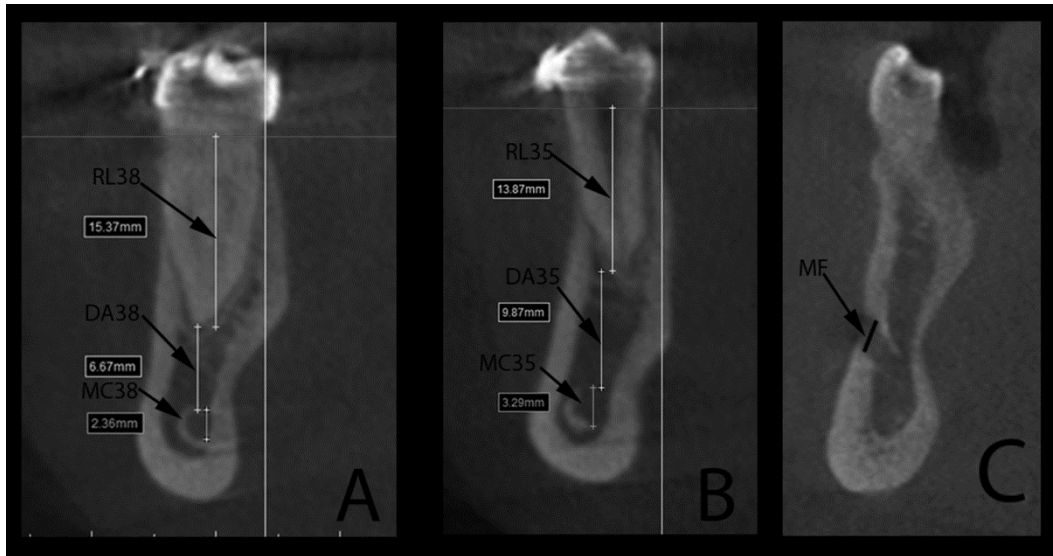


Figure 7.1: Cross-sectional images of mandibular canal at molar (A) and pre-molar (B) regions and of mental foramen (C). The first image at left (A) shows the measurements conducted at molar region, RL 38: root length 38; DA38: distance canal to root apex 38; MC38: mandibular canal diameter at molar region. The image (B) shows the measurements conducted at premolar region, RL 35: root length 35; DA35: distance canal to root apex 35; MC35: mandibular canal diameter at molar region. In image (C) it is shown a cross-sectional image of mental foramen (MF).

Besides these continuous measurements, categorical variables such as presence of bifid mandibular canal and anterior loop (figure 7.2) were also reported. For the incisive canal, continuous variables were: diameter at start point (IC) and below the canine tooth (IC33), vertical distance of the incisive canal to the root apex (DA33) and lower canine root length (RL33) (figure 7.3).

The presence of the incisive canal, the number of bifurcations, its end-point and the connection to the lingual canals were the categorical variables described. At the lingual canal (LC), measurements consisted of buccal (DB) and lingual canal (DL) diameters, canal length (CL) and total bone width below the canal (BW) (figure 7.4). A graphic representation of all these measurements has been presented before by Liang et al (2009). Furthermore, the lingual canal was divided into midline and lateral canals, being described as midline lingual canal when localized at the mandibular middle line and as lateral lingual canal when deviating to left or to right side of the mandible. The lingual canals were also categorized as upper, middle or lower canal, according to its vertical position related to the genial tubercles.

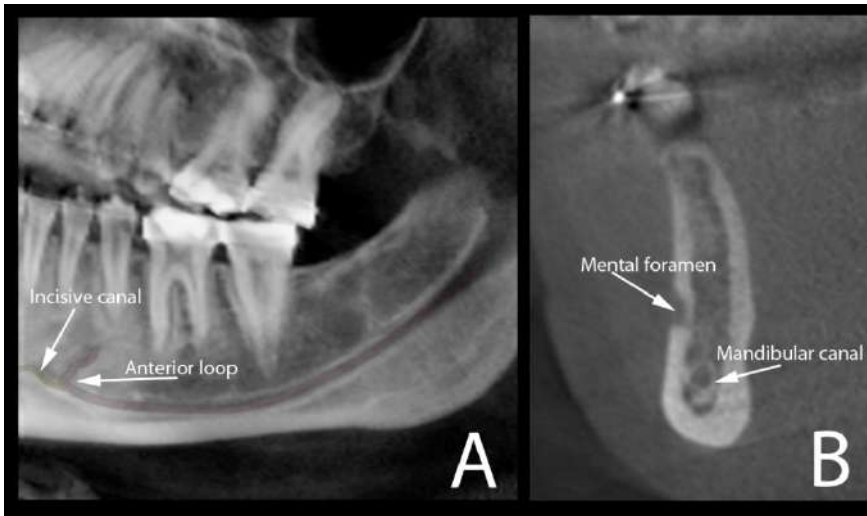


Figure 7.2: Image (A) shows the oblique reconstruction of CBCT volume at region of premolars. In this reconstruction the anterior loop of the mandibular canal can be clearly observed before the start of the incisive canal. The appearance of this anterior loop in a cross-sectional view is shown in image (B).

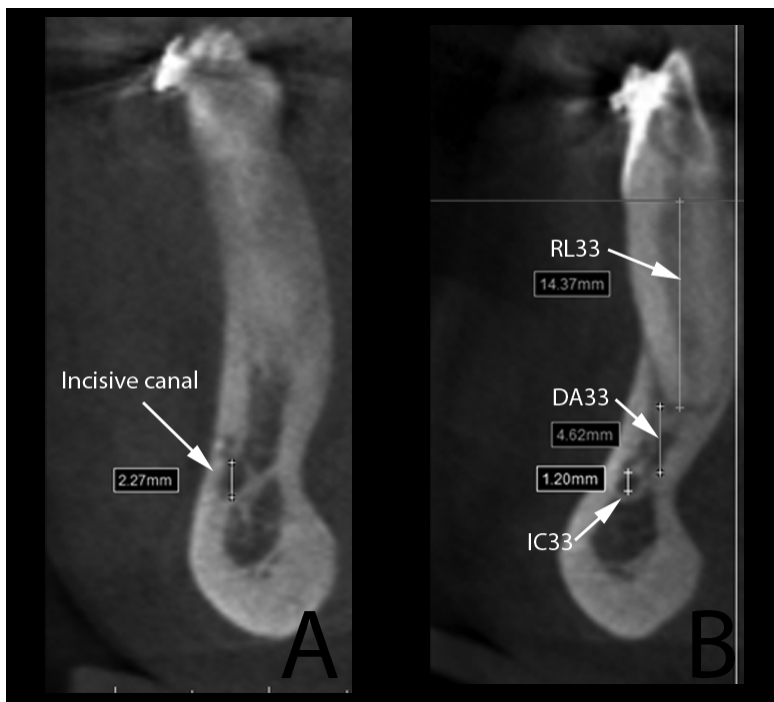


Figure 7.3: Image (A) shows the cross-sectional view of incisive canal at its start point and image (B) the cross-sectional view of the incisive canal below the canine tooth (IC33), at this image were measured the root length of the canine (RL33) and the distance canal to root apex (DA33).

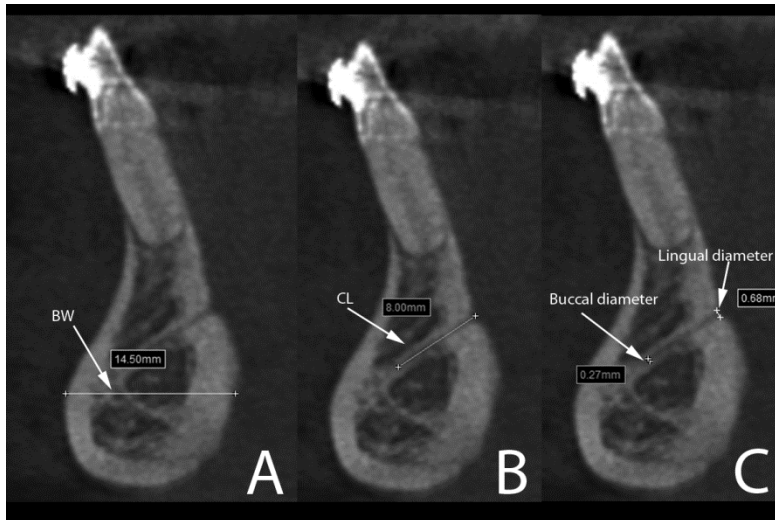


Figure 7.4: Cross-sectional views from the lingual canal. Images (A), (B) and (C) show the measurement of bone width (BW), canal length (CL) and lingual canal diameter (buccal and lingual), respectively.

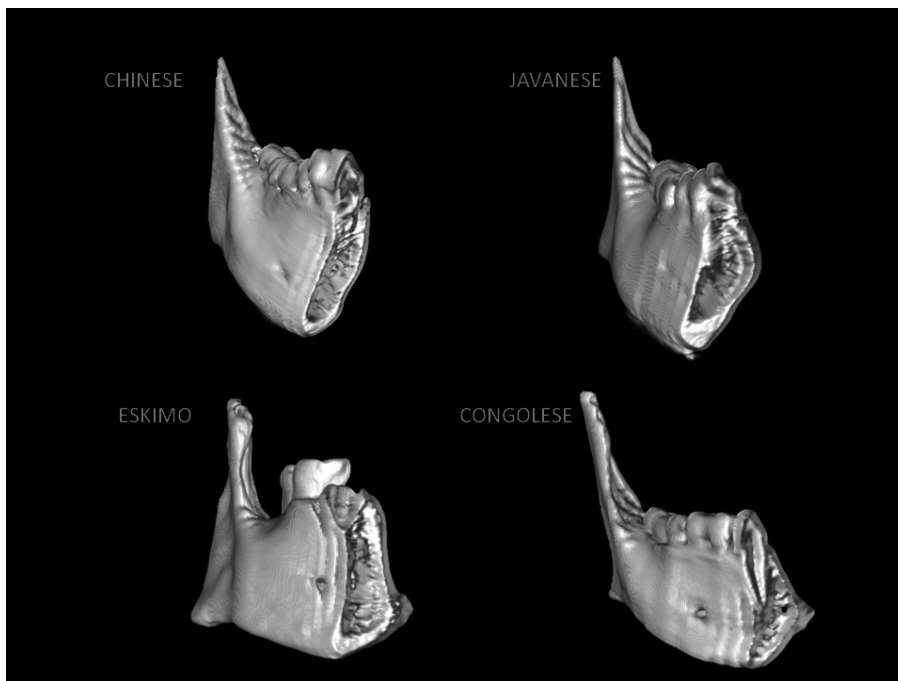


Figure 7.5: Examples of different mandibles included in the study. The 3D reconstructions of CBCT volumes obtained from Chinese, Javanese, Eskimo and Congolese mandibles illustrate the morphological variability frequently seen in the mandibular bone.

Firstly, intraspecific variability was assessed by determining the secular and geographical variability in humans. Human mandibles from prehistoric, medieval and contemporary periods in Belgium were compared to assess secular variability. Contemporary human mandibles from 7 geographical locations, corresponding to 4 continents, namely Africa, America, Asia and Europe, were used to assess geographical variability. In this way, Congolese, Brazilian, Indian, Chinese, Javanese and Belgian mandibles were included in this analysis together with Eskimo

mandibles, the most isolated population in the sample, completing the Contemporary dataset (figure 7.5). Secondly, interspecific variability was determined by comparing contemporary human and great ape mandibles. In this analysis, mandibles from the different geographical locations were grouped in the human group, and then compared to mandibles of chimpanzees and gorillas.

Statistical methods:

To avoid data clustering, just one side of the mandible was chosen for statistical analyses. All data were gathered and statistically analyzed using JMP 8 (SAS Institute Inc., SAS Campus Drive, Cary, North Carolina 27513, USA) for Windows Software Version 7, choosing a 5% level of significance. Descriptive statistics were used to describe variability within groups. The Kruskal–Wallis Non-Parametric test and Dunn’s All Pairs for Joint Ranks were applied to identify which variables differ between groups. For categorical variables, the Contingency Analysis and Chi-Square tests were applied to define how responses distribute differently between groups. Principal component analysis (PCA) on correlations and linear discriminate analysis (LDA) were conducted in order to identify any redundant information, patterning in the sample, and whether the groups could be differentiated by the studied variables.

Results

The results showed significant differences in the dimensions of neurovascular canals and tooth roots in primates. Intra and interspecific analyses revealed that neurovascular mandibular canals, root lengths and the distance between these structures can vary significantly among humans from different eras, geographical locations and within primates.

The mental foramen, incisive canal and lingual canal showed significantly different dimensions in the secular variability analysis. Contemporary group showed significantly larger mental foramen (median/25%-75% interquartiles: 4.1mm/3.4-4.6mm) compared to Medieval (3mm/2.4-3.7mm) and Prehistoric (2.6mm/1.7-3.4mm) groups. The same trend was observed for the incisive canal at its start point and for the lingual canal length (table 7.2). For the root lengths, the Contemporary group presented a significantly longer second premolar (14mm/13.4-16.5mm) than the

Prehistoric group (11mm/9.4-12.2mm); in addition to a longer canine (16mm/13.8-17.8mm) than the Medieval group (12mm/10.5-15.8mm).

Table 7.2: Medians and 25% and 75% interquartiles (mm) of incisive canal and lingual canal length in the secular variability analysis. Note that no incisive canal could be measured at this point in the Prehistoric group. Medians connected with the same letter were statistically significant. IC=incisive canal; N=number

GROUP	IC (start)				Canal Length			
	N	Median	25%	75%	N	Median	25%	75%
CONTEMPORARY (Belgian)	18	3.0^a	2.1	3.1	25	3.9^a	2.7	6.0
MEDIEVAL	16	1.6^a	1.3	2.0	31	2.3^a	1.6	4.5
PREHISTORIC	11	3.0	2.3	4.8

Geographical variability showed significant results for mandibular canal, mental foramen and incisive canal. In Brazilian (1.6mm/1.1-2.1mm) and Belgian (1.8mm/1.6-2.1mm) groups, mandibular canal diameter at second premolar was significantly smaller than in Indian group (2.5mm/2.2-3.0mm). Although presenting small dimensions for the mandibular canal, Belgian group showed the largest mental foramen (4.1mm/3.4-4.6mm) in the geographical sample. It was significantly larger than Indian (2.9mm/2.4-3.7mm) and Chinese (3mm/2.6-3.1mm) groups. Similarly to the mental foramen, the Belgian group showed an incisive canal (3mm/2.1-3.1mm) at its start point, just after the mental foramen, significantly larger than most of the groups considered in the geographical sample.

In Chinese and Javanese groups the longest second premolars were observed, measuring in average 17mm, while in Brazilian and Congolese groups, premolars measured between 15-16mm and in Belgian, Indian and Eskimo, between 13-14mm. The Eskimo group presented shorter canine root lengths (around 12mm) as opposed to an overall range of 14-16mm in the geographical sample.

In general, the mandibular canal was observed closer to the root apices than incisive canal, with a large variability within groups for both canals. Contrary to the secular analysis, the geographical sample yielded significant results on these distances. The longest distances were observed in Eskimo group at molar (8.0mm/5.6-9.2mm) and canine (13mm/9.7-18.9mm) regions, being significant longer compared to Congolese (0.7mm/0.0-2.0mm) and Javanese (1.3mm/0.71-1.55mm),

at molar region, and to Javanese (3.2mm/2.3-5.9mm) and Belgium (3.5mm/2.0-5.8mm) at the canine region. Apart from Eskimo group, the overall distance range in the geographical sample was found in between 0.7 to 3.8 mm at molar region and 3.2 to 6.5mm at canine region.

Human, Chimpanzee and Gorilla groups showed significant differences in the dimensions of the mandibular canal, mental foramen, incisive canal, lingual canal and in the bone width at anterior region. Gorilla group showed significant higher medians for the mandibular canal, lingual canal length and bone width than Human and Chimpanzee groups (table 7.3).

Table 7.3: Medians and 25% and 75% interquartiles (mm) mandibular canal, lingual canal length and bone width in the interspecific analysis. Medians connected with the same letter were statistically significant. N=number

GROUP	N	MC38			Canal Length			Bone Width		
		Median	25%	75%	Median	25%	75%	Median	25%	75%
HUMANS	94	2.6^c	2.2	3.0	3.9^c	3.0	5.3	12.5^b	11.0	14.0
CHIMPANZEE	18	2.8	2.4	3.8	3.0^{bc}	1.9	3.6	9.6^b	8.7	11.1
GORILLA	8	3.5^c	3.5	4.0	5.6^b	3.6	8.6	18.4^b	16.1	24.3

On the other side, Human group showed significant larger mental foramen (3.3mm/2.7-4.0mm) compared to Chimpanzee (2.1mm/1.7-2.7mm) and Gorilla (2.1mm/1.9-2.9mm). Although no incisive canal could be observed in the Gorilla group and a few were presented in Chimpanzee, significant results were found between Human (IC/start: 1.9mm/1.6-2.6mm) and Chimpanzee (IC/start: 0.9mm/0.8-1.1mm) groups. For the root lengths, the longest third molar was observed in the Gorilla group (13mm/10.1-14.8mm), whereas the Human group presented the longest second premolar (14.5mm/13.4-16.4mm) and Chimpanzee, the longest canine (18.1mm/15.4-21.9mm).

No statistically significant results were found for the categorical variables, although interesting findings could be observed in our sample. Bifid mandibular canals and anterior loop were anatomical variations most frequently observed in the Gorilla, Medieval, Prehistoric and Brazilian groups (Table 7.4). No bifid canal or anterior loop could be observed in Chimpanzee. Anterior loop was mostly seen in Medieval, Prehistoric, Chinese and Indian groups.

Table 7.4: Overview sample size and frequency (%) of bifid mandibular canal and its anterior loop in the study sample. N=number

Group	Sample size	Bifid Mandibular Canal	Anterior Loop
		%(N)	%(N)
BRAZILIAN	20	25 (5)	5 (1)
INDIAN	27	3.7(1)	14.8 (4)
BELGIAN	21	4.8(1)	0
CHINESE	8	0	25 (2)
CONGOLESE	8	0	0
JAVANESE	7	0	0
ESKIMO	5	0	0
RAPANUI	2	0	0
TASMANIAN	1	0	0
MEDIEVAL	21	33.3 (7)	52.3 (11)
PREHISTORIC	5	20 (1)	20 (1)
CHIMPANZEE	20	0	0
GORILLA	15	40 (6)	0

Interestingly, incisive canal was present in 100% of Contemporary Belgian group, whereas just 86% in the Medieval and 40% in the Prehistoric groups. Incisive canal was observed in all geographic groups and ended mostly at midline in all groups, but Congolese, Eskimo and Belgian groups. In the Congolese group, this canal ended frequently at the premolar region, as for the Eskimo, the canine region was the end position of all 5 specimens. Interestingly, when visible, most of incisive canal bifurcations were found at the canine and first premolar region. Moreover, the incisive canal was mostly connected to lingual canal in Chinese and Indian groups. Different distributions were observed in the lingual canal, related to vertical and horizontal position (Table 7.5).

Regarding to the horizontal position, this canal was mostly found at midline in Human group, whereas it was frequently found in the midline and left position in Gorillas and Chimpanzee groups. Vertically, it was more frequently observed above the superior genial tubercle in the Contemporary group, in contrast to a more middle position in the Medieval, Prehistoric, Chimpanzee and Gorilla groups. Most of human

mandibles, although coming from different geographical locations, presented lingual canals located above and below the genial tubercles. Only the Indian group presented the highest percentage of middle canals compared to upper and lower positions. The greatest number of extra lingual canals was found in the geographical dataset, mainly in Javanese, Indian and Brazilian. In Javanese mandibles, a high number of extra lingual canals was found in the view of its small sample size (table 7.5). A higher number of extra lingual canals were also observed in the Medieval and Chimpanzee groups.

Table 7.5: Overview sample size and frequency of midline and lateral canals (horizontal location of the canals). The lingual canal location variable determined if the canal was situated upper, lower or at the same level as the genial spine (vertical location canals).

Group	Sample Size	total n Lingual Canals	Lingual Canal (horizontal location) % (N)			Lingual Canals (vertical location) % (N)		
			LEFT	MIDLINE	RIGHT	LOWER	MIDDLE	UPPER
BRAZILIAN	20	38	15.8 (6)	76.3 (29)	7.9 (3)	47.4 (18)	10.5 (4)	42.1 (16)
INDIAN	27	47	14.9 (7)	72 (34)	12.8 (6)	31.9 (15)	40.4 (19)	27.6 (13)
BELGIAN	21	32	12.5 (4)	78.1 (25)	9.4 (3)	25 (8)	18.7 (6)	56.2 (18)
CHINESE	8	16	18.7 (3)	75 (12)	6.2 (1)	56.2 (9)	6.2 (1)	37.5 (6)
CONGOLESE	8	19	26.3 (5)	52.6 (10)	21 (4)	36.8 (7)	5.3 (1)	57.9 (11)
JAVANESE	7	28	35.7 (10)	46.4 (13)	17.8 (5)	53.6 (15)	35.7 (10)	10.7 (3)
ESKIMO	5	14	21.4 (3)	64.3 (9)	14.3 (2)	57.1 (8)	28.6 (4)	14.3 (2)
MEDIEVAL	21	49	22.4 (11)	63.3 (31)	14.3 (7)	36.7 (18)	57.1 (28)	6.1 (3)
PREHISTORIC	5	16	12.5 (2)	68.7 (11)	18.7 (3)	25 (4)	62.5 (10)	12.5 (2)
CHIMPANZEE	20	78	35.9 (28)	35.9 (28)	28.2 (22)	29.5 (23)	37.2 (29)	33.3 (26)
GORILLA	15	28	42.8 (12)	35.7 (10)	21.4 (6)	21.4 (6)	57.1 (16)	21.4 (6)

Multivariate analysis showed variable redundancies, patterning in data sample and that some groups could be differentiated by variables (figures 7.6 to 7.10). Loading plots generated by principal component analysis (figures 7.6 and 7.7)

confirmed that variables related to the same structure provide similar information for data characterization, e.g. variables related to teeth presented similar loading in the same factor, showing similar importance to explain sample variability. In spite of a high distribution overlapping, some sample patterning was revealed by this analysis in the intra and interspecific approaches (figure 7.6).

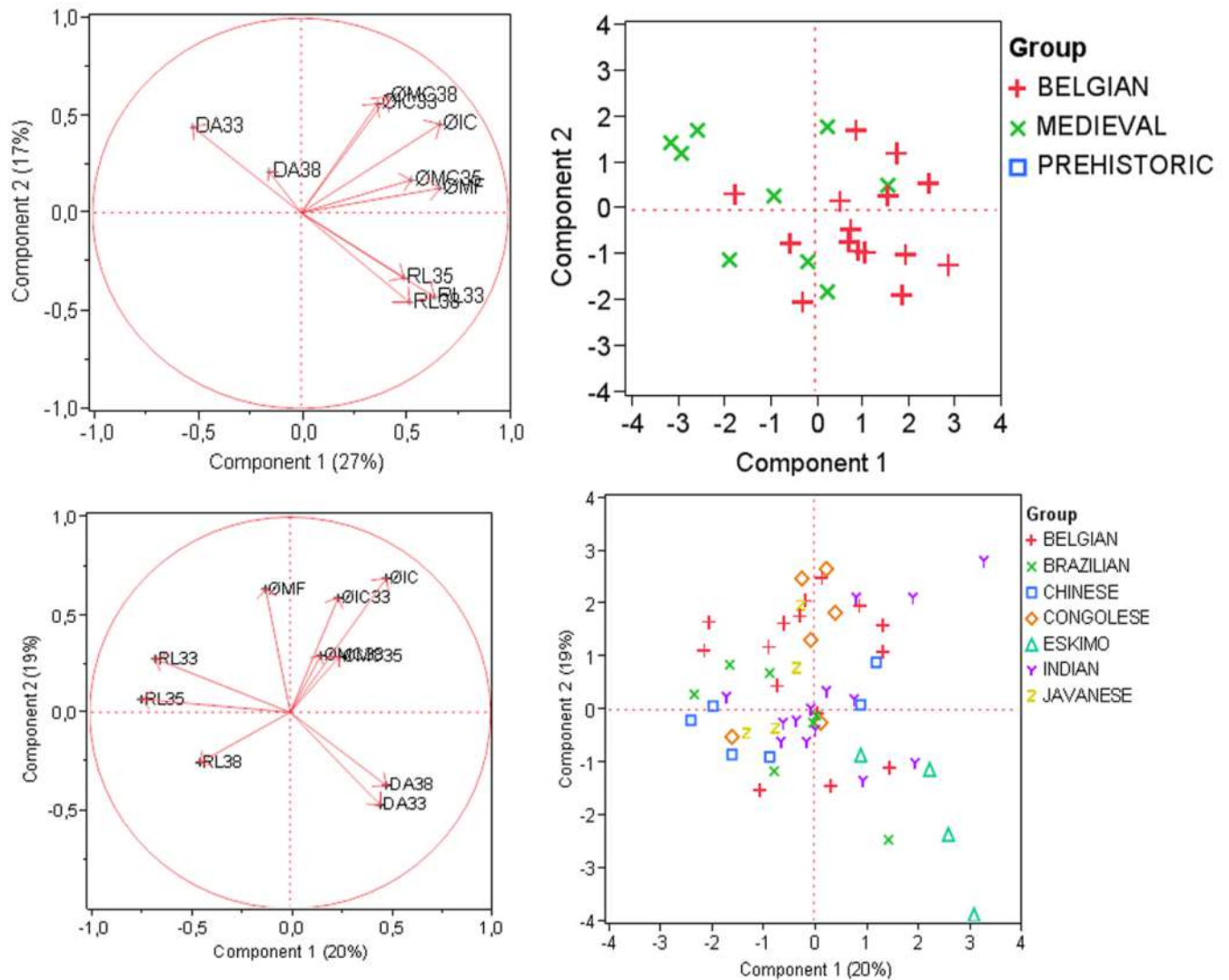


Figure 7.6: Principal component analysis score plots. The graphics show the loading and score plots from secular and geographical analyses

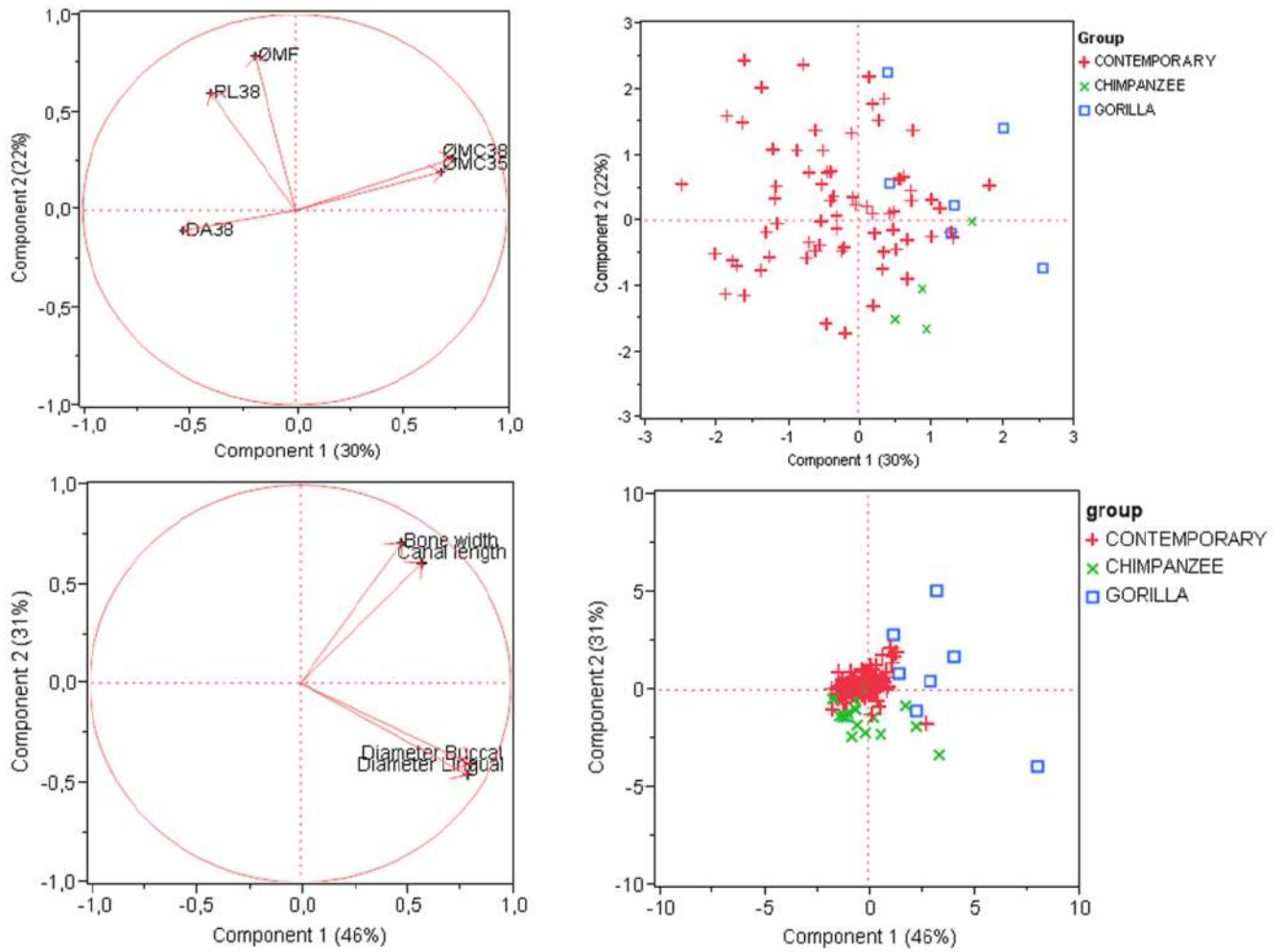


Figure 7.7: Principal component analysis score plots. The graphics show the loading and score plots from interspecific analyses.

Discriminant analysis could differentiate medieval and contemporary mandibles amongst humans from different period of time (figure 7.8). Furthermore, Eskimo mandibles could be differentiated from other geographically distributed human mandibles (figure 7.9). Finally, a differentiation between primates was possible, without overlapping in their distributions (figure 7.10). Furthermore, Brazilian and Belgian mandibles also showed no distribution overlapping with Indian and Congolese mandibles (figure 7.9).

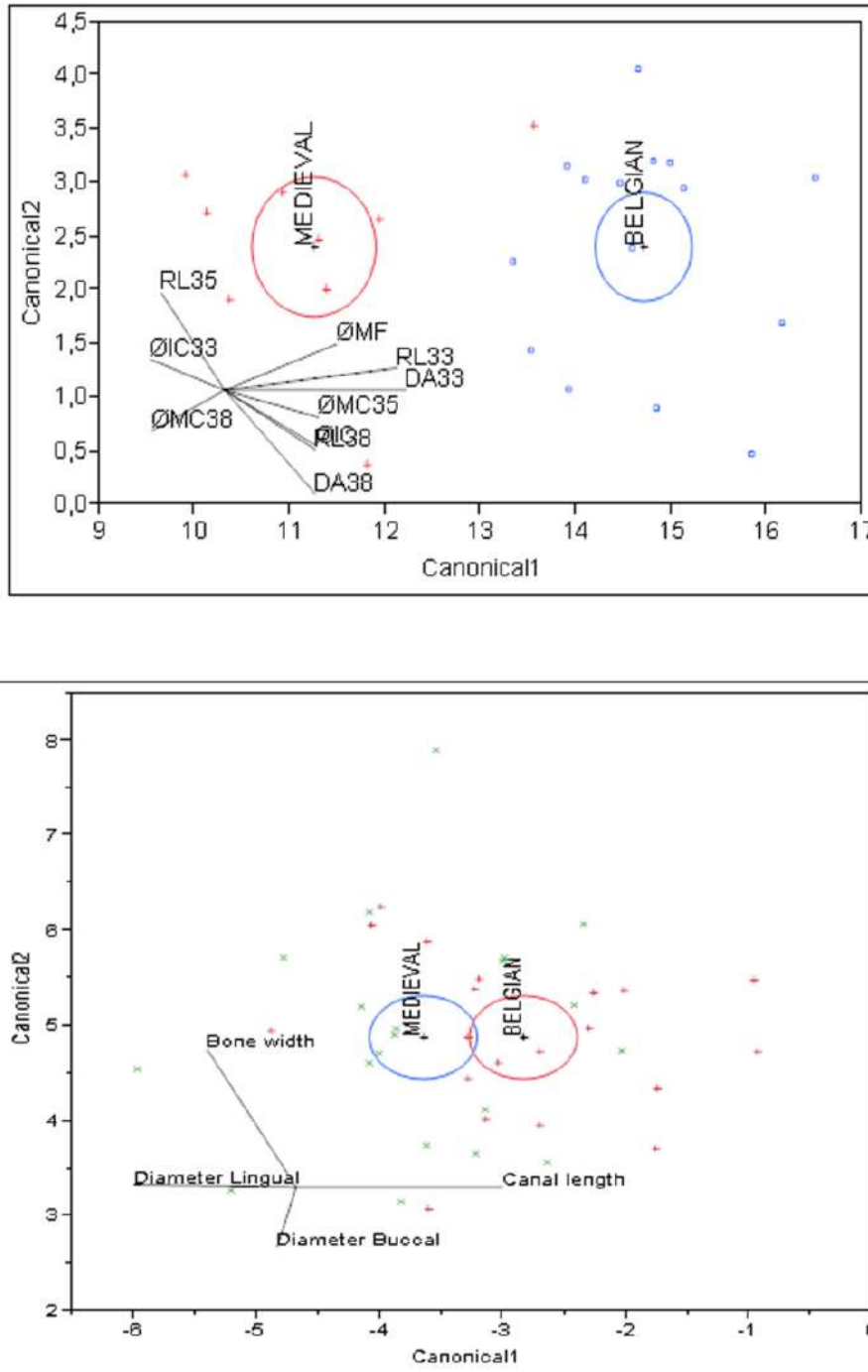


Figure 7.8: Linear discriminant analysis canonical plot. The graphics show the canonical plot in secular analysis.

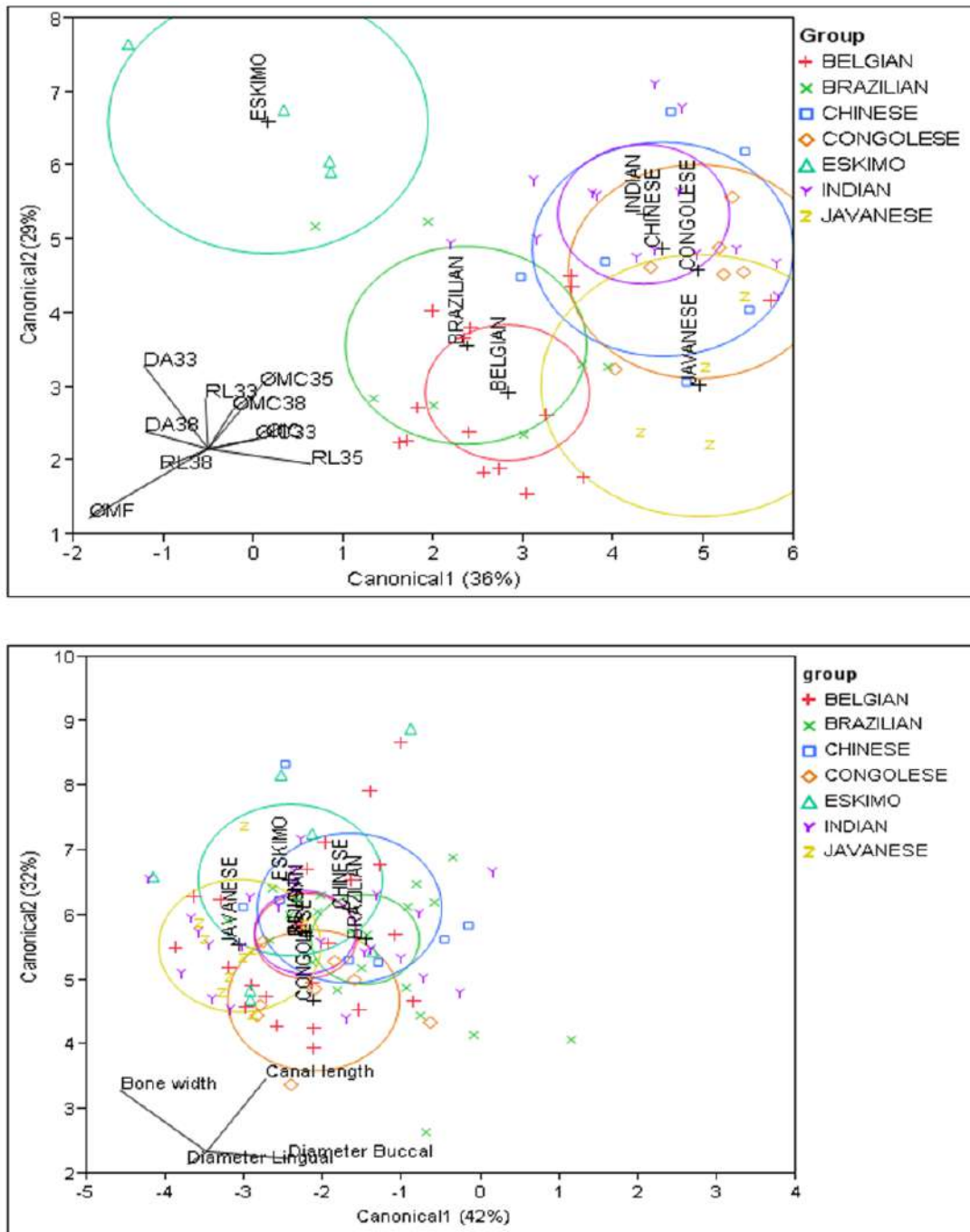


Figure 7.9: Linear discriminant analysis canonical plot. The graphics show the canonical plot in geographical analyses.

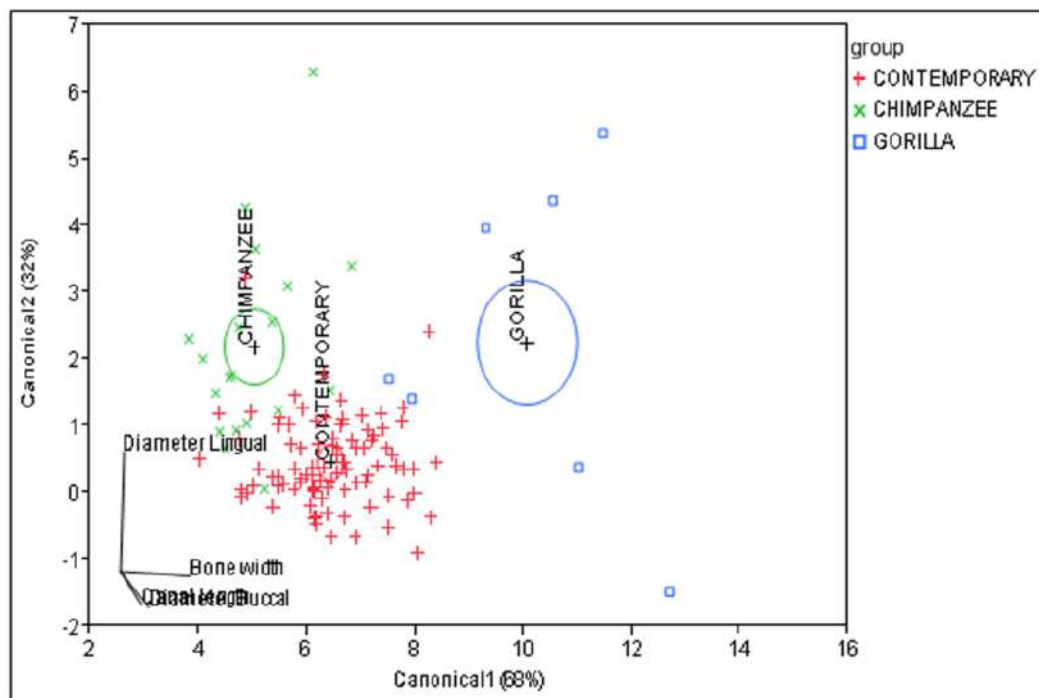
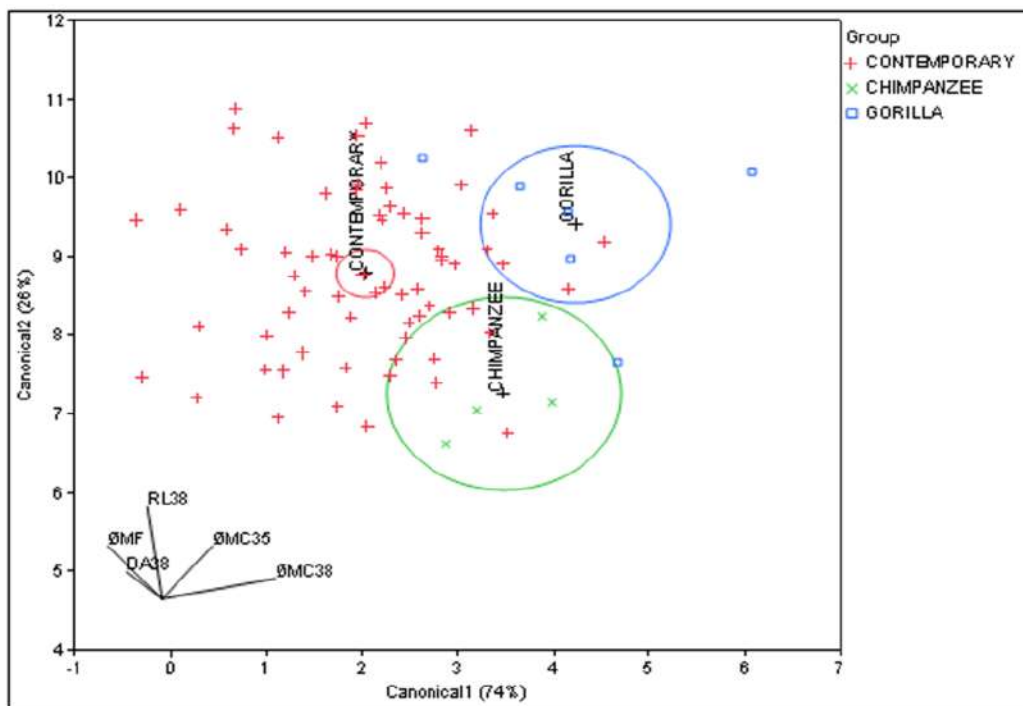


Figure 7.10: Linear discriminant analysis canonical plot. The graphics show the canonical plot in interspecific analyses.

Discussion

This study has evaluated anatomical variability of mandibular neurovascular canals and tooth roots searching for differences and similarities within humans from different period of time, regions and within primates. The morphology of neurovascular canals and their relation with adjacent tooth roots revealed some clinical and research applications.

The anatomical variations pointed in this study might also result from differences in growth rate and remodelling at key locations on the mandible that take place from before birth until adulthood. For instance, mental foramen, a milestone structure associated to mandibular growth (*Park et al 2010*), showed significant differences between groups in all three study approaches. This foramen is located at one of the six functional units (growth units) of mandible (*Curien et al 2011; Park et al 2010*), therefore it is exposed to the influence of the environment and more prone to variability. On the other hand, mandibular canal showed a lower variability among groups, as expected for a more stable unit of mandibular growth (*Curien et al 2011*). The average diameter for mental foramen, for mandibular canal and for incisive canal were similar to previous literature reports in contemporary humans (*Gintaras et al 2010; Neiva et al 2004; Jacobs et al 2002*). The mental foramen and incisive canal in modern humans not only presented an increase through time within humans, but were also larger than in great apes.

Yet, no similar report about the mental foramen was found in the literature. In spite of being constantly addressed as a descriptor of divergences among fossil mandibles and extant animals (*Plavcan and Daegling 2006; Royer et al 2009; Humphrey et al 1999*), unlike the present research, previous studies have investigated differences of mental foramen position (*for review: Robinson and Williams 2010*). Nevertheless, similar efforts to describe contemporary variability from a historical perspective has been reported before by Reich et al (2011) in an attempt to understand atrophy of the mandibular residual alveolar ridge following tooth loss.

As in previous observations (*Dean and Vesey 2008*), the average root length found in contemporary humans was between 11mm and 13mm in third molars, between 13-16mm in second premolars and 13-17mm in canines. Interestingly, tooth roots showed an increase of 1 to 3mm from prehistoric to contemporary period of

time. Although previous studies have reported differences in tooth crown and mandibular sizes in modern humans (*for review: Humphrey et al 1999*), through our literature search only few studies (*Kupczik and Hublin 2010; Fukase and Suwa 2010; Royer et al 2009; Smith et al 1989; Smith et al 1986*) could be found approaching root length variability over time.

By means of micro-computed tomography, Kupczik and Hublin (2010) reported a third molar root length (12.8mm) similar to our results, although shorter than in earlier humans (Aterian) and Neanderthals. In contrast, Fukase and Suwa (2010) found a longer canine in a modern Japanese population compared to prehistoric Jomon Japanese. Yet, recent studies (*Plavcan and Daegling 2006; Kupczik and Dean 2008*) have addressed tooth root variability among species and they raised the discussion around the relation between tooth root size and mandibular size. Further comparison with our results could not be made since the mandibular size was not taken into consideration in our analysis. According to Dean and Vesey (2008), root growth differs between tooth types in both pattern and rate and between taxa. In our study, the third molar root was longer in gorillas, while the longest canine was found in chimpanzees, as well reported by Kupczik and Dean (2008), whereas the longest second premolar was observed in modern humans.

The longest tooth roots of contemporary mandibles were associated with a slightly smaller distance to the neurovascular canals comparing to mandibles of anatomically modern humans from medieval time. However, the same was not true within contemporary human mandibles from different regions. The longest tooth root in Congolese mandibles, in the molar region did not imply the smallest distances to the canals, neither in Brazilian mandibles, in the canine region. Hence, it is suggested that the relation of neurovascular mandibular canals with adjacent tooth roots might be influenced either by biomechanical factors or by some other features that might be genetically regulated.

Furthermore, considering the high variability of these distances within groups, it is suggested that the relation between tooth roots and neurovascular canals might be physiologically determined. This suggests that many factors may influence this distance, like those factors influencing physiological loads and their distribution inside the mandibular bone, e.g. type of occlusion, trabecular bone geometry, canal

corticalization, and bone morphology. This physiologically determined distance should be used as a guide to define the safety margin for dental implant placement in the mandibular bone. According to our results, this safety margin would be around 2.67 to 7.61mm for the canine region. Kovisto et al (2011) has reported an average distance between 1.51 and 3.43mm in the premolar and molar region, the posterior teeth being located closer to canal than anterior teeth. In this way, the reported safety margin of 1.0mm (*Bavitz et al 1993*) to 2.0mm (*Froum et al 2011*) between dental implant and nerve bundle should be reconsidered regarding other functional, morphological and structural characteristics. Some individuals might need greater distances between tooth and canal in order to impose lower stresses on mandibular neurovascular structures. In this case, a high risk for sensory disturbances can be expected when this distance cannot be maintained, e.g. after placement of a dental implant.

However, biomechanical studies involving mandibular bone structure are needed to confirm a correlation between canal-to-root distances and load distribution in the mandible. Furthermore, clinical studies should verify the correlation between the incidence of neurosensory disturbances after implant treatment and distance between implants and the surrounding neurovascular canals. Recently, a correlation between bone trabeculation and canal corticalization was proposed (*Oliveira-Santos et al 2011; Naitoh et al 2009*), and it is clear that further correlations of these features with canal-tooth distances should also be assessed.

Apart from distance canal-to-root, some other characteristics presented by the different groups from the geographical sample were interpreted according to potential risk it could imply to surgical procedures (table 7.6). For example, the presence of a wider incisive canal, mostly branching, suggested that the canine region can be a risk area for nerve trauma and injury. Other high risk features consisted of the presence of bifid mandibular canal and anterior loop, large foramen and high number of lingual canals.

Table 7.6: Geographical trends and surgical risk prediction based on study observations.

Features related to potential surgical risks	<i>Brazilian</i>	<i>Belgian</i>	<i>Indian</i>	<i>Chinese</i>	<i>Javanese</i>	<i>Congolese</i>
Large canals		X (incisive)	X (mandibular)	X (mandibular)		
Long roots	X				X	X
Large mental foramen		X				
Small distances root to canal		X			X	X
Bifid canal	X	X	X			
Anterior loop	X		X	X		

Since the prevalence of bifid canals (*Kuribayashi et al 2010; Naitoh et al 2009b; Rouas et al 2007; Claeys and Wackens 2005*); and anterior loop (*Oliveira-Santos et al 2011b; Neiva et al 2004*) are contradictory in the literature, the geographical variability demonstrated in this study is likely to explain the lack of agreement among studies. Besides, the high risk of tumour spreading associated to a neurovascular network established by the intrabony canals (*Fanibunda and Matthews 2000; Fanibunda and Matthews 1999; Trikeriotis et al 2008*) should be investigated since our results indicated a high number of extra lingual canals and more anteriorly extended incisive canals in humans, also reported previously by De Andrade (*De Andrade et al 2001*).

As expected, more differences were observed in the interspecific than in the intraspecific analysis. The largest bone width at anterior regions of gorillas was followed by the longest lingual canal and highest prevalence of lateral canals. Most interestingly, no gorillas and just a few chimpanzees presented on incisive canal, whereas high incidence was observed in modern humans, in agreement with Mraiwa et al (2003). We suggest that the highest prevalence of lateral canals in great apes, as well as the highest prevalence of incisive canal in modern humans might be related to some morphological and functional characteristics of those two different taxa, e.g. the superior transverse torus or simian shelf in great apes and a protruding mentum osseum or chin in anatomically modern humans.

In fact, the simian shelf, which is a lingual protuberance responsible to provide a more robust mandible, characterizes great apes' mandibles (*Gröning et al 2012*). On the other hand, the chin is a feature unique to modern humans that was speculatively related to our speech ability (*Ichim et al 2007*), although other hypotheses explain it by

the functional and biomechanical significance of the mental protuberance (*Gröning et al 2012; Achermann 2004; Schwartz and Tattersall 2000*). In this way, the incisive canal might be related to the emergence of the mental protuberance in humans. Furthermore, morphology and function must be likewise responsible for divergences in the lingual canal position since its foramina are close to muscle attachments. Those muscles are intimately involved in the function and support of the tongue and its associated soft tissues (*Silverstein et al 2000*).

Although some patterning could be identified by multivariate analysis, the redundant information and the overlapping of population distributions suggested that further observations should be made considering other parameters. This can help to better explain population variability on mandibular neurovascular canals and tooth roots, consequently, providing a better differentiation of populations by those parameters. Mandibular canal, root lengths and mental foramen could clearly differentiate mandibles from different historical periods suggesting further investigations in order to better correlate those findings with other physiological factors. According to Rak et al (2007), modern humans, chimpanzees, orang-utans, and many other primates share the morphology of mandibular ramus which differs from that of gorillas, so that the gorilla anatomy must represent a unique condition, and its appearance must represent an independently derived morphology. Indeed, gorillas did not share the same dimensions for tooth root and mandibular canals with humans, neither with chimpanzees. However, unlike the morphology of mandibular ramus, humans also did not share the same dimensions for tooth roots and mandibular canals with chimpanzees.

Finally, we believe that future collaborations bringing together the multiple research areas involving mandibular anatomy and physiology will result in a better understanding of morphological variations and their clinical and research applications.

Conclusions

This study could describe the significant variability of neurovascular canals and tooth roots in modern humans and great apes. Tooth root, mental foramen and incisive canal presented a high variability for mandibles from different periods of time, geographical origins and species. Similar mandibular canal diameters and canal-to-root distances are expected over the time in humans, whereas more variability may be expected for the lingual canal length. Differences in geographical origin and species may account for a high variability in the mandibular canal diameter and canal-to-root distances in primates.

References

- Abarca M, van Steenberghe D, Malevez C, De Ridder J, and Jacobs R. Neurosensory disturbances after immediate loading of implants in the anterior mandible: an initial questionnaire approach followed by a psychophysical assessment. *Clin Oral Investig* 2006; 10:269-277.
- Ackermann RR, Cheverud JM. Detecting genetic drift versus selection in human evolution. *Proc Natl Acad Sci U S A* 2004; 101:17946-51.
- Bagheri SC, Meyer RA, Khan HA, Wallace J, and Steed MB. Microsurgical repair of the peripheral trigeminal nerve after mandibular sagittal split ramus osteotomy. *J Oral Maxillofac Surg* 2010; 68:2770-2782.
- Bavitz JB, Harn SD, Hansen CA, and Lang M. An anatomical study of mental neurovascular bundle-implant relationships. *Int J Oral Maxillofac Implants* 1993; 8:563-567.
- Captier G, Lethuillier J, Oussaid M, Canovas F, and Bonnel F. Neural symmetry and functional asymmetry of the mandible. *Surg Radiol Anat* 2006; 28:379-386.
- Claeys V, and Wackens G. Bifid mandibular canal: literature review and case report. *Dentomaxillofac Radiol* 2005; 34:55-58.
- Colella G, Cannavale R, Vicidomini A, and Lanza A. Neurosensory disturbance of the inferior alveolar nerve after bilateral sagittal split osteotomy: a systematic review. *J Oral Maxillofac Surg* 2007; 65:1707-1715.
- Curien R, Braun M, Perez M, Bravetti P, and Coqueugniot H. Discriminant study of the development of the mandibular units in a neural reference system. *Surg Radiol Anat* 2011; 33:191-196.
- Dao TT, and Mellor A. Sensory disturbances associated with implant surgery. *Int J Prosthodont* 1998; 11:462-469.
- De Andrade E, Otomo-Corgel J, Pucher J, Ranganath KA, and St George N, Jr. The intraosseous course of the mandibular incisive nerve in the mandibular symphysis. *Int J Periodontics Restorative Dent* 2001; 21:591-597.
- de Oliveira Junior MR, Saud AL, Fonseca DR, De-Ary-Pires B, Pires-Neto MA, and de Ary-Pires R. Morphometrical analysis of the human mandibular canal: a CT investigation. *Surg Radiol Anat* 2011; 33:345-352.
- de Oliveira-Santos C, Souza PH, de Azambuja Berti-Couto S, Stinkens L, Moyaert K, Rubira-Bullen IR, and Jacobs R. Assessment of variations of the mandibular

- canal through cone beam computed tomography. *Clin Oral Investig* 2012; 16:387-393.
- De Vos W, Casselman J, and Swennen GR. Cone-beam computerized tomography (CBCT) imaging of the oral and maxillofacial region: a systematic review of the literature. *Int J Oral Maxillofac Surg* 2009; 38:609-625.
- Dean MC, and Vesey P. Preliminary observations on increasing root length during the eruptive phase of tooth development in modern humans and great apes. *J Hum Evol* 2008; 54:258-271.
- Fanibunda K, and Matthews JN. Relationship between accessory foramina and tumour spread in the lateral mandibular surface. *J Anat* 1999; 195:185-190.
- Fanibunda K, and Matthews JN. The relationship between accessory foramina and tumour spread on the medial mandibular surface. *J Anat* 2000; 196 :23-29.
- Froum S, Casanova L, Byrne S, and Cho SC. Risk assessment before extraction for immediate implant placement in the posterior mandible: a computerized tomographic scan study. *J Periodontol* 2011; 82:395-402.
- Fuakami K, Shiozaki K, Mishima A, Shimoda S, Hamada Y, and Kobayashi K. Detection of buccal perimandibular neurovascularisation associated with accessory foramina using limited cone-beam computed tomography and gross anatomy. *Surg Radiol Anat* 2011; 33:141-146.
- Fukase H, Suwa G. Influence of size and placement of developing teeth in determining anterior corpus height in prehistoric Jomon and modern Japanese mandibles. *Anthropological Science* 2010; 118:75-86.
- Gintaras J, Hom-Lay W, Gintautas S. Anatomy of Mandibular Vital Structures. Part II: Mandibular Incisive Canal, Mental Foramen and Associated Neurovascular Bundles in Relation with Dental Implantology. *J Oral Maxillofac Res* 2010; 1: e2.
- Greenstein G, Cavallaro J, and Tarnow . Practical application of anatomy for the dental implant surgeon. *J Periodontol* 2008; 79:1833-1846.
- Greenstein G, and Tarnow D. The mental foramen and nerve: clinical and anatomical factors related to dental implant placement: a literature review. *J Periodontol* 2006; 77:1933-1943.
- Gröning F, Liu J, Fagan MJ, O'Higgins P. Why do humans have chins? Testing the mechanical significance of modern human symphyseal morphology with finite element analysis. *Am J Phys Anthropol* 2011; 144:593-606.
- Guerrero ME, Jacobs R, Loubele M, Schutyser F, Suetens P, and van Steenberghe D. State-of-the-art on cone beam CT imaging for preoperative planning of implant placement. *Clin Oral Investig* 2006; 10:1-7.
- Hanihara T, and Ishida H.. Frequency variations of discrete cranial traits in major human populations. I. Supernumerary ossicle variations. *J Anat* 2001 a;198:689-706.
- Hanihara T, and Ishida H. Frequency variations of discrete cranial traits in major human populations. II. Hypostotic variations. *J Anat* 2001 b;198:707-725.
- Hanihara T, and Ishida H. Frequency variations of discrete cranial traits in major human populations. III. Hyperostotic variations. *J Anat* 2001 c; 199:251-272.
- Hanihara T, and Ishida H. Frequency variations of discrete cranial traits in major human populations. IV. Vessel and nerve related variations. *J Anat* 2001 d; 199:273-287.
- Hegedus F, and Diecidue RJ. Trigeminal nerve injuries after mandibular implant placement--practical knowledge for clinicians. *Int J Oral Maxillofac Implants* 2006; 21:111-116.

- Humphrey LT, Dean MC, and Stringer CB. Morphological variation in great ape and modern human mandibles. *J Anat* 1999; 195:491-513.
- Ichim I, Kieser J, Swain M. Tongue contractions during speech may have led to the development of the bony geometry of the chin following the evolution of human language: a mechanobiological hypothesis for the development of the human chin. *Med Hypotheses* 2007; 69:20-4.
- Jacobs R, Lambrichts I, Liang X, Martens W, Mraiwa N, Adriaensens P, and Gelan J. Neurovascularization of the anterior jaw bones revisited using high-resolution magnetic resonance imaging. *Oral Surg Oral Med Oral Pathol Oral Radiol Endod* 2007; 103:683-693.
- Jacobs R, Mraiwa N, vanSteenberghe D, Gijbels F, and Quirynen M. Appearance, location, course, and morphology of the mandibular incisive canal: an assessment on spiral CT scan. *Dentomaxillofac Radiol* 2002; 31:322-327.
- Juodzbalys G, Wang HL, Sabalys G, Sidlauskas A, Galindo-Moreno P. Inferior alveolar nerve injury associated with implant surgery. *Clin Oral Implants Res* 2013; 24:183-90.
- Katakami K, Mishima A, Kuribayashi A, Shimoda S, Hamada Y, and Kobayashi K. Anatomical characteristics of the mandibular lingual foramina observed on limited cone-beam CT images. *Clin Oral Implants Res* 2009; 20:386-390.
- Kim ST, Hu KS, Song WC, Kang MK, Park HD, and Kim HJ. Location of the mandibular canal and the topography of its neurovascular structures. *J Craniofac Surg* 2009; 20:936-939.
- Kingsmill VJ. Post-extraction remodeling of the adult mandible. *Crit Rev Oral Biol Med* 1999; 10:384-404.
- Kovisto T, Ahmad M, and Bowles WR. Proximity of the mandibular canal to the tooth apex. *J Endod* 2011; 37:311-315.
- Kupczik K, and Dean MC. Comparative observations on the tooth root morphology of *Gigantopithecus blacki*. *J Hum Evol* 2008; 54:196-204.
- Kupczik K, and Hublin JJ. Mandibular molar root morphology in Neanderthals and Late Pleistocene and recent *Homo sapiens*. *J Hum Evol* 2010; 59:525-541.
- Kuribayashi A, Watanabe H, Imaizumi A, Tantanapornkul W, Katakami K, and Kurabayashi T. Bifid mandibular canals: cone beam computed tomography evaluation. *Dentomaxillofac Radiol* 2010; 39:235-239.
- Kuzmanovic DV, Payne AG, Kieser JA, and Dias GJ. Anterior loop of the mental nerve: a morphological and radiographic study. *Clin Oral Implants Res* 2003;14:464-471.
- Levine MH, Goddard AL, and Dodson TB. Inferior alveolar nerve canal position: a clinical and radiographic study. *J Oral Maxillofac Surg* 2007; 65:470-474.
- Liang X, Jacobs R, Hassan B, Li L, Pauwels R, Corpas L, Souza PC, Martens W, Shahbazian M, Alonso A et al. A comparative evaluation of Cone Beam Computed Tomography (CBCT) and Multi-Slice CT (MSCT) Part I. On subjective image quality. *Eur J Radiol* 2010; 75:265-269.a
- Liang X, Jacobs R, and Lambrichts I. An assessment on spiral CT scan of the superior and inferior genial spinal foramina and canals. *Surg Radiol Anat* 2006; 28:98-104.
- Liang X, Jacobs R, Lambrichts I, and Vandewalle G. Lingual foramina on the mandibular midline revisited: a macroanatomical study. *Clin Anat* 2007; 20:246-251.
- Liang X, Lambrichts I, Corpas LS , Politis C, Vrielinck L, Ma GW, Jacobs R. Neurovascular Disturbance Associated with Implant Placement in the Anterior

- Mandible and its Surgical Implications: literature review including report of a case. *Chinese Journal of Dental Research* 2008; 11: 56-64.
- Liang X, Lambrichts I, Sun Y, Denis K, Hassan B, Li L, Pauwels R, and Jacobs R. A comparative evaluation of Cone Beam Computed Tomography (CBCT) and Multi-Slice CT (MSCT). Part II: On 3D model accuracy. *Eur J Radiol* 2010; 75:270-274.b
- Loubele M, Guerrero ME, Jacobs R, Suetens P, and van Steenberghe D. A comparison of jaw dimensional and quality assessments of bone characteristics with cone-beam CT, spiral tomography, and multi-slice spiral CT. *Int J Oral Maxillofac Implants* 2007; 22:446-454.
- Loubele M, Van Assche N, Carpentier K, Maes F, Jacobs R, van Steenberghe D, and Suetens P. Comparative localized linear accuracy of small-field cone-beam CT and multislice CT for alveolar bone measurements. *Oral Surg Oral Med Oral Pathol Oral Radiol Endod* 2008; 105:512-518.
- Morris CD, Rasmussen J, Throckmorton GS, and Finn R. The anatomic basis of lingual nerve trauma associated with inferior alveolar block injections. *J Oral Maxillofac Surg* 2010; 68:2833-2836.
- Mraiwa N, Jacobs R, Moerman P, Lambrichts I, van Steenberghe D, and Quirynen M. Presence and course of the incisive canal in the human mandibular interforaminal region: two-dimensional imaging versus anatomical observations. *Surg Radiol Anat* 2003; 25:416-423.a
- Mraiwa N, Jacobs R, van Steenberghe D, and Quirynen M. Clinical assessment and surgical implications of anatomic challenges in the anterior mandible. *Clin Implant Dent Relat Res* 2003; 5:219-225. b
- Naitoh M, Hiraiwa Y, Aimiya H, and Arijji E. Observation of bifid mandibular canal using cone-beam computerized tomography. *Int J Oral Maxillofac Implants* 2009; 24:155-159. a
- Naitoh M, Hiraiwa Y, Aimiya H, Gotoh K, and Arijji E. Accessory mental foramen assessment using cone-beam computed tomography. *Oral Surg Oral Med Oral Pathol Oral Radiol Endod* 2009;107:289-294. b
- Naitoh M, Katsumata A, Kubota Y, Hayashi M, and Arijji E. Relationship between cancellous bone density and mandibular canal depiction. *Implant Dent* 2009; 18:112-118. c
- Neiva RF, Gapski R, and Wang HL. Morphometric analysis of implant-related anatomy in Caucasian skulls. *J Periodontol* 2004;75:1061-1067.
- de Oliveira Junior MR, Saud AL, Fonseca DR, De-Ary-Pires B, Pires-Neto MA, and de Ary-Pires R. Morphometrical analysis of the human mandibular canal: a CT investigation. *Surg Radiol Anat* 2011; 33:345-352.
- Oliveira-Santos C, Souza PH, De Azambuja Berti-Couto S, Stinkens L, Moyaert K, Van Assche N, and Jacobs R. Characterisation of additional mental foramina through cone beam computed tomography. *J Oral Rehabil* 2011; 38:595-600.
- Orhan K, Aksoy S, Bilecenoglu B, Sakul BU, and Paksoy CS. Evaluation of bifid mandibular canals with cone-beam computed tomography in a Turkish adult population: a retrospective study. *Surg Radiol Anat* 2011; 33:501-507.
- Park W, Kim BC, Yu HS, Yi CK, and Lee SH. Architectural characteristics of the normal and deformity mandible revealed by three-dimensional functional unit analysis. *Clin Oral Investig* 2010; 14:691-698.
- Plavcan JM, and Daegling DJ. Interspecific and intraspecific relationships between tooth size and jaw size in primates. *J Hum Evol* 2006; 51:171-184.

- Poort LJ, van Neck JW, and van der Wal KG. Sensory testing of inferior alveolar nerve injuries: a review of methods used in prospective studies. *J Oral Maxillofac Surg* 2009; 67:292-300.
- Quevedo LA, Ruiz JV, and Quevedo CA. Using a clinical protocol for orthognathic surgery and assessing a 3-dimensional virtual approach: current therapy. *J Oral Maxillofac Surg* 2011; 69:623-637.
- Rak Y, Ginzburg A, and Geffen E. Gorilla-like anatomy on *Australopithecus afarensis* mandibles suggests *Au. afarensis* link to robust australopiths. *Proc Natl Acad Sci U S A* 2007; 104:6568-6572.
- Reich KM, Huber CD, Lippnig WR, Ulm C, Watzek G, and Tangl S. Atrophy of the residual alveolar ridge following tooth loss in an historical population. *Oral Dis* 2011; 17:33-44.
- Renton T, Adey-Viscuso D, Meechan JG, and Yilmaz Z. Trigeminal nerve injuries in relation to the local anaesthesia in mandibular injections. *Br Dent J* 2010; 209:E15.
- Robinson CA, and Williams FL. Quantifying mental foramen position in extant hominoids and *Australopithecus*: implications for its use in studies of human evolution. *Anat Rec (Hoboken)* 2010; 293:1337-1349.
- Romanos GE, and Greenstein G. The incisive canal. Considerations during implant placement: case report and literature review. *Int J Oral Maxillofac Implant.* 2009; 24:740-745.
- Rosano G, Taschieri S, Gaudy JF, Testori T, and Del Fabbro M. Anatomic assessment of the anterior mandible and relative hemorrhage risk in implant dentistry: a cadaveric study. *Clin Oral Implants Res* 2009; 20:791-795.
- Rouas P, Nancy J, and Bar D. Identification of double mandibular canals: literature review and three case reports with CT scans and cone beam CT. *Dentomaxillofac Radiol* 2007; 36:34-38.
- Royer DF, Lockwood CA, Scott JE, and Grine FE. Size variation in early human mandibles and molars from Klasies River, South Africa: comparison with other middle and late Pleistocene assemblages and with modern humans. *Am J Phys Anthropol* 2009; 140:312-323.
- Schwartz JH and Tattersall I. The human chin revisited: what is it and who has it? *J Hum Evol* 2000; 38:367-409.
- Sessle BJ. Mechanisms of oral somatosensory and motor functions and their clinical correlates. *J Oral Rehabil* 2006; 33:243-261.
- Silverstein K, Costello BJ, Giannakopoulos H, and Hendler B. Genioglossus muscle attachments: an anatomic analysis and the implications for genioglossus advancement. *Oral Surg Oral Med Oral Pathol Oral Radiol Endod* 2000; 90:686-688.
- Smith P, Wax Y, Adler F. Population variation in tooth, jaw, and root size: a radiographic study of two populations in a high-attrition environment. *Am J Phys Anthropol.* 1989;79:197-206.
- Smith P, Wax Y, Adler F, Silberman U, Heinic G. Post-pleistocene changes in tooth root and jaw relationships. *Am J Phys Anthropol.* 1986;70:339-48.
- Spoor F, Jeffery N, and Zonneveld F. Using diagnostic radiology in human evolutionary studies. *J Anat* 2000; 197:61-76.
- Tay AB, and Zuniga JR. Clinical characteristics of trigeminal nerve injury referrals to a university centre. *Int J Oral Maxillofac Surg* 2007; 36:922-927.

- Trikeriotis D, Paravalou E, Diamantopoulos P, and Nikolaou D. Anterior mandible canal communications: a potential portal of entry for tumour spread. *Dentomaxillofac Radiol* 2008; 37:125-129.
- Van Assche N, van Steenberghe D, Guerrero ME, Hirsch E, Schutyser F, Quirynen M, and Jacobs R. Accuracy of implant placement based on pre-surgical planning of three-dimensional cone-beam images: a pilot study. *J Clin Periodontol* 2007; 34:816-821.
- Vandenberghe B, Jacobs R, and Bosmans H. Modern dental imaging: a review of the current technology and clinical applications in dental practice. *Eur Radiol* 2010; 20:2637-2655.
- Venta I, Lindqvist C, and Ylipaavalniemi P. Malpractice claims for permanent nerve injuries related to third molar removals. *Acta Odontol Scand* 1998; 56:193-196.
- Walton JN. Altered sensation associated with implants in the anterior mandible: a prospective study. *J Prosthet Dent* 2000; 83:443-449.
- Ziccardi VB, and Steinberg MJ. Timing of trigeminal nerve microsurgery: a review of the literature. *J Oral Maxillofac Surg* 2007; 65:1341-1345.

Chapter 8

Mandibular neurovascular canals

Influence of oral status and implant treatment

Publication related to this chapter:

Corpas LS, Vandenberghe B, Politis C, Schepers S, Lambrichts I, Naert I, Jacobs R. Anatomical changes in the mandibular bone after tooth extraction and implant rehabilitation in edentulous patients. (in prep)

Dimensional changes of the mandibular bone and neurovascular canals after tooth extraction and implant treatment: 2-year follow-up study

ABSTRACT

Objectives: The aim of this study was to compare the anatomy of mandibular jaw bone and neurovascular canals in dentate and edentate mandibles after implant treatment. **Materials & methods:** Twenty four patients needing implant treatment were selected to take part in this study. All patients were selected at the Maxillo-Facial Surgery department of East Limburg Hospital (ZOL, Genk, Belgium). Twelve patients composed the dentate group, whereas the edentulous and total extraction groups comprised 6 patients each. Cone beam computed tomography scans were taken as part of their clinical treatment. Two-dimensional measurements included the mental foramen (MF) diameter, mandibular (MC), incisive (IC) canal for their diameter and spatial relation within the jaw bone (distance to the borders) at different mandibular regions. Statistical analyses were carried out with repeated measures analysis, paired t-test and one way Anova and Tukey-Kramer HSD (honestly significant difference). Least square regression analyses were conducted to check any association between the dimensions of the mandibular bone and the neurovascular canals. **Results:** Most anatomical structures presented only slight dimensional changes after the one-year follow-up period of this study. Furthermore, dentate and edentulous groups showed comparable ranges of the neurovascular canal diameters. Statistically significant changes over time only occurred for the upper distance of the incisive canal in the total extraction group ($p=0.04$) and for the total bone length at the anterior region of the edentulous group. **Conclusions:** The study suggested that although there is a significant resorption of mandibular bone after tooth extraction, no significant changes occurred in neurovascular canals.

Introduction

Many studies have reported the consequences of tooth loss and associated residual ridge resorption (*Blahout et al 2007, Carlsson 2004; Jaul et al., 1980; Hirai et al., 1993; Klemetti, 1996; Tallgren 1972*). It is well accepted that mandibular bone undergoes resorption after tooth extraction as a result of the mandibular bone remodeling. In general, bone remodeling can be defined as a process where bone gradually alters its morphology in an attempt to adapt to any new external load (*Isidor 2006*). Already in 1892, Wolff formulates his theory based on a direct link between mechanical loading and bone adaptation (*Coelho et al 2009; Mullender et al 1995*). Wolff's law implies that resorption can take a place due to certain decrease in magnitude of mechanical load. On the other hand, bone deposition could be caused by a certain increase in mechanical load (*Dunlop et al 2009; Doblare et al 2002*). The post-extraction remodeling of the adult mandible has been widely addressed previously and recently as well (*Panchbhai 2013; Mahnama et al 2013; Canger and Celenk 2012; Chrcanovic et al 2011; Reich et al 2011 Unger et al 1992; Bras et al 1983; Atwood 1979; Mercier and Lafontant 1979; Enlow et al 1976; Pietrokovski et al 1976; Berg et al 1975; Carlsson et al 1969*).

Scientific endeavours have indeed confirmed that mechanical loads decrease extensively in completely edentulous patients and affect the morphology and material properties of their mandibular bone (*Schwartz –Dabney and Dechow (2002); Klemetti (1996)*). In fact, complete denture wearers present both lower masticatory efficiency and lower bite force than dentate subjects. The maximum bite force was reported to be only 20–40% of that of persons with a full natural dentition (*Trulsson et al 2012*). In the past, several studies were conducted to estimate resorption rate of jaw bones related to the dental status (*Carlsson and Pearson 1967, Atwood 1971, Tallgren 1972*). As such, the classical studies of Tallgren (1972) have quantitatively shown the mandibular, and maxillar, bone resorption in edentulous patients after 13.5- 25 years of complete dentures wear. The average reduction of 9-10mm and 2-3.5mm was reported for anterior mandible and anterior maxilla, respectively, during 25 years of wearing complete dentures (*Tallgren 1972*), with highest resorption rate being reported in the first year of edentulism (around 7mm).

According to previous studies, implant rehabilitation in edentulous patients results in a lower residual ridge resorption, mainly in cases that a fixed prosthesis or overdenture is supported by 4 implants (*de Jong et al 2010; von Wowern and Gottfredsen 2001; Jacobs et al 1992*). After implant treatment, the mandibular bone receives a new functional recruitment, unlike that existing in either natural dentition or complete edentulous status. Compared to patients with a conventional denture, the maximum bite force of patients with a mandibular denture supported by implants was found to be 60–200% higher (*Trulsson et al 2012*). By supporting a lower complete denture with implants, a beneficial effect on the preservation of the peri-implant bone has been observed (*de Jong et al 2010; Kordatzis et al 2003; Wright et al 2002; Jacobs et al 1992*). In turn, implant rehabilitation, unlike complete dentures, can sustain mandibular mechanical loads closer to the physiological thresholds needed to maintain the residual bone ridge. However, it is not known if rehabilitation with implants immediately after complete tooth extraction would reduce the high resorption rates reported in the first years of edentulism (*Tallgren 1972, Jacobs et al 1992*).

It is important to note that apart from the two cited remodeling scenarios (e.g. resorption and deposition), there are also two different types of phenomenological description of bone remodeling, known as “surface” and “internal” remodeling (*Lin et al, 2009*). Schwartz –Dabney and Dechow (2002) suggested that cortical microstructural changes accompany ridge resorption following edentulism. In an early study, those authors showed significant material property variation within human dentate mandibles, some of which were associated with function. They found that mandibular cortical bone in edentulous mandibles differed from that of dentate mandible in cortical thickness, elastic and shear moduli, anisotropy, and orientation of the axis of maximum stiffness (*Schwartz –Dabney and Dechow 2002*). Whereas the mandibular bone resorption results most likely from surface remodeling, the internal process of bone resorption might be responsible for morphological changes in the internal structures of the mandible. Therefore, it is likely that those morphological changes may affect the mandibular canal walls after total tooth extraction. However, there is no consensus about the relation of mandibular canal morphology and the dental status (*Jacobs et al 2007; Jacobs et al 2004; Jacobs et al 2002; Polland et al 2001; Xie et al 1997*).

Considering that the lack of mechanical stimulation results in surface and internal bone remodeling, we hypothesize that edentulism might be associated not only to changes in the mandibular bone morphology, but also to that in the mandibular canals. In addition, the influence of implants on bone resorption and mandibular canal changes was investigated up to 2 years after implant rehabilitation in the mandible and compared to that found in dentate mandibles.

Material and Methods

Patients

The study protocol was approved by the Ethical Committees of East Limburg Hospital (ZOL, Genk, Belgium) (protocol: 08/052L) and all patients gave their informed consent allowing their images to be included in the study. Sixty-two consecutive patients, edentulous or undergoing total tooth extraction, were preliminarily selected at the Maxillo-Facial department of ZOL. After 2 years, 24 out of 62 patients had a second CBCT taken due to treatment reasons and were finally included in the study. They were allocated in 3 groups, based on their treatment needs, as follow: Group *Total Extraction* consisted of patients who had a initial dentate mandible, however, due to periodontal and endodontic complications, a total tooth extraction was planned; Group *Edentulous* comprised images of patients who had edentulous mandible and were seeking implant rehabilitation; in Group *Dentate* was allocated patients who had a dentate mandible and multiple implants planned in the maxillae.

The Dentate group comprised of 12 patients, 7 completely dentate and 5 partially dentate (at least till second premolar at one side), Edentulous group consisted of 6 patients, from those, two patients have received 4 implants to support fixed prosthesis, two patients received 2 implants to support an overdenture and the others patients received 6 implants to support a fixed prosthesis. In the Total extraction group, 3 patients received 4 implants and 3 others received 6 implants to support a fixed prosthesis. The antagonist arch for the dentate group comprised fixed prosthesis supported by implants, and for the edentulous and total extraction group, natural dentition, complete dentures and implant-supported prostheses.

Image Acquisition

Our study analysed preoperative cone beam computed tomography (CBCT) datasets obtained with CBCT system GALILEOS[®] (Sirona Dental Systems, Bensheim, Germany). All patients gave their informed consent to use their CBCT data in the study. After 2 years, patients who had a second CBCT image taken from 6 months to 2 years after surgery were finally selected to comprise the total sample of images observed in the study.

Cone beam computed tomography (CBCT) images were taken prior to surgery, as part of the clinical treatment in order to obtain 3D information and perform treatment planning. For all patients, image acquisition parameters of the GALILEOS[®] CBCT unit were set to 85kv and 28mAs with a scan time of 14 seconds and 2.6 seconds of actual exposure time. The field-of-view (FOV) was 15cm in diameter and 12cm in height and the obtained voxel size was 0.29mm. According to literature, the effective dose of radiation generated by such protocol would be approximately 84 μ Sv corresponding to an average of 4 panoramic images (*Pauwels et al 2012*). Each CBCT dataset was exported as DICOM files using the software provided with the CBCT system (Sidexis, Sirona Dental Systems, Bensheim, Germany) for import and analysis in a customized software platform (developed by KU Leuven, Leuven, Belgium) for quantitative analysis (2D and 3D) of jaw bone over time.

Image Analysis

The goal was to establish a reproducible and precise protocol to measure the rates of horizontal and vertical changes in dimensions after tooth extraction and implant rehabilitation in the mandible. First, two CBCT scans were matched using a rigid registration algorithm (based on mutual information), allowing superimposing and switching views of those specific CBCT datasets. Once the two CBCT scans were registered, a para-axial plane (blue line) was defined through the maxillary arch and used to generate a panoramic overview with cross-sectional reconstructions (perpendicular to the para-axial plane) (figure 8.1). The software used allowed for adjustment of the viewing conditions in the baseline and follow-up images simultaneous, but independently at both images. The centre level (L) and band-width

(W) were individually determined for each pair of CBCT datasets, since scatter and artefacts, inherent of CBCT technology, caused intensity inhomogeneity and did not allow defining standard values for all images.

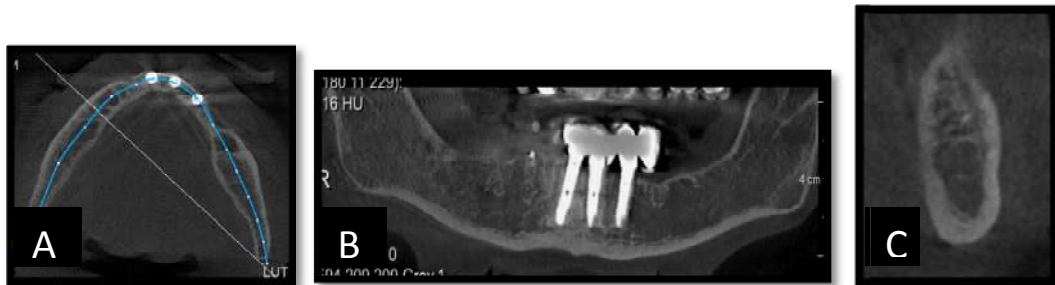


Figure 8.1: CBCT reconstruction views used in the image analysis. Blue line represents the reference line (A) for panoramic (B) and cross-sectional (C) 2D views.

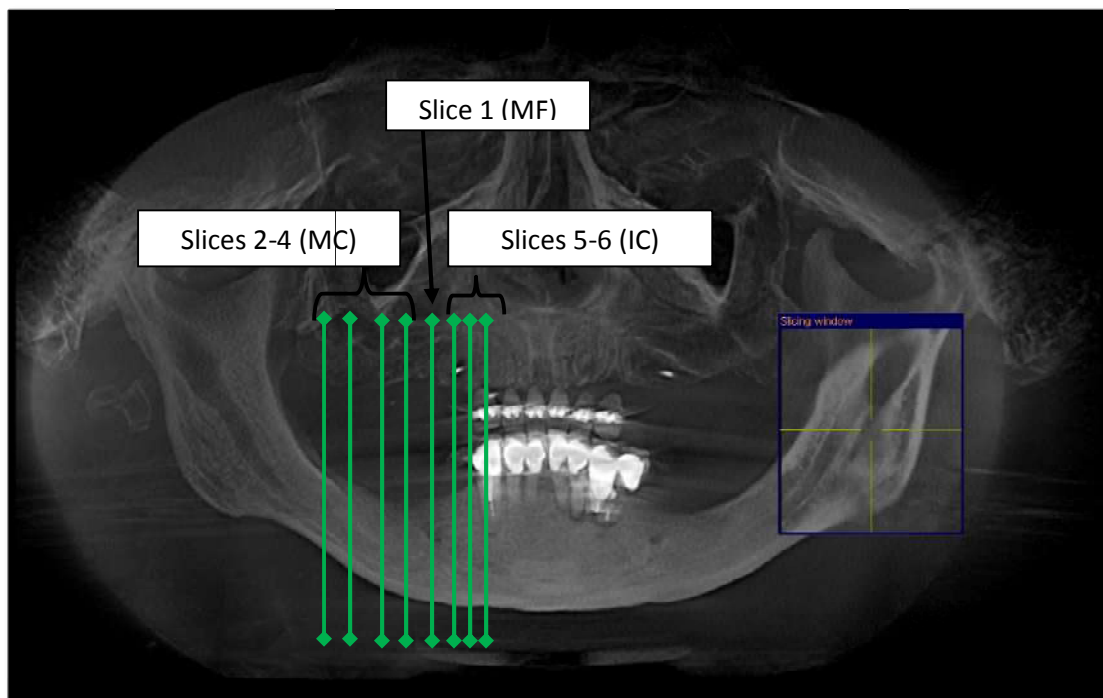


Figure 8.2: Oblique reconstruction of mandibular anterior region showing the location of the regions measured at cross-sectional slices, related to the mental foramen. Slice1 indicates region of measurements related to mental foramen (MF). Slices 2-4 and 5-6 were used for mandibular (MC) and incisive (IC) canal, respectively.

Table 8.1: Detailed description of measurements conducted in the mental foramen region, at 4 mandibular canal regions and 3 incisive canal regions.

Anatomical Structures	N	Measurements	Abbreviations
MF-mental foramen	1	diameter mental foramen (MF)	MF
	2	distance MF to upper ridge	MF dist sup
	3	distance MF to lower border	MF dist inf
	4	bone width above MF	width sup mf
	5	bone width below MF	width inf mf
	6	total bone length	total length
MC-mandibular canal	1	diameter vertical mandibular canal	MC length
	2	diameter horizontal mandibular canal	MC width
	3	distance to the superior border of the mandible	upper dist
	4	distance to the inferior border of the mandible	lower dist
	5	distance to the anterior region	vest dist
	6	distance to the posterior region	lingual dist
	7	total bone length	total bone length
	8	total bone width	total bone width
	9	thickness cortical bone upper ridge	cortical upper
	10	thickness cortical bone lower border	cortical lower
	11	thickness cortical bone vestibular above the canal	cortical vest above
	12	thickness cortical bone lingual above the canal	cortical ling above
	13	thickness cortical bone vestibular below the canal	cortical vest below
	14	thickness cortical bone lingual below the canal	cortical lingual below
IC-incisive canal	1	diameter vertical mandibular canal	MC length
	2	diameter horizontal mandibular canal	MC width
	3	distance to the superior border of the mandible	upper dist
	4	distance to the inferior border of the mandible	lower dist
	5	distance to the anterior region	vest dist
	6	distance to the posterior region	lingual dist
	7	total bone length	total bone length
	8	total bone width	total bone width
	9	thickness cortical bone upper ridge	cortical upper
	10	thickness cortical bone lower border	cortical lower
	11	thickness cortical bone vestibular above the canal	cortical vest above
	12	thickness cortical bone lingual above the canal	cortical ling above
	13	thickness cortical bone vestibular below the canal	cortical vest below
	14	thickness cortical bone lingual below the canal	cortical lingual below

The measurements of vertical and horizontal diameters and distances to upper ridge and lower border of the mandible were carried at 2 mandibular neurovascular canals, e.g. mandibular canal and incisive canal, and at the mental foramen, besides the measurements of mandibular length and width, all of them at the reconstructed cross-sectional images. At baseline (pre) and follow-up (post) images, 4 cross-sectional slices at 5mm, 10mm, 15mm and 20mm posterior to the mental foramen (MF) were observed for the mandibular canal and 3 slices at 2mm; 4mm and 6mm anterior to MF, for the incisive canal. The detailed description of measurements done is found in table 8.1 and figures 8.2-8.5. Fifteen percent of measurements were repeated 3 months after the first measurements to test the intraobserver reliability.

The following questions were formulated in our study:

1. Do mandibular neurovascular canals undergo changes after total tooth extraction?
2. Are dimensional changes in the mandibular neurovascular canals correlated to mandibular dimensional changes?
3. Do those changes influence the spatial positioning of mandibular canals related to mandibular borders?
4. Are those changes related to change in the mandibular cortical thickness?
5. Are mandibular changes depicted by CBCT images similar to those reported in the literature?

Statistic analysis

All data were collected and statistically analyzed using JMP 8 (SAS Institute Inc., SAS Campus Drive, Cary, North Carolina 27513, USA) for Windows Software Version 7, choosing a 5% level of significance. Across Groups analysis corresponded to a repeated measures analysis where two F-tests determine whether the across-groups values were different: Mean Difference tests if the change across the pair of responses is different in among groups and Mean- Mean tests if the average response for a subject is different in different groups. When mean-difference tests showed significant results, paired t-test was used to compare differences between

baseline (pre) and follow-up (post) measurements. One way Anova and Tukey-Kramer HSD (honestly significant difference) were used to determine which groups were different between each other. Least square regression analysis was conducted to check for any association between mandibular bone and neurovascular canals dimensions. The intraclass correlation was computed as a measure of agreement between the first and second measurements done by the same observer.

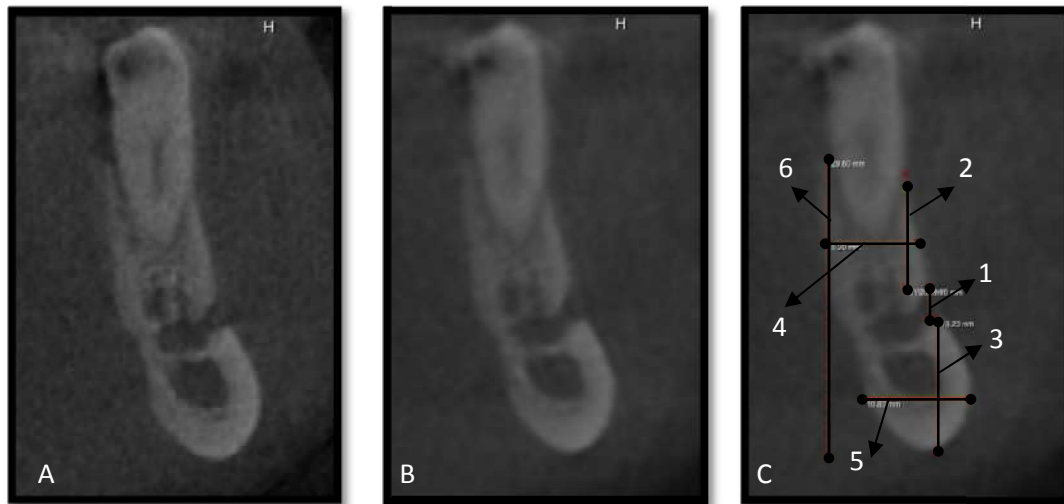


Figure 8.3: Cross-sectional slices pre (A) and post (B) in the mental foramen region of Group Dentate. (C) shows the measurements done at this region. The numbers here are correspondent to those in table 8.1.

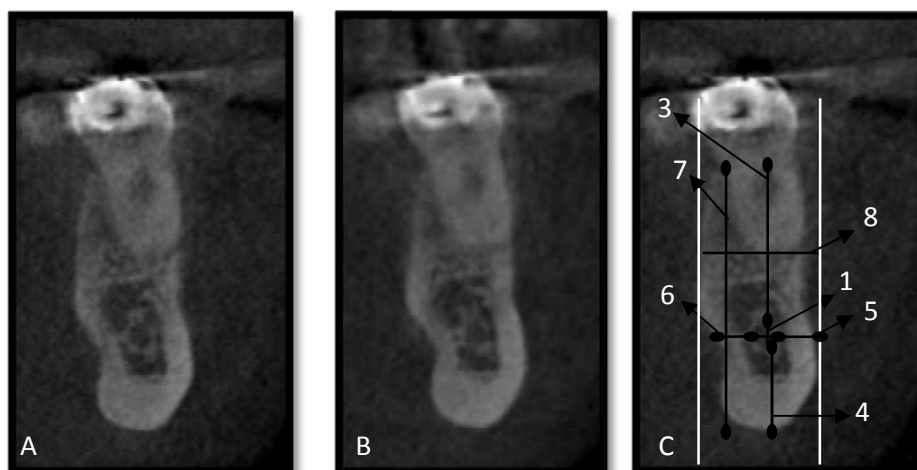


Figure 8.4: legend page 222.

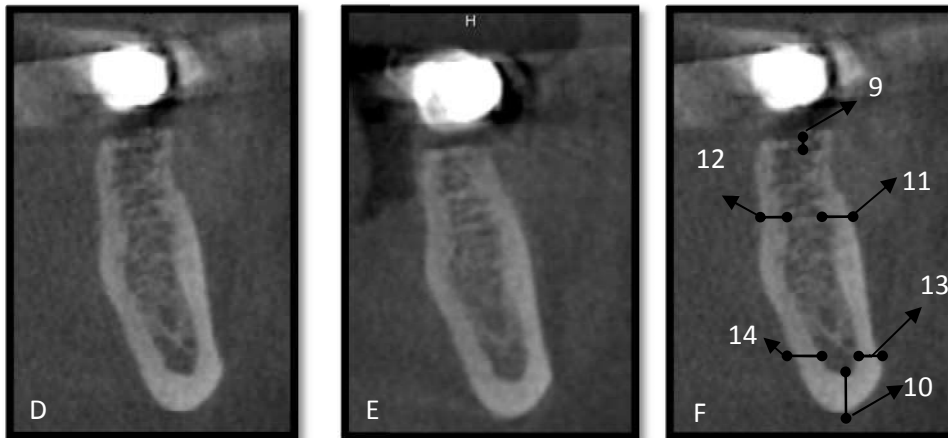


Figure 8.4: Cross-sectional slices from the mandibular canal of Group Dentate from pre (A) and post (B) CBCT datasets. (C) show measurements number 1 to 8. (D) and (E) show pre and post slices for measurement at the mandibular canal of Edentulous group and the measurements 9 to 13 are shown in (F).The numbers here are correspondent to those at table 1. White lines were used to measure the total bone width.

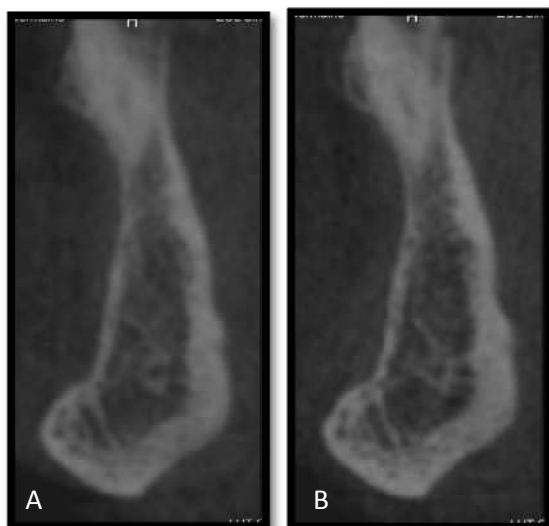
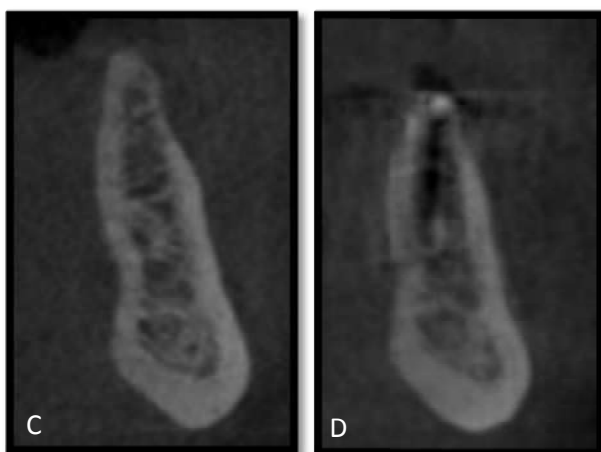


Figure 8.5: Cross-sectional slices from the incisive canal of Group Dentate from pre (A) and post (B) CBCT datasets. (C) and (D) show pre and post slices for measurement at the incisive canal of Edentulous group.



Results

Our results showed that most of anatomical structures presented only slightly dimensional changes after the follow-up period of this study. The measurement pre and post and the mean dimensional changes in the mandibular and incisive canal by region measured are shown in tables 8.2 and 8.3. No statistical significant difference was found over the follow-up time within the groups. Considering that material properties are variable along the mandible, the results were reported by slice measured representing different positions at posterior and anterior regions. A high ICC coefficient (0.89) was found after repeating 15% of measurements.

Table 8.2: Mean pre and post measurements of mandibular canal length and width in each group by mandibular region (5mm/10mm/15mm/20mm). Diff = mean dimensional changes in the mandibular canal over the time by group and mandibular region. Mean diff = overall mean difference in each group. sd= standard deviation.

		Mandibular region												Mean diff
		5MM			10MM			15MM			20MM			
		PRE	POS	diff	PRE	POS	diff	PRE	POS	diff	PRE	POS	diff	
MC length	DENTATE	3,4	3,2	-0,3	3,5	3,3	-0,2	3,1	3,1	0,0	4,0	3,5	-0,4	-0,2
	sd	0,8	0,9	0,5	0,9	0,7	0,6	0,6	0,8	0,5	1,2	0,8	0,9	0,6
	EDENTATE	3,1	2,8	-0,4	2,9	2,8	-0,1	2,8	2,8	0,1	3,1	3,4	0,3	0,0
	sd	1,3	1,2	0,4	0,4	0,5	0,2	0,7	0,6	0,2	0,7	0,4	0,3	0,3
	TOTAL EXTRACTION	3,2	3,0	-0,2	3,1	2,8	-0,3	3,6	2,8	-0,8	2,8	2,6	-0,2	-0,4
	sd	0,7	0,9	0,7	0,8	0,6	0,5	1,1	1,2	0,9	0,5	0,4	0,3	0,6
MC width	DENTATE	2,8	2,9	0,0	2,7	2,7	0,0	2,8	2,8	0,0	3,0	2,9	-0,1	0,0
	sd	1,1	1,1	0,3	0,7	0,7	0,2	0,8	0,8	0,2	0,7	0,8	0,4	0,3
	EDENTATE	2,7	2,7	-0,1	2,4	2,3	0,0	2,5	2,3	-0,2	3,2	2,7	-0,5	-0,2
	sd	0,9	0,9	0,1	0,3	0,3	0,4	0,3	0,4	0,5	0,8	1,0	0,9	0,5
	TOTAL EXTRACTION	3,0	2,9	-0,1	2,5	2,6	0,0	2,6	2,4	-0,3	2,7	2,6	-0,1	-0,1
	sd	3,3	2,8	0,7	5,2	4,6	0,8	3,7	3,0	0,9	1,9	1,2	0,8	0,8

Table 8.3: Mean pre and post measurements of incisive canal length and width in each group by mandibular region (5mm/10mm/15mm/20mm). Diff = mean dimensional changes in the incisive canal over the time by group and mandibular region. Mean diff = overall mean difference in each group. sd= standard deviation.

		Mandibular region									
		2MM			4MM			6MM			Mean diff
		PRE	POS	diff	PRE	POS	diff	PRE	POS	diff	-
IC length	DENTATE	2,9	2,6	-0,2	2,6	2,3	-0,3	2,7	2,5	-0,2	-0,2
	sd	1,0	1,1	0,4	0,9	0,8	0,4	1,0	1,0	0,5	0,4
	EDENTATE	2,5	2,0	-0,5	1,8	1,5	-0,4	2,0	1,9	0,0	-0,3
	sd	0,6	0,7	0,5	0,6	0,7	0,3	0,7	0,8	0,1	0,3
	TOTAL EXTRACTION	1,8	1,6	-0,2	2,0	1,9	-0,1	1,7	1,5	-0,2	-0,2
	sd	0,6	0,5	0,3	0,8	1,0	0,5	0,4	0,5	0,2	0,3
IC width	DENTATE	2,4	2,3	-0,1	1,9	1,9	0,0	2,3	2,1	-0,2	-0,1
	sd	0,8	0,9	0,2	0,5	0,5	0,3	0,6	0,5	0,5	0,3
	EDENTATE	2,1	1,9	-0,2	1,9	1,6	-0,3	1,3	1,3	0,0	-0,2
	sd	0,5	0,5	0,2	0,6	0,6	0,4	0,5	0,5	0,0	0,2
	TOTAL EXTRACTION	1,7	1,4	-0,4	2,0	1,7	-0,3	1,7	1,6	-0,1	-0,3
	sd	5,5	5,6	0,2	5,5	4,1	1,5	0,2	0,3	0,3	0,7

The observation time was in average 12 months in the dentate group, 16 months for the edentate group and 19 months for the total extraction group. The highest differences were found in the total extraction and edentulous groups and for the upper distance of neurovascular canals (tables 8.6 and 8.7) and total bone length anterior and posterior regions (tables 8.4 and 8.5). However, statistically significant results were only found for the total bone length at the anterior region of the edentulous group ($p=0.04$) (table 8.5) and the differences in the upper distance of the incisive canal in the total extraction group ($p=0.04$) (table 8.7). Table 8.4 and 8.5 show the results for the mandibular bone dimensional changes at anterior and posterior regions. The differences in the positioning of the neurovascular canals related to the mandibular borders are shown in tables 8.6 and 8.7.

Table 8.4: Mean pre and post measurements of total bone length and width at posterior mandible in each group by mandibular region (5mm/10mm/15mm/20mm). Diff = mean dimensional changes over the time by group and mandibular region. Mean diff = overall mean difference in each group. sd= standard deviation.

		Mandibular region												Mean diff
		5MM			10MM			15MM			20MM			
		PRE	POS	diff	PRE	POS	diff	PRE	POS	diff	PRE	POS	diff	
total bone length	DENTATE	28,9	28,9	0,0	28,1	28,1	0,0	26,9	26,5	-0,4	26,4	26,2	-0,2	-0,2
	sd	3,6	3,6	0,1	4,2	4,1	0,3	2,6	2,9	1,5	3,0	3,1	0,8	0,7
	EDENTATE	21,2	20,4	-0,8	20,1	19,0	-1,1	18,2	18,0	-0,3	19,3	18,7	-0,6	-0,7
	sd	7,2	7,1	1,4	7,0	6,8	1,4	7,2	7,2	0,6	7,3	7,4	0,6	1,0
	TOTAL EXTRACTION	23,0	22,5	-0,5	21,8	21,1	-0,7	21,0	21,2	0,2	21,8	21,8	0,0	-0,3
	sd	5,2	4,8	1,5	5,2	4,7	1,4	4,4	4,3	0,6	4,6	4,6	0,3	1,0
total bone width	DENTATE	12,1	12,0	-0,1	13,0	13,0	0,0	14,2	14,2	0,0	16,0	16,0	0,0	0,0
	sd	2,0	2,0	0,3	2,0	2,0	0,3	1,9	2,0	0,3	1,9	2,1	0,2	0,3
	EDENTATE	11,6	11,6	0,0	12,7	12,6	-0,1	13,6	13,3	-0,3	14,6	14,6	-0,1	-0,1
	sd	3,0	3,0	0,2	3,3	3,3	0,3	3,6	3,5	0,5	4,0	3,9	0,3	0,3
	TOTAL EXTRACTION	11,5	11,1	-0,3	12,7	12,5	-0,2	13,9	13,9	0,0	14,8	14,7	-0,1	-0,2
	sd	3,9	3,8	0,4	4,2	3,8	0,6	4,2	4,2	0,4	4,8	4,6	0,2	0,4

Table 8.5: Mean pre and post measurements of total bone length and width at anterior mandible in each group by mandibular region (5mm/10mm/15mm/20mm). Diff = mean dimensional changes over the time by group and mandibular region. Mean diff = overall mean difference in each group. sd= standard deviation.

		Mandibular region										Mean diff
		2MM			4MM			6MM				
		PRE	POS	diff	PRE	POS	diff	PRE	POS	diff		
total bone length	DENTATE	30,4	30,4	0,0	31,1	31,0	-0,1	31,8	31,7	0,0	0,0	
	sd	3,49	3,52	0,40	3,26	3,13	0,22	2,93	2,96	0,21	0,3	
	EDENTATE	21,8	20,6	-1,2	22,1	21,7	-0,5	22,7	21,8	-0,9	-0,9	
	sd	7,5	7,6	1,1	7,8	7,9	0,5	8,2	8,3	1,0	0,9	
	TOTAL EXTRACTION	24,9	23,5	-1,3	25,9	23,1	-2,8	26,6	24,0	-2,6	-2,23	
	sd	5,9	5,6	1,7	6,1	5,7	2,3	6,0	5,7	2,0	2,0	
total bone width	DENTATE	11,2	11,3	0,1	11,5	11,5	0,0	11,9	11,9	0,0	0,0	
	sd	2,11	2,14	0,22	1,74	1,86	0,35	1,76	1,82	0,25	0,3	
	EDENTATE	11,5	11,5	0,1	11,5	11,6	0,1	12,0	11,9	-0,1	0,0	
	sd	3,1	3,1	0,3	3,1	3,1	0,3	3,3	3,3	0,2	0,9	
	TOTAL EXTRACTION	11,7	11,8	0,1	12,0	12,0	0,1	12,3	12,3	0,0	0,0	
	sd	3,8	3,5	0,4	3,8	3,8	0,1	2,9	2,9	0,1	2,0	

Table 8.6: Mean pre and post measurements of mandibular canal distance to the mandibular borders in each group by mandibular region (5mm/10mm/15mm/20mm). Diff = mean dimensional changes over the time by group and mandibular region. Mean diff = overall mean difference in each group. Vest=vestibular; dist= distance. sd= standard deviation.

		Mandibular region												Mean diff
		5MM			10MM			15MM			20MM			
		PRE	POS	diff	PRE	POS	diff	PRE	POS	diff	PRE	POS	diff	
upper dist	DENTATE	16,8	17,1	0,3	16,9	16,8	0,0	14,9	14,4	-0,6	13,1	12,5	-0,6	-0,2
	sd	2,7	2,7	0,6	2,7	2,8	0,3	2,6	2,5	1,4	3,3	3,1	1,3	0,9
	EDENTATE	8,2	7,7	-0,5	6,8	6,0	-0,7	6,3	6,1	-0,2	5,7	5,4	-0,3	-0,5
	sd	5,2	5,3	1,4	5,7	5,7	1,3	5,0	4,8	0,7	4,5	4,7	0,8	1,0
	TOTAL EXTRACTION	10,2	9,8	-0,4	8,6	8,5	-0,1	9,3	9,7	0,5	9,0	8,9	-0,1	0,0
	sd	3,0	2,7	1,7	3,0	2,4	1,4	3,2	3,2	0,8	2,8	2,8	0,4	1,1
lower dist	DENTATE	8,5	8,5	0,0	7,7	7,9	0,2	7,3	7,4	0,2	6,8	6,9	0,1	0,1
	sd	1,2	1,2	0,4	1,4	1,6	0,4	1,1	1,2	0,4	1,1	1,3	0,7	0,5
	EDENTATE	9,1	9,3	0,2	8,4	8,5	0,1	8,0	8,1	0,1	8,0	8,0	0,0	0,1
	sd	2,3	2,4	0,3	2,1	2,1	0,3	2,0	2,1	0,4	2,0	1,9	0,3	0,3
	TOTAL EXTRACTION	7,8	7,9	0,1	7,1	7,3	0,2	6,3	6,6	0,3	6,4	6,5	0,1	0,2
	sd	2,0	2,1	0,4	2,0	2,2	0,4	2,2	2,2	0,3	1,9	1,9	0,3	0,3
vest dist	DENTATE	3,5	3,7	0,2	4,8	4,7	-0,1	5,2	5,3	0,1	5,4	5,6	0,2	0,1
	sd	0,6	0,6	0,5	0,9	1,0	0,2	1,0	1,1	0,3	1,0	0,8	0,2	0,3
	EDENTATE	4,4	4,5	0,1	5,2	5,3	0,1	5,1	5,4	0,4	5,6	5,6	0,0	0,1
	sd	1,2	1,2	0,2	1,3	1,4	0,1	1,3	1,4	0,5	1,3	1,4	0,3	0,3
	TOTAL EXTRACTION	3,9	3,9	0,0	4,1	4,1	0,0	4,3	4,4	0,1	4,6	4,9	0,2	0,1
	sd	1,4	1,5	0,3	1,5	1,6	0,3	1,3	1,4	0,5	1,2	1,0	0,4	0,4
lingual dist	DENTATE	4,4	4,2	-0,2	3,0	3,2	0,1	2,6	2,6	0,0	2,4	2,5	0,1	0,0
	sd	1,5	1,6	0,3	1,0	1,0	0,3	0,9	0,7	0,5	0,9	0,8	0,4	0,4
	EDENTATE	3,9	3,8	-0,1	3,5	3,5	0,0	4,2	3,9	-0,3	3,6	4,0	0,3	0,0
	sd	1,5	1,6	0,3	1,1	1,1	0,2	1,3	1,2	0,4	1,2	1,4	0,6	0,4
	TOTAL EXTRACTION	2,9	2,3	-0,6	2,7	3,0	0,3	2,3	2,5	0,2	2,0	2,2	0,2	0,0
	sd	6,8	6,4	0,7	7,2	6,7	0,6	6,9	6,4	0,7	6,4	6,1	0,4	0,6

Table 8.7: Mean pre and post measurements of incisive canal distance to the mandibular borders in each group by mandibular region (5mm/10mm/15mm/20mm). Diff = mean dimensional changes over the time by group and mandibular region. Mean diff = overall mean difference in each group. Dist= distance. sd= standard deviation.

		Mandibular region									
		2MM			4MM			6MM			Mean diff
		PRE	POS	diff	PRE	POS	diff	PRE	POS	diff	-
upper dist	DENTATE	16,9	16,9	0,0	18,3	18,5	0,2	20,1	20,2	0,1	0,1
	sd	2,7	2,8	0,2	2,0	2,1	0,4	2,5	2,7	0,2	0,3
	EDENTATE	7,9	8,0	0,1	9,2	8,8	-0,5	10,9	10,3	-0,6	-0,2
	sd	5,7	5,6	1,2	6,3	6,5	0,5	6,3	6,5	0,7	0,8
	TOTAL EXTRACTION	12,7	10,8	-1,9	13,9	12,2	-1,8	16,0	14,8	-1,2	-1,2
	sd	4,4	3,8	2,2	4,0	3,3	1,9	4,4	3,9	1,5	1,9
lower dist	DENTATE	10,1	10,4	0,3	9,5	9,8	0,3	8,7	8,7	0,0	0,2
	sd	1,4	1,3	0,5	1,9	2,2	0,5	1,9	1,8	0,3	0,4
	EDENTATE	10,9	10,8	0,0	10,5	10,8	0,3	9,1	9,2	0,2	0,1
	sd	2,7	2,6	0,8	2,8	2,9	0,4	2,5	2,5	0,2	0,4
	TOTAL EXTRACTION	8,2	8,2	0,0	7,6	7,8	0,2	8,3	8,3	0,0	0,1
	sd	2,9	2,9	0,7	2,9	3,0	0,3	2,0	2,0	0,1	0,4
vest dist	DENTATE	2,9	2,8	0,0	3,5	3,7	0,2	3,9	4,2	0,3	0,1
	sd	1,0	1,0	0,3	1,2	1,2	0,2	1,0	1,0	0,6	0,4
	EDENTATE	3,2	3,1	0,0	3,4	3,6	0,2	3,4	3,5	0,1	0,1
	sd	1,2	1,2	0,1	1,3	1,3	0,3	1,2	1,2	0,2	0,2
	TOTAL EXTRACTION	3,5	3,8	0,3	3,9	3,8	-0,1	4,9	5,0	0,1	0,1
	sd	1,2	1,3	0,4	1,2	1,2	0,4	1,6	1,7	0,1	0,3
lingual dist	DENTATE	4,8	5,1	0,2	4,6	4,7	0,2	4,1	4,3	0,2	0,2
	sd	1,7	1,6	0,5	2,1	2,0	0,4	1,7	1,7	0,3	0,4
	EDENTATE	5,2	5,4	0,2	4,9	5,3	0,5	6,1	6,2	0,1	0,2
	sd	1,3	1,4	0,3	1,5	1,7	0,6	1,8	1,9	0,2	0,4
	TOTAL EXTRACTION	4,4	4,5	0,1	3,9	4,5	0,7	3,2	3,5	0,3	0,3
	sd	6,9	6,8	0,3	7,4	6,1	1,5	2,2	2,1	0,3	0,7

Least square regression analysis showed significant association between total bone length and neurovascular canal diameter (length), for both incisive and mandibular canals. Least square regression equation produced the best, or most accurate predictions for neurovascular length given the total mandibular length. This regression equation (or line of best fit) is depicted graphically in figures 8.6-8.7.

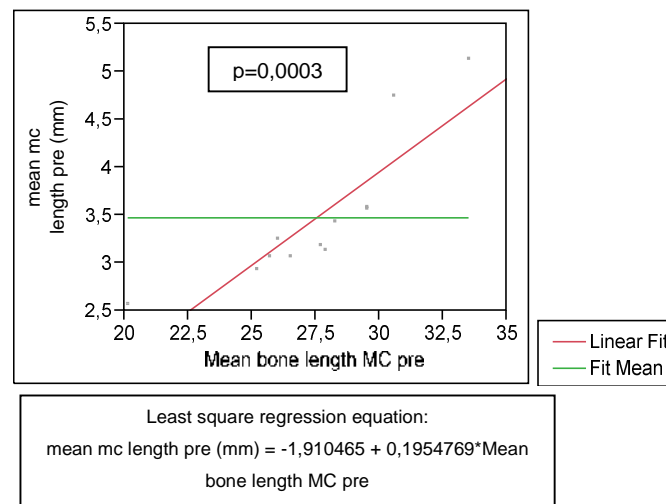


Figure 8.6: The regression line fitted to the scatter plot of values of mandibular canals (mc) and bone length in all dentate mandibles.

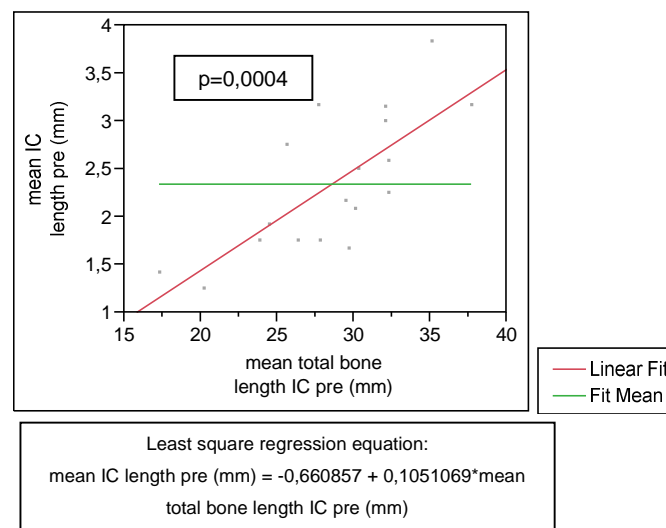


Figure 8.7: The regression line fitted to the scatter plot of values of incisive canals (IC) and bone length in all dentate mandibles.

Besides, small not statistically significant differences were observed in cortical thickness over the time. Those results are shown in table 8.8 for posterior regions and table 8.9 for anterior region.

Table 8.8: Mean pre and post measurements of cortical thickness at posterior region in each group by mandibular region (5mm/10mm/15mm/20mm). Diff = mean dimensional changes over the time by group and mandibular region. Mean diff = overall mean difference in each group. sd= standard deviation.

		Mandibular region												Mean diff
		5MM			10MM			15MM			20MM			
		PRE	POS	diff	PRE	POS	diff	PRE	POS	diff	PRE	POS	diff	
cortical upper	DENTATE	1,1	1,5	0,4	1,9	2,0	0,1	1,5	1,7	0,2	1,2	1,4	0,1	0,2
	sd	1,3	1,7	0,9	3,8	3,8	0,2	1,2	1,6	0,4	1,9	1,8	0,7	0,6
	EDENTATE	2,4	2,1	-0,3	2,7	2,2	-0,5	2,1	2,1	0,0	2,3	2,2	0,0	-0,2
	sd	1,5	1,3	0,6	1,5	1,2	0,6	1,2	1,5	0,5	1,3	1,3	0,6	0,6
	TOTAL EXTRACTION	2,2	2,2	0,0	1,9	1,9	0,0	3,3	3,2	-0,1	2,2	2,2	0,0	0,0
sd	1,0	0,5	0,9	1,3	0,9	0,8	1,8	1,7	0,4	1,2	1,2	0,3	0,6	
cortical lower	DENTATE	4,4	4,5	0,0	4,8	4,8	0,0	4,6	4,8	0,2	4,5	4,5	0,0	0,0
	sd	0,8	0,8	0,3	0,9	0,8	0,3	0,9	1,0	0,2	0,9	0,8	0,2	0,3
	EDENTATE	4,4	4,4	0,0	3,9	4,2	0,4	4,2	4,5	0,3	4,5	4,6	0,1	0,2
	sd	1,1	1,1	0,2	0,9	1,0	0,5	1,1	1,2	0,3	1,1	1,1	0,2	0,3
	TOTAL EXTRACTION	3,6	3,7	0,2	3,3	3,5	0,3	3,6	3,6	0,0	3,4	3,4	0,0	0,1
sd	1,0	1,0	0,2	0,9	1,0	0,5	0,9	0,9	0,2	0,9	1,0	0,1	0,3	
cortical vest above	DENTATE	2,7	2,8	0,1	3,1	3,4	0,3	3,3	3,5	0,1	3,7	3,7	0,0	0,2
	sd	0,7	0,8	0,3	1,4	1,4	0,7	0,4	0,5	0,3	0,7	0,7	0,2	0,3
	EDENTATE	2,7	2,8	0,2	2,5	2,9	0,4	3,5	3,5	0,0	3,8	3,7	0,0	0,2
	sd	0,6	0,8	0,3	0,7	0,6	0,5	1,0	1,0	0,3	1,1	1,0	0,3	0,3
	TOTAL EXTRACTION	2,4	2,8	0,4	2,8	3,0	0,2	3,4	3,4	-0,1	3,0	3,5	0,5	0,3
sd	0,7	0,8	0,3	0,8	0,9	0,5	0,9	1,1	0,4	0,7	0,9	0,5	0,3	
cortical lingual above	DENTATE	2,7	2,9	0,2	2,7	2,9	0,3	3,0	3,0	0,1	3,0	3,3	0,3	0,2
	sd	0,5	0,5	0,3	0,7	0,8	0,4	0,6	0,7	0,2	0,6	0,6	0,5	0,4
	EDENTATE	2,6	2,8	0,2	3,3	3,2	-0,1	3,0	2,8	-0,3	2,5	2,6	0,1	0,0
	sd	0,9	1,0	0,3	1,0	0,9	0,4	0,9	0,8	0,4	0,8	0,9	0,5	0,4
	TOTAL EXTRACTION	2,8	3,0	0,2	2,8	3,2	0,4	2,9	3,0	0,1	2,6	3,1	0,5	0,3
sd	0,7	0,7	0,3	0,7	0,8	0,4	1,0	0,9	0,5	0,8	1,0	0,5	0,4	
cort vest below	DENTATE	3,2	3,5	0,4	3,5	3,6	0,1	3,3	3,5	0,2	3,4	3,5	0,1	0,2
	sd	0,5	0,5	0,4	0,4	0,4	0,2	0,5	0,4	0,2	0,5	0,6	0,2	0,3
	EDENTATE	2,8	2,9	0,1	2,8	2,9	0,1	3,2	3,2	0,0	3,1	3,0	-0,1	0,0
	sd	0,8	0,8	0,2	0,9	1,0	0,1	1,1	1,2	0,2	1,0	1,1	0,3	0,2
	TOTAL EXTRACTION	2,9	3,1	0,2	3,0	3,1	0,1	2,9	3,0	0,1	3,0	3,0	0,0	0,1
sd	0,7	0,9	0,4	0,7	0,7	0,2	0,6	0,7	0,2	0,7	0,7	0,2	0,2	
cort lingual below	DENTATE	3,3	3,4	0,1	3,2	3,3	0,1	3,0	3,1	0,0	3,0	3,2	0,2	0,1
	sd	0,5	0,7	0,3	0,3	0,4	0,3	0,8	0,8	0,1	0,3	0,5	0,4	0,3
	EDENTATE	3,1	3,2	0,1	3,0	2,9	-0,1	2,6	2,6	0,0	2,9	2,7	-0,2	0,0
	sd	1,0	1,0	0,2	1,0	1,0	0,2	0,7	0,7	0,1	0,8	0,8	0,4	0,2
	TOTAL EXTRACTION	3,4	3,4	0,0	2,9	2,7	-0,2	2,5	2,7	0,2	2,3	2,4	0,0	0,0
sd	1,1	1,0	0,2	0,8	0,9	0,3	0,7	0,8	0,3	0,7	0,8	0,4	0,3	

Table 8.9: Mean pre and post measurements of cortical thickness at anterior region in each group by mandibular region (5mm/10mm/15mm/20mm). Diff = mean dimensional changes over the time by group and mandibular region. Mean diff = overall mean difference in each group. Cort=cortical; vest=vestibular. sd= standard deviation.

		Mandibular region									
		2MM			4MM			6MM			Mean diff
		PRE	POS	diff	PRE	POS	diff	PRE	POS	diff	-
cortical upper	DENTATE	1,3	1,3	0,1	1,0	1,1	0,1	0,7	0,8	0,1	0,1
	sd	1,6	1,6	0,3	1,5	1,5	0,3	0,6	0,7	0,3	0,3
	EDENTATE	2,5	2,2	-0,3	1,8	1,9	0,1	1,6	1,4	-0,2	-0,1
	sd	1,8	1,7	0,4	0,7	0,8	0,7	0,7	0,9	0,7	0,6
	TOTAL EXTRACTION	3,7	2,8	-0,9	2,9	2,3	-0,6	3,0	3,8	0,8	-0,2
	sd	1,8	1,7	1,1	1,0	1,1	1,3	2,2	3,0	1,4	1,3
cortical lower	DENTATE	4,6	4,8	0,2	5,0	5,0	0,0	4,9	5,0	0,0	0,1
	sd	0,8	0,9	0,3	0,8	0,8	0,1	1,2	1,2	0,1	0,2
	EDENTATE	3,8	4,2	0,3	4,2	4,5	0,3	4,0	4,2	0,1	0,2
	sd	1,5	1,5	0,2	1,3	1,3	0,2	1,0	1,0	0,2	0,2
	TOTAL EXTRACTION	3,4	3,7	0,3	3,4	3,4	0,0	4,1	4,1	0,0	0,1
	sd	1,3	1,4	0,2	1,2	1,4	0,3	1,1	1,1	0,2	0,2
cortical vest above	DENTATE	2,4	2,7	0,3	2,6	2,7	0,1	2,3	2,3	0,0	0,1
	sd	0,5	0,6	0,2	0,6	0,8	0,3	0,6	0,5	0,2	0,2
	EDENTATE	2,6	2,7	0,1	3,0	3,2	0,2	2,4	2,5	0,1	0,1
	sd	1,0	0,9	0,8	0,8	0,8	0,1	0,7	0,7	0,1	0,4
	TOTAL EXTRACTION	2,4	2,5	0,1	2,2	2,7	0,5	2,1	2,0	-0,1	0,1
	sd	0,9	0,8	0,6	0,6	0,7	0,3	0,6	0,6	0,4	0,4
cortical lingual above	DENTATE	2,9	2,9	0,0	2,7	2,8	0,1	2,7	2,9	0,2	0,1
	sd	0,5	0,7	0,3	0,6	0,6	0,3	0,6	0,7	0,3	0,3
	EDENTATE	2,1	2,3	0,2	2,1	2,3	0,2	2,3	2,3	0,0	0,1
	sd	1,0	1,1	0,4	0,8	0,7	0,4	0,8	0,8	0,2	0,3
	TOTAL EXTRACTION	2,4	2,6	0,2	2,5	2,6	0,1	2,2	2,3	0,1	0,1
	sd	0,6	0,6	0,3	0,7	0,6	0,5	0,7	0,9	0,6	0,5
cort vest below	DENTATE	3,0	3,3	0,2	3,2	3,3	0,1	3,1	3,2	0,2	0,1
	sd	0,5	0,6	0,3	0,4	0,4	0,1	0,4	0,5	0,2	0,2
	EDENTATE	2,2	2,3	0,1	2,5	2,7	0,2	2,5	2,6	0,1	0,1
	sd	0,8	0,8	0,2	0,8	0,8	0,2	0,7	0,7	0,2	0,2
	TOTAL EXTRACTION	2,9	3,1	0,2	3,2	3,3	0,1	3,0	3,1	0,1	0,1
	sd	0,9	0,9	0,2	0,9	1,0	0,3	0,9	1,0	0,2	0,2
cort lingual below	DENTATE	3,1	3,7	0,5	3,6	3,6	0,0	4,0	4,0	0,0	0,1
	sd	0,4	0,7	0,7	0,7	0,8	0,3	0,8	0,7	0,4	0,5
	EDENTATE	2,9	2,9	0,0	3,0	3,2	0,1	3,5	3,6	0,1	0,1
	sd	1,3	1,4	0,6	1,3	1,3	0,3	1,2	1,3	0,4	0,4
	TOTAL EXTRACTION	2,6	2,7	0,0	3,0	3,1	0,2	3,1	3,1	0,0	0,1
	sd	1,0	1,1	0,2	0,7	0,9	0,3	0,9	0,9	0,2	0,2

Table 8.10 shows the results of mental foramen dimensions and the distance between mandibular and canal borders at the mental foramen region. No statistical

significant differences were found within the follow-up time. The distance from the lower border were maintained over the time (figure 8.8) and total bone length reduction was correspondent to the decrease in the distance between the mental foramen and the upper border of the mandible (figure 8.9).

Table 8.10: Mean pre and post measurements of mental foramen (mf) and the distance from mf foramen borders to the upper (mf dist sup) and lower (mf dist inf) mandibular border. Diff = mean dimensional changes over the time by group. Dist= distance. sd= standard deviation.

Group	mf pre	mf post	diff	mf dist sup pre	mf dist sup post	diff	mf dist inf pre	mf dist inf post	Mean diff
dentate	3,7	3,7	0,0	13,0	13,0	0,0	13,1	13,1	0,1
sd	0,9	1,0	0,3	3,2	3,2	0,9	1,2	1,1	0,2
edentulous	2,7	2,6	-0,2	5,4	5,0	-0,4	12,8	12,8	-0,1
sd	0,9	0,9	0,2	4,9	4,8	0,9	3,4	3,4	0,2
total extraction	2,7	2,5	-0,2	7,1	5,8	-1,3	14,4	14,3	0,0
sd	0,7	0,7	0,3	2,7	2,8	1,3	3,1	3,1	0,3

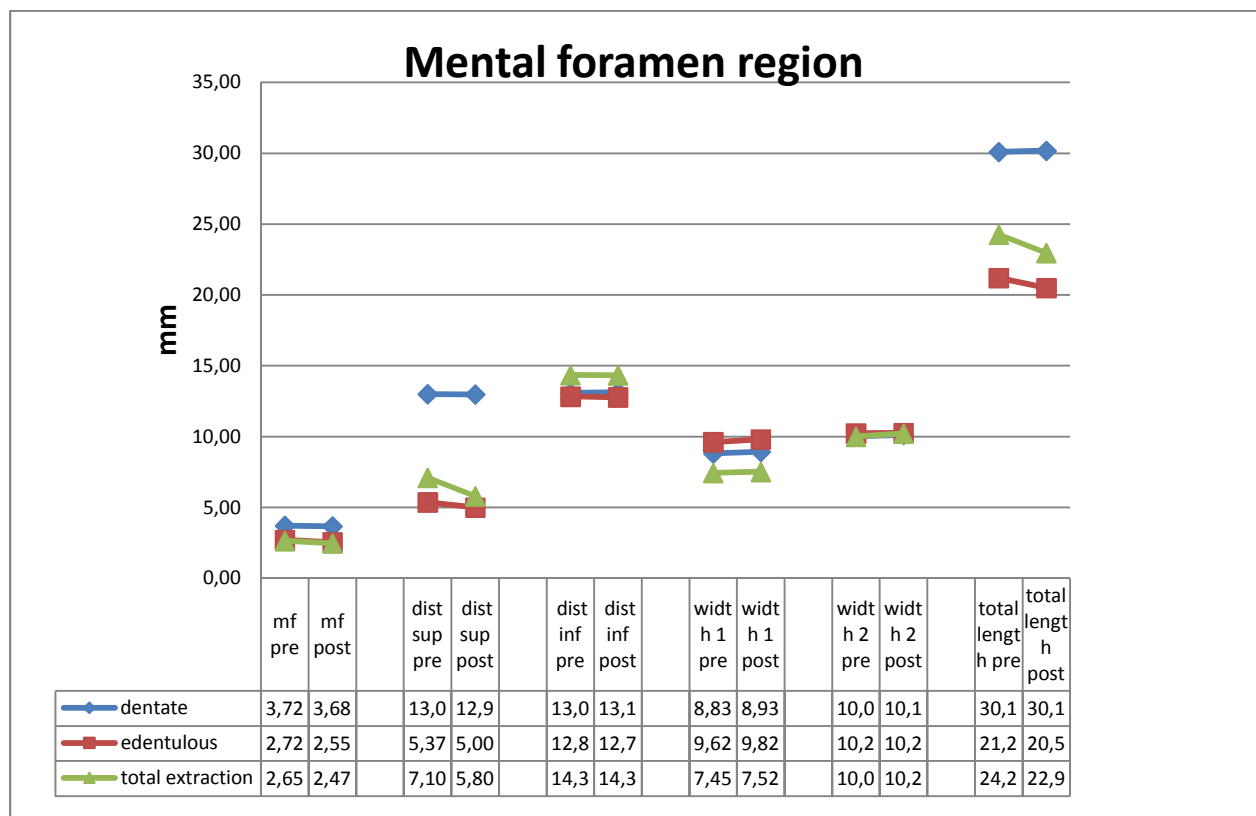


Figure 8.8: Dimensional changes at mental foramen region at each group. mf=mental foramen; dist sup= distance mental foramen to the upper border of the mandible; dist inf= distance mental foramen to the lower border of the mandible; width 1= total mandibular width above the mental foramen; width 2 = total mandibular width below the foramen; total length=total mandibular bone length at anterior region.

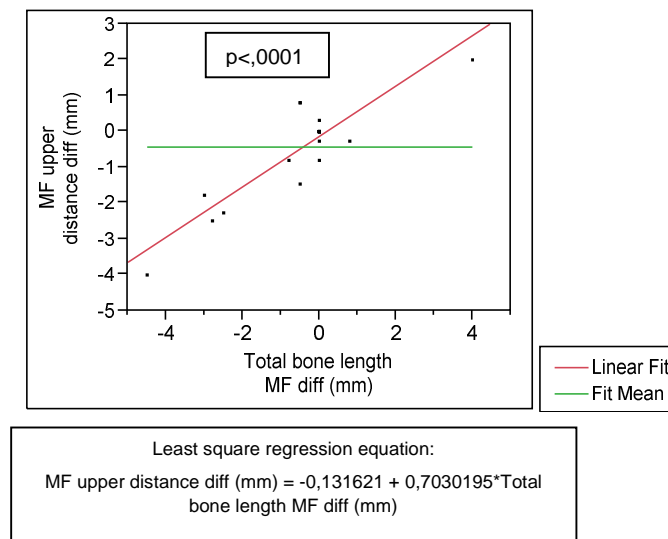


Figure 8.9: The regression line fitted to the scatter plot of values of upper distance difference (diff) and total bone length MF difference in all dentate mandibles.

The resorption rates (mm bone loss/year) was calculated for each group, however, no statistical significant differences were found. Those results are presented figure 8.10 and tables 8.11 and 8.12.

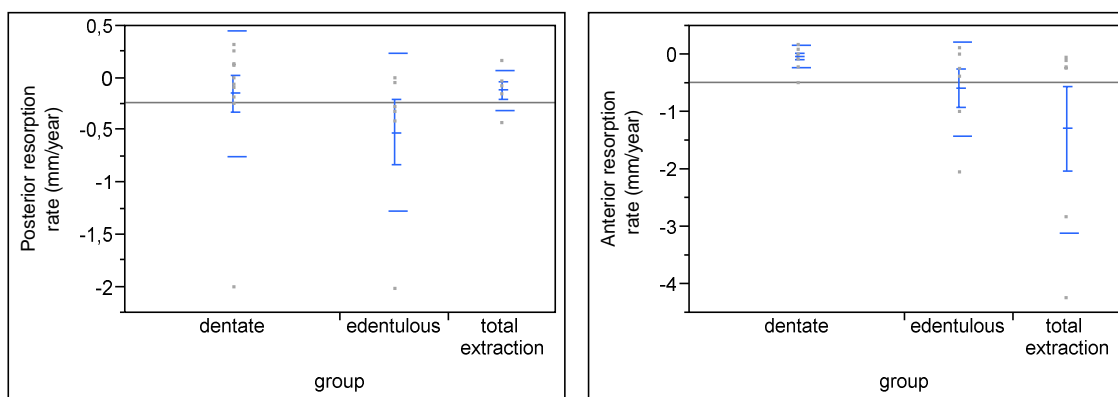


Figure 8.10: Mean posterior and anterior resorption rates in dentate, edentulous and total extraction groups. Lines indicate mean, standard deviation and 95% confidence interval.

Table 8.11: Means for Oneway Anova of resorption rate (mm/year) for mandibular posterior region ($p=0.39$).

Level	Number	Mean	Std Error	Lower 95%	Upper 95%
dentate	12	-0,15	0,17	-0,50	0,20
edentulous	6	-0,52	0,24	-1,01	-0,02
total extraction	6	-0,12	0,24	-0,61	0,37

Table 8.12: Means for Oneway Anova of resorption rate (mm/year) for mandibular anterior region ($p=0.05$).

Level	Number	Mean	Std Error	Lower 95%	Upper 95%
dentate*	12	-0,03	0,28	-0,61	0,56
edentulous	6	-0,60	0,40	-1,43	0,24
total extraction*	6	-1,29	0,40	-2,12	-0,46

*dentate x total extraction group ($p=0.04$)

Discussion

The present study has shown by means of CBCT images that only few changes occur in the mandibular neurovascular canals after tooth extraction. This was shown by the subtle changes observed in patients followed for 1 year and 7 months after tooth extraction and implant treatment. The mandibular bone dimensional alterations during the observational period did not influence the dimensions, neither the positioning, of the neurovascular canals inside this jaw bone. Moreover, the similar canal diameters found for the dentate and edentulous patients, for both the incisive canal and mandibular canal, further suggested that neurovascular canals do not undergo significant alterations in edentulous mandibles.

According to our results, the mandibular bone length was related to the length of neurovascular canals, in the posterior and anterior region of the mandible. Therefore, the average bone loss for both regions could be calculated for the edentulous group in order to be compared to previous study (*Tallgren 1972*). This

allowed us to suggest the possible range of years of edentulism of those patients, since this information could not be reliably gathered in the study. Using the least square regression equation presented in figures 8.6 and 8.7, the mean bone loss for the edentulous group was found around 6mm, for the anterior region, and 4mm at the posterior regions. This bone resorption at anterior region corresponded to patients within 7 years of edentulism, according to the study of Tallgren (1972).

It is worth to note that the mandibular bone resorption found might be influenced by the implant treatment received by the patients participating in our study. The resorption rate (mm bone loss/year) of edentulous patients was compared to rates reported previously, although such extrapolation is limited as earlier studies were carried on two dimensional projection images (*Sağlam 2002; Batenburg et al 1997; Tallgren 1972*). Tallgren (1972) reported a resorption rate of 0.68mm/year between 3 years and 7 years edentulism. Although we have found a lower resorption rate (0.59mm/year) for edentulous patients, this difference might be caused by the different years of edentulism and not only by the implant treatment. Interestingly, the resorption rate for a period of one year after extraction was reported to be around 2.54mm/year, almost double the resorption rate found in our study for a similar observation period. In fact, the resorption rate of patients undergoing total extraction was found to be around 1.3mm/year. This suggests that implant treatment may reduce mandibular resorption rate after total tooth extraction.

Using the same CBCT system of the present study, Sheikhi et al (2012) and Ganguly et al (2011) evaluated the accuracy of linear measurements in ideal and rotate position, as well as in simulated clinical conditions. The mean difference between physical measurements and radiographic measurements was lower than 0.2mm (*Sheikhi et al 2012*). Besides, strong inter and intra observer agreement has been reported to this CBCT system (*Sheikhi et al 2012; Ganguly et al 2011*), in agreement with our study. Cone beam images allow for a 3D visualization of the mandibular bone in a higher image resolution compared to previous images techniques, such as panoramic and cephalometric images used in similar previous studies (*Sağlam 2002; Batenburg et al 1997; Tallgren 1972*). Additionally, cone beam images overcome the drawback of structures overlapping and magnification inherent to projection images. This can be responsible for some disagreement among the

results previously found in the mandibular bone loss. The large inter-individual variability further limited comparison across studies.

On the other hand, even not using the same imaging technique, the thickness of the cortical bone of the mandible was in agreement with previous studies and was maintained over the observation time. Similarly, Katranji et al (2007) reported no difference of cortical thickness between dentate and edentulous mandible. In general, the changes in the dimensions of the mandibular structures were not clinically significant regarding the mandibular canal diameter and positioning, as well as for the cortical thickness. In healthy patients, the neurovascular canals seemed to maintain their original position related to the mandibular borders, but to the upper mandibular border. Yet, this change in upper distance was directly related to the mandibular bone resorption, and not resorption of canal walls. According to Polland et al (2001), the wall of the mandibular canal was similar in dentate and edentulous mandibles, and was highly perforated.

Although previous studies have suggested that myelinated nerve fibres are degenerated after tooth extraction (*Heasman and Beynon 1986; Hansen 1980*), no study was found reporting on changes in the mandibular canal dimensions over time after tooth extraction. However, no difference in the course and distribution of the inferior alveolar nerve has been found earlier in the study of Kieser et al (2005). The fibre diameter distribution curves of human inferior alveolar nerves are often bimodal distribution with peaks in the A δ (pain and temperature) and A β (touch and pressure) ranges. The bimodality characteristic appeared to be independent of the age and the number of teeth present (*Heasman and Beynon 1986*). However Heasman and Beynon (1986) suggested that, if any fibres had undergone atrophy following tooth loss, they would have been from the large diameter types, those representing touch and pressure. In turn, those innervating the periodontal ligament and teeth. It has been reported that edentulous jaw did not contain any large size axons, compared with the dentulous jaw (*Nonaka et al 2003*). Interestingly, large fibres are not the most found in the alveolar inferior nerve (*Heasman 1984*) suggesting that most of IAN fibres might maintain their functional significance in the bone physiology, even after total tooth extraction.

It can be concluded that the neurovascular canals do not undergo clinically significant changes after tooth extraction. Future studies should be conducted in larger and more homogeneous samples during longer follow-up period, besides considering the influence of other factors, such as type of treatment, in the mandibular bone loss over the time. In further studies, the relation between structures will be revisited in the mandible, as such alveolar bone loss indices, influence of bone quality classification and neurovascular bone corticalization.

Conclusions:

1. The study suggested that no significant changes of neurovascular canals occurs after tooth extraction.
2. Although mandibular bone loss could be observed over time, no association was found with dimensional changes in the neurovascular canals.
3. The length of neurovascular canals was positively related to the mandibular bone length in the anterior and posterior region.
4. Subtle changes, not clinically significant, were observed in the position of the mandibular canals and cortical thickness after tooth extraction and implant treatment.
5. Although using a different imaging technique, our study showed some similar results as previously reported in the literature concerning cortical thickness, bone loss and neurovascular dimensions. However, the resorption rate of mandibular bone after implant treatment in the first years after tooth extraction were lower than those reported in literature.

References:

- Atwood DA. Reduction of residual ridges: a major oral disease entity. *J Prosthet Dent* 1971; 26:266-79.
- Atwood DA. Bone loss of edentulous alveolar ridges. *J Periodontol* 1979; 50:11-21.
- Batenburg RH, Stellingsma K, Raghoobar GM, Vissink A. Bone height measurements on panoramic radiographs: the effect of shape and position of edentulous mandibles. *Oral Surg Oral Med Oral Pathol Oral Radiol Endod* 1997; 84:430-5.
- Berg H, Carlsson GE, Helkimo M. Changes in shape of posterior parts of upper jaws after extraction of teeth and prosthetic treatment. *J Prosthet Dent* 1975; 34:262-8.

- Blahout RM, Hienz S, Solar P, Matejka MH, Ulm CW. Quantification of bone resorption in the interforaminal region of the atrophic mandible. *Int J Oral Maxillofac Implants* 2007; 22:609-15.
- Bras J, van Ooij CP, Duns JY, Wansink HM, Driessen RM, van den Akker HP. Mandibular atrophy and metabolic bone loss. A radiologic analysis of 126 edentulous patients. *Int J Oral Surg* 1983; 12:309-13.
- Canger EM, Celenk P. Radiographic evaluation of alveolar ridge heights of dentate and edentulous patients. *Gerodontology* 2012; 29:17-23.
- Carlsson GE. Responses of jawbone to pressure. *Gerodontology* 2004; 21:65-70.
- Carlsson GE, Persson G. Morphologic changes of the mandible after extraction and wearing of dentures. A longitudinal, clinical, and x-ray cephalometric study covering 5 years. *Odontol Revy* 1967; 18:27-54.
- Carlsson GE, Ragnarson N, Astrand P. Changes in height of the alveolar process in edentulous segments. II. A longitudinal clinical and radiographic study over 5 years of full upper denture patients with residual lower anteriors. *Sven Tandlak Tidskr* 1969; 62:125-36.
- Chrcanovic BR, Abreu MH, Custódio AL. Morphological variation in dentate and edentulous human mandibles. *Surg Radiol Anat* 2011; 33:203-13.
- Coelho PG, Fernandes PR, Rodrigues HC, Cardoso JB, Guedes JM. Numerical modeling of bone tissue adaptation--a hierarchical approach for bone apparent density and trabecular structure. *J Biomech* 2009 11; 42:830-7.
- de Jong MH, Wright PS, Meijer HJ, Tymstra N. Posterior mandibular residual ridge resorption in patients with overdentures supported by two or four endosseous implants in a 10-year prospective comparative study. *Int J Oral Maxillofac Implants* 2010; 25:1168-74.
- Doblaré M, García JM. Anisotropic bone remodeling model based on a continuum damage-repair theory. *J Biomech* 2002; 35:1-17.
- Dunlop JW, Hartmann MA, Bréchet YJ, Fratzl P, Weinkamer R. New suggestions for the mechanical control of bone remodeling. *Calcif Tissue Int* 2009; 85:45-54.
- Enlow DH, Bianco HJ, Eklund S. The remodeling of the edentulous mandible. *J Prosthet Dent* 1976; 36:685-93.
- Ganguly R, Ruprecht A, Vincent S, Hellstein J, Timmons S, Qian F. Accuracy of linear measurement in the Galileos cone beam computed tomography under simulated clinical conditions. *Dentomaxillofac Radiol.* 2011; 40:299-305
- Hansen HJ. Neuro-histological reactions following tooth extractions. *Int J Oral Surg* 1980; 9:411-26.
- Heasman PA. The myelinated fibre content of human inferior alveolar nerves from dentate and edentulous subjects. *J Dent* 1984; 12:283-6.
- Heasman PA, Beynon AD. Myelinated fibre diameters of human inferior alveolar nerves. *Arch Oral Biol* 1986; 31:785-7.
- Hirai T, Ishijima T, Hashikawa Y, Yajima T. Osteoporosis and reduction of residual ridge in edentulous patients. *J Prosthet Dent* 1993; 69:49-56.
- Isidor F. Influence of forces on peri-implant bone. *Clin Oral Implants Res* 2006; 17:8-18.
- Jacobs R, Lambrichts I, Liang X, Martens W, Mraiwa N, Adriaenssens P, Gelan J. Neurovascularization of the anterior jaw bones revisited using high-resolution magnetic resonance imaging. *Oral Surg Oral Med Oral Pathol Oral Radiol Endod* 2007; 103:683-93.

- Jacobs R, Mraiwa N, van Steenberghe D, Sanderink G, Quirynen M. Appearance of the mandibular incisive canal on panoramic radiographs. *Surg Radiol Anat* 2004; 26:329-33.
- Jacobs R, Mraiwa N, vanSteenberghe D, Gijbels F, Quirynen M. Appearance, location, course, and morphology of the mandibular incisive canal: an assessment on spiral CT scan. *Dentomaxillofac Radiol* 2002; 31:322-7.
- Jacobs R, Schotte A, van Steenberghe D, Quirynen M, Naert I. Posterior jaw bone resorption in osseointegrated implant-supported overdentures. *Clin Oral Implants Res* 1992; 3:63-70.
- Jaul DH, McNamara JA Jr, Carlson DS, Upton LG. A cephalometric evaluation of edentulous Rhesus monkeys (*Macaca mulatta*): a long-term study. *J Prosthet Dent* 1980; 44:453-60.
- Katranji A, Misch K, Wang HL. Cortical bone thickness in dentate and edentulous human cadavers. *J Periodontol* 2007; 78:874-8.
- Kieser J, Kieser D, Hauman T. The course and distribution of the inferior alveolar nerve in the edentulous mandible. *J Craniofac Surg* 2005; 16:6-9.
- Klemetti E. A review of residual ridge resorption and bone density. *J Prosthet Dent* 1996; 75:512-4.
- Kordatzis K, Wright PS, Meijer HJ. Posterior mandibular residual ridge resorption in patients with conventional dentures and implant overdentures. *Int J Oral Maxillofac Implants* 2003; 18:447-52.
- Lin D, Li Q, Li W, Swain M. Dental implant induced bone remodeling and associated algorithms. *J Mech Behav Biomed Mater* 2009; 2:410-32.
- Mahnama A, Tafazzoli-Shadpour M, Geramipannah F, Mehdi Dehghan M. Verification of the mechanostat theory in mandible remodeling after tooth extraction: Animal study and numerical modeling. *J Mech Behav Biomed Mater* 2013; 20:354-62.
- Mercier P, Lafontant R. Residual alveolar ridge atrophy: classification and influence of facial morphology. *J Prosthet Dent* 1979; 41:90-100.
- Mullender MG, Huiskes R. Proposal for the regulatory mechanism of Wolff's law. *J Orthop Res* 1995; 13:503-12.
- Nonaka N, Ezure H, Goto N, Hagiwara Y, Goto J, Yamamoto T. Differences in the axonal compositions of the human mandibular nerve between dentulous and edentulous jaws. *Okajimas Folia Anat Jpn* 2003; 79:191-3.
- Panchbhai AS. Quantitative estimation of vertical heights of maxillary and mandibular jawbones in elderly dentate and edentulous subjects. *Spec Care Dentist* 2013;33:62-9.
- Pauwels R, Beinsberger J, Collaert B, Theodorakou C, Rogers J, Walker A, Cockmartin L, Bosmans H, Jacobs R, Bogaerts R, Horner K; SEDENTEXCT Project Consortium. Effective dose range for dental cone beam computed tomography scanners. *Eur J Radiol* 2012; 81:267-71.
- Pietrokovski J, Sorin S, Hirschfeld Z. The residual ridge in partially edentulous patients. *J Prosthet Dent* 1976; 36:150-8.
- Reich KM, Huber CD, Lippnig WR, Ulm C, Watzek G, Tangl S. Atrophy of the residual alveolar ridge following tooth loss in an historical population. *Oral Dis* 2011; 17:33-44.
- Sağlam AA. The vertical heights of maxillary and mandibular bones in panoramic radiographs of dentate and edentulous subjects. *Quintessence Int* 2002; 33:433-8.
- Sheikhi M, Ghorbanizadeh S, Abdinian M, Goroochi H, Badrian H. Accuracy of linear measurements of galileos cone beam computed tomography in normal and different head positions. *Int J Dent* 2012:214954.

- Schwartz-Dabney CL, Dechow PC. Edentulation alters material properties of cortical bone in the human mandible. *J Dent Res* 2002; 81:613-7.
- Tallgren A. The continuing reduction of the residual alveolar ridges in complete denture wearers: a mixed-longitudinal study covering 25 years. *J Prosthet Dent* 1972; 27:120-32.
- Trulsson M, van der Bilt A, Carlsson GE, Gotfredsen K, Larsson P, Müller F, Sessle BJ, Svensson P. From brain to bridge: masticatory function and dental implants. *J Oral Rehabil* 2012; 39:858-77.
- Unger JW, Ellinger CW, Gunsolley JC. An analysis of the effect of mandibular length on residual ridge loss in the edentulous patient. *J Prosthet Dent* 1992; 67:827-30.
- von Wowern N, Gotfredsen K. Implant-supported overdentures, a prevention of bone loss in edentulous mandibles? A 5-year follow-up study. *Clin Oral Implants Res* 2001; 12:19-25.
- Xie Q, Wolf J, Tilvis R, Ainamo A. Resorption of mandibular canal wall in the edentulous aged population. *J Prosthet Dent* 1997; 77:596-600.
- Wright PS, Glantz PO, Randow K, Watson RM. The effects of fixed and removable implant-stabilised prostheses on posterior mandibular residual ridge resorption. *Clin Oral Implants Res* 2002; 13:169-74.

:

Chapter 9

General discussion and conclusions

I. General discussion and conclusions

After extraction, teeth can be replaced by dental implants. Those are titanium screws that are placed inside the bone and which will integrate to jaw bone due to bone formation around the implant surface. This prosthetic replacement of teeth is comparable to other prosthetic replacements elsewhere in the body, since tooth loss can be also considered as a limb amputation. The utmost goal of any prosthetic rehabilitation is to recover function approaching normal physiological conditions. In this way, patients would be able to feel their prosthesis as part of their body, rather than interpret it as a foreign body. Thus, dental implants should be incorporated in the body allowing natural functioning, such as natural teeth, in order to be considered physiologically integrated.

During tooth extraction, a large number of sensory fibres are damaged. Since the target organ is removed, it is possible that the axonal sprouting of the damaged nerve fibres may result in the formation of a traumatic neuroma rather than a guided regeneration that occurs when the nerve is transected (*Mason and Holland 1993*). However, previous studies showed that the initial degeneration is followed by a nerve fibre proliferation that ends after the socket healing is complete, reaching similar levels of “normal” bone.

After implant placement, the innervation pattern of nerve fibres involved in bone remodeling and repair have been found similar to that found in healed socket (*Sawada et al 1993; Buma et al 1995; Ysander et al 1995; Gunjigake et al 2006; Mason and Holland 1993*). Electrophysiological techniques (*Linden and Scott 1988*) have shown that mechanoreceptive fibres represented in the mesencephalic nucleus were still present within the bone 6 months after tooth extractions; however those fibres could not be mechanically stimulated. Linden and Scott (1988) concluded that the majority of those fibres do not appear to reinnervate new tissues in which they can be mechanically stimulated, which implies that the nerve endings were present deep within the alveolar bone. Similarly, Bonte et al (1993) could not find any response in the trigeminal ganglion after mechanical stimulation of dental implants, though an inhibitory reflex in temporal muscle has been observed. However, a recent study (*Habre-Hallage et al 2012*) demonstrated that punctate mechanical stimulation of oral implants activates both primary and secondary cortical somatosensory areas.

This cortical activation may represent the underlying mechanism of osseoperception (*Habre-Hallage et al 2012*), and might happen by activating the remaining fibres with cell bodies in the mesencephalic nucleus described by Linden and Scott (1989) after extraction socket healing. Another mechanism underlying osseoperception might be the way mechanical forces are sensed and codified in bone. For example, mechanoreception in implants may be an adaptation of existing function in bone. It is not a mechanosensory function identical to what happens in teeth, but rather a new mechanoreception process, which is part of the bone adaptation to new mechanical demands after implant rehabilitation.

From chapter 2, one can conclude that mechanoreceptors have their morphology, location, distribution and physiological characteristics directly related to the biomechanical environment within they are located. After tooth extraction, the degeneration of those mechanoreceptors takes place since those fibres seem to not innervate new tissues in which they could be mechanically stimulated (*Linden and Scott 1989*). One hypothesis is that implant placement would be able to stimulate fibres located deep in the alveolar bone whose cell bodies are located at the mesencephalic nucleus. Besides, implants may also stimulate nerve regeneration by restoring functional significance of nerve fibres. This nerve regeneration has also been suggested for specialized nerve endings after trauma at IAN, and may also occur at peri-implant region. However, no specialized endings have been demonstrated in this region in previous studies, neither in chapter 5.

In that chapter, no intimate contact was noted between implant and nerve fibres. One cannot affirm that the implant would be responsible for the new functional significance of those fibres, since their function could not be determined in the present study. It has not been prove yet by previous studies if implants can improve or stimulate nerve regeneration. Whether implants can influence nerve fibres or not, they seem not to impair nerve fibres as shown by the study of Onur et al (2006) and the proximity of implants and anterior mandibular canals of patients observed in chapter 8. A close spatial interrelation between implants and the incisive canal (and its branches), indicates that nerve fibres from those canals might be innervating the peri-implant region (figure 9.1).

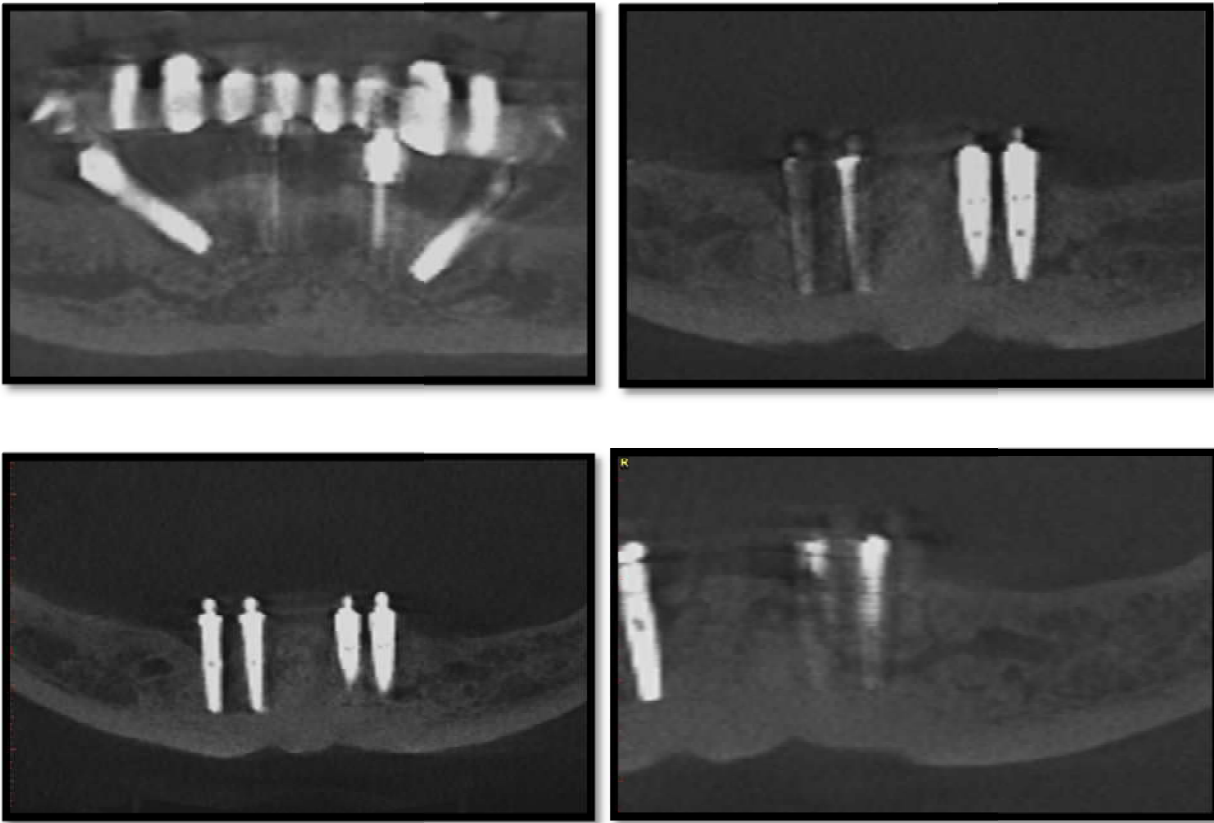


Figure 9.1: Illustration of good spatial interrelation between implant and neurovascular canals in the mandible. CBCT images from clinical cases observed in chapter 8.

The effect of different implant material and surface in the nerve conduction characteristics has been reported as minimal (*Onur et al 2006*), but no study has been found discussing differences in nerve fibre morphology, distribution pattern or molecular processes. Wada et al (2001) found no differences between loaded and unloaded approaches or implant surfaces, although further studies applying a controlled design are still required to approach the influence of those factors in bone innervation.

In chapter 2 periodontal innervation and mechanoreception was reviewed in order to describe the existing knowledge about this function in normal physiological conditions. This review was mainly based in the current concepts related to the PDL innervation. Five literature reviews and the subsequent studies published in the last 6 years were consulted to identify the relevant elements as well as the future needs in the study of the PDL innervation. Special attention was given to the spatial arrangement of nerve fibres within the PDL, after observing how limited are the extrapolation done from 2D analysis. A 3D approach was proposed using the

histological slices obtained for the study of myelinated nerve fibres distribution in the periodontal ligament, presented in chapter 3.

PDL is a complex, fibre-reinforced substance that responds to force in a viscoelastic and nonlinear manner. The PDL consists of 53–74% collagen fibres and 1-2% blood vessels and nerve endings that are embedded into an amorphous mucopolysaccharide matrix. Fibrous collagen elements resist tensile forces and the highly hydrated viscous ground substance into which fibrous proteins are embedded forms the extracellular matrix. The ground substance is responsible for the PDL's viscoelastic properties when subject to loading. Also, the PDL's cellular response to mechanical loading results in a metabolic response, e.g. remodeling of the ground substance and fibrous tissue (*Fill et al 2011*).

Although 2D histological slices have great impacts on quantification and visualization of clinical and research data, 3D volume reconstruction from these 2D slices is required in order to fully appreciate anatomical structures. Further approaches should combine information from different imaging techniques, such as histological and radiological 3D reconstructions.

Periodontal ligament and peri-implant bone are directly related to the distribution of mechanical loads in the jaw bones. Nevertheless, those structures differ in their components and physiological characteristics. In this thesis, both structures were assessed by means of histological images in chapters 3-5. The discussion aimed to highlight their importance for mechanoreception function.

In chapters 3 and 4, original research was conducted related to the distribution of nerve fibres and the function of other specialized structures found within human PDL. In chapter 3, it was observed that PDL nerve fibres were evenly distributed along the root of a human canine, with slightly higher concentration at the tooth apex. However this observation was done in one canine and further extrapolation should be made with caution. Yet, findings are in agreement with previous study in animals (*Loescher and Holand 1991*). Besides, the fibre diameter range of 5-8µm was similar to that reported in the inferior alveolar nerve and in the PDL in humans (*Heasman and Beynon 1986; Griffin and Spain 1972*). Interestingly, those fibres did correspond to the ones that were reported to degenerate in the IAN after tooth extraction (*Heasman 1984*). However, this range is not the most commonly found in the IAN of humans

(Heasman and Beynon 1986; see table 4: chapter 2), suggesting that most of myelinated nerve fibres of IAN maintain their functionality after tooth extraction.

Other PDL structures were assessed in Chapter 4 in order to identify their influence in the PDL function and relation to the PDL innervation. A brief literature review was conducted to identify the current information about the epithelial rests of Malassez and cementicles. The function of those structures remains unclear in the literature, although several researches pointed out their importance for the PDL maintenance, regeneration and prevention of ankylosis. Furthermore, the intimate relation of those structures with PDL nerve fibres has been demonstrated. The case-report of tooth autotransplantation in Chapter 4 added new evidence to the relation between ERM, PDL innervation and regeneration in humans. Future studies should further assess the ERM morphological alterations reported in this chapter, as well as, the role of ERM in periodontal regeneration and its association to PDL innervation.

Osseointegration and osseoperception are two important concepts in the field of implant dentistry (Brånemark et al 1997). Both are relevant processes during successful oral implant rehabilitation. Osseointegration stands for bone tissue formation around implants, creating a direct bone-implant contact, while Osseoperception deals with the peripheral feedback arising from osseointegrated implants evoking brain activation after mechanical stimulation (Jacobs and van Steenberghe 2006; Trulsson 2005; Klineberg 2005). It is believed that nerve fibres found within peri-implant bone may act as mechanoreceptors during load application on implants. In this way, studying the peri-implant bone innervation may help in unravelling the osseoperception phenomenon and assessing the related clinical impact of this phenomenon.

Peri-implant bone innervation might be influenced by several factors e.g. implant surface and functional load application. Studies on bone response to titanium implant have 3 main focuses: 1) describe the osseointegration process, 2) report the percentage of bone-implant contact and 3) determine or compare the factors influencing this process as such surgical technique, implant surface, shape and loading approaches. Unfortunately, regarding bone innervation and nerve tissue regeneration after implant rehabilitation, the literature is still scarce (Ysander et al 2001).

The osseointegration process is frequently described without any reference to tissue re-innervation as part of a successful osseointegration.

To address the clinical relevance of osseoperception phenomenon, one should understand the link amongst osseoperception, physiological integration, patient satisfaction/adaptation and implant success. Osseoperception, the perception of mechanical stimulus via osseointegrated implants, contributes to the physiological integration of the implanted prosthesis leading to better patient satisfaction and adaptation to the treatment. However some patient-centered aspects should be considered to assess the implant success, namely physiological and psychological impact of the treatment (*Papaspyridakos et al 2012*). Up till now, no clinical protocol is available to predict or improve the physiological impact of implant treatment. A physiologically integrated implant should be understood as an implant considered as being part of the body and, therefore, it would contribute to maintain the functional equilibrium of the oral system.

This physiological integration has been addressed by functional, psychophysical, neurophysiological and histological studies (*Habre et al 2012; Habre et al 2011; Jacobs and van Steenberghe 2006; Lambrichts 1998*). Evidence from these studies may strengthen the role of osseointegrated implants in the peripheral feedback mechanism during oral function. However, several aspects involved in oral physiology are not similar between patients with natural teeth and patients rehabilitated with osseointegrated implants. For example, unlike patients with natural teeth, who display bite-to-bite variation in jaw muscles activity, implant patients chew with approximately the same pattern of muscle activity during the whole masticatory function (*Turker et al 2007*).

Nevertheless, functional findings and psychophysical studies have reported an improved oral function in implant rehabilitated patients compared to conventionally rehabilitated patients. Functional studies show a higher bite force and a better masticatory efficiency for implant patients (*Haraldson and Carlsson 1977; 1979*). In the same way, psychophysical studies report markedly lower tactile thresholds in those patients. Whereas clinically health dentate patients can perceive micro-thickness from 8-20 μm (*Siirla and Laine 1969; Jacobs and van Steenberghe 1991*), this tactile threshold is found around 50 μm for implant rehabilitated patients and 150 μm patients

wearing mucosa-supported prosthesis. However, these differences between implant-supported prosthesis and mucosa-supported prosthesis are less pronounced for the tactile threshold related to load application. Whereas patients with a natural dentition can perceive down to 2 grams (g) of occlusal load, once wearing total mucosa-supported prosthesis and implant-supported prosthesis, this threshold increases to 150g and 100g, respectively (*Jacobs and van Steenberghe 1993*).

Since tactile threshold for load perception is remarkably higher for implant rehabilitated patients compared to patients with a natural dentition, considerable amount of occlusal overload is less prone to be perceived by implant rehabilitated patients. This fact should be highlighted when establishing patient occlusion after implant rehabilitation. High precision tools for occlusion determination might be required in order to avoid overload on the implant-bone complex, mainly in cases where immediate loading approach is being applied. In those cases, avoiding initial overload will be crucial to the process of implant osseointegration (*Klineberg et al 2012*). Moreover, it may also play a role in the maintenance of this osseointegration and of the balance in the oral musculoskeletal system.

Besides scientific evidences on the perception of mechanical stimulus via osseointegrated implants provided by functional and psychophysical tests (*Trulsson et al 2012; Enkling et al 2010; Batista et al 2008; Jacobs and van Steenberghe 2006; Mericske-Stern et al 2000; Hämmerle et al 1995; Jacobs and van Steenberghe 1993; Jacobs and van Steenberghe 1991*), scientific evidences are also provided by neurophysiological studies, namely functional resonance magnetic imaging (*Habre-Hallage et al 2012; Yan et al 2008; Lundborg et al 1996*), neural recordings (*Trulsson 2005*) and evoked related potentials (*Van Loven et al 2000*) studies. However, the conclusions generated by those studies are still unclear regarding the location of the main receptors responsible for mechanoreceptive function in implant rehabilitated patients. Similar doubt was faced in the earlier studies related to mechanoreceptive function present in natural dentition.

Clinical and experimental studies on the effect that sympathetic and sensory denervation have on bone dynamics, have suggested a role for the nervous system in bone blood flow, fracture repair and maintenance of bone tissue, regeneration and osteopathology (*Herkovitz et al 1995*). Reports on bone mechanosensibility function

can be found in the literature older than the osseointegrated implants, although not receiving this specific denomination. Firstly, Leriche (1930) announced that bone contained nerves fibres which supply both marrow and bone tissue and originated of sympathetic system and from the brain and spinal cord. In this way, they would mediate pain as well as position and space perception (*Herkovitz et al 1995*). Following this same idea, Miller and Kasahara (1963) report that myelinated nerve fibres found in the trabeculae of the epiphysis and metaphysis and on the under surface of the articular cartilage probably play a role in position sense and give information concerning pressure and movement in the internal structures of the ends of long bones.

The role of the bone innervation in the feedback controlling oral function remains unclear. Unfortunately, histological studies have been unsuccessful in demonstrating the involvement of these fibres in the tactile function, similarly to mechanoreceptors in the periodontal ligament. Actually, sensory function allowing force and pressure feedback, as such provided by specialized mechanoreceptors in the periodontal ligament, might not rely on mechanoreceptors in the peri-implant bone. However, neurophysiologic and functional findings in implant patients provide scientific evidences that a physiological adaptation occurs after implant treatment and this feedback might happen in a different pathway. These evidences can be found in studies showing brain neuroplasticity after implant rehabilitation (*Habre-Hallage et al 2012; Yan et al 2008; Lundborg et al 1996*), as well as higher chewing efficiency, bite force, better food manipulation ability and lower active and passive tactile threshold (*Svensson et al 2013; Trulsson et al 2012; Jacobs and van Steenberghe 2006; Trulsson and Gunne 1998; Jacobs and van Steenberghe 1993 Haraldson et al 1979; Haraldson and Carlsson 1977*) compared to edentulous patients rehabilitated with conventional prosthesis.

According to Sessle (2006), the modulatory mechanisms underlying these neuroplastic changes are still unclear, but do not appear to be accounted for by morphological changes (e.g. collateral sprouting) in the uninjured low-threshold mechanosensitive afferent endings in the trigeminal brainstem complex or by alterations in certain central inhibitory circuits or pre-synaptic regulatory processes. The neuromuscular system can be reflexly influenced by the afferent inputs into the brainstem from receptors that signal pain, touch, joint position, muscle stretch or

tension, etc. Reflex responses in jaw muscle have been demonstrated in some human subjects with mechanical stimulation of implant-supported prostheses.

Electrophysiological studies in cats (*Linden and Scott 1988*) showed that implant stimulated by purely mechanical loads generate response in the trigeminal ganglion but not at the mesencephalic nucleus. In the periodontal ligament, fibres with cell bodies at the mesencephalic nucleus are considered responsible for the sensory feedback during oral function in dentate subjects (*Linden and Scott 1989*). Hence, this function is expected to remain impaired in

“A key question in the perspective of the phenomenon of osseoperception is whether the transfer of forces through the implants to the bone could modify the peripheral input to the trigeminal motoneurone pool.”

van Steenberghe 1998

implant oral rehabilitation. Indeed, studies evaluating passive threshold on implants and teeth, found that this function, although better than in a fully edentulous condition, remains impaired when mechanically stimulating implants (*Jacobs and van Steenberghe 1993*). On the other hand, the research group in Habre et al (2012) is the first to demonstrate a sensory cortical response in humans after purely mechanical implant stimulation. Those findings (*Habre et al 2012*) confirmed that central plasticity occurs after implant rehabilitation, which may allow some functional adaptation controlled by other areas in the central nervous system, the central projection trajectories are no more the same observed in normal oral status.

In chapter 5, we addressed the mechanosensibility in implants by reviewing previous studies about peri-implant innervation. Besides, an original research was conducted in humans searching for mechanoreceptors in osseointegrated implants. Although our study could confirm the presence of nerve fibres in the peri-implant region in humans, and their diameter range corresponded to those carrying touch and pressure information, no clear conclusion could be made about the function of those nerve fibres. Nevertheless, techniques limitations should also be considered since they may also impair the histological description of nerve fibres. A single histological technique is not able to depict all types of nerve fibres associated with a tissue. In our study, we used light microscopy for initial identification of neural structures, electron microscopy was used to confirm the presence of nerve fibres and when any structure similar to mechanoreceptors was observed in the histological slices in order to confirm our findings.

Although no differences have been found in the nerve density after implant osseointegration, the influence in nerve fibre proliferation, molecular and structural changes have been reported by Ysander et al (2001) and Wang et al (1998), respectively. Ysander et al (2001) found a higher neuropeptide activity in marrow cells associated with bone remodeling during osseointegration, whereas Wang et al (1998) observed more fatty changes in the marrow of edentulous site compared to the implant site. Besides, the bone with implant has shown many varicose fibres in almost all remodeling cavities (*Lambrichts 1998; Buma et al 1995*).

Other techniques such as immunohistochemistry use immunoreactive substances to unravel the physiological role of nerve fibres located in the bone tissue. Mach et al (2002) show that the mineralized bone, the bone marrow and the periosteum receive innervation from both unmyelinated and myelinated sensory neurons, which would presumably include A- β , A- δ and C fibres, all of which could conduct sensory input from the periphery to the central system. Previous reports have suggested that in addition to the afferent role that sensory neurons play in conveying nociceptive information from mineralized bone, these may regulate bone metabolism together with sympathetic fibres that innervate a mineralized bone (*Mach et al 2002*). To better understand bone innervation and its influence in the mechanosensory function, the role of nerve fibres found in the peri-implant region should be characterized according to the same parameters studied for those fibres found in the PDL. In turn, peri-implant innervation should address the morphology of nerve endings, distribution of nerve fibres and endings, their central connections, neurophysiological aspects, as well as the biomechanical environment in which they are confined.

The study of osseoperception should focus on the functional significance of this phenomenon, such as it has been done in the study of the mechanosensory phenomenon in teeth. In this way, the clinical application of osseoperception can be determined for oral implants. It is suggested that the ability to perceive loads through osseointegrated implants allow those to be well integrated into the oral functions, before relied on natural teeth. The physiological integration of the implant prosthesis is the most important consequence of an optimized osseoperception after implant rehabilitation. This is mainly required for a better masticatory function and adaptation of the patient to the artificial tooth. Identifying the elements that influence

osseoperception is the first step to determine which of them can be controlled clinically as such osseoperception can be optimized in implant treatment. The literature may give some suggestions about how this optimization can be obtained. For example, it is known that, in man, tapping an implant in the upper jaw leads to an inhibitory reflex in the jaw closing muscle as observed through electromyography (*Bonte and van Steenberghe 1991*). However, this inhibitory reflex in the jaw closing muscle, as well as the post-stimulus EMG complexes, was very dependent on the presence of periodontal neural receptors, either in the ligament or the gingiva (*Jacobs and van Steenberghe 1995, Bonte and van Steenberghe 1991*). Thus apparently the maintenance of some remaining teeth may help in the prosthetic integration and patient's adaptation.

There is an agreement between animal and human data that tapping an implant only elicits a reflex in jaw closing muscles if some part of the natural dentition remains. Thus the latter is probably triggered by vibrations caused by the tap and conveyed through bone conduction. In turn, the nerve fibres histologically observed at the implant-to-bone interface cannot elicit a jaw reflex. It raises the question about the functional significance of those fibres for the implant treatment. Other suggestions could be that they are involved in the mechanoreception and remodeling processes in bone. Yet, to test this hypothesis more studies are needed about how those processes occur in association with bone innervation. In this way, further application of this knowledge can be suggested in the clinical practice.

"The physiology and biology of skeletal and alveolar bone are supported by a dynamic and complex milieu."

Lin et al (2012)

In case those fibres are involved in the perception of mechanical loads through oral implants, they might influence the hold-and-split task of masticatory function. An improved ability to perceive loads would allow a better motor control according to the characteristics of the food. However, it is not known how this ability of perceiving loads can be improved. One suggestion would be by a specialized training on oral motor control after prosthetic rehabilitation. Besides, this improvement could be also possible by stimulating the regeneration of nerve fibres in the peri-implant bone or when some remnants of PDL mechanoreceptors would be present. If the latter hypothesis is correct, another question would be how to stimulate this regeneration?

If the first hypothesis would be the right one, immediate implant placement would be more likely to have regenerated mechanoreceptors than delayed placement. In this way, immediate implant placement would improve physiological integration of implants due to a better mechanosensory function.

PDL mechanoreception is a complex function which components are specialized engines that has built up their distribution and morphology according to the biomechanical conditions endure throughout patient's life. Taking this into consideration, it is hard to believe that such a specialized engine would survive after tooth extraction, either regenerate after implant placement.

It has been reported that large nerve fibres undergo degeneration after tooth extraction (*Tang et al 2008*), corresponding to the calibre of nerve fibres found around a canine in chapter 3. Nerve degeneration caused by loss of the tooth is an important reason for the jaw bone resorption. Mechanical loading is the primary factor in bone remodeling and can also maintain innervation (*Tang et al 2008*).

The characterization of the peri-implant bone in humans in chapter 5 allowed us to determine if bone density and structure can be determined applying the newest imaging techniques of clinical use. The possibility to describe those bone parameters precisely would help to simulate this biomechanical environment allowing to assess strain/stress around implants (*Lin et al 2012*). Bone density is related to bone turn over and remodeling process, whereas bone structure is related to bone geometry and load distribution.

In chapter 6, we showed that bone density cannot be accurately determined in CBCT images. This radiographic bone parameter, however, is suggested as a feasible feature to be used for the assessment of bone density in intra-oral radiographs. This chapter showed a strong association between bone density before implant placement and bone loss after 3 months healing in animals. Similar clinical studies should be conducted to further confirm this relation in humans. Concerning bone structure, more information can be visualised in CBCT images as showed by figure 6.12 in chapter 6. However, this information could not be expressed numerically by means of fractal analysis. This means that more research is still needed till bone parameters as density and structure can be determined by means of radiographic images used in clinical practice. The images below show clearly that

even though more bone trabeculae can be visualized on CBCT slices (figure 9.2), they do not seem to match with the trabeculae morphology identified in histological slices. This difference is explained by divergences in methods to obtain the images, as such the image resolution, cutting direction and slice thickness. In turn, the current images techniques used in clinical practice are of limited application for the study of the mechanoreception in implants.

The study of bone density and structure, in chapter 6, brought the expectation to be able to correlate them with any possible alteration in the mandibular canal. In case those properties would be reliably detected in CBCT images, this correlation could be done in chapter 8. This hypothesis was also supported by the observation of Tang et al (2008) that “besides preventing implants from excessive occlusal loads, the sensory nerve successfully established can enhance bone formation via its effect on bone cells.” Wadu et al (1997) showed that the radiographic appearance of mandibular canal is related to trabecular number, distribution and pattern around the canal. Radiographic appearance of the mandibular canal has been recently related to trabecular bone volume (*Bertl et al 2013*) and trabecular classification (*Oliveira-Santos 2012*). In this way, such bone characteristics could be associated to the mandibular canal's radiographic appearance. Unfortunately, the actual state of imaging technology did not allow a reliable measure of those bone features. However, the question about the radiographic appearance of the mandibular canal related to changes in the alveolar bone might be relevant to study influence of implants in the oral physiology.

In chapters 7 and 8, mandibular canal variability was studied, since large variations of those canals have been reported before. In chapter 7, this variability was studied and could be partially explained by differences in species and geographical position. Mandibular canal dimensions were directly related to mandibular bone size. This relation may explain the differences in size inside the secular sample. In chapter 8, CBCT imaging technique was used to study the influence of implant treatment on jaw bone and mandibular canal changes related to the oral status. Although, the mandibular canal has a large variability within the population, the oral status was not confirmed as a factor influencing mandibular canal dimensional changes. Finally, our results suggested that implant treatment may decrease bone resorption in the first year after tooth extraction.



Figure 9.2: Manual segmentation of trabecular space and registration of corresponding histological and CBCT slices.

II. Conclusions and Future perspectives

The knowledge on periodontal ligament (PDL) and peri-implant bone tissue innervation is relevant to explain the mechanisms underlying the oral function. Although differing in their components and structures, both tissues may play an important role in fine oral motor control, providing sensory feedback to the Central Nervous System (CNS). Although our hypotheses were in part confirmed, future studies are needed in order to morphologically and functionally describe the physiological integration of implants.

This thesis addressed several aspects related to the osseoperception phenomenon and discussed the related clinical impact on osseointegrated implant treatment. Future researches on mechanosensory function in teeth and implants should address the cellular and molecular processes underlying this function. A better description of the tridimensional arrangement of PDL could further explain how loads are transmitted within a bone and translated into neural processes.

In the same way, the 3D arrangement of bone will influence the transmission of loads around the peri-implant bone. More reliable description of peri-implant bone structure and density may explain part of the biomechanical properties of bone. This understanding will help to understand the mechanosensory function in implants.

To investigate the possible role of peri-implant innervation in the mechanosensory function, peri-implant nerve fibres should be further investigated in the light of their cellular and molecular processes, neurophysiological aspects, morphological characteristics, distribution and central connections.

Summary

Samenvatting

Summary:

This thesis is composed of 2 literature reviews and 6 scientific studies focusing on the mechanosensory function related to periodontal ligament (PDL) and peri-implant region. The scientific research first started with the exploration of PDL nerve fibre distribution in humans (1) and the investigation of special PDL structures, namely the epithelial rests of Malassez (ERM) (2). This was followed by the histological search for mechanoreceptors in the peri-implant tissue of humans (3). Besides these histological approaches, more clinically accessible tools were investigated as possible indication for physiological changes of bone, especially dental radiographs which are daily used in clinic. Thus, morphological aspects of peri-implant bone were assessed by cone beam computed tomography (CBCT) and intra-oral (IO) radiography, using histological imaging as gold-standard (4). Finally, the influence of implant treatment on mandibular anatomy and innervation was investigated using 3D CBCT images. For this, the variability of neurovascular canals in the mandibular bone had first to be addressed (5, 6).

PDL innervation and mechanoreceptors have been extensively described according to their morphology, neurophysiological aspects, spatial arrangement and functional significance (*chapter 2*). Yet, researches exploring the 3D reconstruction of the PDL and mechanoreception function at cellular and molecular levels are expected to further our understanding of mechanosensory function in teeth. Three-dimensional volume reconstruction from 2D histological slices showed some potential in visualising the complex PDL anatomy, spatial arrangement and interrelationship among the different PDL structures (*chapter 2*).

Regarding nerve fibre distribution in human PDL, bundles of nerve fibres were mostly found at the alveolar related part of the PDL and in the vicinity of blood vessels (*chapter 3*). The highest number of fibres was found at the buccal and mesial region as well as at the root apex. The diameter of PDL fibres ranged between 2-15µm, and those that were myelinated and in the range of 5-6µm were most frequently seen in the human PDL. Overall, the lingual region showed higher concentration of nerve fibres of larger diameter (8-9µm). The highest concentration of isolated fibres was found at the intermediate region between apex and tooth fulcrum, and this in the cemental part of the PDL.

Other PDL special structures such as ERM and cementicles have been described in the literature, however their role in the PDL function is not fully understood (*chapter 4*). An altered ERM morphology after tooth autotransplantation suggested that this structure is related to PDL regeneration. Additional studies are needed to confirm this finding and to research the likely influence of this finding in PDL regeneration treatments.

For the first time in humans, myelinated and unmyelinated nerve fibres were shown in the peri-implant bone mostly localized in the Haversian canals close to the bone-implant interface (*chapter 5*). However in this study, no structure even resembling a mechanoreceptor was observed in the peri-implant region, which does not explain why some PDL mechanoreceptor functions are partially restored after implant treatment. Therefore, the exact location and mechanism of the structures that

would be responsible for those functions remains mostly unknown in fully implant rehabilitated patients.

Regarding peri-implant bone tissue estimations, significant correlations could be observed between bone levels histologically assessed and bone levels measured on IO radiographs and CBCT images (*chapter 6*). Tissue parameters as measured on IO radiographs correlate significantly with some histomorphometric parameters. However, such correlation could not be established for CBCT images. An increased bone loss (>2mm) seemed more likely to occur at low density bones (<5mmAl_{eq}). No reliable information about geometrical arrangement of trabecular bone could be obtained from radiographic images since IO and CBCT fractal analysis did not correlate to histological fractal analysis.

Using 3D CBCT scans, the anatomical variability of neurovascular canals of the mandible was addressed, not only between modern humans from different time-periods and different geographical regions, but also between mandibles of human and non-human primates. This contributed to an elaborate overview about neurovascular canal anatomy and the relation with adjacent tooth roots (*chapter 7*). Geographically, anatomical features which characterize some populations could be related to potential surgical and pathological risks. Furthermore, the incisive canal is suggested to be a unique feature of human mandibles (*chapter 7*). Considering some study limitations, this thesis suggested that neurovascular canals do not change significantly after tooth extraction and that the resorption rate of mandibular bone after implant treatment in the first years after tooth extraction seemed to be about 50% less than the rate reported in literature (*chapter 8*).

To conclude, PDL and peri-implant tissue were assessed to understand the underlying mechanisms of osseoperception influencing the oral implant rehabilitation. A special focus was also given to the innervation of those tissues, their functional relation and spatial arrangement with other adjacent structures.

Samenvatting:

Dit proefschrift bestaat uit 2 literatuurstudies en 6 wetenschappelijke onderzoeken gericht op de mechanosensorische functie gerelateerd aan het parodontale ligament (PDL) en de peri-implantaat regio. Het wetenschappelijk werk begon met het verkennen van de distributie van PDL zenuwvezels bij de mens (1) en met het onderzoek naar bijzondere PDL structuren, namelijk de epitheliale resten van Malassez (ERM) (2). Vervolgens werd een histologische zoektocht ondernomen naar mechanoreceptoren in het peri-implantaat weefsel van de mens (3). Naast deze histologische aanpak, werden meer bruikbare klinische tools onderzocht als mogelijke indicatoren voor fysiologische veranderingen van bot, en meer bepaald dental radiografieën die dagelijks in de tandheelkundige praktijk gebruikt worden. Zo werden meer morfologische aspecten van het peri-implantaat bot beoordeeld aan de hand van intra-orale (IO) en cone beam computed tomography (CBCT) radiografie, met als gouden standaard de histologische beeldvorming (4). Tenslotte, werd de invloed van de implantaat behandeling op de onderkaak anatomie en innervatie onderzocht aan de hand van 3D CBCT beelden. Hiervoor moest eerst de variabiliteit van neurovasculaire kanalen in de onderkaak aangekaart worden (5,6).

PDL innervatie en mechanoreceptoren werden tot nu toe reeds uitgebreid beschreven op basis van hun morfologie, neurofysiologische aspecten, ruimtelijke rangschikking en functionele betekenis (hoofdstuk 2). Toch wordt verwacht dat onderzoeken die de 3D-reconstructie van het PDL en die de mechanoreceptor-functie ervan op cellulair en moleculair niveau verkennen, ons een beter begrip van mechanosensorische functie in tanden kan bijbrengen. Driedimensionale volume reconstructie van 2D histologische coupes toonde effectief potentieel aan in het visualiseren van de complexe PDL anatomie, de ruimtelijke rangschikking en verwevenheid tussen de verschillende PDL structuren (hoofdstuk 2).

Met betrekking tot de zenuwvezel verdeling in het menselijke PDL werden zenuwvezelbundels meestal gevonden in het alveolaire deel van het PDL en in de nabijheid van bloedvaten (hoofdstuk 3). Het hoogste aantal vezels werd gevonden op de buccale en mesiale regio's, alsmede aan de wortel apex. De diameter van PDL vezels varieerde tussen 2-15 μm , waarvande gemyeliniseerde vezels in het bereik van 5-6 μm het vaakst voorkomen. De linguale regio vertoonde over het algemeen de hoogste concentratie aan zenuwvezels van grotere diameter (8-9 μm) i. Het hoogste aantal geïsoleerde vezels werd gevonden in het intermediaire gebied tussen apex en tand rotatiepunt, en dit ter hoogte van het cement-gedeelte van het PDL.

Andere bijzondere PDL structuren zoals ERM en cementicles werden in de literatuur reeds beschreven, maar hun rol in de PDL functie is nog niet volledig begrepen (hoofdstuk 4). Een veranderde ERM morfologie na tand autotransplantatie suggereert dat deze structuur gerelateerd is aan PDL regeneratie. Bijkomende studies zijn nodig om dit te bevestigen en om de waarschijnlijke invloed ervan te onderzoeken in PDL regeneratie- behandelingen.

Voor het eerst bij mensen, werden niet-myeliniseerde en gemyeliniseerde zenuwvezels in het peri-implantaat bot gelokaliseerd, vooral ter hoogte van de Haversse kanalen dichtbij het bot-implantaat grensvlak (hoofdstuk 5). In deze studie werden er weliswaar geen enkele structuren die ook maar op mechanoreceptoren

gelijken, waargenomen in de peri-implantaat regio, wat dus geen verklaring geeft waarom sommige PDL mechanoreceptor functies gedeeltelijk worden hersteld na behandeling met implantaten. Hierdoor blijft de exacte locatie en werking van de structuren die verantwoordelijk zijn voor deze functies nog vrijwel onbekend in volledig implantaat gerehabiliteerde patiënten.

Op het gebied van de berekening van peri-implantaat botweefsel, konden significante correlaties waargenomen worden tussen het botniveau dat histologisch geëvalueerd werd en het bot dat opgemeten werd op CBCT en IO röntgenfoto's (hoofdstuk 6). Bepaalde weefselparameters opgemeten op IO röntgenfoto's correleren significant met enkele histomorfometrische parameters. Weliswaar kon een dergelijke correlatie niet worden vastgesteld voor CBCT beelden. Een verhoogd botverlies (> 2 mm) leek vaker op te treden bij beenderen met lage dichtheid (<5mmAeq). Geen betrouwbare informatie over de geometrische configuratie van trabeculair bot kon worden verkregen van de radiografische beelden aangezien IO en CBCT fractaal-analyse niet bleek te correleren met de histologische fractaal-analyse.

Aan de hand van 3D CBCT opnames, werd de anatomische variabiliteit van de neurovascularisatie binnen onderkaken aangekaart, niet alleen voor de moderne mens uit verschillende tijdsperiode en tussen verschillende geografische regio's, maar ook tussen menselijke en niet-menselijke primaten. Dit heeft bijgedragen tot een uitgebreid overzicht van de neurovasculaire kanaal anatomie en de relatie met aangrenzende tandwortels (hoofdstuk 7). Geografisch worden sommige anatomische kenmerken gerelateerd aan mogelijke chirurgische en pathologische risico's. Verder blijkt het incisale kanaal een uniek kenmerk te zijn van de menselijke onderkaak (hoofdstuk 7). Uitgaande van een aantal methodologische beperkingen, suggereert dit proefschrift dat neurovasculaire kanalen niet significant veranderen na het trekken van tanden en dat de botresorptie ratio na behandeling met implantaten in het mandibulaire bot in de eerste jaren na het trekken van tanden 50% minder was dan wat reeds beschreven werd in de literatuur (hoofdstuk 8).

Tot slot, PDL en peri-implantaat weefsel werden beoordeeld om de onderliggende mechanismen van osseoperceptie te begrijpen. Ook werd een bijzondere aandacht besteed aan de innervatie van deze weefsels, hun functionele relatie en ruimtelijke rangschikking met andere aangrenzende structuren.

References

References:

- Batista M, Bonachela W, Soares J. Progressive recovery of osseoperception as a function of the combination of implant-supported prostheses. *Clin Oral Implants Res* 2008; 19:565-9.
- Beertsen W, McCulloch CA, Sodek J. The periodontal ligament: a unique, multifunctional connective tissue. *Periodontol* 2000 1997; 13:20-40.
- Berkovitz BK. The structure of the periodontal ligament: an update. *Eur J Orthod* 1990;12:51-76.
- Bertl K, Heimel P, Reich KM, Schwarze UY, Ulm C. A histomorphometric analysis of the nature of the mandibular canal in the anterior molar region. *Clin Oral Investig*. 2013 Mar 20. [Epub ahead of print]
- Bonte B, Linden RW, Scott BJ, van Steenberghe D. Role of periodontal mechanoreceptors in evoking reflexes in the jaw-closing muscles of the cat. *J Physiol* 1993; 465:581-94.
- Bonte B, van Steenberghe D. Masseteric post-stimulus EMG complex following mechanical stimulation of osseointegrated oral implants. *J Oral Rehabil* 1991; 18:221-9.
- Bosshardt DD, Nanci A. Immunocytochemical characterization of ectopic enamel deposits and cementicles in human teeth. *Eur J Oral Sci* 2003; 111:51-9.
- Brånemark PI, Rydevik B, Skalak R. Osseointegration in skeletal reconstruction and joint replacement. Quintessence publishing Co Inc, Carol Stream, Ill.1997.
- Brånemark PI. Osseoperception and musculo-skeletal function. In: Williams E, Rydevik B, Johns R, Brånemark P-I (eds). *Osseoperception and musculoskeletal function*. Gothenburg: Institute of Applied Biotechnology 1999: 6-10.
- Buma P, Elmans L, Oestreicher AB. Changes in innervation of long bones after insertion of an implant: immunocytochemical study in goats with antibodies to calcitonin gene-related peptide and B-50/GAP-43. *J Orthop Res* 1995; 13:570-7.
- Cassetta M, Stefanelli LV, Di Carlo S, Pompa G, Barbato E. The accuracy of CBCT in measuring jaws bone density. *Eur Rev Med Pharmacol Sci* 2012; 16:1425-9.
- Enkling N, Heussner S, Nicolay C, Bayer S, Mericske-Stern R, Utz KH. Tactile sensibility of single-tooth implants and natural teeth under local anesthesia of the natural antagonistic teeth. *Clin Implant Dent Relat Res* 2012; 14:273-80.
- Enkling N, Utz KH, Bayer S, Stern RM. Osseoperception: active tactile sensibility of osseointegrated dental implants. *Int J Oral Maxillofac Implants* 2010; 25:1159-67.
- Enkling N, Nicolay C, Utz KH, Jöhren P, Wahl G, Mericske-Stern R. Tactile sensibility of single-tooth implants and natural teeth. *Clin Oral Implants Res* 2007; 18:231-6.
- El-Sheikh AM, Hobkirk JA, Howell PG, Gilthorpe MS. Changes in passive tactile sensibility associated with dental implants following their placement. *Int J Oral Maxillofac Implants* 2003; 18:266-72.
- Fill TS, Toogood RW, Major PW, Carey JP. Analytically determined mechanical properties of, and models for the periodontal ligament: critical review of literature. *J Biomech* 2012 3; 45:9-16.
- Griffin CJ, Spain H. Organization and vasculature of human periodontal ligament mechanoreceptors. *Arch Oral Biol* 1972; 17:913-21.
- Gunjigake KK, Goto T, Nakao K, Konoo T, Kobayashi S, Yamaguchi K. Correlation between the appearance of neuropeptides in the rat trigeminal ganglion and reinnervation of the healing root socket after tooth extraction. *Acta Histochem Cytochem* 2006; 39:69-77.

- Habre-Hallage P, Bou Abboud-Naman N, Reyhler H, van Steenberghe D, Jacobs R. Assessment of changes in the oral tactile function of the soft tissues by implant placement in the anterior maxilla: a prospective study. *Clin Oral Investig* 2010; 14:161-8.
- Habre-Hallage P, Abboud-Naaman NB, Reyhler H, van Steenberghe D, Jacobs R. Perceptual changes in the peri-implant soft tissues assessed by directional cutaneous kinaesthesia and graphaesthesia: a prospective study. *Clin Implant Dent Relat Res* 2011; 13:296-304.
- Habre-Hallage P, Dricot L, Jacobs R, van Steenberghe D, Reyhler H, Grandin CB. Brain plasticity and cortical correlates of osseoperception revealed by punctate mechanical stimulation of osseointegrated oral implants during fMRI. *Eur J Oral Implantol* 2012; 5:175-90.
- Haku K, Muramatsu T, Hara A, Kikuchi A, Hashimoto S, Inoue T, Shimono M. Epithelial cell rests of Malassez modulate cell proliferation, differentiation and apoptosis via gap junctional communication under mechanical stretching in vitro. *Bull Tokyo Dent Coll* 2011; 52:173-82.
- Hämmerle CH, Wagner D, Brägger U, Lussi A, Karayiannis A, Joss A, Lang NP. Threshold of tactile sensitivity perceived with dental endosseous implants and natural teeth. *Clin Oral Implants Res* 1995; 6:83-90.
- Hansen HJ. Neuro-histological reactions following tooth extractions. *Int J Oral Surg* 1980; 9:411-26.
- Haraldson T, Carlsson GE. Bite force and oral function in patients with osseointegrated oral implants. *Scand J Dent Res* 1977; 85:200-8.
- Haraldson T, Carlsson GE, Ingervall B. Functional state, bite force and postural muscle activity in patients with osseointegrated oral implant bridges. *Acta Odontol Scand* 1979; 37:195-206.
- Haraldson T, Ingervall B. Muscle function during chewing and swallowing in patients with osseointegrated oral implant bridges. An electromyographic study. *Acta Odontol Scand* 1979 a; 37:207-16.
- Haraldson T, Ingervall B. Silent period and jaw jerk reflex in patients with osseointegrated oral implant bridges. *Scand J Dent Res* 1979 b; 87:365-72.
- Haraldson T, Carlsson GE. Chewing efficiency in patients with osseointegrated oral implant bridges. *Swed Dent J* 1979; 3:183-91.
- Heasman PA. The myelinated fibre content of human inferior alveolar nerves from dentate and edentulous subjects. *J Dent* 1984; 12:283-6.
- Heasman PA, Beynon AD. Myelinated fibre diameters of human inferior alveolar nerves. *Arch Oral Biol* 1986; 31:785-7.
- Herkovitz MS, Singh, Sandhu HS. Innervation of bone. In: Hall BK (ed). *Bone matrix and bone specific products*. CRC Press. 1991: 166-185.
- Holton WL, Hancock EB, Pelleu GB Jr. Prevalence and distribution of attached cementicles on human root surfaces. *J Periodontol*. 1986; 57:321-4.
- Hua Y, Nackaerts O, Duyck J, Maes F, Jacobs R. Bone quality assessment based on cone beam computed tomography imaging. *Clin Oral Implants Res* 2009; 20:767-71.
- Huang Y, Van Dessel J, Liang X, Depypere M, Zhong W, Ma G, Lambrichts I, Maes F, Jacobs R. Effects of Immediate and Delayed Loading on Peri-Implant Trabecular Structures: A Cone Beam CT Evaluation. *Clin Implant Dent Relat Res* 2013 Apr 2. doi: 10.1111/cid.12063.

- Jacobs R, van Steenberghe D. Comparative evaluation of the oral tactile function by means of teeth or implant-supported prostheses. *Clin Oral Implants Res* 1991; 2:75-80.
- Jacobs R, van Steenberghe D. Comparison between implant-supported prostheses and teeth regarding passive threshold level. *Int J Oral Maxillofac Implants* 1993; 8:549-54.
- Jacobs R, van Steenberghe D. Role of periodontal ligament receptors in the tactile function of teeth: a review. *J Periodontal Res* 1994; 29:153-67.
- Jacobs R, van Steenberghe D. Qualitative evaluation of the masseteric poststimulus EMG complex following mechanical or acoustic stimulation of osseointegrated oral implants. *Int J Oral Maxillofac Implants* 1995; 10:175-82.
- Jacobs R, Olmarker K, Rydevik B, Brånemark P-I and van Steenberghe D. Comparison of the vibrotactile threshold for limb amputees with bone-anchored and conventional socket prostheses. (SIROT 7th World Congress, Amsterdam) 1996.
- Jacobs R, van Steenberghe D, Brånemark P-I and Rydevik B. Evaluation of osseoperception following mechanical stimulation of osseointegrated implants. *J Dent Res* 1997 76:375.
- Jacobs R, Bou Serhal C, van Steenberghe D. The stereognostic ability of natural dentitions versus implant-supported fixed prostheses or overdentures. *Clin Oral Investig* 1997; 1:89-94.
- Jacobs R. Neurological versus psychophysical assessment of osseoperception. In: Jacobs R. (ed) *Osseoperception*. Leuven KULeuven.1998:75-88.
- Jacobs R, Brånemark R, Olmarker K, Rydevik B, van Steenberghe D, Brånemark P-I. Evaluation of the psychophysical detection threshold level for vibrotactile and pressure stimulation of prosthetic limbs using bone anchorage or soft tissue support. *Prosthet Orthot Int* 2000; 24:133-42.
- Jacobs R, Wu CH, Goossens K, Van Loven K, van Steenberghe D. Perceptual changes in the anterior maxilla after placement of endosseous implants. *Clin Implant Dent Relat Res* 2001; 3:148-55.
- Jacobs R, Mraiwa N, van Steenberghe D, Gijbels F, Quirynen M. Appearance, location, course, and morphology of the mandibular incisive canal: an assessment on spiral CT scan. *Dentomaxillofac Radiol* 2002; 31:322-7.
- Jacobs R, Mraiwa N, van Steenberghe D, Sanderink G, Quirynen M. Appearance of the mandibular incisive canal on panoramic radiographs. *Surg Radiol Anat* 2004; 26:329-33.
- Jacobs R, van Steenberghe D. From osseoperception to implant-mediated sensory-motor interactions and related clinical implications. *J Oral Rehabil* 2006; 33:282-92.
- Jang KS, Kim YS. Comparison of oral sensory function in complete denture and implant-supported prosthesis wearers. *J Oral Rehabil* 2001; 28:220-5.
- Kannari K. Sensory receptors in the periodontal ligament of hamster incisors with special reference to the distribution, ultrastructure and three-dimensional reconstruction of Ruffini endings. *Arch Histol Cytol* 1990; 53:559-73.
- Keller D, Hämmerle CH, Lang NP. Thresholds for tactile sensitivity perceived with dental implants remain unchanged during a healing phase of 3 months. *Clin Oral Implants Res* 1996; 7:48-54.
- Klineberg IJ, Trulsson M, Murray GM. Occlusion on implants - is there a problem? *J Oral Rehabil* 2012; 39:522-37.

- Klineberg I. Introduction: from osseointegration to osseoperception. The functional translation. *Clin Exp Pharmacol Physiol* 2005; 32:97-9.
- Klineberg I, Calford MB, Dreher B, Henry P, Macefield V, Miles T, Rowe M, Sessle B, Trulsson M. A consensus statement on osseoperception. *Clin Exp Pharmacol Physiol* 2005; 32:145-6.
- Lambrichts I, Creemers J, van Steenberghe D. Morphology of neural endings in the human periodontal ligament: an electron microscopic study. *J Periodontal Res* 1992; 27:191-6.
- Lambrichts I, Creemers J, van Steenberghe D. Periodontal neural endings intimately relate to epithelial rests of Malassez in humans. A light and electron microscope study. *J Anat* 1993;182 :153-62.
- Lambrichts I. Histological and ultrastructural aspects of bone innervation. In: Jacobs R. (ed) *Osseoperception*. Leuven: KULeuven 1998:13-20.
- Lin D, Li Q, Li W, Swain M. Dental implant induced bone remodeling and associated algorithms. *J Mech Behav Biomed Mater* 2009; 2:410-32.
- Lin D, Li Q, Li W, Duckmanton N, Swain M. Mandibular bone remodeling induced by dental implant. *J Biomech* 2010 19; 43:287-93.
- Linden RW, Scott BJ. The site and distribution of mechanoreceptors in the periodontal ligament of the cat represented in the mesencephalic nucleus and their possible regeneration following tooth extraction. *Prog Brain Res*1988; 74:231-6.
- Linden RW, Scott BJ. The effect of tooth extraction on periodontal ligament mechanoreceptors represented in the mesencephalic nucleus of the cat. *Arch Oral Biol* 1989; 34:937-41.
- Linden RWA. An update on innervation of the periodontal ligament. *Eur J Orthod* 1990; 12:91-100.
- Liu SM, Zhang ZY, Li JP, Liu DG, Ma XC. [A study of trabecular bone structure in the mandibular condyle of healthy young people by cone beam computed tomography]. *Zhonghua Kou Qiang Yi Xue Za Zhi*. 2007; 42:357-60.
- Loescher AR, Holland GR. Distribution and morphological characteristics of axons in the periodontal ligament of cat canine teeth and the changes observed after reinnervation. *Anat Rec* 1991; 230:57-72.
- Long A, Loescher AR, Robinson PP. A quantitative study on the myelinated fiber innervation of the periodontal ligament of cat canine teeth *J Dent Res* 1995; 74:1310-1317.
- Lundborg G, Brånemark P-I and Rosen B. Osseointegrated thumb prosthesis: a concept for fixation of digit prosthetic devices. *J Hand Surg* 21-A:216-221.
- Lundqvist S, Haraldson T. Oral function in patients wearing fixed prosthesis on osseointegrated implants in the maxilla. *Scand J Dent Res* 1990; 98:544-9.
- Mach DB, Rogers SD, Sabino MC, Luger NM, Schwei MJ, Pomonis JD, et al. Origins of skeletal pain: sensory and sympathetic innervation of the mouse femur. *Neuroscience* 2002; 113:155-66.
- Maeda T, Ochi K, Nakakura-Ohshima K, Youn S, Wakisaka S. The Ruffini ending as the primary mechanoreceptor in the periodontal ligament: Its morphology, cytochemical features, regeneration, and development. *CROBM* 1999:307-327.
- Manzano GM, Giuliano LM, Nóbrega JA. A brief historical note on the classification of nerve fibers. *Arq Neuropsiquiatr* 2008; 66:117-9.
- Mason AG, Holland GR. The reinnervation of healing extraction sockets in the ferret. *J Dent Res* 1993; 72:1215-21.

- Mericske-Stern R, Venetz E, Fahrländer F, Bürgin W. In vivo force measurements on maxillary implants supporting a fixed prosthesis or an overdenture: a pilot study. *J Prosthet Dent* 2000; 84:535-47.
- Miller RM, Kasahara M. Observations on the innervation of human long bones. *Anat Rec* 1963; 145: 13-23.
- Nackaerts O, Jacobs R, Devlin H, Pavitt S, Bleyen E, Yan B, Borghs H, Lindh C, Karayianni K, van der Stelt P, Marjanovic E, Adams JE, Horner K. Osteoporosis detection using intraoral densitometry. *Dentomaxillofac Radiol* 2008; 37:282-7.
- Nackaerts O, Jacobs R, Horner K, Zhao F, Lindh C, Karayianni K, van der Stelt P, Pavitt S, Devlin H. Bone density measurements in intra-oral radiographs. *Clin Oral Investig* 2007; 11:225-9.
- Nackaerts O, Jacobs R, Pillen M, Engelen L, Gijbels F, Devlin H, Lindh C, Nicopoulou-Karayianni K, van der Stelt P, Pavitt S, Horner K. Accuracy and precision of a densitometric tool for jaw bone. *Dentomaxillofac Radiol* 2006; 35:244-8.
- Naitoh M, Aimiya H, Hirukawa A, Arijii E. Morphometric analysis of mandibular trabecular bone using cone beam computed tomography: an in vitro study. *Int J Oral Maxillofac Implants* 2010; 25:1093-8.
- Oliveira-Santos C, Souza PH, de Azambuja Berti-Couto S, Stinkens L, Moyaert K, Rubira-Bullen IR, Jacobs R. Assessment of variations of the mandibular canal through cone beam computed tomography. *Clin Oral Investig* 2012; 16:387-93.
- Onur MA, Sezgin A, Gurpinar A, Sommer A, Akca K, Cehreli M. Neural response to sandblasted/acid-etched, TiO₂-blasted, polished, and mechanochemically polished/nanostructured titanium implant surfaces. *Clin Oral Implants Res* 2006;17:541-7.
- Papaspyridakos P, Chen CJ, Singh M, Weber HP, Gallucci GO. Success criteria in implant dentistry: a systematic review. *J Dent Res* 2012; 91:242-8.
- Polland KE, Munro S, Reford G, Lockhart A, Logan G, Brocklebank L, McDonald SW. The mandibular canal of the edentulous jaw. *Clin Anat* 2001; 14:445-52.
- Rydevik B. Amputation prostheses and osseoperception in the lower and upper extremity. In: Brånemark P-I, Rydevik B, Skalak R (eds). *Osseointegration in skeletal reconstruction and joint replacement*. Quintessence publishing Co Inc, Carol Stream, Ill. 1997
- Rydevik B. The role of osseoperception in limb amputees with bone-anchored prostheses. In: Jacobs R. (ed) *Osseoperception*. Leuven KULeuven.1998:47-59.
- Sawada, M., Kusakari, H., Sato, O., Maeda, T. & Takano, Y. Histological investigation on chronological changes in peri-implant tissues, with special reference to response of nerve fibres to implantation. *The Journal of the Japanese Prosthodontic Society* 1993; 37:144–158
- Seeman E. From Density to Structure: Growing Up and Growing Old on the Surfaces of Bone. *J Bone Miner Res* 1997; 12: 509–52.
- Sessle BJ. Mechanisms of oral somatosensory and motor functions and their clinical correlates. *J Oral Rehabil* 2006; 33:243-61.
- Siirilä HS, Laine P. Occlusal tactile threshold in denture wearers. *Acta Odontol Scand* 1969; 27:193-7.
- Stenfelt S, Jacobs R, Olmarker K, Rydevik B, Brånemark P-I. A technique for determination of vibrotactile force threshold levels in patients with orthopaedic osseointegrated implants. In: Jacobs R. (ed) *Osseoperception*. Leuven KULeuven 1998:105-123.

- Sun Y, De Dobbelaer B, Nackaerts O, Loubele M, Yan B, Suetens P, Politis C, Vrielinck L, Schepers S, Lambrechts I, Horner K, Devlin H, Jacobs R. Development of a clinically applicable tool for bone density assessment. *Int J Comput Assist Radiol Surg* 2009; 4:163-8.
- Svensson KG, Grigoriadis J, Trulsson M. Alterations in intraoral manipulation and splitting of food by subjects with tooth- or implant-supported fixed prostheses. *Clin Oral Implants Res* 2013; 24:549-55.
- Tang L, Chen Y, Wang Y, Liang X, Zhang N. Peripheral nerve may regulate the jaw bone resorption after tooth extraction. *Med Hypotheses* 2008; 71:414-7.
- Trulsson M, Gunne HS. Food-holding and -biting behavior in human subjects lacking periodontal receptors. *J Dent Res* 1998; 77:574-82.
- Trulsson M. Sensory-motor function of human periodontal mechanoreceptors. *J Oral Rehabil* 2006; 33:262-73.
- Trulsson M. Sensory and motor function of teeth and dental implants: a basis for osseoperception. *Clin Exp Pharmacol Physiol* 2005; 32:119-22.
- Trulsson M, van der Bilt A, Carlsson GE, Gottfredsen K, Larsson P, Müller F, Sessle BJ, Svensson P. From brain to bridge: masticatory function and dental implants. *J Oral Rehabil* 2012; 39:858-77.
- Türker KS, Sowman PF, Tuncer M, Tucker KJ, Brinkworth RS. The role of periodontal mechanoreceptors in mastication. *Arch Oral Biol* 2007; 52:361-4.
- Van Loven K, Jacobs R, Swinnen A, Van Huffel S, Van Hees J, van Steenberghe D. Sensations and trigeminal somatosensory-evoked potentials elicited by electrical stimulation of endosseous oral implants in humans. *Arch Oral Biol* 2000; 45:1083-90.
- van Steenberghe D. The structure and function of periodontal innervation. A review of the literature. *J Periodontal Res.* 1979; 14:185-203.
- van Steenberghe D; Trigeminal reflexes elicited by means of endosseous implants. In: Jacobs R. (ed) *Osseoperception*. Leuven KULeuven.1998:157-167.
- Wada S, Kojo T, Wang YH, Ando H, Nakanishi E, Zhang M, Fukuyama H, Uchida Y. Effect of loading on the development of nerve fibres around oral implants in the dog mandible. *Clin Oral Implants Res* 2001; 12:219-24.
- Wadu SG, Penhall B, Townsend GC. Morphological variability of the human inferior alveolar nerve. *Clin Anat* 1997; 10:82-7.
- Wang, Y.-H., Kojo, T., Ando, H., Nakanishi, E., Yoshizawa, H., Zhang, M., Fukuyama, H., Wada, S., Uchida, Y. Nerve regeneration after implantation in peri-implant area. A histological study on different implant materials in dogs. In: Jacobs R. (ed) *Osseoperception*. Leuven KULeuven1998:3-11.
- Yan C, Ye L, Zhen J, Ke L, Gang L. Neuroplasticity of edentulous patients with implant-supported full dentures. *Eur J Oral Sci* 2008; 116:387-93.
- Ysander M, Brånemark R, Olmarker K, Myers RR. Intramedullary osseointegration: development of a rodent model and study of histology and neuropeptide changes around titanium implants. *J Rehabil Res Dev* 2001; 38:183-90.

Curriculum vitae

Livia Corpas was born on April 24th 1978 in Rio de Janeiro, Brazil. At the end of 1998, Livia obtained her bachelor in Dentistry and, later in 2000, her specialized diploma in Prosthetics, both at the Federal University of Rio de Janeiro. Between 2001 and 2004 she worked as assistant professor at the Prosthetic departments of the Federal University of Rio de Janeiro, the University of Grande Rio and the University Veiga de Almeida (Rio de Janeiro / Brazil), besides participating and lecturing in specialized courses. After several years of clinical practice, she continued her academic training with a Master of Oral Rehabilitation at the University of São Paulo in Bauru (FOB/USP; Brazil, 2003-2005) and a Master of Medical Imaging at the Catholic University of Leuven (KULeuven; Belgium, 2007), where 1 year earlier she was selected for a PhD-granted programme for Latin American students (SBA-Selective Bilateral Agreement). Her PhD trajectory started in 2007 at the Oral Imaging Centre (KULeuven) where she focused on the study of physiological integration of oral implants and on new imaging methods to approach the topic. Since 2012, Livia is a scientific collaborator at the Prosthetic unit of the Dept. of Oral Health Sciences, KU Leuven where she is involved in research projects, more specifically on the integration of new digital technologies in the dental practice. Since 2010, Livia also teaches courses at Advimago (Centre for Advanced Oral Imaging) in Brussels on digital dentistry and 3D imaging. Livia is reviewer for Brazilian and other international journals, author and co-author of international publications. She was a finalist for the Research Award of the International Association of Dentomaxillofacial Radiology (IADMFR) in 2009 and 2013, while she received a "Research Fellowship" for the European Academy of Dentomaxillofacial Radiology (EADMFR 2012) for a scientific collaboration project between universities in Brazil, Belgium and Spain.

Articles in internationally peer-reviewed journals:

1. **Corpas** LS, Jacobs R, Quirynen M, Huang Y, Naert I, Duyck J. *Peri-implant bone tissue assessment by comparing the outcome of intra-oral radiograph and cone beam computed tomography analyses to the histological standard.* Clin Oral Implants Res 2011; 22:492-9. (see chapter 6)

2. Huang Y, **Corpas** LS, Martens W, Jacobs R, Lambrichts I. *Histomorphological study of myelinated nerve fibres in the periodontal ligament of human canine*. Acta Odontol Scand 2011; 69:279-86. (see chapter 3)
3. Struys T, Schuermans J, **Corpas** LS, Politis C, Vrielinck L, Schepers S, Jacobs R, Lambrichts I. *Proliferation of epithelial rests of Malassez following auto-transplantation of third molars: a case report*. J Med Case Reports 2010; 19;4:328. (see chapter 4)
4. Duyck J, **Corpas** LS, Vermeiren S, Ogawa T, Quirynen M, Vandamme K, Jacobs R, Naert I. *Histological, histomorphometrical, and radiological evaluation of an experimental implant design with a high insertion torque*. Clin Oral Implants Res 2010; 21:877-84. (related to chapter 6)
5. Vandenberghe B, **Corpas** LS, Bosmans H, Yang J, Jacobs R. *A comprehensive in vitro study of image accuracy and quality for periodontal diagnosis. PART 1: The influence of X-ray generator on periodontal measurements using conventional and digital receptors*. Clin Oral Investig 2011; 15:537-49.
6. Berti SA, Couto Souza PH, Jacobs R, Lambrichts I, **Corpas** LS, Arruda EP, Martins WD, Westphalen FH, Tolazzi AL. *Spontaneous resolution of a central giant-cell granuloma after incisional biopsy: a case report*. J Oral Maxillofac Surg 2009; 67:1543-7.
7. Liang X, Jacobs R, **Corpas** LS, Semal P, Lambrichts I. *Chronologic and geographic variability of neurovascular structures in the human mandible*. Forensic Sci Int 2009 10; 190:24-32.
8. Liang X, Jacobs R, Hassan B, Li L, Pauwels R, **Corpas** LS, Souza PC, Martens W, Shahbazian M, Alonso A, Lambrichts I. *A comparative evaluation of Cone Beam Computed Tomography (CBCT) and Multi-Slice CT (MSCT) Part I. On subjective image quality*. Eur J Radiol 2010; 75:265-9.
9. Calderon P dos S, Kogawa EM, **Corpas** LS, Lauris JR, Conti PC. *The influence of gender and bruxism on human minimum interdental threshold ability*. J Appl Oral Sci 2009; 17:224-8.
10. Liang X, Lambrichts I, **Corpas** LS, Politis C, Vrielinck L, Ma GW, Jacobs R. *Neurovascular disturbance associated with implant placement in the anterior mandible and its surgical implications: literature review including report of a case*. Chin J Dent Res 2008; 11: 56-64.

Presentations at international scientific conferences:

1. **Corpas**, LS, Nackaerts O, ROCKENBACH, M. I., Duyck, Joke, Jacobs, R. Radiographic and histological density of peri-implant bone in animal study In: IADR general session, 2012, Foz do Iguacu. **90th General Session and Exhibition of the IADR/ IADR Latin American regional meeting**, 2012. p.120.

2. **Corpas**, LS, Lambrichts, I., Semal, P., Collaert B, Quiryne, Marc, Jacobs, R. Periodontal and peri-implant tissues: morphological and structural aspects related to oral function In: XXIIIrd congress of International Society of Biomechanics, 2011, Brussels. **ISB2011**, 2011. p.24.
3. Huang Y, **Corpas**, LS, ZHANG, G., Maes F, Lambrichts, I., Jacobs, R. Three dimensional reconstruction of Mallassez epithelial rests using light microscopic imaging. In: **18th International Congress of DentoMaxillofacial Radiology**, Hiroshima,. 2011. p.199.
4. **Corpas**, LS, Huang Y, Zang G, Maes F, Lambrichts I, Jacobs R. Three Dimensional Reconstruction of Human Periodontal Ligament Structures using Light Microscopic Imaging In: **12th European Congress of Dento-Maxillo-Facial Radiology**, Istanbul, 2010.
5. **Corpas**, LS., Huang Y, Collaert B, Vrielinck L, Zang G, Struys T, Lambrichts I, Jacobs R. Presence of myelinated nerve fibers in the periodontal ligament , peri-implant bone and bone substitute materials, **ITI Symposium**, Switzerland 2010.
6. **Corpas**, LS, Jacobs, R., Lambrichts, I., Naert, Ignace, Quiryne, Marc, Duyck, J. Peri-implant bone tissue assessment during osseointegration by comparing the outcome of 6 radiographic analysis methods to the histological standard In: 17th International Congress of Dentomaxillofacial Radiology Imaging in Perspective, 2009, Amsterdam. **17th International Congress of Dentomaxillofacial Radiology Imaging in Perspective**, 2009.
7. Liang X, Jacobs R, Hassan B, Li L, Pauwels R, **Corpas**, LS, Couto Souza, Paulo H., Martens W, Shahbazian M, Alonso A, Lambrichts I. A comparative evaluation on subjective image quality of cone beam computed tomography (CBCT) and multi-slice CT (MSCT) In: 17th International Congress of Dentomaxillofacial Radiology Imaging in Perspective, 2009, Amsterdam. **17th International Congress of Dentomaxillofacial Radiology Imaging in Perspective**, 2009.
8. Liang X, Jacobs R, **Corpas**, LS, Semal P, Gilissen E, Lambrichts I. Characteristic comparative anatomy of the nasopalatine canal using CBCT imaging. In: 11th Congress of the European Academy of Dento-Maxillo-Facial Radiology, 2008, Budapest. **11th Congress of the European Academy of Dento-Maxillo-Facial Radiology**, 2008.
9. **Corpas**, LS, Liang X, Semal P, Lambrichts I, Jacobs R. Modern human variability in mandibular neurovascularization and its evolutionary aspects. In: 11th Congress of the European Academy of Dento-Maxillo-Facial Radiology, 2008, Budapest. **11th Congress of the European Academy of DentoMaxilloFacial Radiology**, 2008.
10. Liang X, Jacobs R, Semal P, **Corpas**, LS, Martens W, Raymundo Junior, R, Lambrichts I. Modern human variability of neurovascular structures in the anterior

mandible In: 16th International Congress of Dentomaxillofacial Radiology Imaging in Perspective, 2007, Beijing. **16th International Congress of Dentomaxillofacial Radiology Imaging in Perspective, 2007.**

Presentations at other conferences and symposia:

Corpas, LS. The use of CBCT and optical scanning in imaging diagnosis, 2013. *Ribeirão Preto; Event: 35^a Jornada Odontológica de Ribeirão Preto, Institution: University of São Paulo/ Dentistry Faculty of Ribeirão Preto.*

Corpas, LS. Optimalisatie CBCT, 2013. *Kortrijk; Event: Studieclub, Institution: Verbond der Vlaamse Tandartsen.*

Corpas, LS. Diagnostic imaging for Implant Dentistry, 2013. *São Paulo; Event: invited lecturer- Specialization of Implantology; Institution: São Leopoldo Mandic (Dentistry Faculty)*

Corpas, LS. Digital solutions for Implant Dentistry, 2012. *Curitiba; Event: invited lecturer- Master Implantology; Institution: ILAPEO (Latin American Institute of Dental Research and Education)*

Corpas, LS. Basic concepts of CBCT in Dentistry, 2012. *Langdorp; Event: Studieclub, Institution: Verbond der Vlaamse Tandartsen.*

Vandenberghe B, **Corpas, LS. Les empreintes optiques, 2011.** *Brussels; Event : Congrès de la Societe de Medecine Dentaire; Institution: Societe de Medecine Dentaire*

Corpas, L.S. Use of Cone Beam Computed Tomography in Implant Dentistry, 2010. *Gramado; Event: VIII CONABRO; Instution: ABRO (Brazilian association of Oral Maxillofacial Radiology)*

Jacobs, R., **Corpas, LS. The osseoperception phenomenon: an anatomical and physiological integration, 2007.** *Bauru; Event: Digital Imaging, Implantology. Institution: FOB/USP (São Paulo University/ Dental school Bauru)*

Corpas, LS. Experience as brazilian phd student at KULeuven. 2012. *Leuven; Event: Visit ABRUEM (Brazilian Association of State Universities) Institution: KULeuven*

Corpas, LS. Sharing experience as foreign student at KULeuven, 2008 *Leuven; Event: Meeting schorlarship programme Selective Bilateral Agreement (SBA-grant program for Latin America); Institution: KULeuven*